TOPCAT

Template Offshore Platform Capacity Assessment Tools

The TOPCAT software and TOPCAT manual are provided "as is" by the Marine Technology and Management Group (MTMG) at the University of California at Berkeley to sponsors of the research project entitled "Screening Methodologies for Use in Platform Assessments and Requalifications." Any express or implied warranties of merchantability and fitness for a particular purpose are disclaimed. In no event shall the MTMG be liable for any direct, indirect, incidental, special, exemplary, or consequential damages (including, but not limited to, procurement of substituted goods or services; loss of use, data or profits; or business interruption) however caused by any theory of liability, whether in contract, strict liability, or tort (including negligence or otherwise) arising in any way out of the use of this software or manual, even if advised of the possibility of such damage.

TOPCAT

Template Offshore Platform Capacity Assessment Tools

Programming Credits:

TOPCAT v0.71 James D. Stear, Zhaohui Jin, Robert G. Bea

TOPCAT is an outgrowth of the ULSLEA (Ultimate Limit State Limit Equilibrium Analysis) Program. Credits for the development of ULSLEA are as follows:

ULSLEA v3.0 James D. Stear, Robert G. Bea

ULSLEA v2.1 James D. Stear, Mehrdad M. Mortazavi, Robert G. Bea

ULSLEA v2.0 Mehrdad M. Mortazavi, Robert G. Bea

ULSLEA v1.0 Mehrdad M. Mortazavi, Robert G. Bea

TABLE OF CONTENTS

APPENDIX T

CHAPTER ONE: INTRODUCTION

1.0 Introduction

TOPCAT is an analysis program intended for the preliminary structural design and assessment of fixed steel offshore platforms. The name stands for Template Offshore Platform Capacity Assessment Tools. TOPCAT is an outgrowth of the ULSLEA (Ultimate Limit State Limit Equilibrium Analysis) program, previously developed by the Marine Technology and Management Group at U. C. Berkeley.

TOPCAT enables a user to quickly develop a simple structural model for one of several standard platform types and then analyze the model for the following conditions:

- Loads from the action of wind, wave and current.
- Loads from earthquakes.
- Fatigue from cyclic wave loading.

TOPCAT is oriented towards the evaluation of major structural members (unbraced deck legs, diagonal braces, caisson guy-wires, piles) in platforms; features such as decks, boat-landings, and conductors as input as non-structural members, but are modeled for the purpose of determining attracted loads. The program has been developed to allow for analysis of the following types of platforms:

- Four-, six-, eight- and twelve-leg jacket-type structures. The program will accept input for jackets which are either unbattered, have symmetric batter on one or both principal axes, or have a single vertical or single battered face. The legs supporting the deck section should be unbattered. All corner legs and main piles must be of the same type; for platforms with six or more legs, the interior legs and piles may be of a different type than the corner legs and piles.
- Three-leg (tripod) jackets. The program will accept input for tripods with either equilateral or isosceles plan layouts. Legs may be vertical, battered such that the centroid of the jacket top plan is directly above the centroid of the jacket bottom plan, or a single vertical leg may be specified. If a single vertical leg is specified, this leg must be opposite the odd-size face for jackets with isosceles plan. All corner legs and main piles must be of the same type.
- Braced (two identical braces at right angles in plan) or guyed (three identical wires, 120° apart in plan) caissons, with supporting braces or wires attached to vertical piles.
- Multi-jacket structures, which consist of several multi-leg jackets all supporting a common deck structure. The user specifies a single jacket type, and then may specify the layout of these jackets relative to one another.

All platforms are assumed to be roughly symmetric, and assumed to possess no significant mass or projected area eccentricities which will result in torsion. The jacket-type platforms are assumed to be piled through the legs, but may also include skirt piles. Analysis options allow the strength contributions of conductors, mud mats and mudline braces to be included. The soil beneath the platform can be specified as having up to ten layers of either sand or clay, with different strength properties. Users analyzing platforms with diagonal bracing have the option of

specifying braces or tubular joints as be grouted, or specifying braces as having significant out-of-straightness or denting damage.

TOPCAT has been developed to function in the Microsoft Excel 7.0 environment together with Windows 95. The program consists of a single workbook, which contains all calculation, pre-processor and post-processor functions. Algorithms controlling the program input, output and calculations have been written in Microsoft Visual Basic, the macro language of Microsoft Excel 7.0. Input files generated by the program are saved as separate workbooks consisting of a single Excel spreadsheet.

1.1 How is TOPCAT Different from ULSLEA?

TOPCAT represents major modifications to the ULSLEA series of programs. The following changes have been made:

- All program functions are controlled by a single Excel 7.0 workbook. Previous versions of ULSLEA relied upon a companion workbook to control the program menus and the taking and saving of input.
- Users now have the ability to directly access output tables from within the program, as opposed to having to print them out. These tables have been expanded to provide all values used to define the graphical output provided by the program. Output tables and graphs have been added for fatigue damage to tubular joints and platform horizontal mode shapes.
- Users can now enter and store data on fatigue analysis parameters and earthquake analysis parameters.
- Special input has been developed for caissons and tripod structures.
- Users may directly add deck bay diagonal braces, without having to "fool" the program as with ULSLEA v3.0. Input files from v3.0 of platforms that have deck bay bracing are automatically corrected to the new format used by TOPCAT.
- Users may now model jackets with a single vertical end-on face, and tripods with a single vertical leg. In addition, for jackets with more than six legs, users may specify the corner legs and piles as being of a different type than those in the center portions of the jacket.
- Users may designate up to ten soil layers of sand and clay, as opposed to a single layer.
- Users may input information on conductors and mud mats, and include these members' strength and stiffness contributions (along with those of mudline braces) in the foundation component.
- Users may input specific steel yield strengths, brace effective length factors, and joint stress concentration factors for individual members as opposed to defining these values globally.
- Users now have the option of using Cnoidal wave theory instead of Stokes fifth-order theory to define wave particle horizontal velocities.

1.2 Getting Started with TOPCAT

New users of the TOPCAT program should review Chapter Two, which explains the basic functions of the TOPCAT program, together with key assumptions and limitations, and carefully read through Chapter Three, a tutorial which walks the user though the tasks of program installation, model preparation, analysis parameter specification, analysis, and output processing. It is essential that users read and understand these two chapters prior to using the program.

Following the reading of Chapters Two and Three, the user should review Chapter Four, which contains additional modeling examples.

Users of the original ULSLEA program (v2.0, v2.1 and v3.0) can go directly to Chapter Three, and briefly review the program changes. ULSLEA users are encourages to review the program examples in Chapter Four.

Several reports have been produced by the Marine Technology and Management Group (MTMG) at U. C. Berkeley concerning the theory and verification of the TOPCAT program. This manual makes reference to those reports; in the future, effort will be made to integrate the information contained in these reports into user manual appendices for ease of reference. The reports are:

- "A Probabilistic Screening Methodology for Use in Assessment and Requalification of Steel, Template-Type Offshore Platforms," by M. Mortazavi and R. G. Bea, Report to Screening Methodologies Project Sponsors, Department of Civil Engineering, U. C. Berkeley, January 1996.
- "Earthquake Analysis of Offshore Platforms," by J. D. Stear and R. G. Bea, Bea, Report to Screening Methodologies Project Sponsors, Department of Civil and Environmental Engineering, U. C. Berkeley, June 1997.
- ULSLEA Enhancements: Fatigue Analysis / Earthquake Analysis / Additional Configurations," by J. D. Stear and R. G. Bea, Bea, Report to Screening Methodologies Project Sponsors, Department of Civil and Environmental Engineering, U. C. Berkeley, June 1997.

1.3 Acknowledgments

This software has been developed by the Marine Technology and Management Group at U. C. Berkeley as part of the Screening Methodologies for Offshore Platforms Project. TOPCAT v0.70 has been developed by Research Assistants James D. Stear and Zhaohui Jin working under the supervision of Professor Robert G. Bea. TOPCAT v0.70 is based in part on the ULSLEA program. ULSLEA v1.0 and v2.0 were developed by Research Assistant Mehrdad Mortazavi working under the supervision of Professor Robert G. Bea; ULSLEA v2.1 and v3.0 were developed by Research Assistant James Stear working under the supervision of Professor Robert G. Bea.

The Screening Methodologies for Offshore Platforms Project has been sponsored by ARCO Exploration and Production Technology, Brown & Root International, Incorporated in conjunction with PEMEX/IMP, Chevron Petroleum Technology Company, Exxon Production Research Company, Mobil Technology Company, Shell Deepwater Development Systems, Incorporated, Unocal Corporation, and the U. S. Minerals Management Service in conjunction with the California State Lands Commission. The support and assistance provided by these companies and agencies, and their liaisons to the project, are gratefully acknowledged.

CHAPTER TWO: TOPCAT PROGRAM BASICS

2.0 Introduction

This chapter reviews the basic functions of the TOPCAT program. The goal of this chapter is to give new users an overview of how platforms are idealized for a TOPCAT analysis, what the different analysis types do, and what output is returned to the user. References are made to the User Manual appendices, which contain complete explanations of the principals behind the TOPCAT strength and load calculation procedures.

2.1 How Does TOPCAT Work?

TOPCAT is a simple structural analysis program specifically designed to allow a user to quickly build and analyze models of jacket-type and caisson-type fixed offshore platforms for storms, earthquakes and long-term exposure to waves. The program consists of pre-processing features, which allow a user to quickly input the basic geometry and member characteristics of a platform and the environmental conditions; computational routines for storm, earthquake, and fatigue analysis; and post-processing features, which allow a user to obtain graphical and tabular output on the analyses performed.

TOPCAT idealizes platforms as a series of structural sections or components, as shown in Figure 2-1.

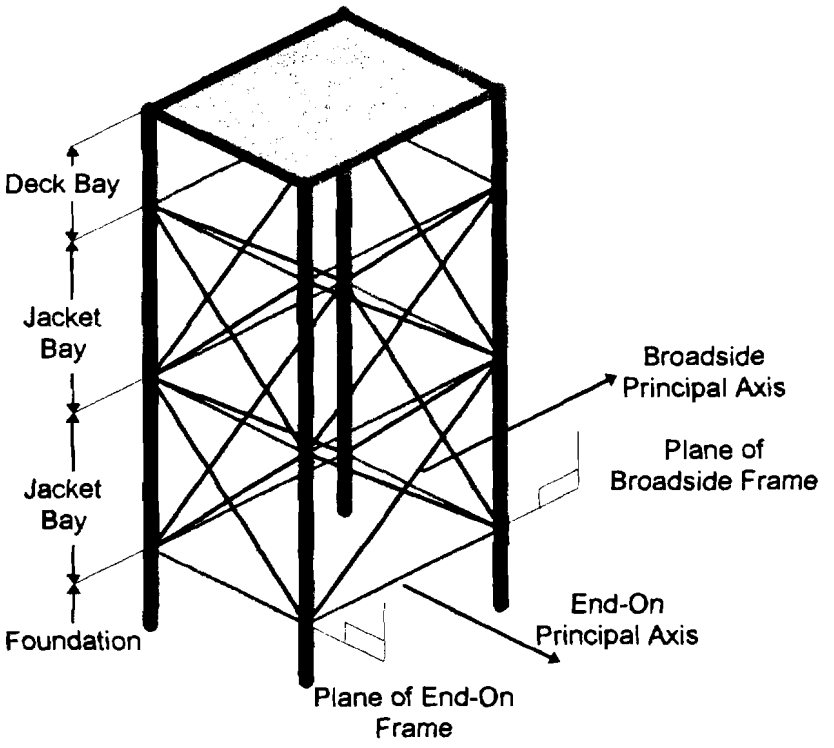

Figure 2-1: Structural Sections of a Jacket Platform

Jacket-type platforms are made up of the following components: a deck bay, jacket bays, and a foundation level. Deck and jacket bay components have a strength and a stiffness on each of the two principal horizontal axes; rotation about these axes is ignored (see Figures 2-2 and 2-3).

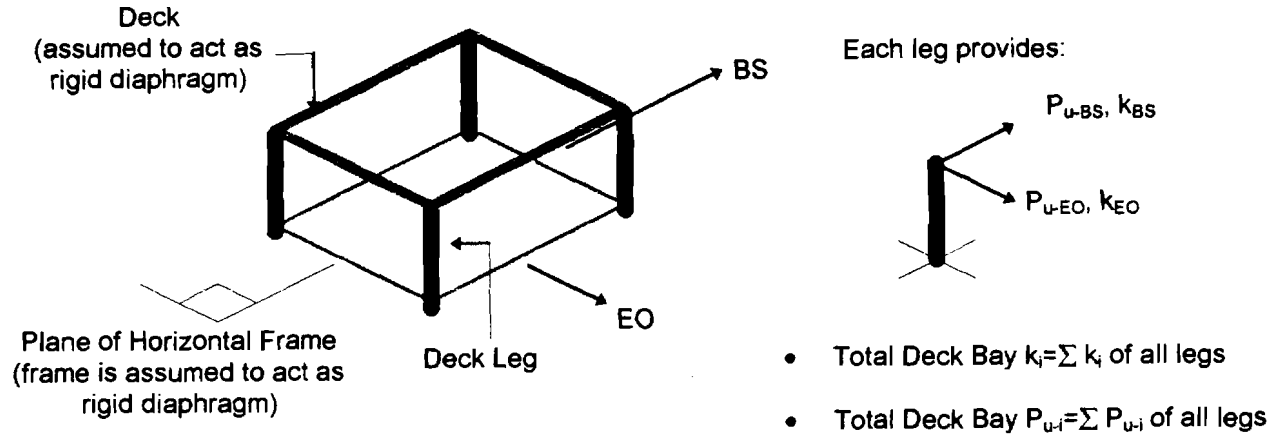

Figure 2-2: Deck Bay Component (Unbraced Deck Bay)

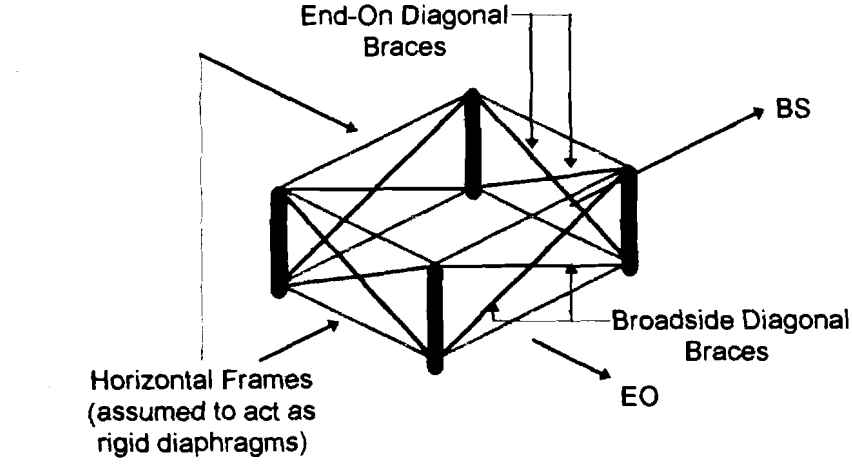

In plane of BS or EO frames:

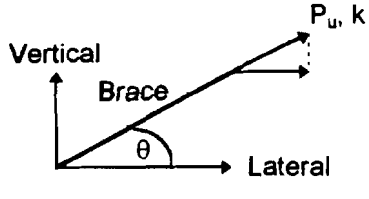

- Horizontal Component of Brace Capacity: $P_{ui\text{-}l}=P_{ui}\cdot\cos\theta$
- Horizontal Stiffness of Brace: $k_{i\text{-}l}= k_i\cdot\cos^2\theta$
- Bay k_j (j = EO or BS) = $\Sigma\, k_{i\text{-}lj}$
- Bay $P_{u\text{-}lj}$ (lower-bound) = $(P_{uMLTF\text{-}lj}/k_{MLTF\text{-}lj})\cdot\Sigma\, k_{i\text{-}lj}$
- Bay $P_{u\text{-}lj}$ (upper-bound) = $\Sigma\, P_{ui\text{-}lj}$

MLTF=Most Likely to Fail Bracing Member

Figure 2-3: Jacket Bay Component

The strengths and stiffnesses are defined by the major structural elements which make up the component: column leg elements for the deck bay (if it is unbraced), tubular brace elements for the jacket bays (and deck bay if it is braced). Bracing elements are assumed to provide strength and stiffness only along the axis of the brace; therefore, braces in the broadside frames do not provide resistance in the end-on frames, and vice-versa. The foundation level component has strength and stiffness on both principal horizontal axes, as well as strength and stiffness for rotation about these axes (see Figure 2-4). The strengths and stiffnesses of the foundation level are defined by the piles which make up the foundation and, if specified as an option, also by conductors and mudline elements such as mud mats and mudline framing via bearing and sliding resistance.

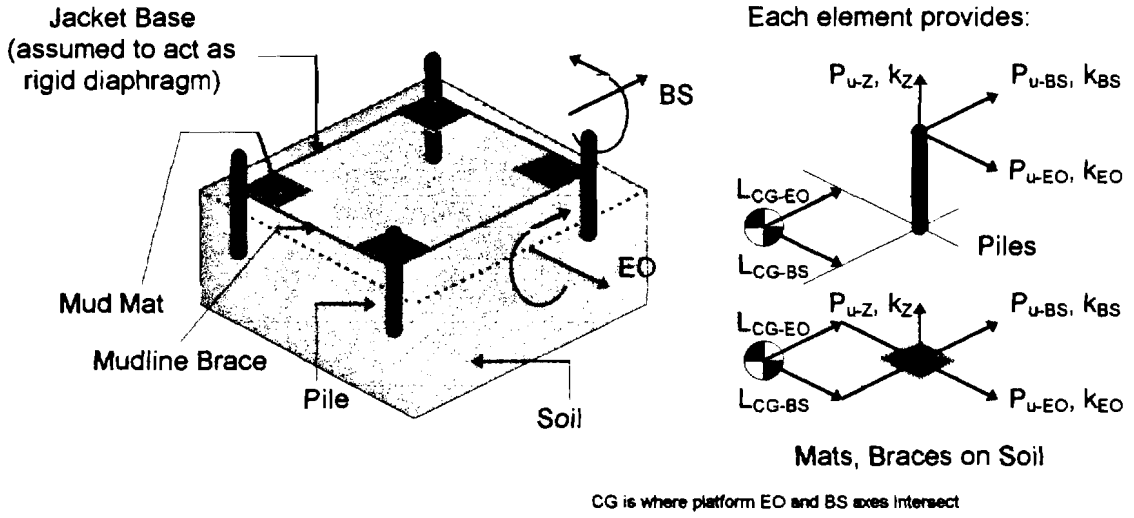

- Lateral $k_i = \Sigma k_i$ of all piles and mudline elements
- Lateral $P_{u\text{-}i} = \Sigma P_{u\text{-}i}$ of all piles and mudline elements

- Vertical $k_z = \Sigma k_z$ of all piles and mudline elements
- Vertical $P_{u\text{-}z} = \Sigma P_{u\text{-}z}$ of all piles and mudline elements

- Rotation $k_{\theta\text{-}i} = \Sigma k_z \cdot L_{i\text{-}CG}^2$ of all piles and mudline elements
- Rotation $M_{u\text{-}i} = \Sigma P_{u\text{-}z} \cdot L_{i\text{-}CG}$ of all piles and mudline elements

Figure 2-4: Foundation Strength and Stiffnesses

Tripod jackets have component strengths and stiffnesses developed for the horizontal axes shown in Figure 2-5. Torsion is not included in the formulation.

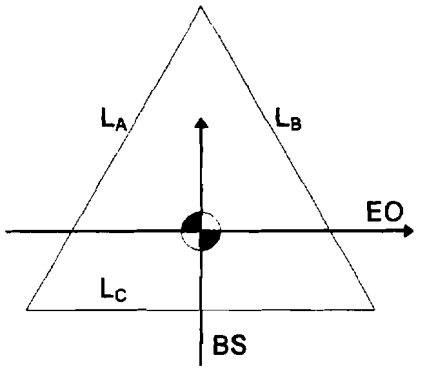

- Sides A, B must have equal lengths
- Frame A, B element strengths and stiffnesses are projected to BS axis to obtain components' BS strengths and stiffnesses
- Frame A, B element strengths and stiffnesses are projected to EO axis to obtain element contributions to EO strengths and stiffnesses together with Frame C elements

Figure 2-5: Tripod Principal Axes

Caissons are assumed to consist of the following components, as shown in Figure 2-6: a top section, which is the portion of the platform above the bracing or guying point, and a supported section, which is the guyed or braced section. The strength and stiffness of the supported section are defined by the following series system: connection of support to the caisson, the support (brace or wire), and the support foundation (pile).

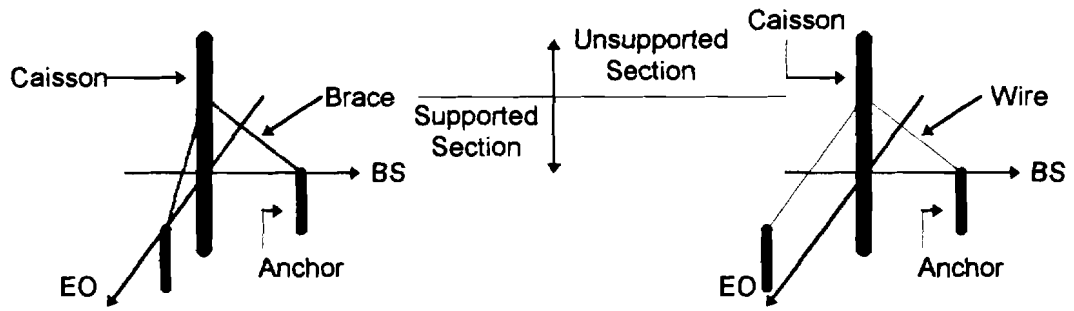

Figure 2-6: Structural Sections of Caissons

Caisson supports must be identical, i.e. the caisson must be supported by either two identical braces or three identical wires. As such, a caisson's strength and stiffness are formulated for only one axis.

In addition to structural components, a TOPCAT model includes non-structural components. These include decks, boat landings, and appurtenances in the structural bays such as conductors and other piping. The non-structural components serve as load-attractors: their projected areas serve to generate additional hydrodynamic and aerodynamic loads, and their masses will affect the vibration properties of the platform. Deck components are located at the top of the deck bay; the boat landing is located at the top of the first jacket bay, and appurtenances exist in any bay.

TOPCAT allows a user to perform the following assessments:

- A deterministic or probabilistic demand-capacity analysis of the platform for storm loading, with platform capacity defined on the two principal axes of the platform.
- A deterministic or probabilistic demand-capacity analysis of the platform for earthquake loading, with platform capacity defined on the two principal axes of the platform.
- A Miner's Rule-type fatigue analysis focused on the tubular joints to which the main diagonals are connected (or connection by which brace or wire is attached to a caisson), using stresses associated with wave action on the two principal axes of the platform.

Each of these analysis procedures is summarized in the following sections. Where necessary, the user is referred to the appendices for further detailed information.

2.2 Storm Analysis

For storm analyses, TOPCAT performs what is referred to as pure demand-capacity analysis. Instead of performing a conventional structural analysis (formulating a complete stiffness matrix for the entire platform model, applying a load vector to the model, solving for the displacements induced by the load vector, and then using the displacements to find forces induced in the platform components), TOPCAT formulates strength capacities for the different individual components, and then compares these component strength capacities with the loads each component must resist. These storm loads, calculated from wind, wave and current, are determined assuming the platform is a rigid structure, hence there is no need for use of a complete structural stiffness matrix.

Strength capacities for the different platform components are estimated by application of plastic analysis. Based on a presumed failure mode for the component, the load needed to force the component to the failure state is estimated; this load is thus taken to be the load capacity of the component. The basics of how these strengths are derived will be summarized; users desiring detailed information on the formulation of deck bay, jacket and foundation component strengths are referred to Appendix B (for leg and jacket members) and Appendix G (for foundation members).

The failure mechanisms used to find the load capacities of jacket-type platform components are:

- Simultaneous hinging of the tops and bottoms of columns in an unbraced bay with lateral load applied at the top, as in Figure 2-7.
- Buckling and yielding of diagonal braces, or yielding or collapse of tubular joints to which braces are connected, in a braced bay with lateral load applied at the top, as in Figure 2-8. Both a lower-bound and an upper-bound capacity are estimated; the lower-bound is the load needed to force the weakest member in the bay to fail, while the upper-bound is based on the post-yield and post-buckling strengths of all members in the bay.
- Simultaneous yielding of all piles in a two-hinge mechanism with lateral load applied at the pile top, or by shear failure in the supporting soil, as in Figure 2-9.
- Rotation of the foundation to the first incidence of axial yielding of a pile, by either yielding of the pile steel or by yielding of all supporting soil around the pile, as in Figure 2-10.

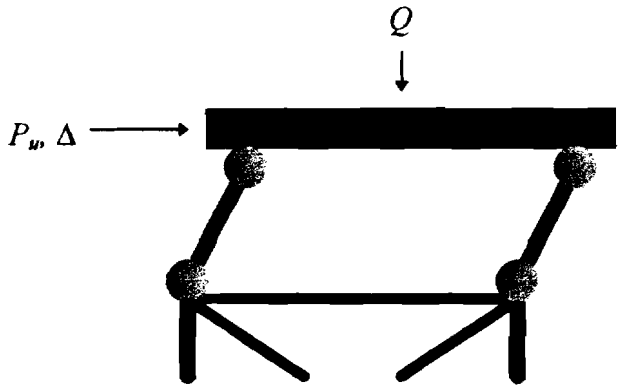

Figure 2-7: Component Mechanism for Lateral Capacity of Unbraced Bays

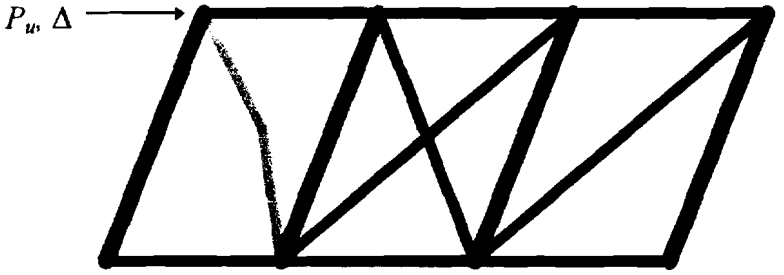

Figure 2-8: Component Mechanism for Lateral Capacities of Braced Bays

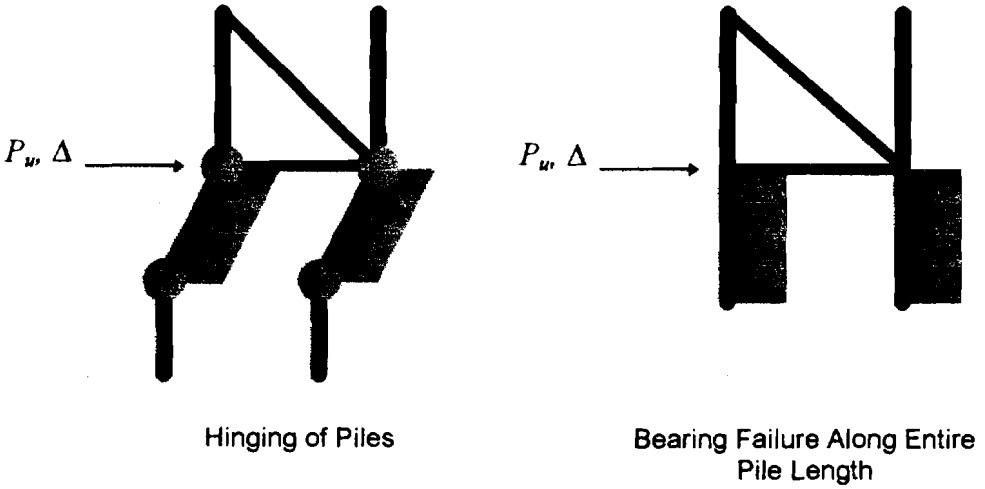

Figure 2-9: Lateral Foundation Mechanism

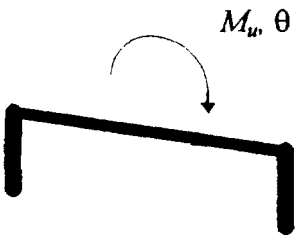

Figure 2-10: Overturning Foundation Mechanism

Limited demand-capacity interaction is accounted for in each of these strength capacity formulations. For unbraced bays, the maximum plastic hinge moment for each column (leg) is determined assuming *M-P* interaction between the moment and the axial load supported by the column. This load is the deck load, which is assumed to be shared equally by all columns in the bay. In addition, the lateral capacity of the bay is reduced by the P-Δ force associated with the deck load and the lateral deflection of the bay top reached when the assumed failure mechanism forms.

For braced bays, the buckling capacities of diagonal braces are calculated using a three-hinge buckling formulation which takes into account the presence of distributed local hydrodynamic load as calculated from wave and current action. These capacities may be formulated assuming the member has significant curvature, has dent damage, or has been grouted. In addition, the horizontal component of the axial force (from overturning) in battered legs is added to the effective lateral capacity of the bay. A reduction in effective capacity is taken for jacket bays immediately beneath an unbraced bay due to the moments which will be induced in the tops of the legs in the braced section.

For foundation lateral capacity, the maximum plastic hinge moment for each pile is determined assuming *M-P* interaction between the moment and the axial load supported by the pile. This load is the deck load, assumed shared equally by all main piles, and the pile self-weight; axial load from overturning is not included by the program for resolution of *P-M* interaction, as this load is assumed to be taken by the soil surrounding the pile. The jacket weight is assumed to be supported by mud mats and mudline elements. The horizontal component of the axial force (from overturning) in battered piles is added to the effective lateral capacity of the foundation level. The axial capacities of piles, used for establishing the platform overturning capacity, are reduced by both the pile's self-weight and the pile's share of deck load, if any, prior to determining the maximum supportable overturning moment.

Tripod capacities are developed much the same as for standard jackets, although the capacity is developed for the axes shown in Figure 2-5. Users should refer to Appendix D for further information on tripod demand and capacity formulations.

The mechanisms used to define the capacities of braced and guyed caissons are:

- Hinging of the unsupported section above the point of support, Figure 2-11:

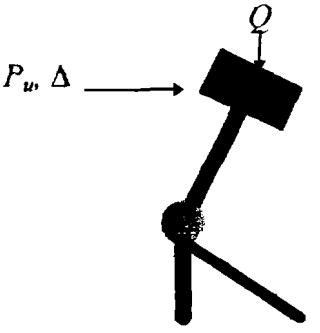

Figure 2-11: Hinging of Unsupported Section of Caisson

- Failure of the connection-support-pile series system which supports the caisson against lateral load (Figure 2-12):

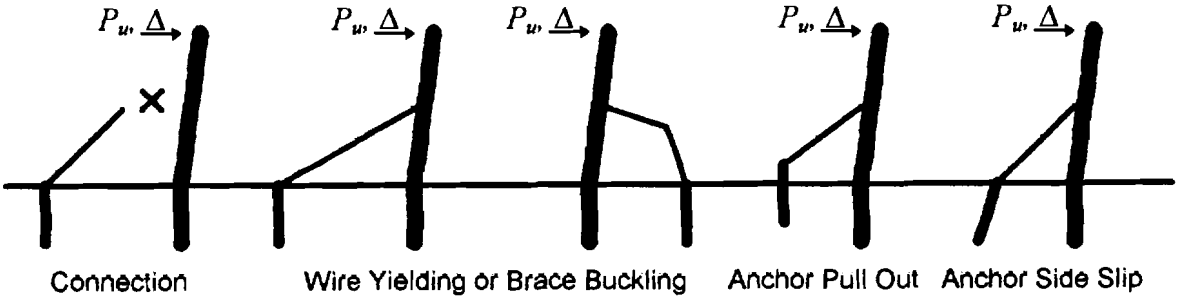

Figure 2-12: Supported Section of Caisson Mechanisms

The calculations used to determine the caisson capacities are documented in Appendix D.

Wind, wave and current loads acting on the platform are calculated based on the projected areas of structural and non-structural platform components (decks, boat landings, appurtenances), assuming all loads are proportional to the square of the fluid velocity. The user specifies drag coefficients to use for decks and tubular members. For the purpose of estimating wave loads, the structure and non-structure areas are all assumed to be located at the wave crest, where fluid velocity is at maximum and fluid acceleration is at minimum; the inertial (fluid acceleration-based) component of the wave hydrodynamic force is neglected. Wave kinematics used in the calculation of hydrodynamic loads are calculated using either Stokes fifth-order theory or Cnoidal wave theory. The program uses the chart below to determine the range of applicability of each theory:

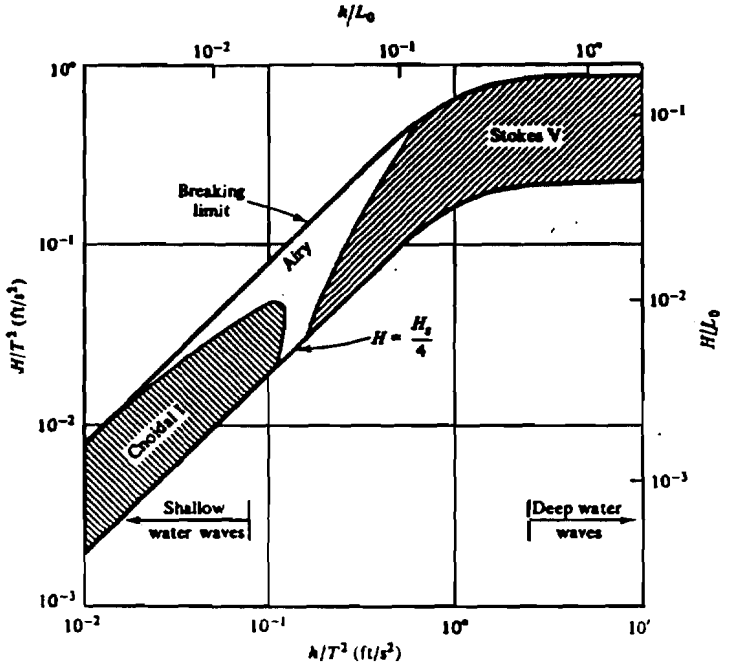

Figure 2-13: Range of Wave Kinematic Theory Applicability

The user is allowed to specify current blockage and a wave kinematics factor to modify the kinematics used to determine loads. Users desiring further information of the procedures used to calculate wave kinematics and hydrodynamic loads are referred to Appendix A.

The forces from wind, wave and current are used to determine the shear and overturning moment the platform is subject to, assuming the platform is a rigid structure. The shear at each level in the structure is compared to the strength capacity of the component at that level (Figure 2-14), while the overturning moment is compared to the moment capacity of the foundation.

The program will return to the user the following information:

- Lateral strengths of all platform components for both principal directions of loading.
- Foundation overturning capacity.
- Axial strengths of all diagonal braces in the platform, formulated including the presence of local hydrodynamic load, or supporting wires if a guyed caisson.
- Axial and lateral strengths of all piles.
- Surface loads which must be supported by all mudline elements in order to function as sources of foundation strength.
- Connection loads for conductors.
- Water kinematics for wave and current.
- Shears induced by aero- and hydrodynamic loading at each component level of the platform, for both principal axes of loading.
- Overturning moments induced by aero- and hydrodynamic loading, about both principal axes of loading.

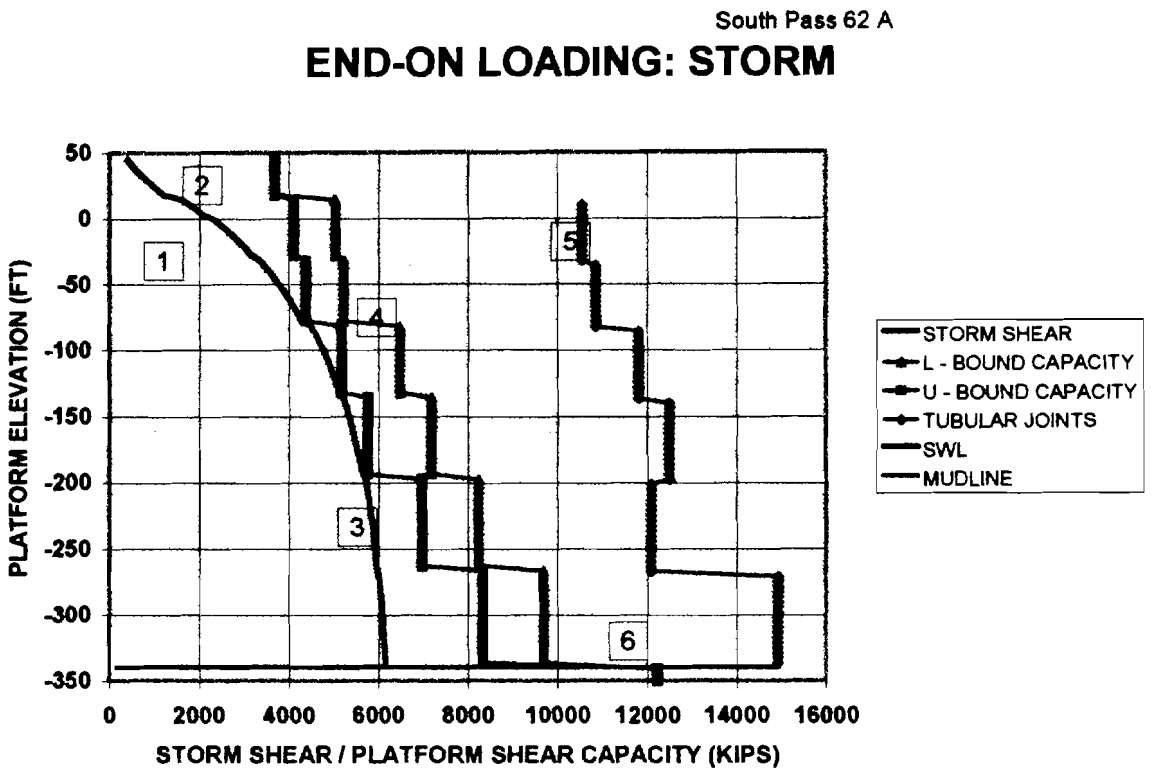

1. Profile of storm shears imposed on platform by user-specified wind, wave and current
2. Lateral load capacity of deck bay
3. Lower-bound lateral load capacity of a jacket bay
4. Upper-bound lateral load capacity of a jacket bay
5. Lateral load capacity of a jacket bay based on tubular joint connection failure as opposed to diagonal brace failure
6. Lateral load capacity of foundation

Figure 2-14: Graphical Display of Storm Shear Imposed on Platform Plotted Together with Platform Component Lateral Capacities (Deck Bay, Six Jacket Bays, and Foundation Lateral Mechanism)

In addition to the demand-capacity analysis, the user may also perform a limited reliability analysis. When the user supplies information on the uncertainties associated with the different strength components and loading mechanisms, the program will, using the component strengths and storm loads described above as the mean component strength and mean component demand, and applying mean-value first-order second-moment reliability theory with a linear limit-state function (capacity minus demand), determine the reliability of each component (Figure 2-15):

The reliability is expressed as a safety index, β. Assuming the platform capacity to be governed by the capacities of its components as a series system, the platform will fail when any one of its components fails. Therefore, the overall reliability of the platform will be equal to the lowest component reliability determined for each principal direction. Users desiring further information of the calculation procedures used to estimate platform reliability are referred to Appendix H.

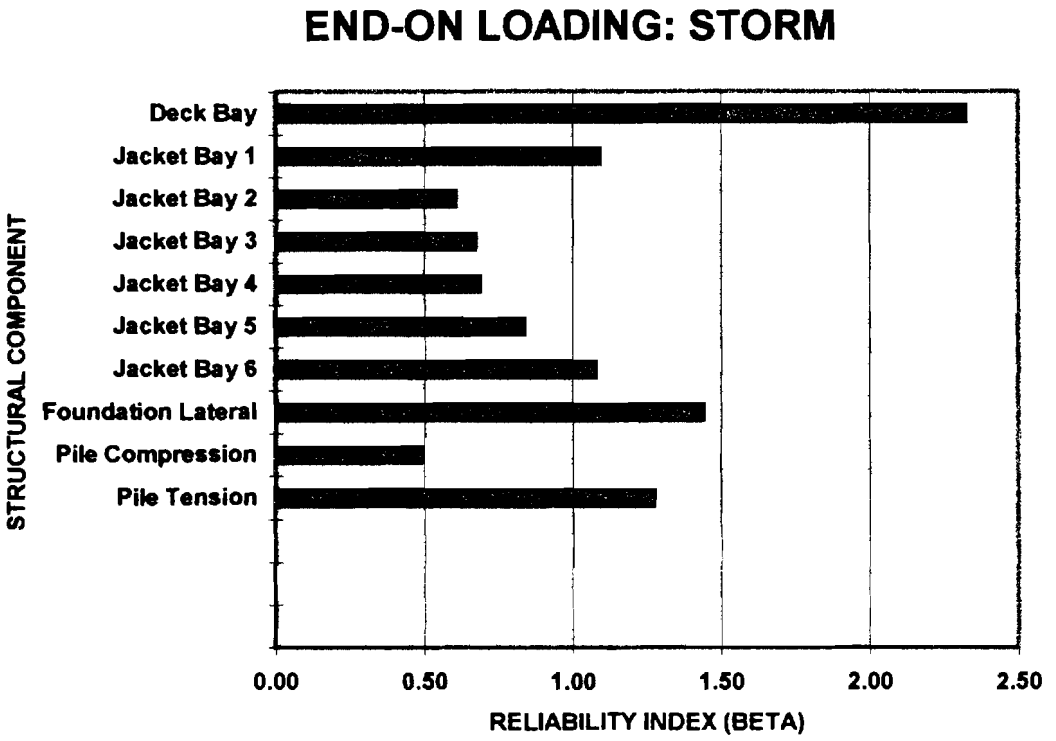

Figure 2-15: Graphical Display of Component Reliability

2.3 Earthquake Analysis

For earthquake analysis, TOPCAT preserves the demand-capacity format for assessing platform performance, but some conventional structural analysis is necessary to determine the demands on components. TOPCAT uses the modal response spectrum method to determine earthquake loads. For jacket-type platforms, the primary tower shear, tower bending, foundation shear, rotation and uplift force-displacement mechanisms are used together with structural and non-structural member masses, including added mass for submerged components (added mass coefficient is specified by the user), to develop simple response models for both principal horizontal and the vertical directions. Users desiring more detailed information should review Appendix E.

A simple approach is taken to determining the horizontal and vertical responses of a platform. For horizontal response, it is assumed the displacements are reflected by shear deformation in the deck bay and jacket bays. Modal analysis is thus applied to find the periods and mode shapes of the platform assuming a fixed base and only considering shear deformations; masses are lumped at the deck level and between the bay sections, hence giving the number of horizontal DOF as one plus the number of jacket bays. Rotational inertia of the platform horizontal cross-sections is ignored. The first horizontal period in each direction is then modified by a lengthening process to account for the additional flexibility of the foundation and tower. For vertical response, a simplified vertical model including only the pile axial and mudline element stiffnesses and the mass of the entire structure is used to estimate the first vertical period; vertical response is treated as SDOF. Figure 2-16 depicts the models for horizontal and vertical response:

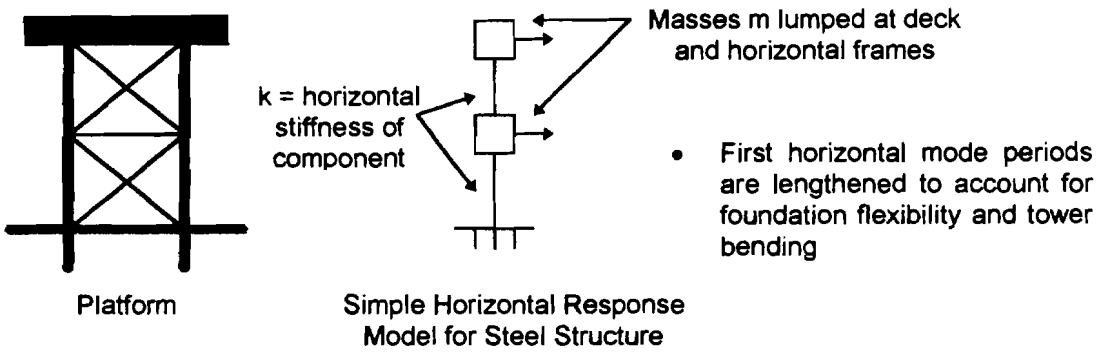

Figure 2-16A: Horizontal Response Model for Jacket-Type Platform

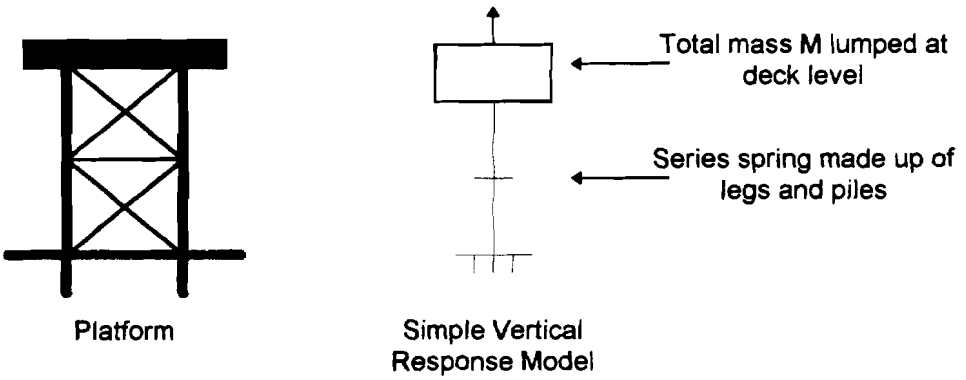

Figure 2-16B: Vertical Response Model for Jacket-Type Platform

Tripod response models are developed for the two axes shown in Figure 2-5. This formulation does not account for any torsion arising from mass or stiffness eccentricities. Further information on tripod stiffnesses is contained in Appendix D.

Caissons are idealized as 2 DOF systems for lateral response, and a simple 1 DOF system for vertical response, as shown in Figure 2-17. For lateral response, the stiffness of the top section is the bending stiffness of the unsupported section, while the supported section stiffness is a parallel spring made up of the caisson and a series spring made up of the support and its anchor pile. For vertical response, the stiffness is a series system made up of the axial stiffness of the unsupported section and a parallel system made up of the supported section of the caisson and the support-anchor series systems.

Modal responses, and hence the total demands on platform components, are calculated using the API Response Spectrum (API, 1993) shown in Figure 2-18. The program can include up to three modes on each of the two principal horizontal axes, and also includes the first vertical mode. The user may choose either ABS or SRSS modal combination rules.

Platform component capacities are determined using the same procedures described in the storm analysis section, except that local load on diagonal braces is established from the response spectrum. The local acceleration acting perpendicular to the axis of the brace is assumed to be equal to the peak spectrum value (which for the API spectrum is ZPA x 2.5).

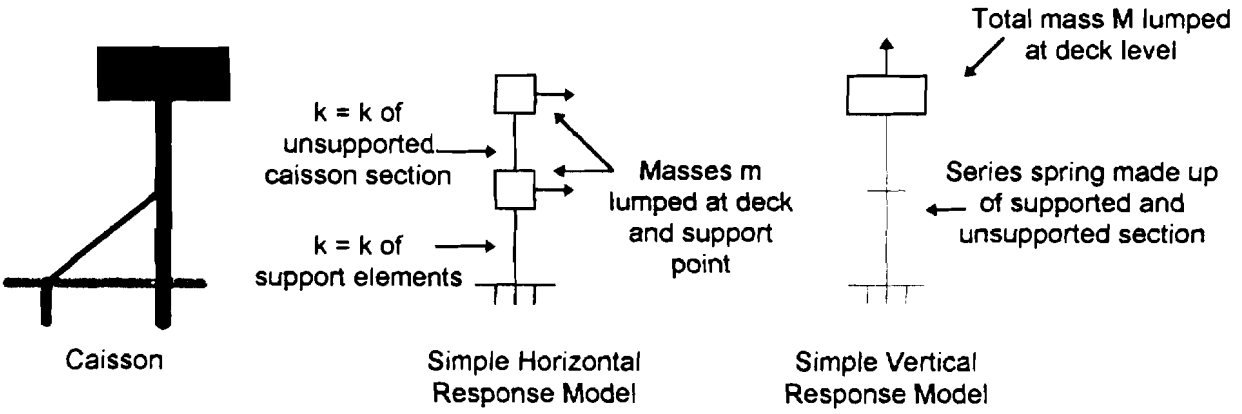

Figure 2-17: Caisson Response Models

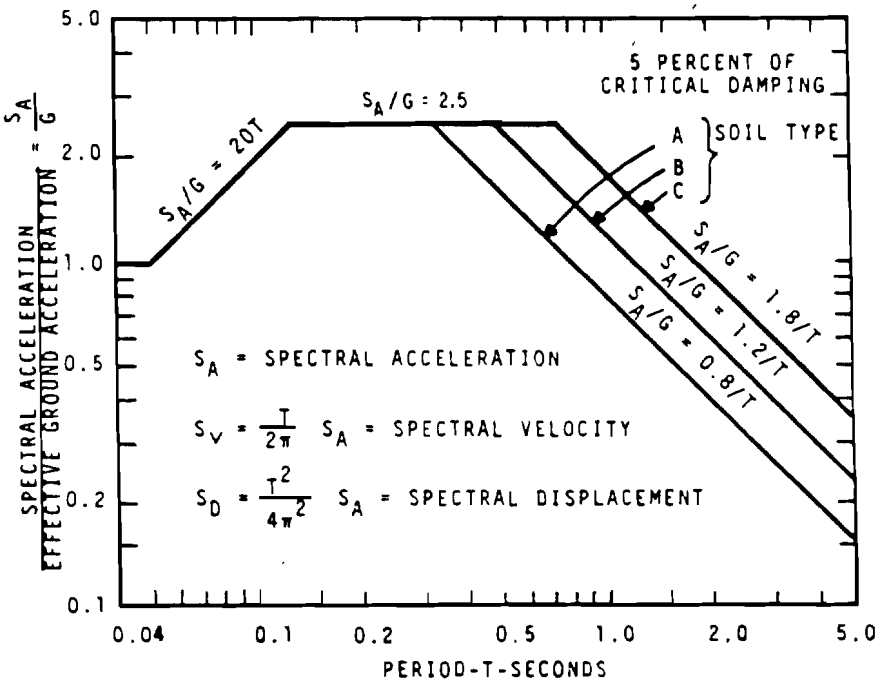

SOIL TYPE

A ROCK – CRYSTALLINE CONGLOMERATE OR SHALE-LIKE MATERIAL GENERALLY HAVING SHEAR WAVE VELOCITIES IN EXCESS OF 914 M/SEC (3000 FT/SEC)

B SHALLOW STRONG ALLUVIUM – COMPETENT SANDS, SILTS AND STIFF CLAYS WITH SHEAR STRENGTHS IN EXCESS OF ABOUT 72 kPa (1500 PSF), LIMITED TO DEPTHS OF LESS THAN ABOUT 61 M (200 FT) AND OVERLYING ROCK-LIKE MATERIALS

C DEEP STRONG ALLUVIUM – COMPETENT SANDS, SILTS AND STIFF CLAYS WITH THICKNESSES IN EXCESS OF ABOUT 61 M (200 FT) AND OVERLYING ROCK-LIKE MATERIALS

Figure 2-18: API Response Spectrum

The *P-M* interaction relationship used to estimate the plastic hinge moment in unbraced deck legs does not include the force from vertical response of the platform; this is assumed to be taken by the soil surrounding the pile. To calculate the rotation capacity of the foundation, the axial strengths of the piles are first reduced by the force from vertical response, which is assumed to be shared equally by all piles.

The program will return to the user the following information:

- Lateral strengths of all platform components for both principal directions of loading.
- Foundation overturning capacity.
- Foundation vertical capacity.
- Axial strengths of all diagonal braces in the platform, formulated including the presence of local acceleration load, or axial strengths of supporting guy-wires
- Axial and lateral strengths of all piles.
- Axial and lateral stiffnesses of all piles.
- Surface loads which must be supported by all mudline elements in order to function as sources of foundation strength.
- Connection loads for conductors.
- Mode shapes and periods for up to three modes on each of the two horizontal axes, and the first vertical period.
- Shears induced by earthquake loading at each component level of the platform, for both principal axes of loading.
- Overturning moments induced by earthquake loading, about both principal axes of loading.
- The vertical force from earthquake loading.

The user may also perform a limited reliability analysis for earthquake loading. When the user supplies information on the uncertainties associated with the different strength components and the earthquake response spectrum ordinate, the program will, using the component strengths and earthquake loads described above as the mean component strength and mean component demand, and applying mean-value first-order second-moment reliability theory with a linear limit-state function (capacity minus demand), determine the reliability of each component. The overall reliability of the platform will be equal to the lowest component reliability determined for each principal direction.

2.4 Fatigue Analysis

The TOPCAT fatigue analysis is oriented towards assessing the accumulated fatigue damage, and hence expected fatigue life, of main lateral load-carrying member connections. For jacket-type platforms, these are diagonal brace tubular joint connections, as shown in Figure 2-19. For caissons, the focus is on three locations: the connections of the main supports, in the caisson directly above the point of support attachment, and in the caisson at the mudline, as shown in Figure 2-20.

Conventional structural analysis methods are used to estimate the fatigue stresses at the joints. Using forces estimated from a storm loading pattern, the axial forces in all diagonal bracing members or guy-wires are estimated. This analysis is performed only on the principal axes of the platform, and it is assumed that members in one set of frames or support direction to not contribute resistance to the other set or direction.

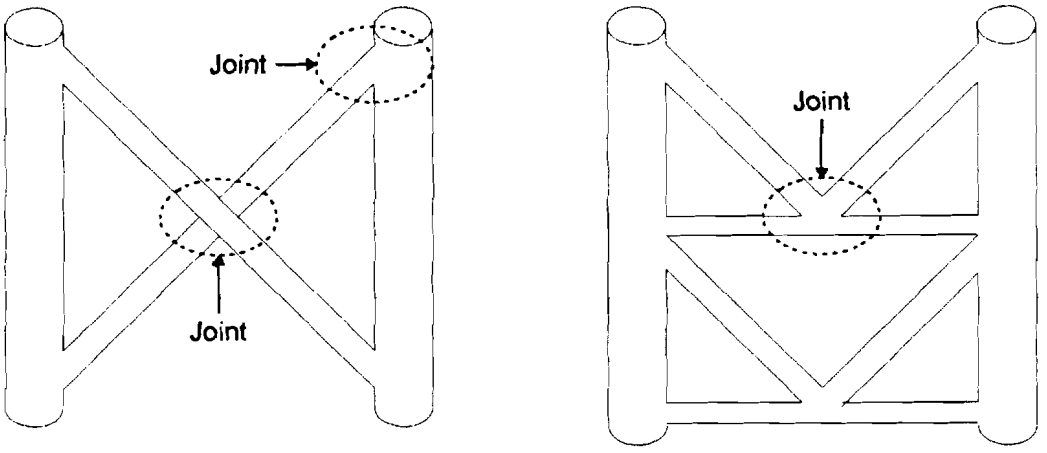

Figure 2-19: Diagonal Brace Joint Connections

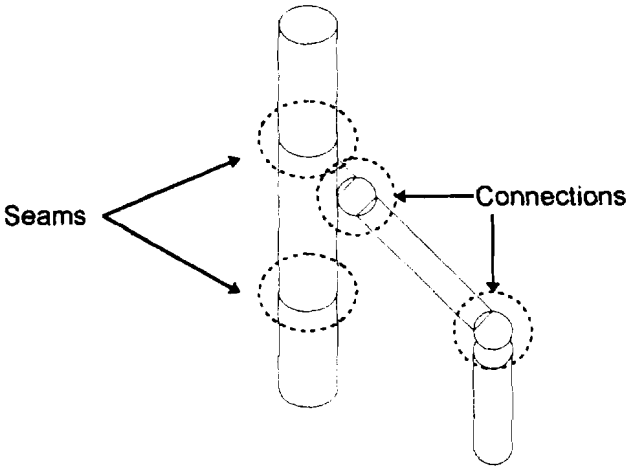

Figure 2-20: Fatigue-Critical Areas in Caissons

The axial force in each brace or wire is converted to stress, which is then modified by either user-supplied or program-calculated stress concentration factors (TOPCAT calculates stress concentration factors for tubular joints from using the relationships in Table Commentary F.1-1 from API RP2A-LRFD, 1993). In addition to the stress from axial force, bending stresses at brace ends due to bending induced by local hydrodynamic loads are calculated. These stresses are also modified by user-supplied or program calculated stress concentration factors. The stresses are based entirely on loads in-plane with the frame or section in which the member is located. No out-of-plane loads are considered.

Once the stresses have been calculated, the program applies a simplified Miner's-Rule approach to estimate the accumulated damage, and hence the fatigue life, for each diagonal brace joint or support attachment point. The approach used is described in Appendix F; stresses at joints are

assumed proportional to a "fatigue design" wave height loading pattern. The stresses are combined with information on the number of cycles of waves at the platform location, to obtain the total number of stress cycles. The wave cycle information is assumed to consist of two parts, as shown in Figure 2-21; a nominal condition spectrum and a storm condition spectrum.

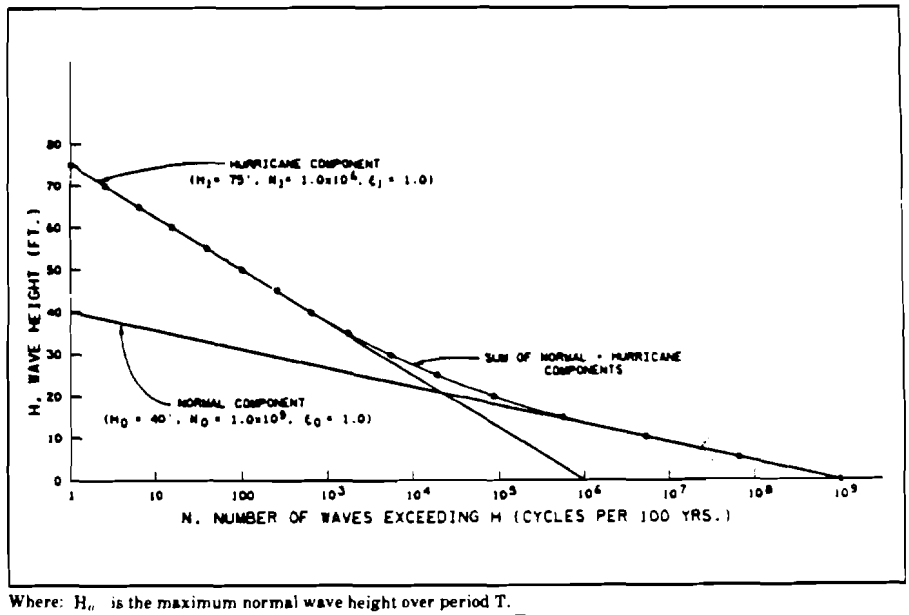

Where: H_n is the maximum normal wave height over period T.
H_t is the maximum hurricane wave height over period T.
N_n is the number of wave cycles from normal distribution over period T.
N_t is the number of wave cycles from hurricane distribution over period T.
T is the duration of the long-term wave height distribution.
ξ_n is the parameter defining the shape of the Weibull normal distribution. Value of 1.0 corresponding to the exponential distribution results in a straight line.
ξ_t is the parameter defining the shape of the Weibull hurricane distribution.

Figure 2-21: Sample Two-Part Wave Height Distribution (API RP2A-LRFD, 1993)

The user specifies both the slope and the intercept of the S-N curve used to evaluate behavior of the joint or connection, as shown in Figure 2-22.

The program returns to the user:

- The accumulated fatigue damage at each diagonal brace-joint (or support connection and caisson seams).
- The expected fatigue life of each diagonal brace-joint (or support connection and caisson seams).

NOTE: Uses must be aware that this analysis is extremely approximate, and is not intended to provide actual fatigue life values. The numbers generated are intended to provide guidance in

ranking connections relative to one another, so that a user can quickly establish which joints might be problematic relative to others.

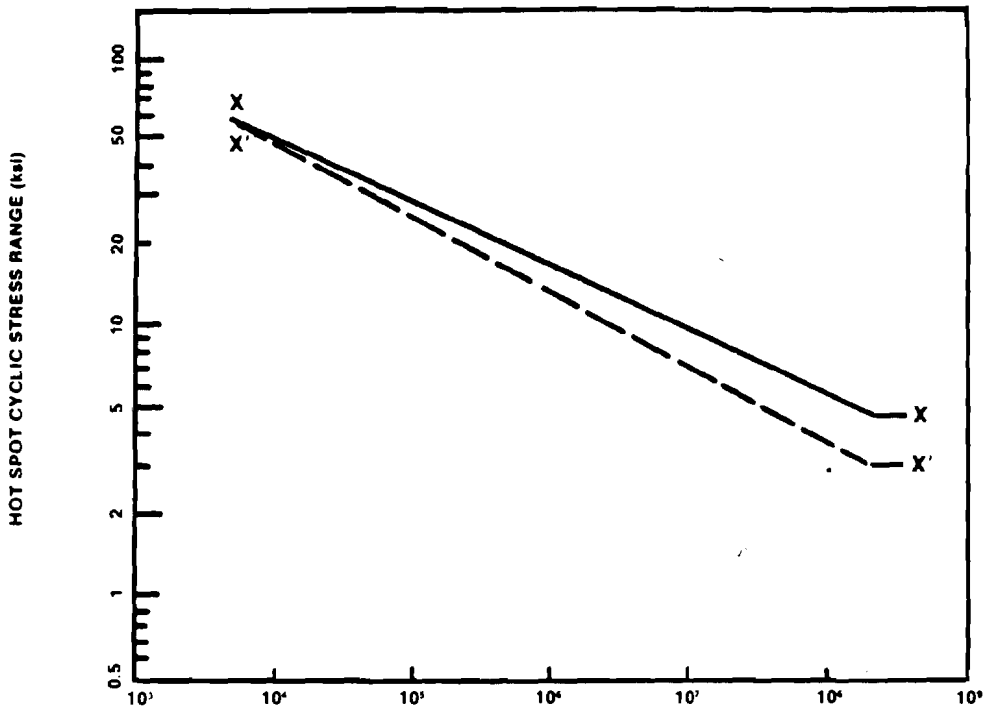

NOTE — These curves may be represented mathematically as

$$N = 2 \times 10^6 \left(\frac{\Delta\sigma}{\Delta\sigma_{ref}}\right)^{-m}$$

where N is the permissible number of cycles for applied cyclic stress range $\Delta\sigma$, with $\Delta\sigma_{ref}$ and m as listed below.

CURVE	$\Delta\sigma_{ref}$ STRESS RANGE AT 2 MILLION CYCLES	m INVERSE LOG-LOG SLOPE	ENDURANCE LIMIT AT 200 MILLION CYCLES
X	100 MPa (14.5 ksi)	4.38	35 MPa (5.07 ksi)
X'	79 MPa (11.4 ksi)	3.74	23 MPa (3.33 ksi)

Figure 2-22: Example S-N Curve

2.5 Program Limitations

Users must be aware of the key simplifying assumptions and limitations of the TOPCAT program:

- The program only assesses structural behavior on the principal axes of the platform. While loads may be declared for directions between these axes, the program will resolve the loads into principal axes components. Torsional loading is not currently considered.
- The program assumes horizontal bracing members either do not carry significant load, or are not in danger of failing from the loads they do carry, and hence are not analyzed as structural members. It is important for users to understand that some bracing configurations, such as

K-braces or single braces oriented in the same direction, will have horizontal members which are subject to loads equal to the horizontal component of the load of the diagonal braces with which they are associated, as shown in Figure 2-23. These braces may need to be checked separately by the user to ensure they are not the weakest elements in the load path.

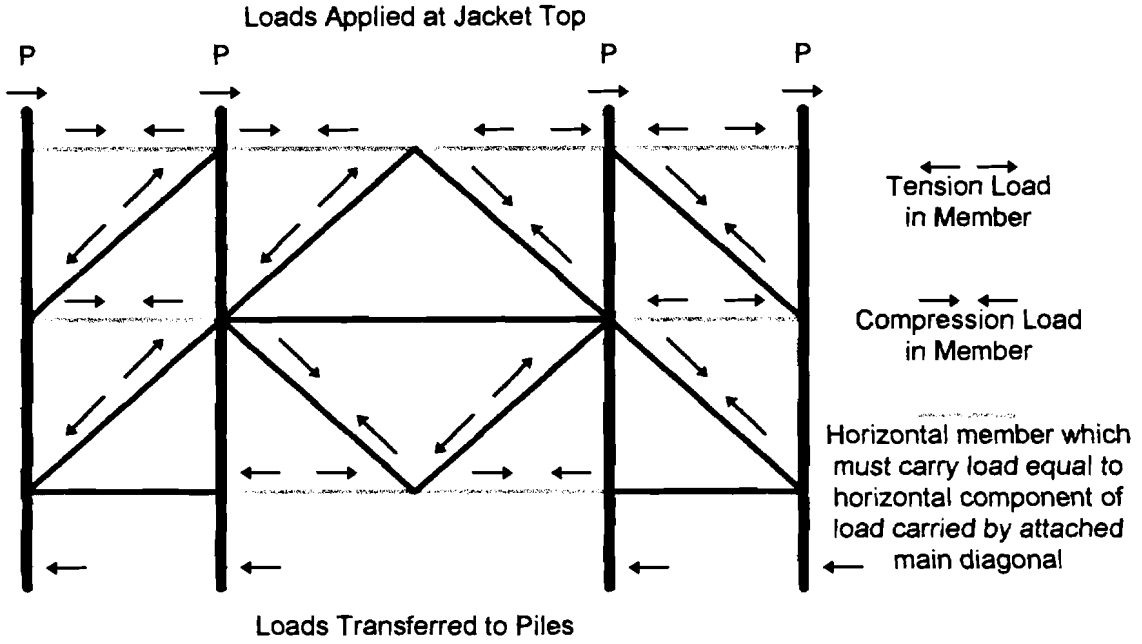

Figure 2-23: Horizontal Braces in the Load Path

- X-braces are assumed to buckle only in-plane, in the mode shown in Figure 2-24:

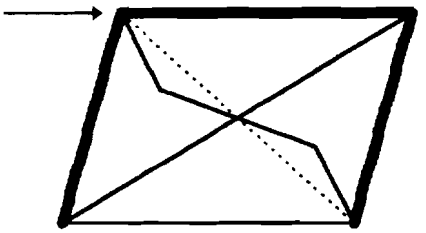

Figure 2-25: Buckling of X-braces

- All joints in the platform are modeled as simple joints as per API RP2A-LRFD (1993). The equations used to develop joint punching and pullout capacities are very conservative, and furthermore, it is known that the simple joint procedure is far too conservative for modeling joints between braces of similar sizes, such as an X-brace intersection or the connection between braces in a K-configuration and the supporting horizontal brace.
- The program assumes piles above the mudline are of uniform construction, and hence only need to be checked for axial force from overturning at the base, where moment is a maximum. This may not be true for newer platforms which are not piled through the legs, which often have very different sections connected together to form legs. The program also

assumes that jacket legs on standard platforms are not in danger of failure, as they are not considered to carry significant load.

- Foundation elements are treated as sharing load equally, irrespective of local stiffnesses. This may be inappropriate in some cases, such as when piles have dramatically different stiffnesses, or, more likely, when more flexible elements such as conductors, mud mats and mudline braces are included in the capacity formulation. Some of these more flexible elements may be unable to achieve full capacity before some of the stiffer platform elements fail completely and suffer strength loss.
- Interaction between pile lateral and axial demand-capacity behavior is not considered by the program. The program currently uses loads from gravity to determine *P-M* interaction when determining the plastic moment capacity of piles. Vertical loads from overturning and earthquake vertical response are not accounted for; it is assumed that these loads are quickly shed with depth due to friction from the surrounding soil. Deck structure weight is assumed to be carried by the main piles, while jacket weight is assumed to be supported by mudline elements. This may be an inappropriate assumption is certain instances; for example, when soil has been scoured away around the mudline elements, or when a jacket has settled over time due to creep in the soil.
- Uses must be aware that the fatigue analysis is extremely approximate, and is not intended to provide actual fatigue life values. The numbers generated are intended to provide guidance in ranking connections relative to one another, so that a user can quickly establish which joints might be problematic relative to others. Also, the program is limited in what critical locations it can evaluate.

Users should be sure they understand the implications of these limitations and analytical simplifications.

CHAPTER THREE:
USING THE PROGRAM

3.0 Introduction

The goal of this chapter is to familiarize the user with using the TOPCAT program. The user will be shown how to install and start the program, and the basic program features will be demonstrated.

Using a small platform as an example, the user will be walked through the process of building a platform analysis file for a standard jacket-type platform. This will familiarize the user with use of the TOPCAT input interface. Once the user has finished building the example analysis file, the user will be walked through the different analyses which TOPCAT can perform. This latter part will include getting the user familiar with using the TOPCAT output interface. Paragraphs headed by the word *TUTORIAL* denote special information relevant to completing the tutorial exercise contained in this chapter.

3.1 Program Installation and Startup

The TOPCAT program has been developed to work in the Microsoft Excel v7.0 environment. The program uses Excel spreadsheets to store platform analysis file data, to hold values for graphing results, and to make output tables. Excel charts are utilized to present graphical output. TOPCAT is menu-driven, and input is handled via a series of dialog boxes which are called up by the input menu.

Installing TOPCAT:

The TOPCAT program consists of one Microsoft Excel v7.0 workbook, TOPCAT.xls. This file may be found on the software distribution diskette issued with this manual. Make a suitable directory on the host machine, and copy this file to the directory.

To start TOPCAT:

Follow these steps:

1. Open Microsoft Excel v7.0.
2. Close the blank workbook. If this is not done, TOPCAT may not function properly.
3. Choose OPEN from the FILE menu; locate and select TOPCAT.xls and press OPEN.

This starts the process of opening the TOPCAT workbook program. The TOPCAT background screen will appear and the usual Excel menu will be replaced by the TOPCAT menu, as shown in Figure 3-1. The program is now ready for use.

TUTORIAL: The user should follow the above steps, installing the program and then starting it.

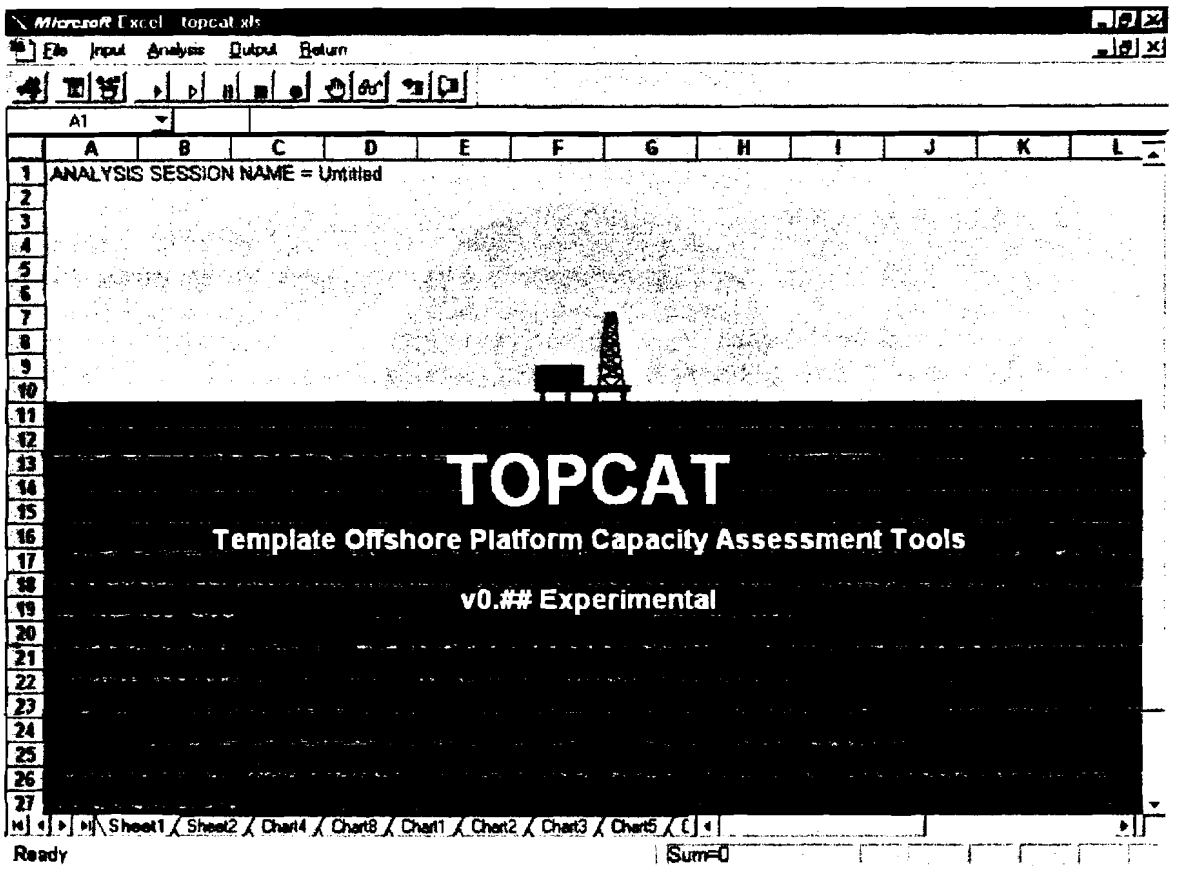

Figure 3-1: TOPCAT Program Environment in Excel

3.2 TOPCAT Operating Environment and Menu Structure

The TOPCAT program has five main menu items:

- The FILE menu. The items in this menu control the opening of existing platform analysis files, the saving of platform analysis files, the closing (without saving) of platform analysis files, and the creation of new (blank) platform analysis files. This menu also allows the user to print output, as well as exit the TOPCAT program and return to Excel. These menu items are shown in Figure 3-2; their use is described in Section 3.3.
- The INPUT menu. This menu controls the input preprocessor functions of TOPCAT. Using this menu, a user can build a platform analysis file. The user also uses this menu to set one or more analysis options which will control how certain analysis tasks are performed. The menu has three sub-menus: ENVIRONMENT, GLOBAL PARAMETERS, and LOCAL PARAMETERS. The INPUT menu and the sub-menu items can be seen in Figures 3-3, 3-4 and 3-5. Use of the INPUT menu to construct a platform analysis file is described in Sections 3.4, 3.5 and 3.6.

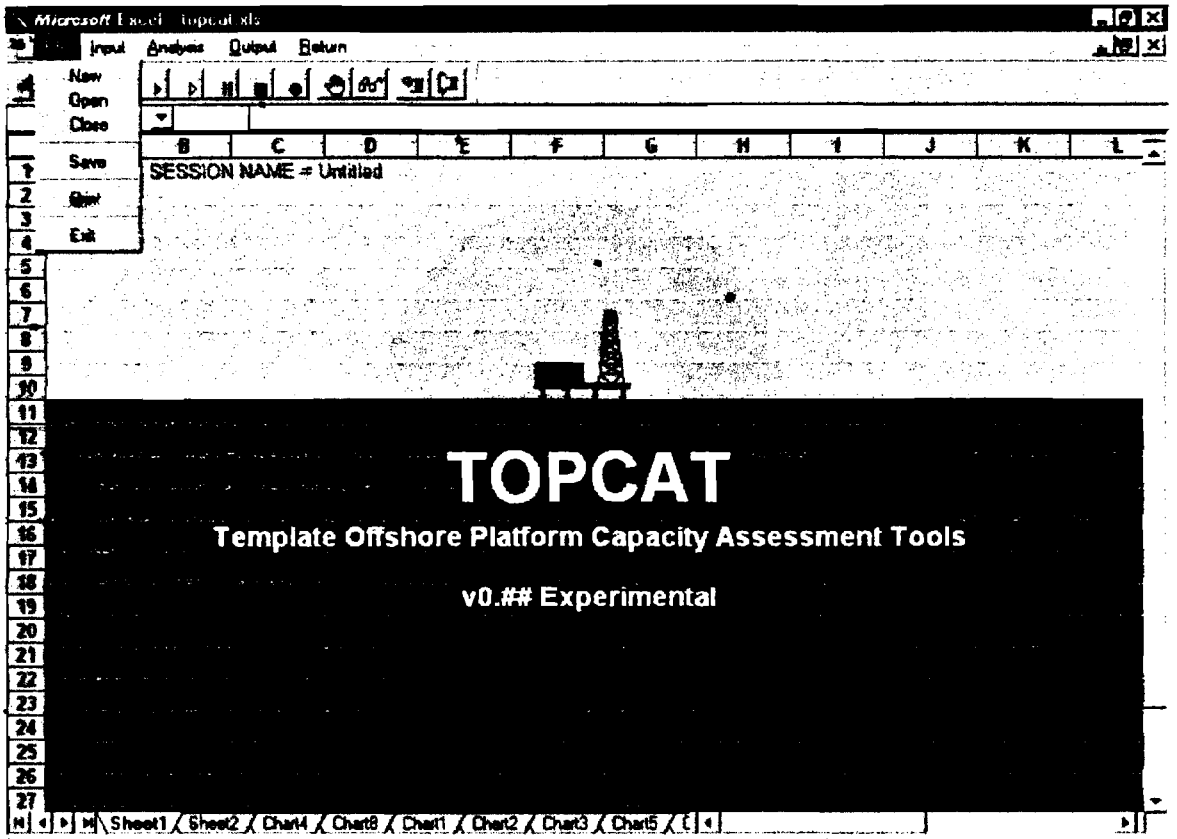

Figure 3-2: TOPCAT FILE Menu

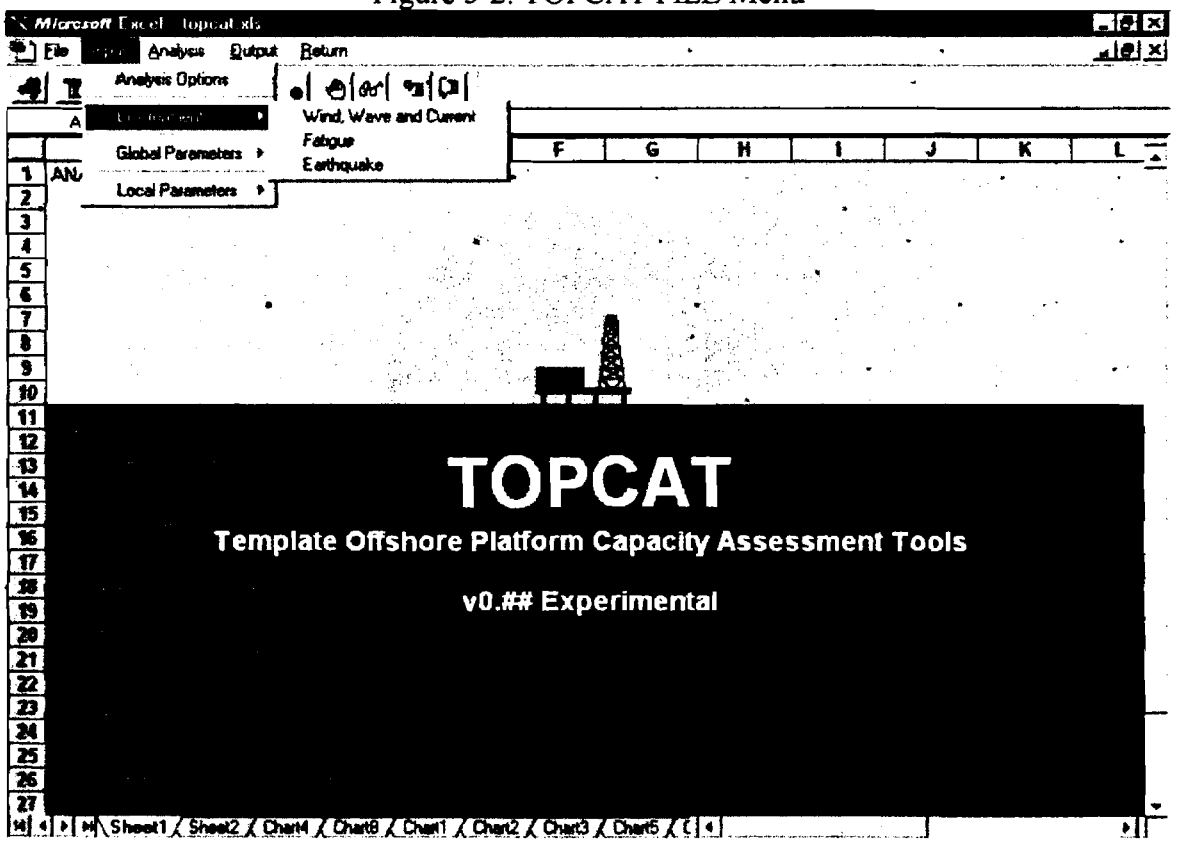

Figure 3-3: TOPCAT INPUT Menu, with ENVIRONMENT Sub-menu

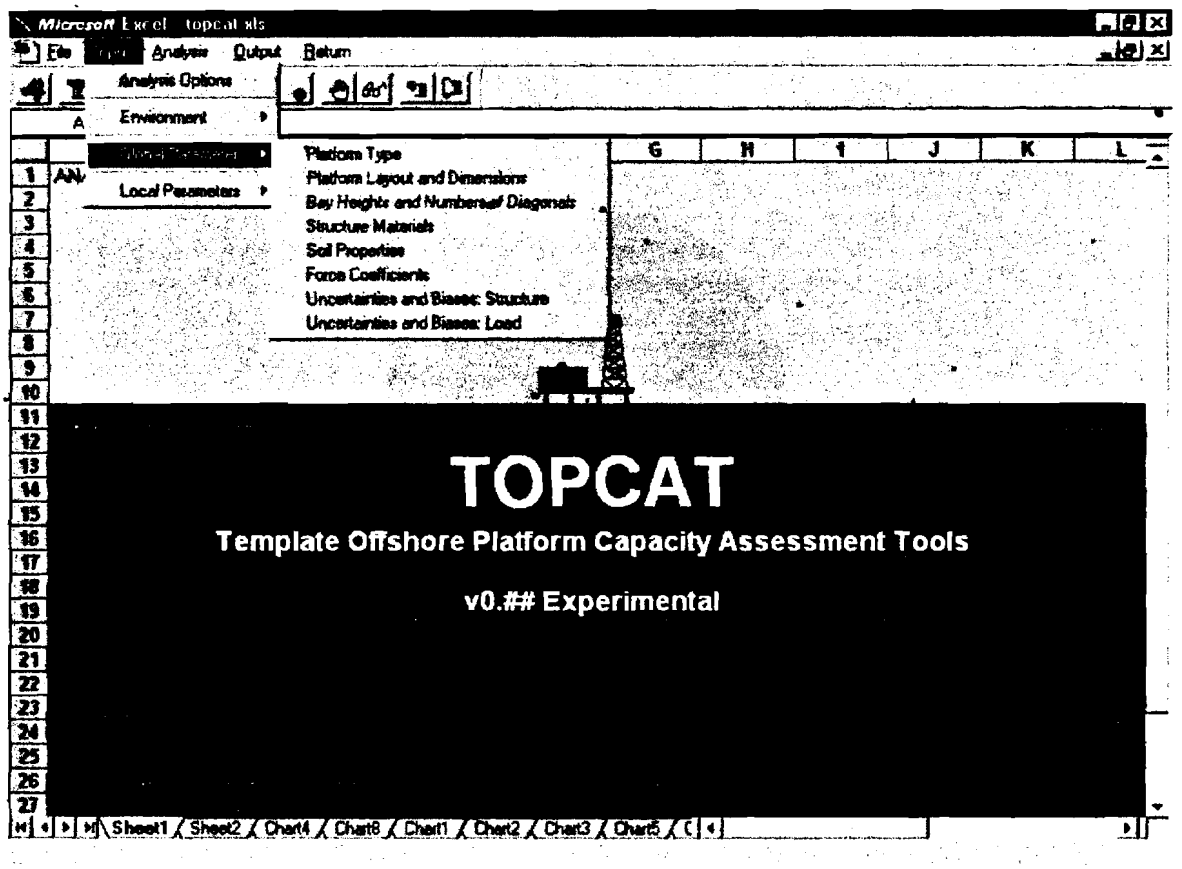

Figure 3-4: TOPCAT INPUT Menu, with GLOBAL PARAMETERS Sub-menu

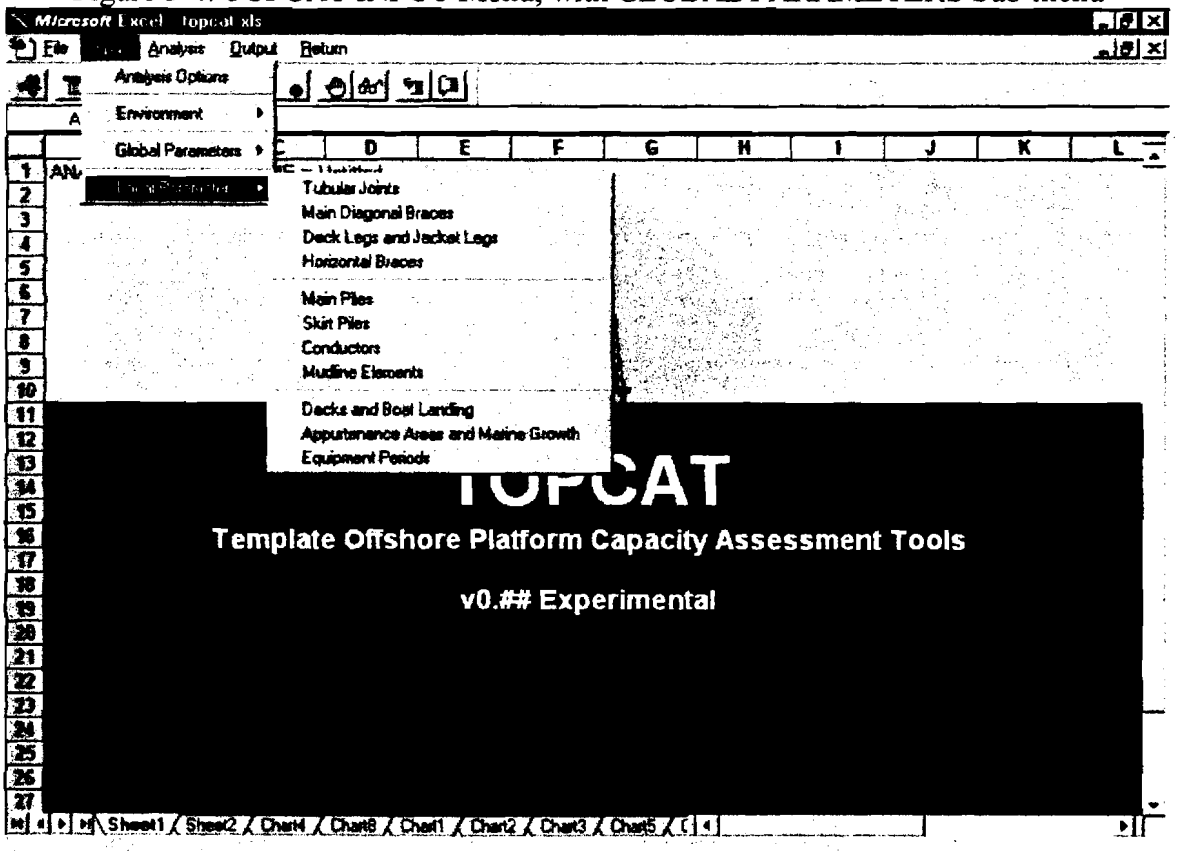

Figure 3-5: TOPCAT INPUT Menu, with LOCAL PARAMETERS Sub-menu

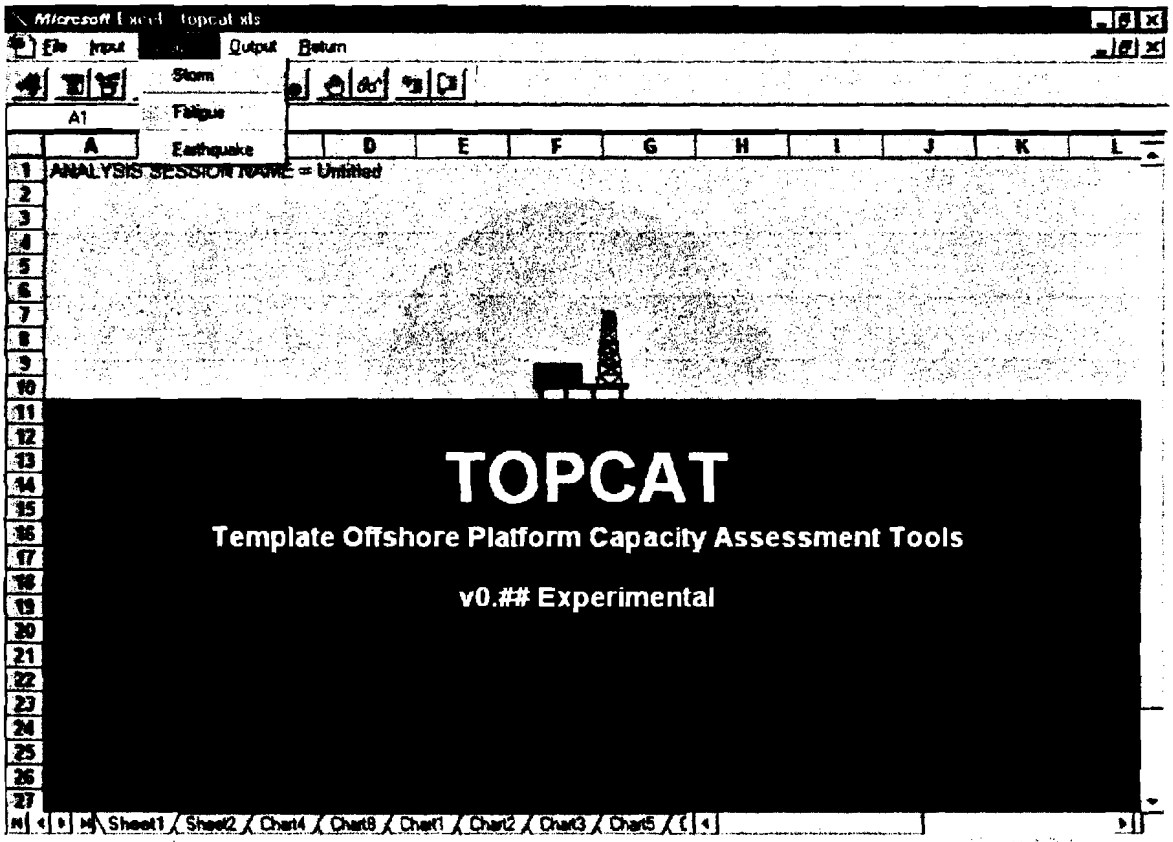

Figure 3-6: TOPCAT ANALYSIS Menu

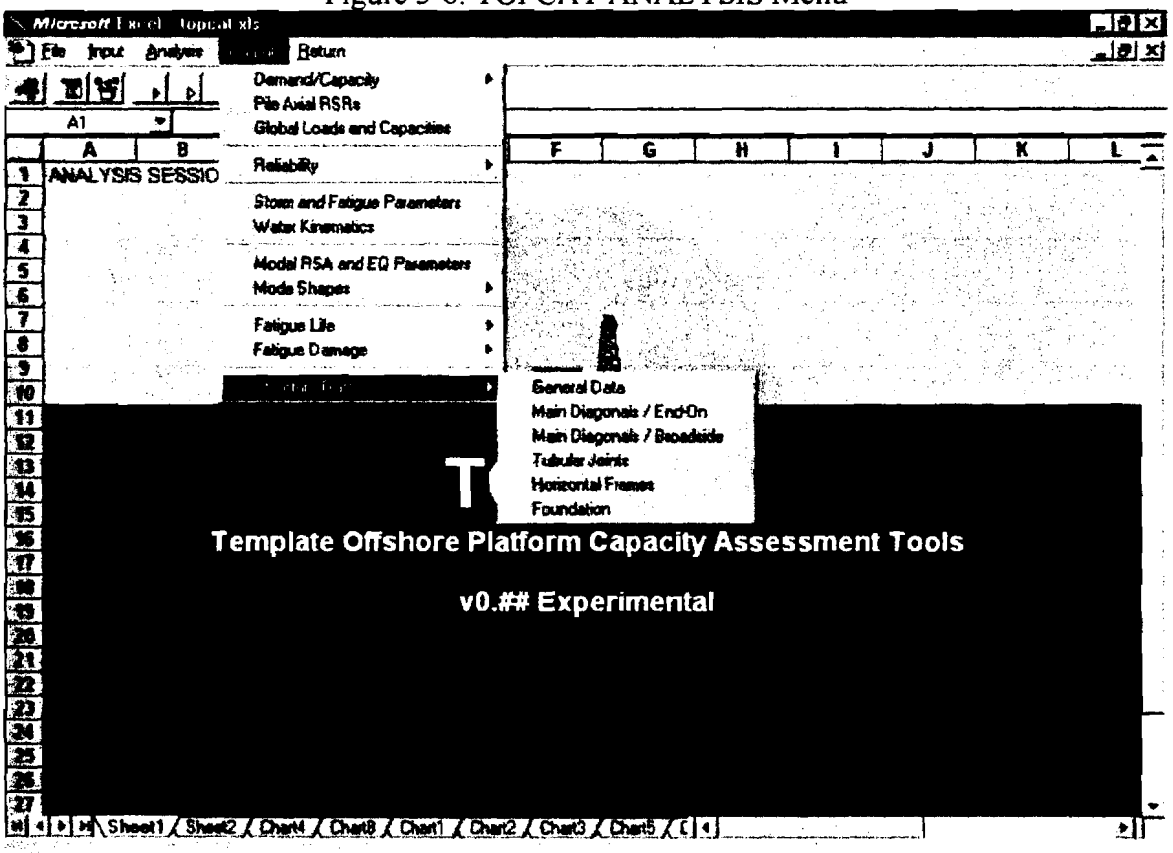

Figure 3-7: TOPCAT OUTPUT Menu, with STRUCTURE Sub-menu

- The ANALYSIS menu. This menu controls the start of the three program analysis options. The user simply selects the desired option, and the program will perform the necessary calculations. This menu may be seen in Figure 3-6. Use of the ANALYSIS menu, and the OUTPUT menu, is described in Sections 3.7, 3.8 and 3.9.
- The OUTPUT menu. This menu acts as a post-processor for TOPCAT. With the items on this menu, a user can view the various graphs and tables which are produced when TOPCAT performs an analysis. The menu contains one sub-menu, STRUCTURE. The OUTPUT menu may be seen in Figure 3-7. Use of the OUTPUT menu, and the ANALYSIS menu, is described in Sections 3.7, 3.8 and 3.9.
- The RETURN menu. This menu is simply a switch which returns the user to the TOPCAT input environment, after examining graphs and tables. It is recommended, but not required, that users always use this menu item to return to the TOPCAT input environment after reviewing output but before making any changes in an analysis file.

3.3 Using the FILE Menu

When a user enters data in TOPCAT, the program creates a new Excel workbook consisting of a single sheet, and then stores the data in the cells of this sheet. This new workbook thus becomes the platform analysis file for whatever platform is being modeled. A user may save this file at any time, and previously-saved files may be opened again. One platform analysis file holds all data on the platform structure and on the three load cases (storm, earthquake and fatigue).

The FILE menu is used to create new (blank) input files, open and close existing input files, save input files, as well as control the printing of output and exiting the program. Each of the menu items is described below:

New

This item closes without saving any open input file, and then creates a new blank input file. This menu item is used to dump a currently open input file from memory and start a new one.

Open

When this item is selected, the user may open previously-saved input files. If this item is selected while an input file is already open in TOPCAT, the file currently open will be closed without saving, and the new file will be opened in its place.

Close

When CLOSE is selected from the FILE menu, the current analysis file is closed, giving the user an opportunity to save any changes, and a new blank file is opened in its place.

Save

This item allows a user to save the current open input file. The program asks for a file name, and allows the user to specify the directory where the file will be saved. The input file is kept open in TOPCAT.

TUTORIAL: In the course of the tutorial steps in this chapter, the user will be asked to assemble an input file. At any time during the tutorial session, the user may save the partially-completed input file, and then exit the program. The user may return to the tutorial exercise by starting TOPCAT, and then opening the previously-saved example input file.

Print

This item activates the printing options dialog box, as shown below. The items on the dialog box are the tables and graphs which can be viewed with the OUTPUT menu. The user simply checks which tables and graphs are desired for printing, and then clicks OK. The selected graphs and tables will be printed.

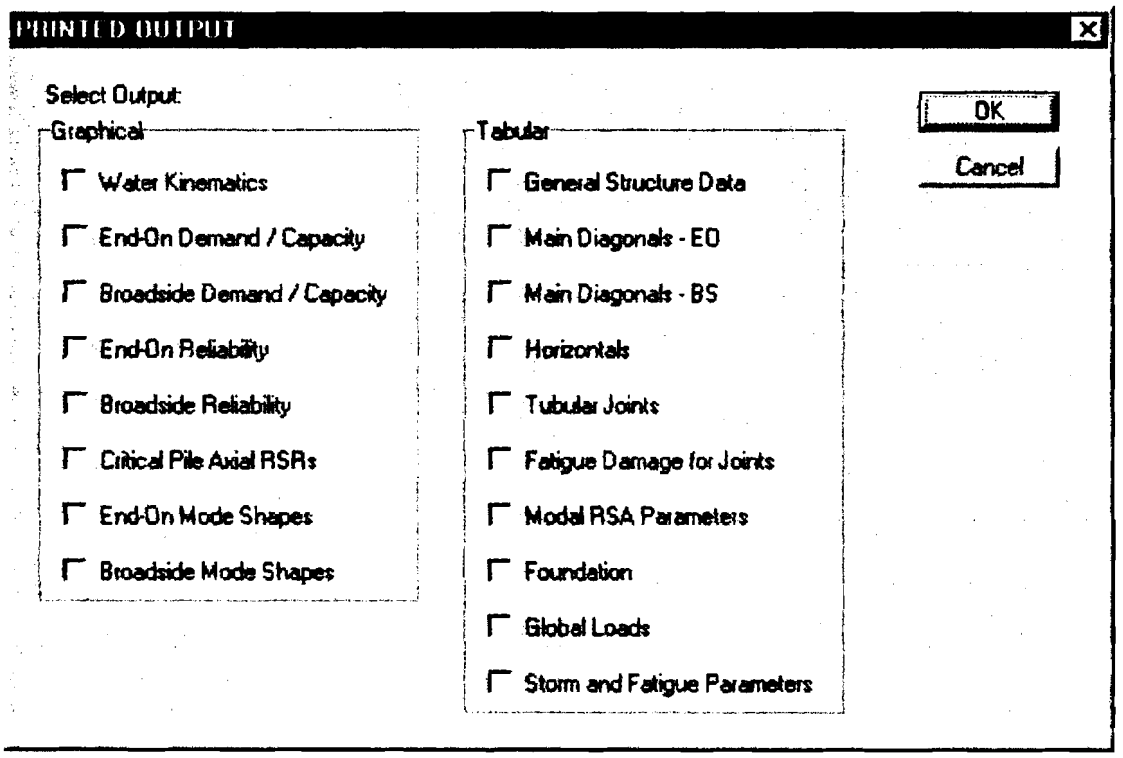

Figure 3-8: Printed Output Selection

Exit

When this item is selected, the TOPCAT program will close any open input file, and then close the TOPCAT workbook. The user will be returned to the Microsoft Excel environment. The user is NOT given the option to save changes to the input file when EXIT is selected, so users should be sure to save their work using SAVE prior to exiting TOPCAT.

3.4 Starting an Input File

To analyze a platform using TOPCAT, the user must build an input file. This file will contain the following information:

- Platform type and global dimensions.
- Location and sizes of main structural members: legs, diagonal braces (or wires, for caissons), joint connections for diagonal braces, and piles.
- Location, sizes and masses of non-structural members: decks, appurtenances, and horizontal braces in the platform, which are not modeled as structural members.
- Location and sizes of optional structural members, such as mud mats and conductors.
- The soil profile beneath the platform.
- Analysis parameters such as material strengths, buckling strength and post-buckling strength factors for diagonal braces, and load and strength biases and uncertainties.
- Load coefficients used to estimate aerodynamic, hydrodynamic and inertia (earthquake) loads.
- Storm, earthquake and fatigue parameters for the different types of analyses.

This information is declared in three stages:

1. Defining global characteristics of the platform, i.e. type, dimensions, arrangement of braces, piles, and non-structural elements, soil characteristics below the platform, and various analysis parameters such as biases and force coefficients.
2. Defining the local characteristics of platform structural and non-structural elements, i.e. diagonal brace diameters, thicknesses, steel yield strengths, joint connections, deck dimensions and weights, etc.
3. Specifying the storm, earthquake and fatigue parameters for analysis cases; i.e. wave height, wave period, current velocity, wind speed, earthquake response spectrum ZPA, fatigue stress nominal wave height and other load-associated variables.

Sections 3.5, 3.6 and 3.7 of this chapter guide the user through the process of completing these tasks when developing input for a four-, six-, eight- or twelve-leg jacket. Use of the INPUT menu items is explained, and their application is demonstrated through reference to a tutorial exercise involving the input and analysis of a small four-leg platform. Additional modeling examples, namely a tripod, a braced caisson and a guyed caisson, are contained in Chapter Four. Users desiring to build input files for tripods and caissons should review this chapter first, and then proceed to the examples in Chapter Four.

3.5 Defining Global Parameters

A user starts building an input file by defining what are termed "global parameters":

- The platform type: three-, four-, six-, eight-, twelve-leg jacket, or guyed or braced caisson.
- The overall dimensions of the platform structure: base dimensions, number of jacket bays, bay heights.
- General structural and non-structural information: the number of diagonal braces in both the end-on and broadside frames, the number of horizontal braces in the bottom of each bay, the number of decks.
- Structure materials: default steel yield strength, modulus of elasticity, default brace buckling length factor, brace post-buckling strength.
- Soil properties: the number of soil layers, and the makeup and strength of those layers.

- Force coefficients: load multipliers on the current load pattern, hydrodynamic drag coefficients for tubular members and decks, added mass coefficients for tubular members, water kinematics modifiers for current blockage and directional spreading.
- Biases and uncertainties: user-specified modifications (biases) and, if reliability results are desired, uncertainties, for brace, joint, pile strengths, and to storm and earthquake load magnitudes.

All of this information is entered using the GLOBAL PARAMETERS sub-menu items on the INPUT menu. The following GLOBAL PARAMETERS sub-menu items must be accessed first, and in the listed order, prior to accessing any others when creating an input file:

1. Platform Type
2. Platform Layout and Dimensions
3. Bay Heights and Numbers of Braces

The remaining GLOBAL PARAMETERS sub-menu items may be accessed in any order, including after the declaration of local parameters (which are described in Section 3.6):

- Structure Materials
- Soil Properties
- Force Coefficients
- Biases and Uncertainties: Structure
- Biases and Uncertainties: Load

The dialog boxes associated with all of these menu items are shown below, along with examples of their use.

TUTORIAL: The user will begin to define an input file for the small platform shown in Figure 3-9.

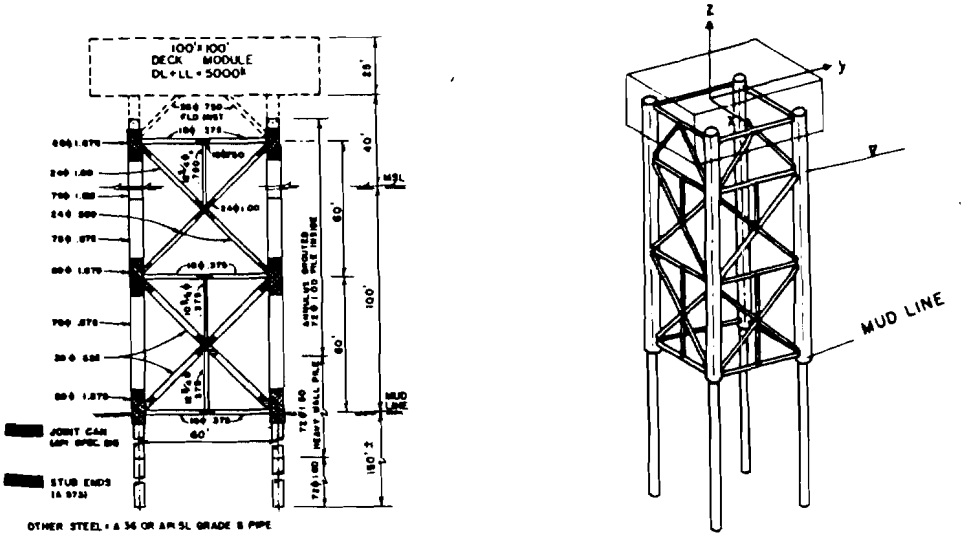

Figure 3-9: Example Platform

This platform, known as the Southern California Example Structure, is a design for a platform for use off Southern California in the San Pedro/Santa Barbara Channel area. The soil beneath the platform is stiff clay, with a surface-level shear strength of 2.5 ksf, and a submerged specific weight of 50 lbs/ft^3. The shear strength increases with depth at a rate of 0.01 ksf/ft. The platform is made entirely of 36 ksi steel. Braces are rigidly connected to the legs, given an effective length factor of 0.5.

GLOBAL PARAMETERS/Platform Type:

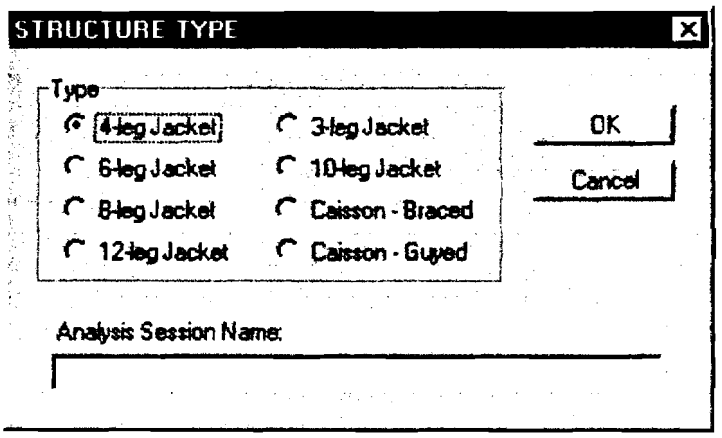

Figure 3-10: Platform Type Declaration

Users can specify the platform type, and provide a name for the analysis session. The analysis session name is not the input file name; it is an identifier printed on all output sheets. NOTE: the "10-Leg Jacket" option is not currently available; it defaults to "8-Leg Jacket" if selected. Plan views of the pile layouts associated with the different standard jacket types are in Figure 3-11, along with the principal axis definitions used by the platform.

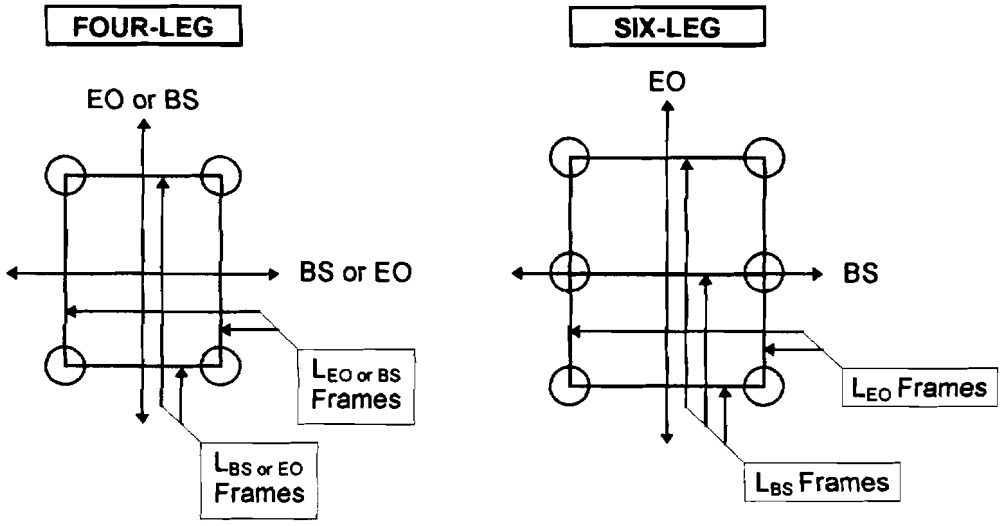

Figure 3-11A: Plan View of Pile Layouts Assumed by TOPCAT for Standard Jackets

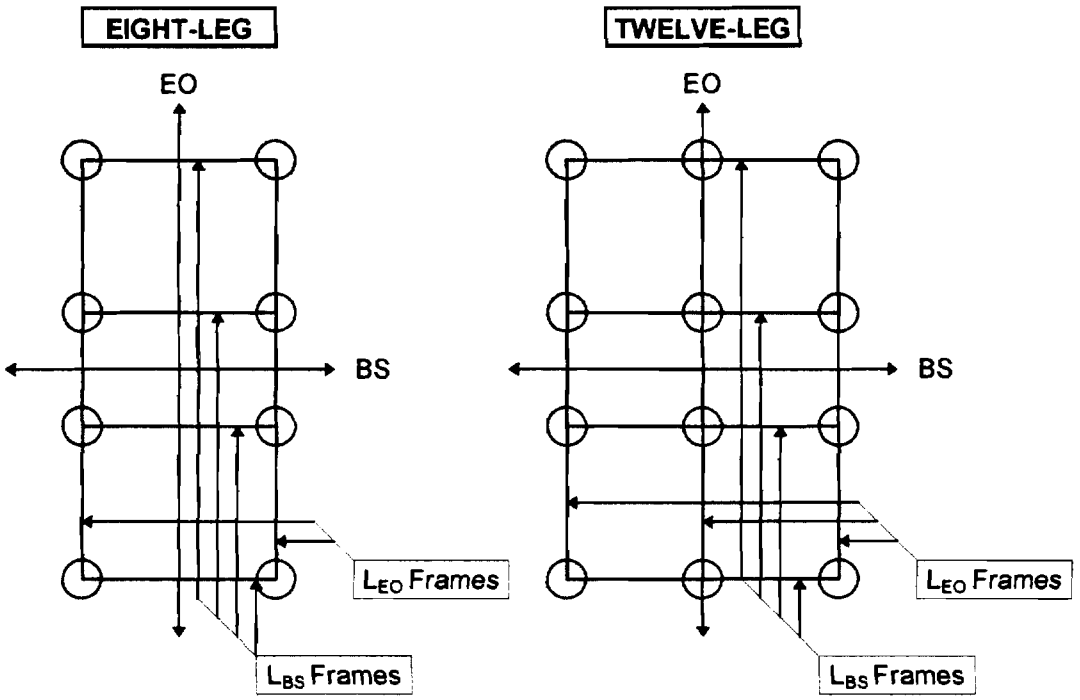

Figure 3-11B: Plan View of Pile Layouts Assumed by TOPCAT for Standard Jackets

NOTE: all dialog boxes in the program will typically have both an OK and a Cancel button. If OK is selected, the input supplied to the dialog box will be entered into the current input file. If Cancel is selected, the input supplied will not be entered into the current input file.

TUTORIAL: enter data on the example platform in Figure 3-9. Select "4-Leg Jacket," and entitle the analysis session as "TUTORIAL 4-LEG." Click OK when done.

GLOBAL PARAMETERS/Platform Layout and Dimensions:

If the platform is a four-, six-, eight-, or twelve-leg jacket, the dialog box in Figure 3-12 is used by the program.

The user would enter the following information, referring to Figure 3-13 for guidance in term definitions:

- Water Depth (ft): the distance from the mudline to the non-storm condition water level. Do not include storm surge or storm tide.
- Sinkage Below Mudline (ft): the distance from the mudline to the bottom horizontal frame of the jacket. If the jacket is resting on the mudline, this distance is zero.
- Number of Decks: the number of decks the platform has. TOPCAT allows a user to specify up to five decks.

- Number of Jacket Bays: the number of bays or stories in the jacket structure, and does not include the deck bay (the bay or section immediately below the decks). The number of jacket bays must be between 1 and 30.
- 1 Vertical Face (EO): some platforms are battered only on three sides, leaving one vertical face. This face must be perpendicular to the end-on axis.
- Skirt Piles: this box should be checked if the platform being modeled has skirt piles (attached to the jacket in the bottom jacket bay) in addition to main piles (which pass through the jacket legs). TOPCAT is not intended for the analysis of platforms which are only supported by skirt piles.
- Plan Dimensions: these inputs define the jacket top plan and bottom plan. Only eight-leg and twelve-leg platforms have middle sections.

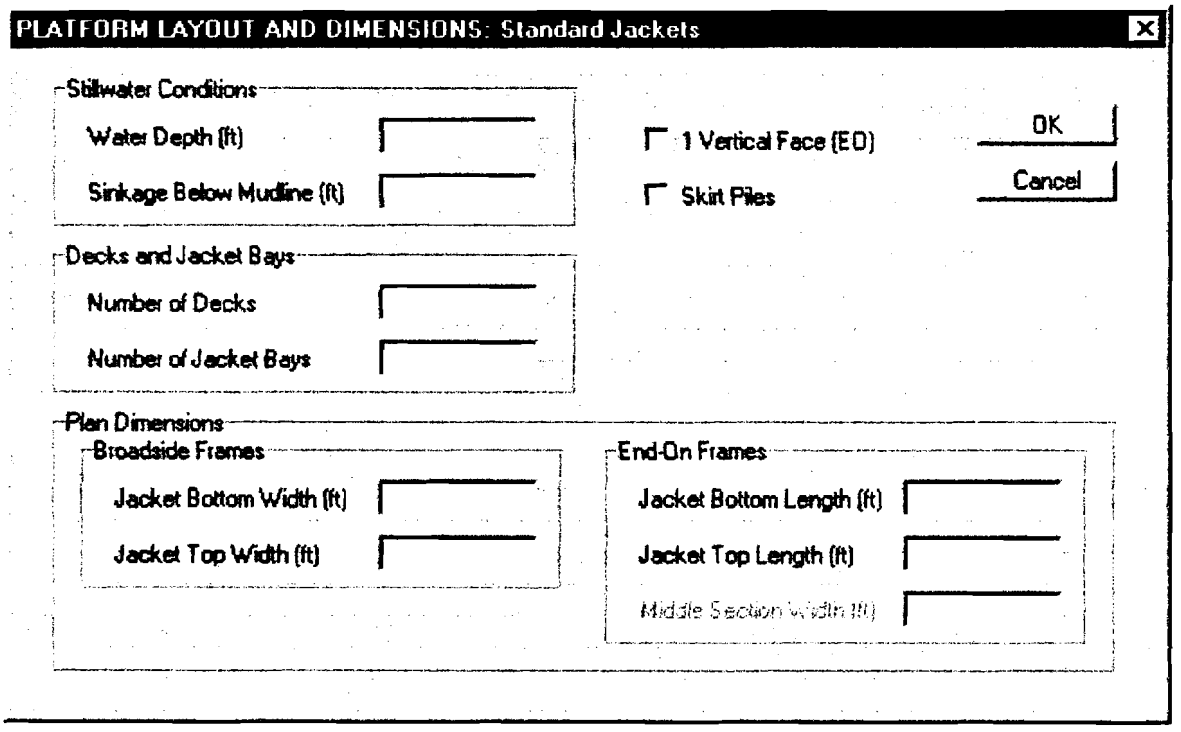

Figure 3-12: Platform Global Layout and Dimensions

TUTORIAL: enter the global layout and dimensions for the example platform in Figure 3-9. This platform is in 100 ft of water, and the jacket is resting on the mudline (sinkage is zero); therefore the user enters "100" and "0". The platform has one deck, and two jacket bays (while the deck bay is braced, it is not part of the jacket). The platform has no skirt piles, and has zero batter on all faces, so both the skirts and single vertical EO face box should remain unchecked. The jacket top and bottom dimensions are 60 ft on a side; therefore the user should enter "60" for all jacket top end-on and broadside and bottom end-on and broadside dimensions. The platform, being a four-leg structure, has no middle section width. Click OK when done.

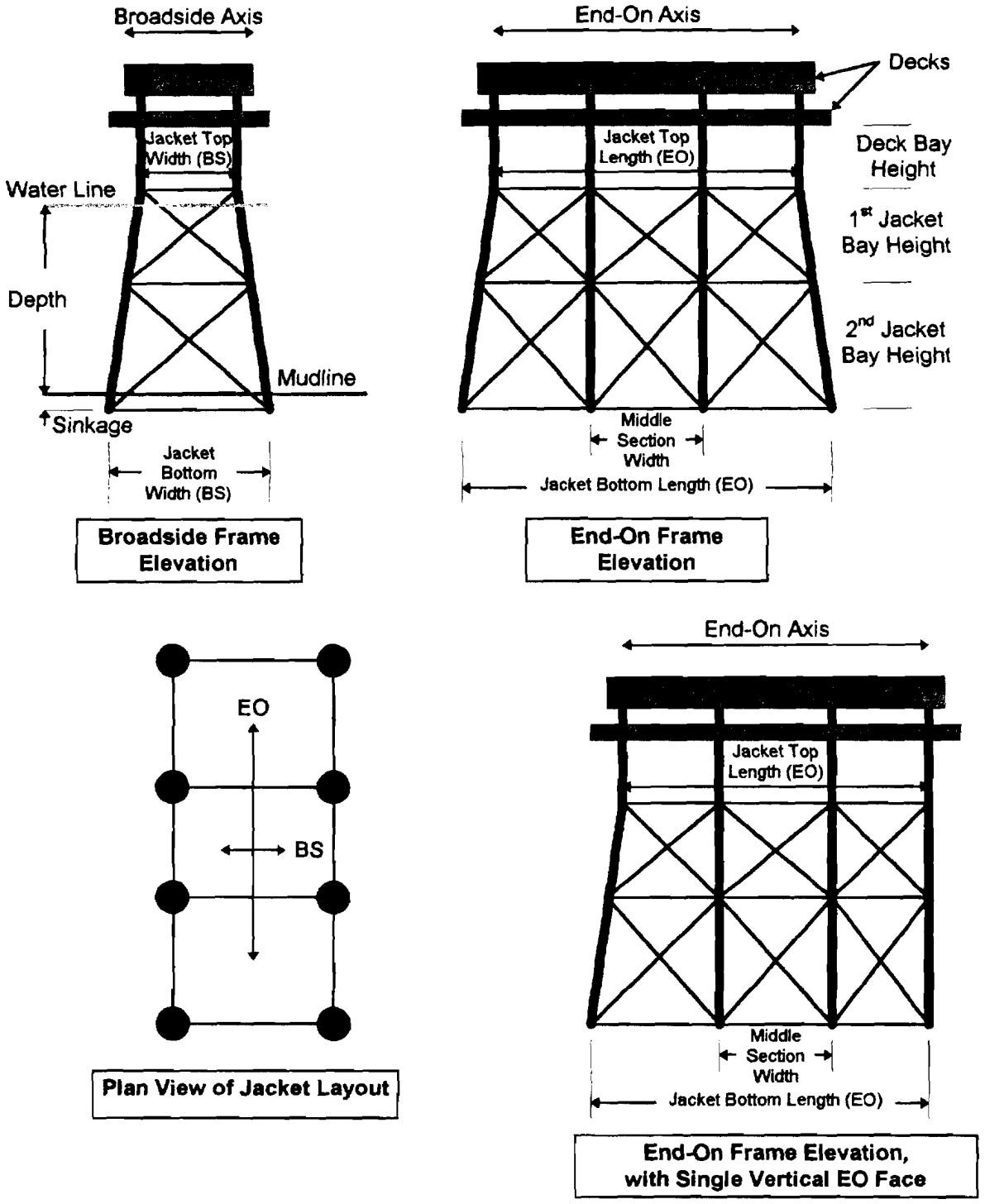

Figure 3-13: Terminology for Platform Global Layout and Dimensions, Using an Eight-Leg Platform for Reference

GLOBAL PARAMETERS/Bay Heights and Numbers of Braces:

The program will display the following dialog box:

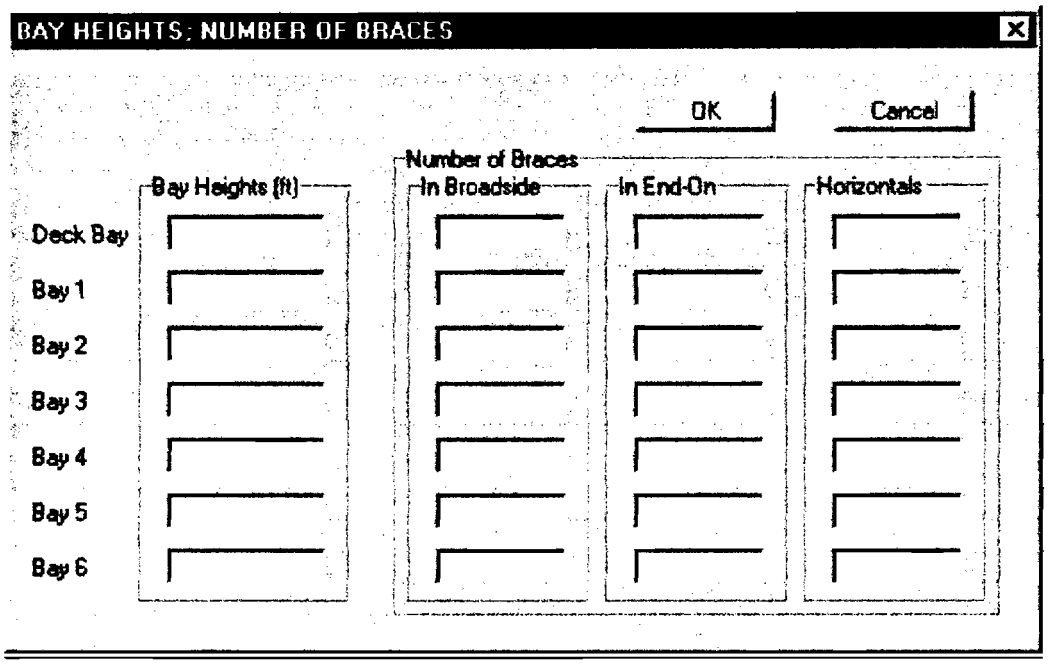

Figure 3-14: Bay Heights and Numbers of Braces

The user inputs data on the elevated dimensions of the platform structure, and also supplies the numbers of broadside and end-on main diagonal and horizontal braces in each bay. The bay heights are the elevated dimension of each structural bay, as shown in Figure 3-13. Figure 3-15 shows the classification of braces into either broadside main diagonal, end-on main diagonal, and horizontal. Main diagonals are organized by which principal set of framing (either end-on or broadside) they are part of. Horizontal braces are organized by which horizontal frame they are in; the horizontal braces associated with a bay are those in the horizontal frame at the bottom of the bay.

The user is required to specify at least one diagonal brace in each jacket bay. A maximum of 100 braces can be specified for each given bay orientation (end-on, broadside or horizontal). The deck bay can have zero braces, as can the horizontal frames.

NOTE: if there are more than six jacket bays, input will be taken by a series of screens until all bays are accounted for.

TUTORIAL: for the example platform in Figure 3-9, enter bay heights, starting with the deck bay and going down: "30", "60", and "60". Next, enter numbers of braces. The platform has four main diagonal braces (K-brace configuration) in each principal direction in the deck bay, and four horizontal braces in the frame at the bottom of the bay; hence, the user will enter "4", "4" and "4" for broadside frame main diagonals, end-on frame main diagonals, and horizontal frame main diagonals for the deck bay. Similarly, the first and second jacket bays of the platform are seen to have four main diagonal braces (X-brace configuration) in each principal direction in the

bay, and four horizontal braces in the frame in the bottom of each bay. The user will enter "4", "4", "4" for the first jacket bay and "4", "4", "4" for the second jacket bay. Click OK.

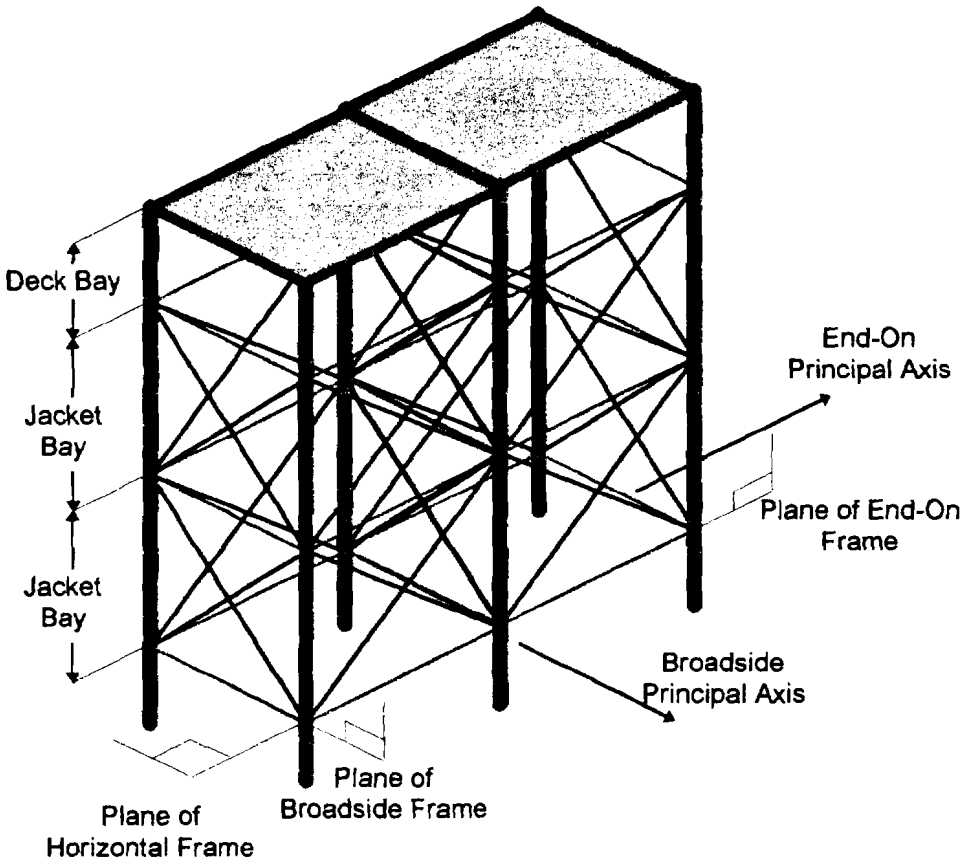

Figure 3-15A: Main Diagonal and Horizontal Bracing

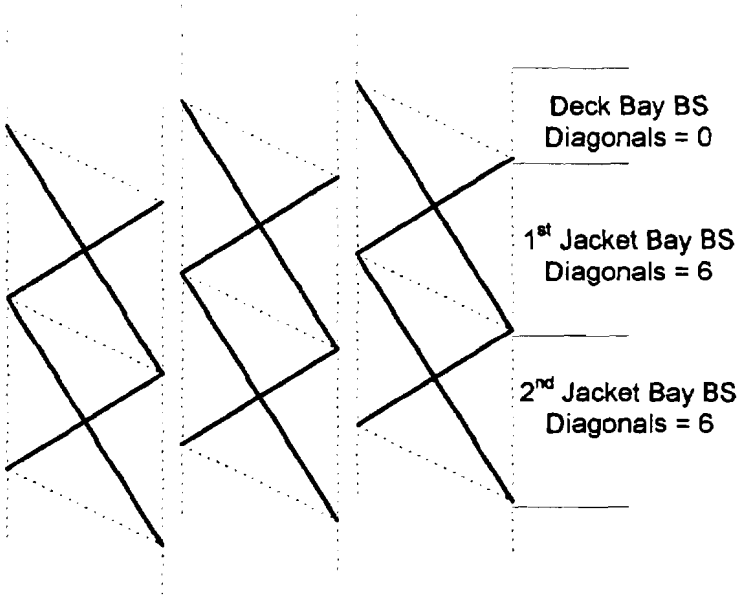

Figure 3-15B: Main Diagonal Braces in Broadside Frames

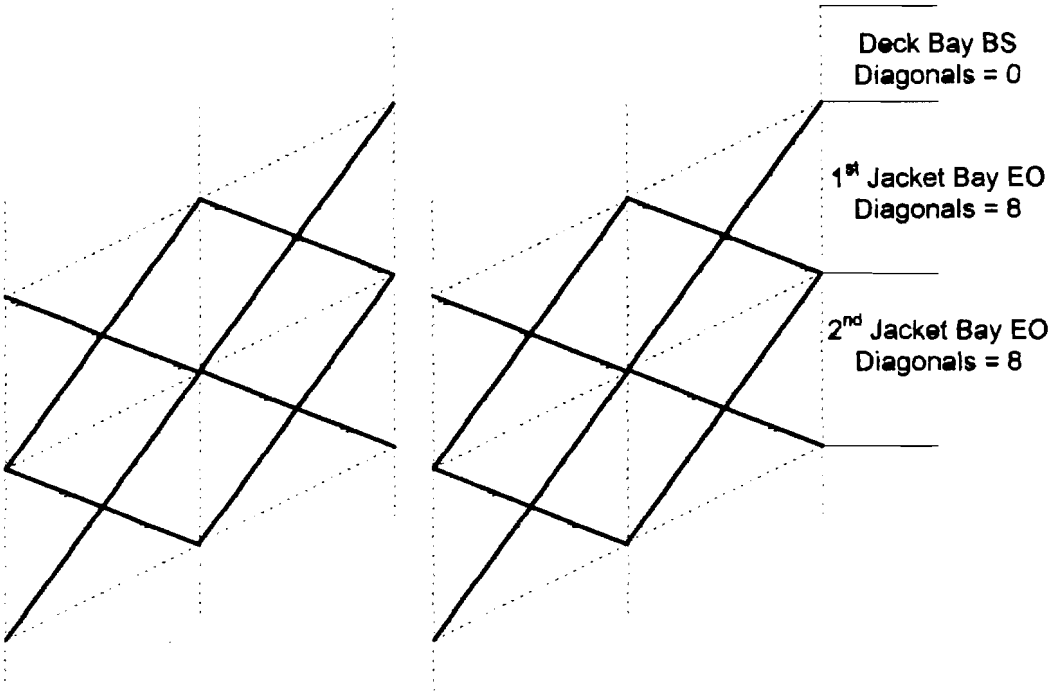

Figure 3-15C: Main Diagonal Braces in End-On Frames

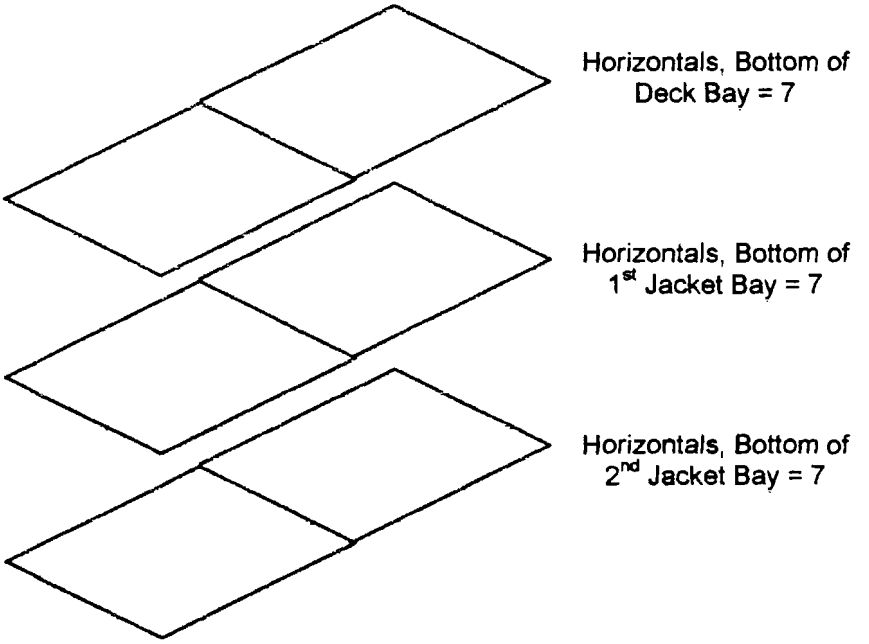

Figure 3-15D: Braces in Horizontal Frames

GLOBAL PARAMETERS/Structure Materials

The program displays the following dialog box:

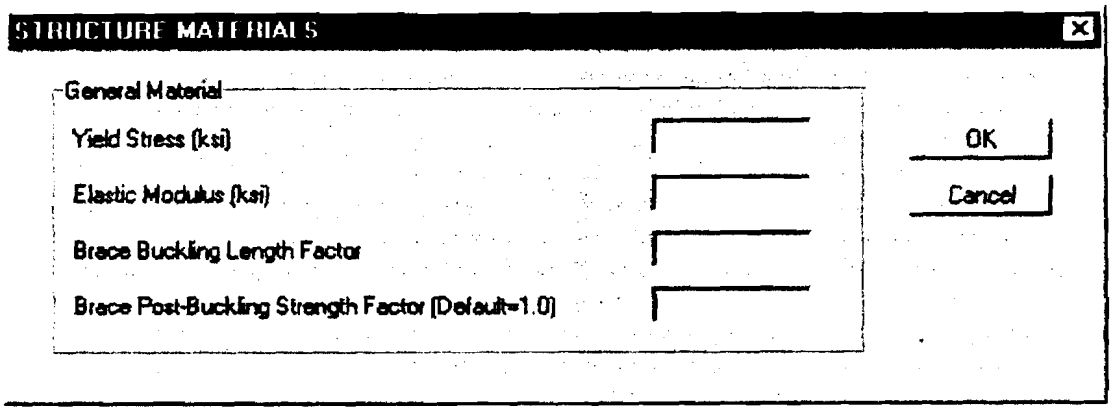

Figure 3-16: Structure Materials

The user designates a "default" steel yield strength, an elastic modulus for steel members, a "default" brace buckling length (k) factor, and a brace post-buckling strength factor. The default steel yield strength and brace buckling length factor can be over-ridden by specifying specific yield strengths for individual members, as discussed later in the local parameters section. The brace post-buckling strength factor is used when the program estimates the "upper-bound" capacity of a braced bay; for the upper-bound capacity, the program assumes all members have reached their plastic limits. For braces in tension, the yield strength is taken to be the plastic strength, so the post-yield strength factor is 1.0 or 100%; for braces in compression, the post-buckling strength is dependent upon both the stockiness of the brace and the amount of imposed inelastic displacement. While the program default for the post-buckling strength of braces is also 1.0, it is recommended that users supply a value which is more indicative of braces which have reached a compression ductility of four or so. For this situation, most braces will have a post-buckling strength of perhaps 30% (0.3) or 20% (0.2), as shown in Figure 3-17.

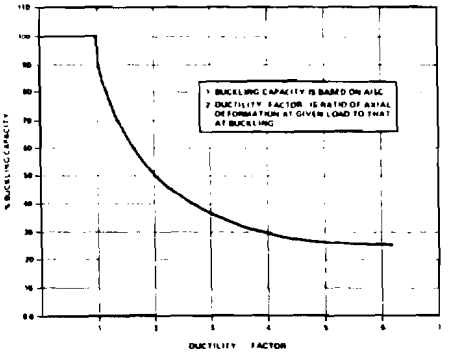

Figure 3-17: Post-Buckling Strength of Braces

TUTORIAL: the example platform is made from 36 ksi steel, with an elastic modulus of 29,000 ksi. Enter "36" for yield strength, and "29000" for elastic modulus. The main diagonal braces in the platform have very rigid end connections, which provide a k factor of 0.5. Enter "0.5" for effective length factor, and enter a post-buckling strength factor of "0.3". Click OK.

GLOBAL PARAMETERS/Soil Properties:

The program will first display this dialog box:

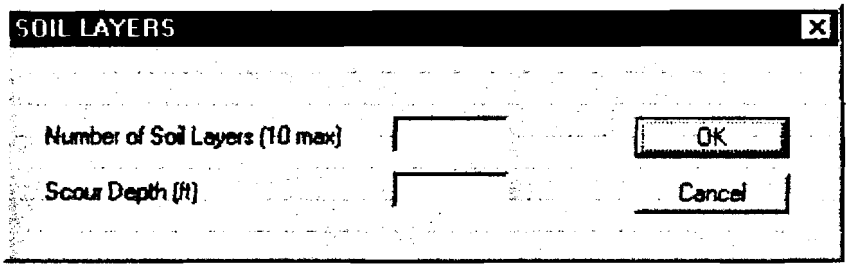

Figure 3-18: Number of Soil Layers

The user can enter up to ten layers of soil, either predominantly clay or predominantly sand, to characterize the soil profile beneath the platform. At least one layer must be specified; the user need only specify the number of layers through which the piles penetrate. A layer can be specified (1) sand with constant angle of friction, (2) clay with constant undrained shear strength, or (3) clay with linearly-varying shear strength through the layer. The scour depth refers to the amount of soil which has been scoured away from the bottom of the platform, as measured from the base of the jacket.

TUTORIAL: the example platform in Figure 3-9 has one major layer of soil beneath it, into which the piles penetrate. There is no scour. Enter "1" and "0" respectively, then click OK.

Upon entering the number of soil layers and clicking OK, the program displays the following dialog box:

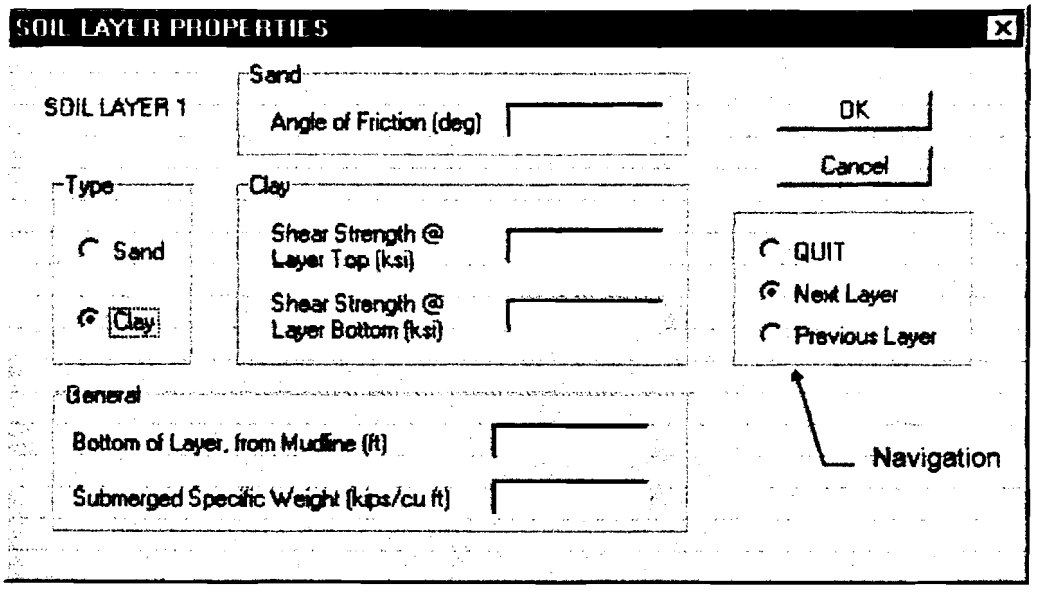

Figure 3-19: Soil Layer Characteristics

The user must now supply information on each soil layer, starting with the shallowest layer and then proceeding downward (see Figure 3-20).

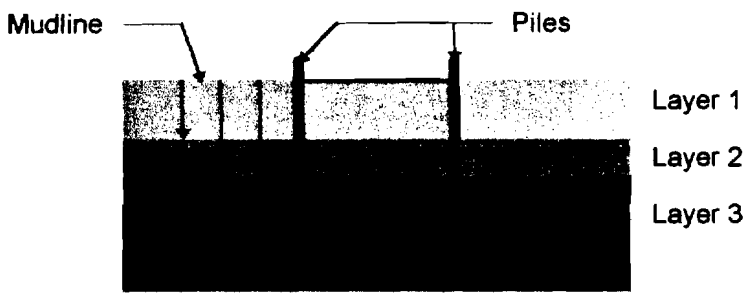

Figure 3-20: Soil Layers Beneath a Platform

When a sand layer is specified, the user must enter the effective angle of friction for the soil. When a clay layer is specified, the user must enter the undrained shear strength of the clay at the top and bottom of the layer. If these two shear strengths are different, the program assumes the strength varies linearly in the layer. For each layer, the user must also supply the submerged specific weight of the soil, and the distance from the mudline to the bottom of the soil layer. For the last layer, the distance needs to be specified such that it is deeper than the pile penetrations.

NOTE: the toggle below the OK/Cancel buttons allows the user to navigate through the different soil layer input. By selected either next or previous layer, the user can sequentially review the soil layer data which has been entered. The entry sequence terminates when either (1) the last soil layer has been entered, and the user clicks OK with advance to next layer specified, or (2) the user selects the QUIT option and clicks OK.

TUTORIAL: the soil beneath the platform is stiff clay, with a surface shear strength of 2.5 ksf. The strength of the soil increases 0.01 ksf/ft with depth. Selects "clay", and enters a top layer strength of "2.5". The bottom layer cut-off must be chosen to be deeper than the pile penetration (150 ft); a depth of 200 ft is chosen for the layer bottom, so enter "200". The bottom layer strength is thus 4.5 ksf, so enter "4.5" for this value. The specific weight of the soil is about 50 lbs/ft^3, so enter "0.05". Click OK to proceed.

GLOBAL PARAMETERS/Force Coefficients:

The program will display the dialog box shown in Figure 3-21. The user specifies:

- A wave kinematics factor and a current blockage factor to modify wave and current horizontal velocities in the water column (Appendix A).
- An added mass coefficient, to determine the amount of added hydrodynamic mass to include with each member when determining platform mass for a modal analysis (Appendix E).
- A hydrodynamic drag coefficient, C_D, to enable drag forces to be calculated on tubular members and appurtenances in the platform (Appendix A).
- Special hydrodynamic drag and wind speed coefficients for each deck, to enable forces to be calculated for waves in the deck and wind on projected areas (Appendix A).

The user may also specify a load factor. This linearly scales the load on the platform from storms, earthquakes, and the baseline analysis used to estimate fatigue stresses. The default value is unity.

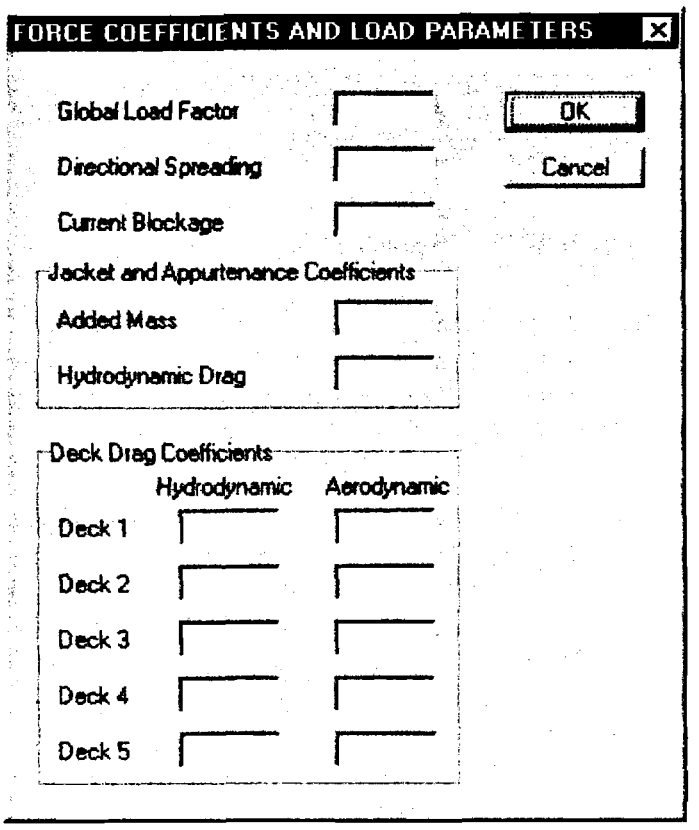

Figure 3-21: Force Coefficients

TUTORIAL: specify the load factor as "1.0". Referring to API RP-2A LRFD (1993), enter wave kinematics factor as "1.0", current blockage as "0.8", and hydrodynamic drag coefficient on tubular members and appurtenances as "1.05". As the platform members are very stiff, use an added mass coefficient of "1.0". The deck can be considered heavily equipped, so enter a deck hydrodynamic drag coefficient of "2.5" and a wind speed coefficient of "1.0" for Deck 1. Click OK.

GLOBAL PARAMETERS/Biases and Uncertainties: Structure:

The program will display the dialog box in Figure 3-22. The user can specify biases and uncertainties for the axial strengths of tubular braces, the punching or pullout strength of tubular joint connections, and pile head axial and lateral strengths and stiffnesses. The biases are simply percentage modifiers to the values of these quantities calculated by the program. The uncertainties, expressed as coefficient of variation or *COV* (standard deviation divided by mean value), are associated with the assumed log-normal distribution of the strength or stiffness characteristic in question; the value calculated by the program and modified by bias is assumed to be the mean value of the characteristic's distribution. The *COV*s are used by the program when performing reliability calculations (Appendix H). The program defaults all biases to unity

if they are unspecified. *COV* input is optional; if no *COV*s are input the program will not return any reliability results.

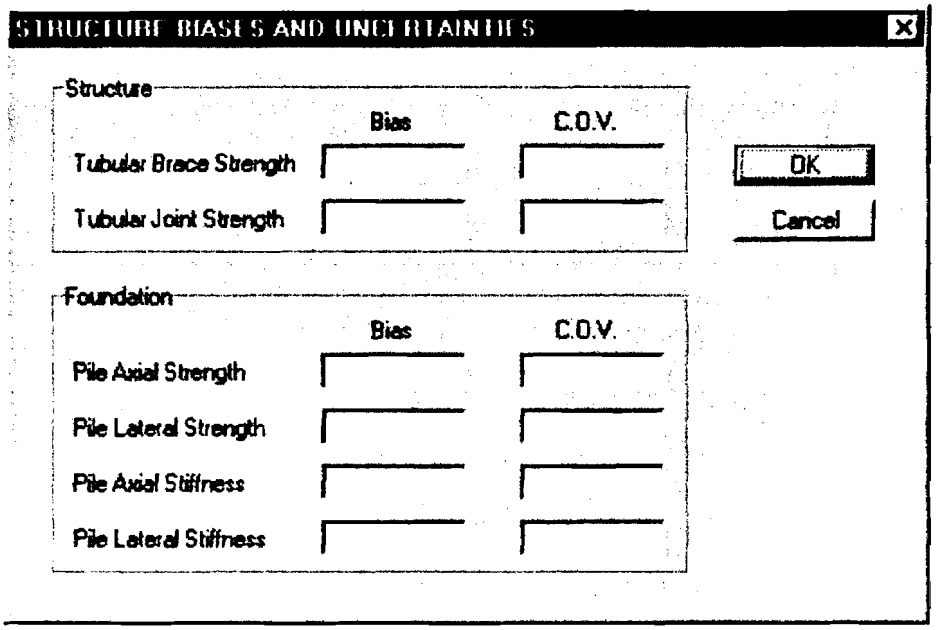

Figure 3-22: Structure Biases and Uncertainties

TUTORIAL: assign biases of "1.0" to all of the above characteristics, except for pile head axial stiffness; for this characteristic, assign a bias of "3". To demonstrate the reliability features of TOPCAT, enter values of *COV* for all components. Assign *COV* of "0.3" to both brace and joint connection strength, and *COV* of "0.4" for pile head axial and lateral strength and pile head axial stiffness and lateral stiffness.

GLOBAL PARAMETERS/Biases and Uncertainties: Load:

The program displays the following dialog box:

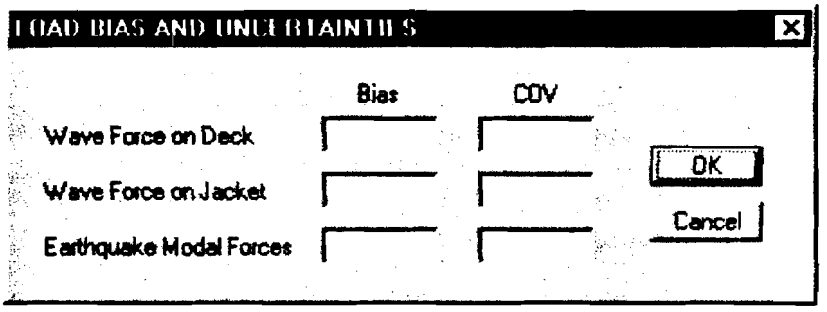

Figure 3-23: Load Biases and Uncertainties

As for structure biases and uncertainties, the user can supply biases and uncertainties for forces from storms and earthquakes. These biases are percentage modifiers to the magnitude of the wave force on the deck, the wave force on the jacket, and the API (1993) acceleration response spectrum ordinate used to calculate loads from response spectrum analysis, while the *COV*s represent the uncertainties associated with the assumed log-normal distributions of these

quantities (the values calculated by the program and modified by bias are assumed to be the mean values). The biases default to unity, while if no *COV*s are input the program will not return reliability results.

TUTORIAL: assign biases of unity ("1.0") to wave force in deck, wave force on jacket, and earthquake modal forces. Assign *COV* of "0.4" to the wave forces, and a *COV* of "0.8" to the earthquake modal forces.

3.6 Defining Local Parameters

With the definition of global parameters complete, the user can now supply information on the "local parameters" of the platform. These are:

1. Tubular joint connection dimensions, and if desired, fatigue stress concentration factors; these are the connections between the main diagonals and either jacket legs or other main diagonals (X-bracing).
2. Main diagonal brace diameter, thickness, orientations, bracing configuration, and if desired, specific strength parameters and/or damage.
3. Deck and jacket leg diameter and thickness.
4. Horizontal brace diameter, thickness, length and orientation.
5. Main pile diameter, thickness, penetration, and if desired, specific strength parameters.
6. Skirt pile diameter, thickness, penetration, and if desired, specific strength parameters. This item can only be selected if the platform was declared as having skirt piles (Section 3.5, GLOBAL PARAMETERS/Platform Layout and Dimensions).
7. Conductor diameter, weight per ft of length, plastic hinge capacity, cross-section moment of inertia, and penetration, if it is desired to include conductors in either an earthquake analysis (modal properties determination) or as strength and stiffness elements in the calculation of foundation strength and stiffness (Appendix E and G).
8. Mud mat areas, and soil bearing and sliding strength and stiffness modifiers if considering the bearing and sliding action of mud mats and mudline braces when calculating foundation strength and stiffness (Appendix G).
9. Projected areas and weights of decks and boat landings.
10. Projected areas of appurtenances, and marine growth on structural members.
11. An equipment period of vibration, if deck-level accelerations from earthquake response are desired for mounted equipment design.

The user must supply items 1, 3 and 5. All other items can be left unassigned. Input for tubular joint connections (connections of main diagonals) need only be input if the user desires to (1) assess the strength of the connections, or (2) perform a fatigue analysis. If either of these two options is desired, tubular joint input must be supplied before diagonal brace input. Otherwise, all local parameter items can be input in any order.

LOCAL PARAMETERS/Tubular Joints

TOPCAT can base the axial strength of main diagonal braces on either the axial tension or buckling capacity of the brace, or on the punching or pullout strength of the tubular joints at either end of the brace by which the brace is attached to other structural members:

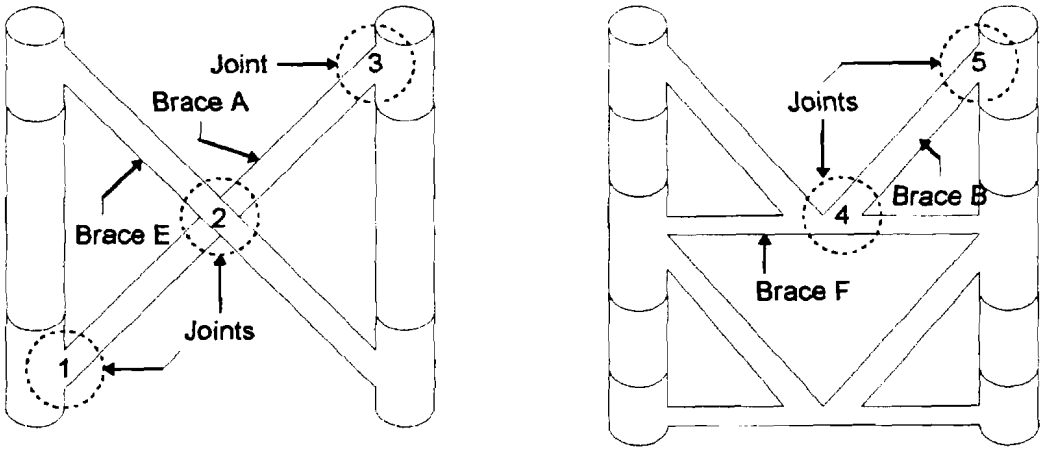

Figure 3-24A: Axial Strength of Diagonal Braces, Accounting for Connections

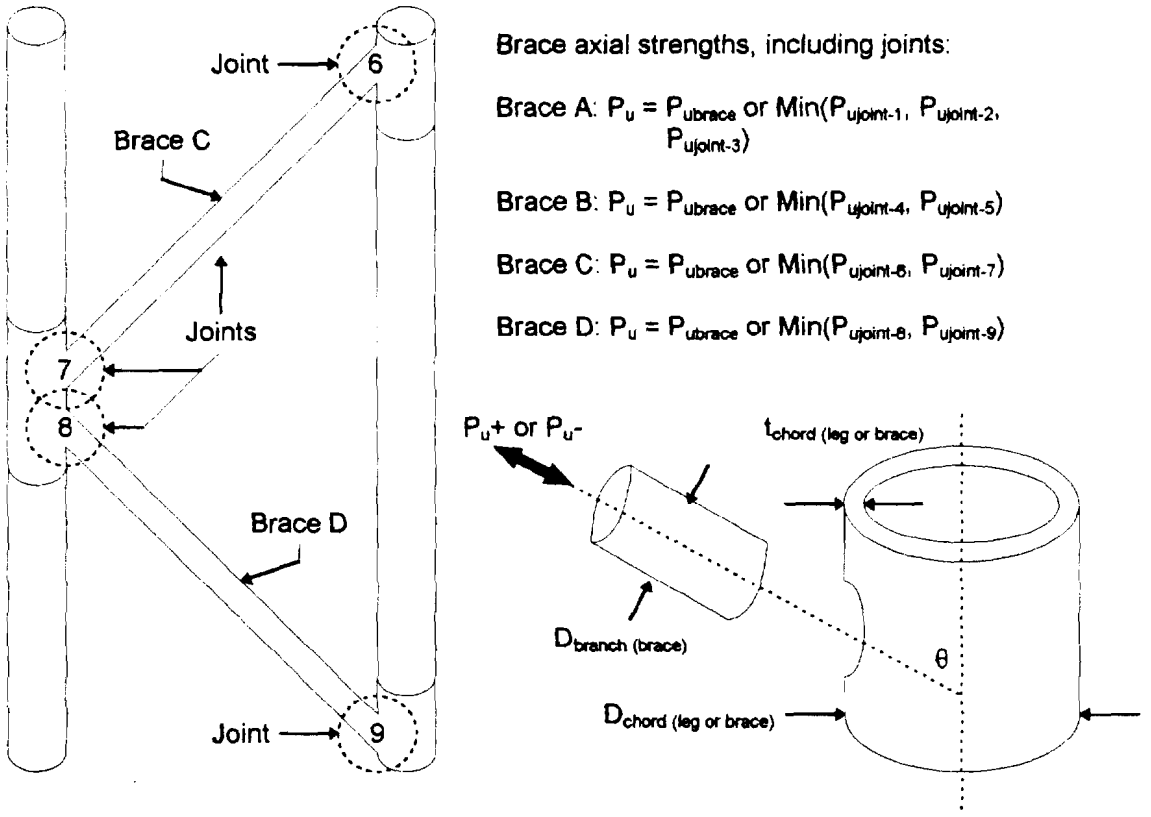

Figure 3-24B: Axial Strength of Diagonal Braces, Accounting for Connections

When entering data on diagonal braces, user must specify tubular joint connection types for both brace ends if the strengths of connections are to be evaluated along with the axial strength of the attached brace. TOPCAT can model tubular joints which fall into the category of "simple" tubular joints, i.e. there is no overlap of principal braces framing into the joint, and the joint has

no gussets, diaphragms or stiffeners. Tubular joint connections are categorized by the load they carry, as per API (1993) suggestions: K, T or Y, and X, as shown in Figure 3-25.

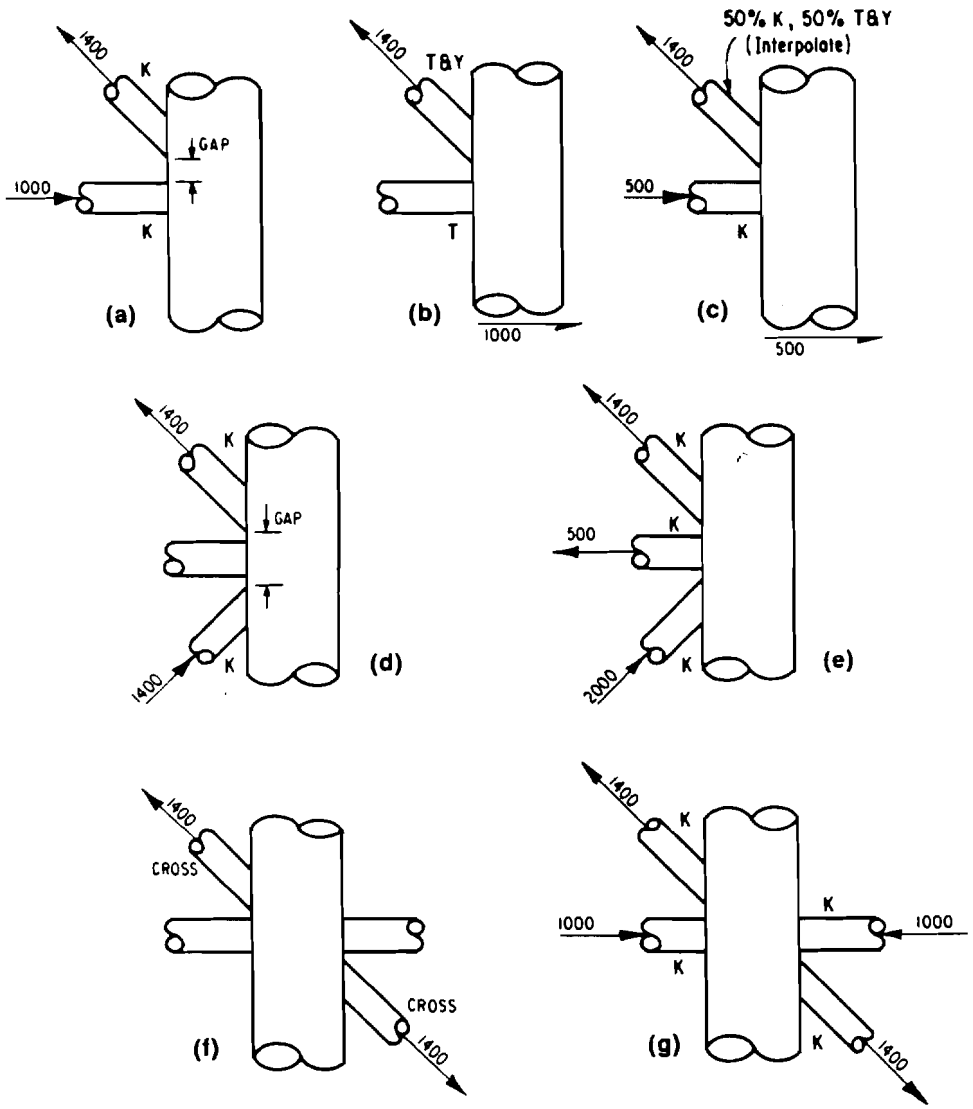

Figure 3-25: API (1993) Joint Classification

For each joint type, the user must enter the chord (member to which the brace attaches) diameter and thickness, the branch (brace) diameter and the angle between the axis of the chord and the axis of the brace, as shown in Figure 3-24. Users must also specify any gap in K-joints. For

braces in an X-brace or K-brace configuration, such as Braces A and B, the X-joint and K-joint to which these braces attach has another bracing member as the chord, not a jacket leg. For example, Brace A is connected to Joint 2. The branch diameter will be the diameter of Brace A, while the chord thickness and diameter will be the diameter and thickness of Brace B.

An X-brace effectively has three connections: two at either end (Joints 1 and 3 for Brace A), and one at the cross-point in the X configuration (Joint 2). TOPCAT only allows a user to specify two connection types per brace, assumed to be at either end. Users entering joint types for X-braces can enter type definitions for each joint (assuming this is necessary, due to differences in joint configurations), and then during the course of an analysis, try the brace with different end joint types to find which two types of the three are limiting in terms of strength.

Users need not enter a joint type for every single joint connection in the platform. For example, Brace D in Figure 3-24 is connected to the jacket legs by Joints 8 and 9. If the chord diameter and thickness for Joints 8 and 9 are the same and both joints have the same load pattern, and Brace D makes the same angle with each chord, then Joints 8 and 9 are of the same type, and thus the user need only declare a single joint type to represent these two connections. Similarly, if Brace C has the same diameter as Brace D, and Joints 6 and 7 have the same chord properties and load pattern as Joints 8 and 9, and Brace C makes the same angle with the chords as Brace D does, then Joints 6, 7, 8, and 9 are all of the same type, and only one joint type need be specified to represent them. Joint types in TOPCAT do not refer to specific connections; they refer to connections which have identical characteristics.

When the TUBULAR JOINTS item is selected, the program displays the following dialog box:

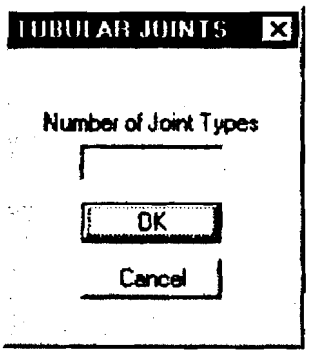

Figure 3-26: Number of Joint Types

The user supplies the total number of joint types for main diagonal brace connections in the platform. After supplying this number, the program displays the dialog box shown in Figure 3-27. For each joint, the user must specify as a minimum the joint load-path type, the chord diameter and thickness, the branch diameter, the angle between the brace and chord, any gap existing in K-joints, and whether or not the joint is grout-filled. Additional information, namely steel yield strength (if the can material is different from the attached braces and legs) and special stress concentration factors (to override the default values used by the program; see Appendix F) can also be supplied.

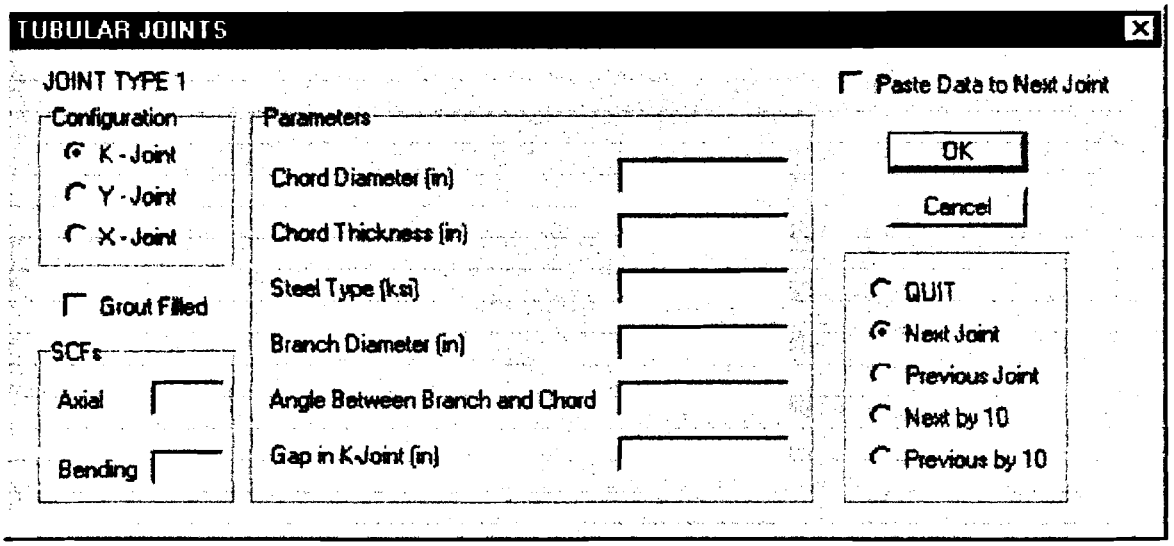

Figure 3-27: Tubular Joints

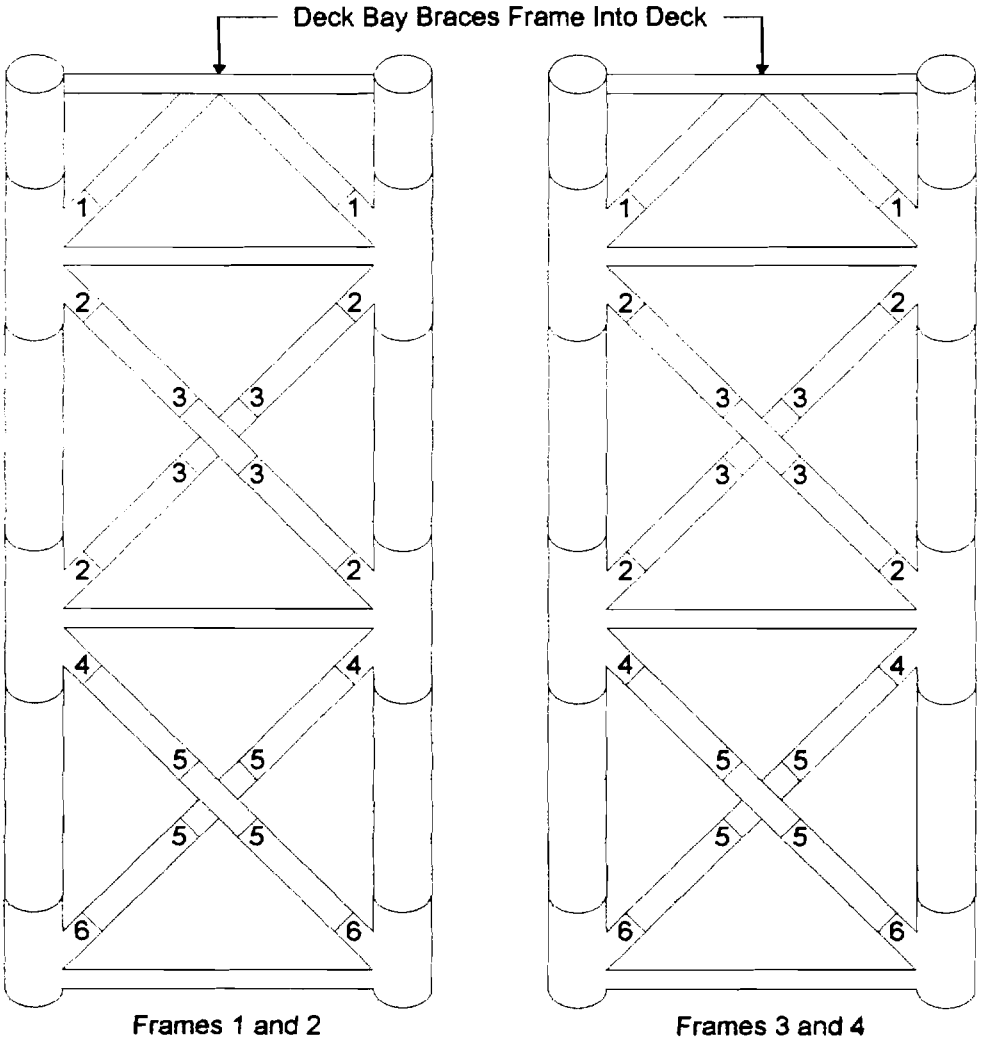

Figure 3-28: Number of Joint Types in Example Platform

The user will declare joints sequentially (the order of input of types is irrelevant). The navigation menu can be used to move backwards and forwards through the joint types, either stepping by one or stepping by ten. The box marked "paste" can be used to copy data from one joint to the next. WARNING: users should be cautious with the paste feature; if it is inadvertently left checked while reviewing previously-entered data, this data will be copied over by the data for whatever joint was being examined when the paste box was first selected.

TUTORIAL: The user will supply input for tubular joints. All of the tubular joint connections of main diagonal braces in the example platform can be represented by six joint types, as seen in Figure 3-28. These joint types are:

1. K-joint, by which the lower ends of the 36" ϕ main diagonals in the deck bay are attached to the top of the jacket legs. The joint can is 80" ϕ with 1.875" w.t. The angle between the brace and the chord is 45°. The gap in the K-joint is 18", effectively the diameter of the horizontal which attaches to the joint can. The steel yield strength of the joint can is 50 ksi.
2. K-joint, by which the upper and lower ends of the X-braced 24" ϕ main diagonals in the first jacket bay are attached to the legs. The joint can is 80" ϕ with 1.875" w.t. The angle between the brace and the chord is 45°. The gap in the K-joint is 18". The steel yield strength of the joint can is 50 ksi.
3. X-joint, the intersection between the X-braced 24" ϕ main diagonals in the first jacket bay. The intersection chord diameter is 24" ϕ with 0.5" w.t. The angle between the brace and the chord is 90°. The steel yield strength of the joint is the same as the braces, so it may be left unassigned, hence taking the default structure value of 36 ksi entered previously in STRUCTURE MATERIALS.
4. K-joint, by which the upper ends of the X-braced 30" ϕ main diagonals in the second jacket bay are attached to the legs. The joint can is 80" ϕ with 1.875" w.t. The angle between the brace and the chord is 45°. The gap in the K-joint is 18". The steel yield strength of the joint can is 50 ksi.
5. X-Joint, the intersection between the X-braced 30" ϕ main diagonals in the second jacket bay. The intersection chord diameter is 30" ϕ with 0.625" w.t. The angle between the brace and the chord is 90°. The steel yield strength of the joint is the same as the braces, so it may be left unassigned, hence taking the default structure value of 36 ksi entered previously in STRUCTURE MATERIALS.
6. T/Y-joint, by which the lower ends of the X-braced 30" ϕ main diagonals in the second jacket bay are attached to the legs. The joint can is 80" ϕ with 1.875" w.t. The angle between the brace and the chord is 45°. The steel yield strength of the joint can is 50 ksi.

The upper ends of the deck bay main diagonals frame into the deck structure, and are assumed to have sufficiently rigid connections to avoid collapse or tearing. The user should step through the input dialog boxes, entering the above information. The stress concentration factor inputs will be left blank (thus accepting the program's default API-based values; see Appendix F).

LOCAL PARAMETERS/Main Diagonal Braces

The user enters information on each main diagonal brace in the platform using the following dialog box:

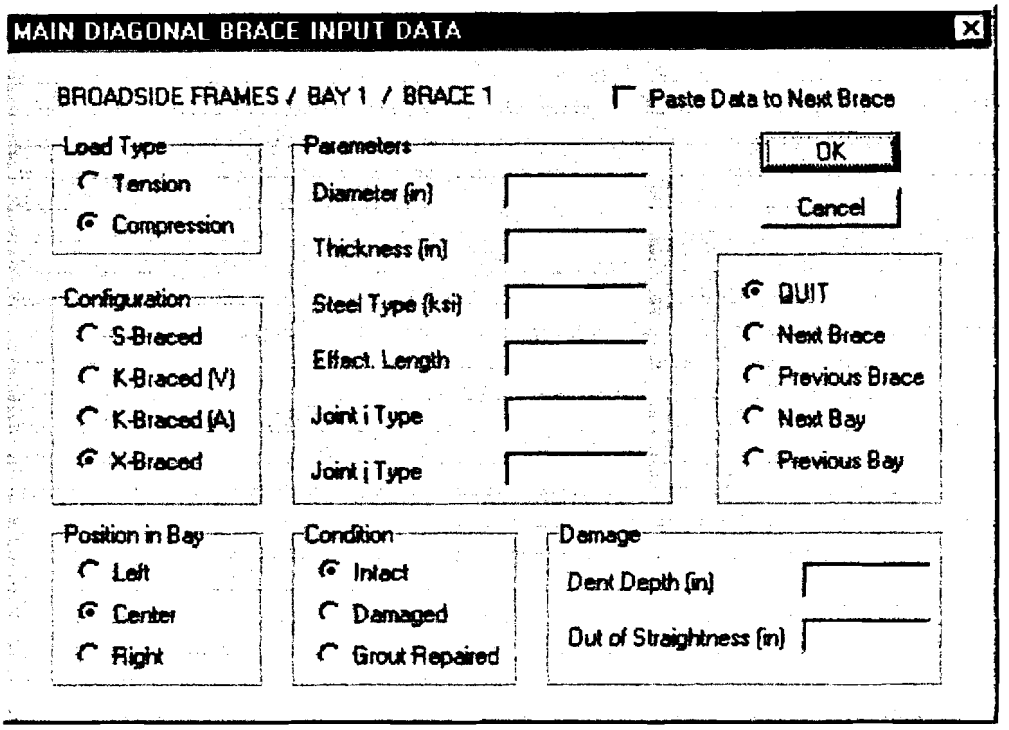

Figure 3-29: Main Diagonal Braces

The program will allow the user to input the braces, one at a time, in the following sequence:

1. Broadside frame main diagonal braces, starting in the first (top) jacket bay and working down.
2. Broadside frame main diagonal braces in the deck bay, if any were declared in BAY HEIGHTS AND BRACE NUMBERS.
3. End-on frame main diagonal braces, starting in the first (top) jacket bay and working down.
4. End-on frame main diagonal braces in the deck bay, if any were declared in BAY HEIGHTS AND BRACE NUMBERS.

In addition to tracking braces by frame and bay, the program makes use of several other characteristics when modeling these members: orientation, configuration, and position within a bay (for platforms with six or more legs). These are used to ensure TOPCAT sizes the braces correctly, and to tell the program to calculate a brace's buckling capacity or tension capacity. It is important that the user understand these terms.

Orientation is characterized by the type of axial load a brace will carry, either tension or compression. The TOPCAT user needs to establish this orientation by idealizing the frame in which the brace is located in an elevation view, and then considering the frame to be loaded at the top from left to right in this view. The loads in the braces in this frame are then established from static considerations: main diagonals running from upper-left to lower-right in the view will be placed in compression, and hence the program will calculate their axial compression capacities, while main diagonals running from lower-left to upper-right in the view will be placed in tension, and hence the program will calculate their axial tension capacities. This

process is demonstrated in Figure 3-30. When the user selects the elevation to be used, the user is effectively choosing the direction the platform will be loaded from for the given axis.

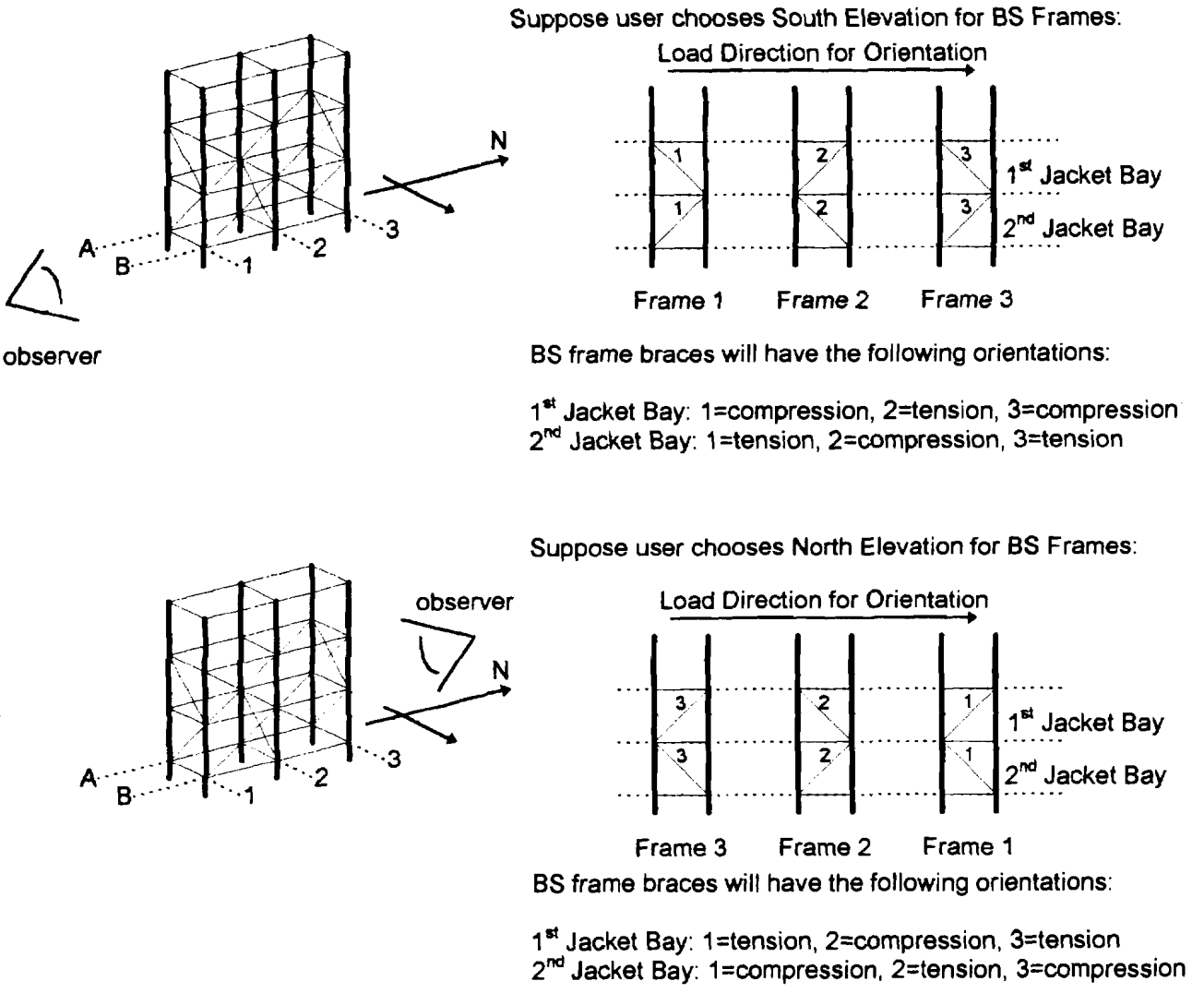

Figure 3-30: Establishing Orientation of Main Diagonal Braces

A brace's configuration identifies the arrangement of a brace in a horizontal section of frame, where a "section" is defined as the space between two jacket legs. The common configurations are single, K-braced (with the "K" directed either up or down) and X-braced. These configurations are shown in Figure 3-31.

Position refers to the where a brace is located in a frame which has more than one horizontal section, where a "section" is defined as the space between two jacket legs. Horizontal sections are identified by reference to the elevation view selected by the user for identifying brace orientation: left, center, right. All broadside frames of four-, six- and eight-leg jackets have one section (center), while broadside frames of twelve-leg jackets have two sections (left, right). End-on frames of four-leg jackets have a single section (center), end-on frames of six-leg jackets have two sections (left, right), while end-on frames of eight- and twelve-leg jackets have three

sections (left, center, right). Figure 3-32 depicts the sections of the end-on frames of the six-leg platform in Figure 3-30.

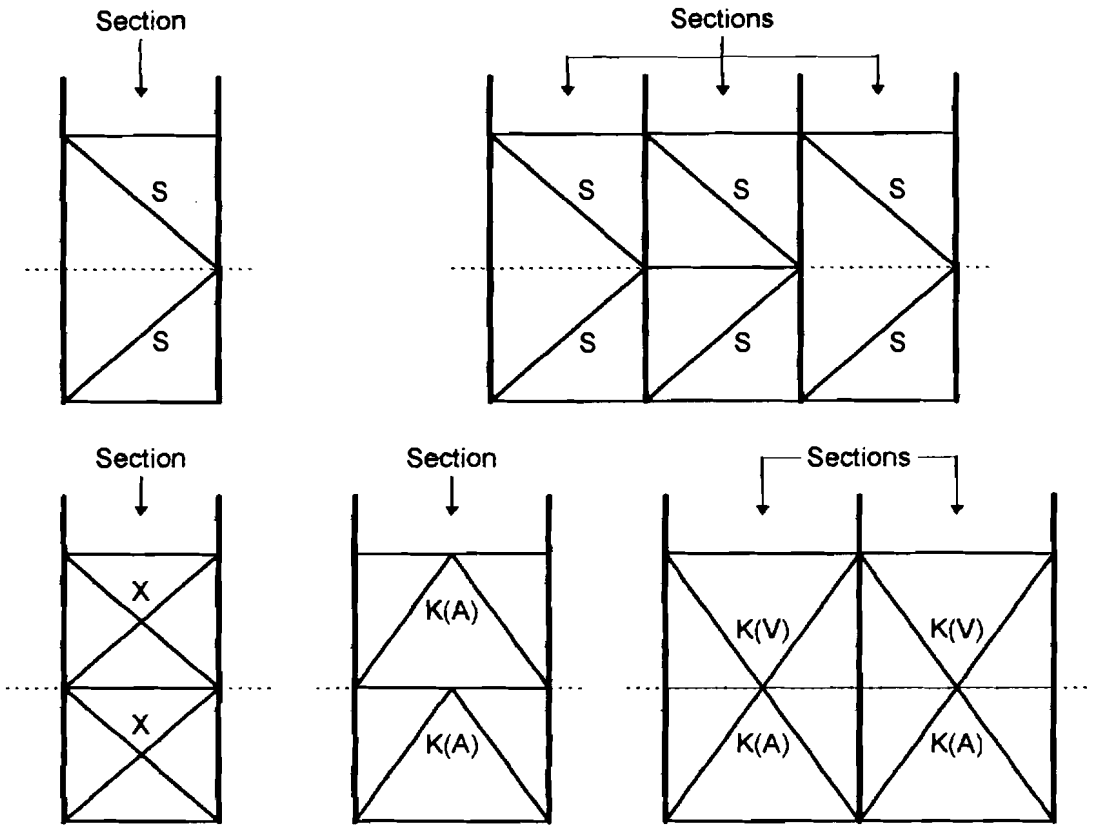

Figure 3-31: Bracing Configurations

The input ordering of braces in a given set of frames for a given jacket bay is irrelevant. For the end-on frames shown in Figure 3-32, the end-on braces in each jacket bay could be entered in any order. It is important that each brace has its orientation, configuration and position correctly identified when entering data for the brace.

As a minimum, a user must input the brace diameter and thickness. In addition, the user can supply specify a specific steel yield strength and specific *k*-factor for a brace, as opposed to using the default set in STRUCTURE MATERIALS. If the user wishes to include the consideration of tubular joint punching or pullout strength, the types of joints at either end of the brace (or one end and the cross-connection, for X-braces) can be entered.

NOTE: platforms with more than six-legs and having batter only on three sides must have an elevation view selected for the end-on frames which places the vertical face section on the right side of the view. For these configurations, TOPCAT assumes the end-on load will always be directed from the battered side to the vertical side, as shown in Figure 3-33.

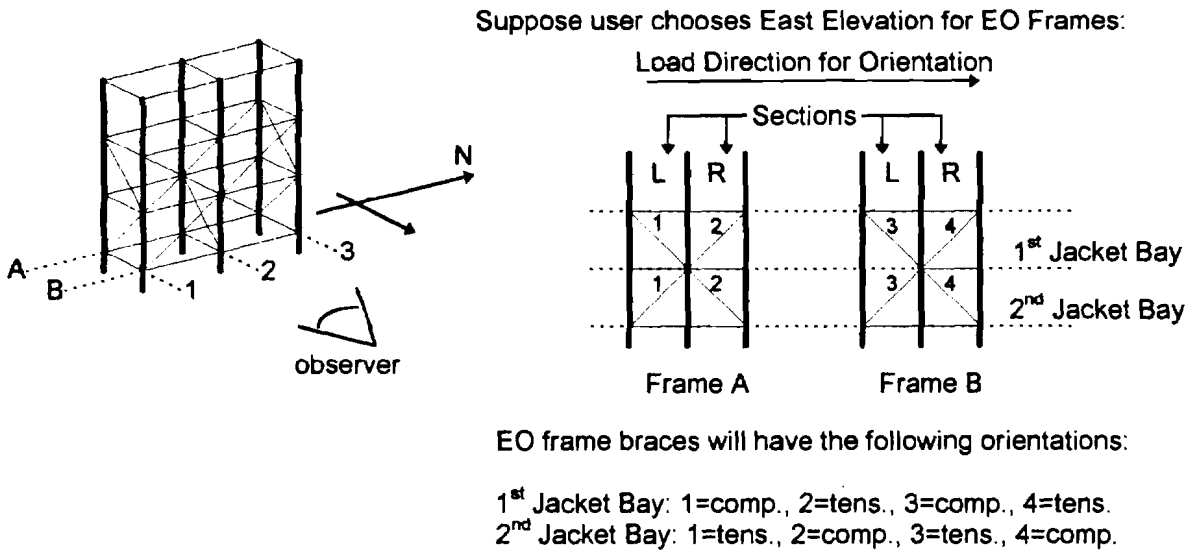

Figure 3-32: Platform Frame Sections

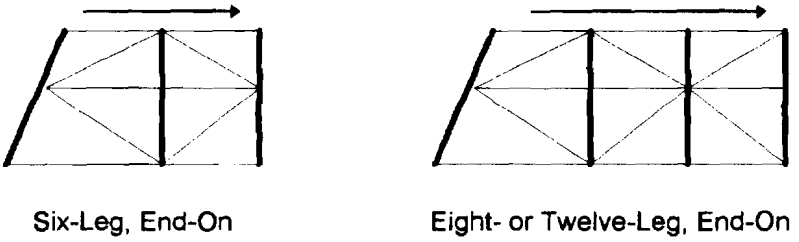

Figure 3-33: Mandatory Elevations for Platforms with Batter on Three Sides

A user may also specify a brace as having local denting damage and/or significant out-of-straightness, by specifying the member as damaged. In addition, the user may also specify a member as being grouted, regardless of whether or not the member is damaged. Dent depth and out-of-straightness are shown for a brace in Figure 3-34.

The user may use the navigation options to move forward and backward in the brace input sequence, as desired. A past feature is included, for copying input from one brace to the next brace in the input sequence. Users are cautioned to ensure the paste box is not checked when they are reviewing previously-entered data; otherwise, this data will be copied over as the user moves through the sequence of brace entries.

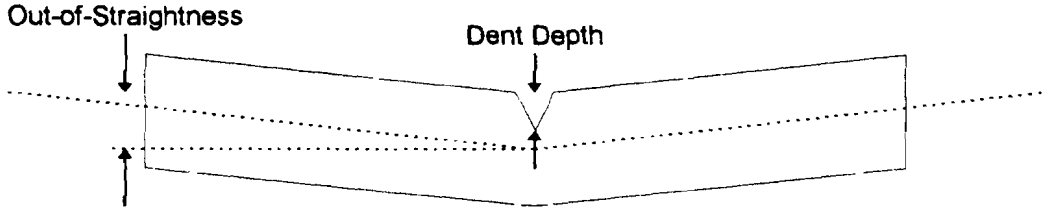

Figure 3-34: Damage to Braces

TUTORIAL: the user will input the main diagonal braces for the example platform in Figure 3-9. As the platform has four legs, the choice of which frames are broadside and which frames are end-on is left up to the user; idealize Frames 1 and 2 as broadside and Frames 3 and 4 as end-on. As the platform is completely symmetric, the choice of elevation is irrelevant; for reference idealize supplying input for a south elevation for the end-on frames, and a west elevation for the broadside frames. Arbitrarily choosing the first jacket bay compression braces in Frame 1 and Frame 3 as the first brace to be input for each broadside and end-on sequence, number the braces as shown in Figure 3-35.

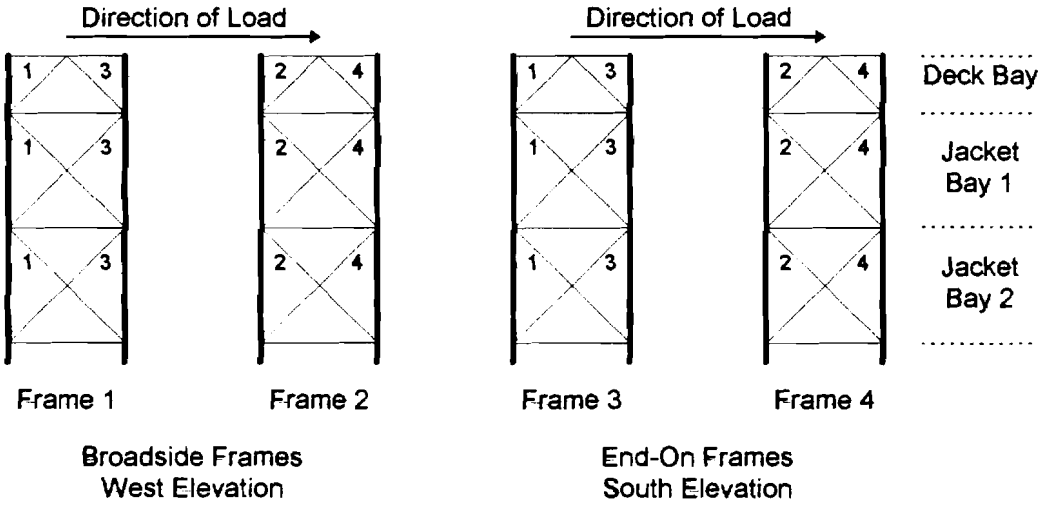

Figure 3-35

Input begins with the first jacket bay of the broadside frames. There are four broadside frame braces in this bay; all are 24 inches in diameter, w.t. 0.5 inch. All braces are part of an X-brace configuration. Two of the braces (1 and 2) will be placed in compression, and two (3 and 4) will be placed in tension. All braces have Type 2 joints at the ends and a Type 3 joint at the X-brace intersection, as shown in Figure 3-28. As the platform is a four-leg structure (one horizontal section), the position of all braces should be center.

Starting with Brace 1, make the following entries:

- Orientation: compression
- Configuration: X-brace
- Position: center
- Diameter: 24″
- Thickness: 0.5″
- Joint Type i: 2
- Joint Type j: 3

Do not click OK yet (if OK was inadvertently selected, switch the navigation option to previous, and click OK. This restores the view of Brace 1 input. Select next for the navigation option before continuing). Either joint type could be entered for slots i and j; the order of entry does not

make a difference to the program. Leave the condition of the brace as intact, and leave the yield strength and *k*-factors blank (the braces will take the default values).

The paste feature can be put to good use for this platform. The only difference in these braces are the orientations. Therefore, to enter the rest of the broadside frame first bay diagonals, do the following steps in order:

1. Select paste
2. Click OK

This now copies the information from Brace 1 to Brace 2. Brace 2 is identical in orientation to Brace 1, so:

3. Click OK. This confirms data for Brace 2, and copies data for Brace 3.
4. Change orientation to tension. This is the correct orientation for the two remaining braces in the bay.
5. Click OK. This confirms data for Brace 3, and copies data for Brace 4.
6. Click OK. This confirms data for Brace 4, and copies data for Broadside Frame Brace 1 in the second jacket bay.

With these steps, the user has finished inputting data for broadside braces in the first jacket bay, and is now ready to begin input for broadside braces in the second jacket bay. With the last action, the user copied information from broadside Brace 4 of the first jacket bay to broadside Brace 1 of the second jacket bay. Obviously, these braces do not have the same dimensions, and they have different end connection types. Also, it is desired to have the first two braces in each bay be compression braces. Hence, the user would make the following changes:

7. Orientation: compression
8. Diameter: 30″
9. Thickness: 0.625″
10. Joint i: 4
11. Joint j: 5 or 6, choose 6
12. Click OK

This enters data for the first broadside brace in the second jacket bay, and copies the data for entry. This bay also has four diagonal braces; the user would take the following steps to complete entering data on the braces in this bay:

13. Click OK. This confirms data for Brace 2, and copies the data for Brace 3.
14. Changes orientation to tension.
15. Click OK. This confirms data for Brace 3, and copies data for Brace 4.
16. Clicks OK. This confirms data for Brace 4.

The dialog box will now be requesting input for Broadside Frame Brace 1 in the deck bay. The following entries would enter all data for the four diagonal braces in this bay:

17. Orientation: compression
18. Configuration: K-brace

19. Diameter: 36″
20. Thickness: 0.75″
21. Joint Type i: 1
22. Joint Type j: leave blank
23. Click OK
24. Click OK
25. Orientation: tension
26. Click OK
27. Click OK

All data on broadside braces have now been entered, and the program will be prompting the user for input on End-On Brace 1 in the first jacket bay. As the end-on and broadside frames are identical, simply repeat the above steps to input data for the end-on frame braces.

LOCAL PARAMETERS/Deck and Jacket Legs

The program will display the following dialog box:

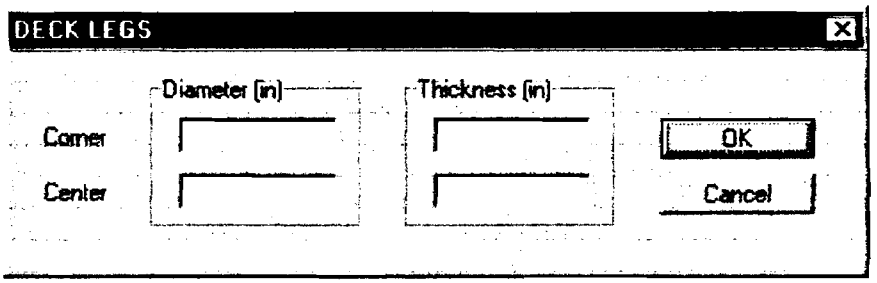

Figure 3-36: Deck Leg Input

The user must input diameter and thickness for deck and jacket legs. The deck leg data is used in formulating the lateral load capacity of the deck bay when there is no deck bay bracing, as well as for determining the mass and projected areas of the deck legs. Another dialog box will appear for jacket leg input after deck leg input is processed, as shown in Figure 3-37.

Jacket legs are treated as non-structural elements; however, their dimensions must be input in order to estimate their mass and projected areas for load purposes. Jacket leg diameter and thickness are defined for sections equal to the height of each bay in the jacket; TOPCAT assumes the breaks in the leg sections correspond roughly with the horizontal frames separating each bay. For platforms with more than four legs, the user has the option of inputting different leg sizes for the corner legs and interior legs. If there are more than six jacket bays, successive dialog boxes will appear until all data has been entered.

TUTORIAL: for the example platform, enter a corner leg diameter of 72 inches, and a corner leg thickness of 1 inch. As this is a four-leg platform, there are no center legs. Click OK. For the jacket legs, enter a corner diameter of 78 inches and a thickness of 1.125 inches for the first jacket bay, and a corner diameter of 78 inches and a thickness of 0.875 inch for the second jacket bay. Click OK.

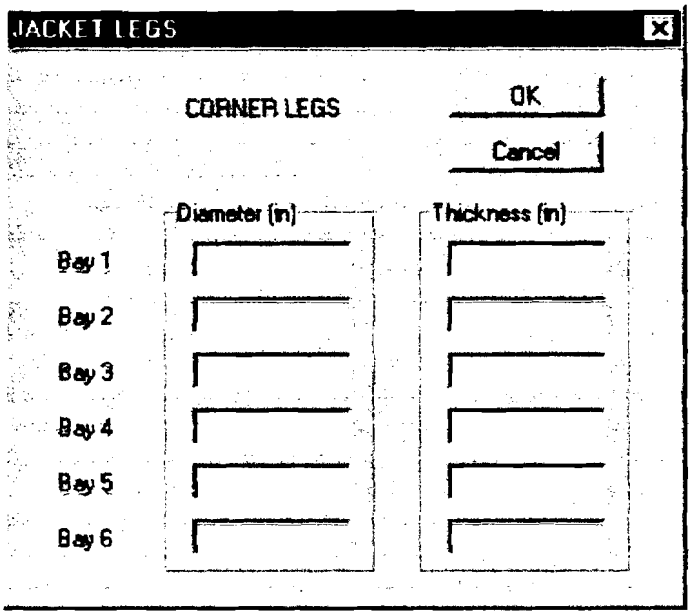

Figure 3-37: Jacket Leg Input

LOCAL PARAMETERS/Horizontal Braces

The program will display the following dialog box, assuming horizontal braces have been specified for the platform:

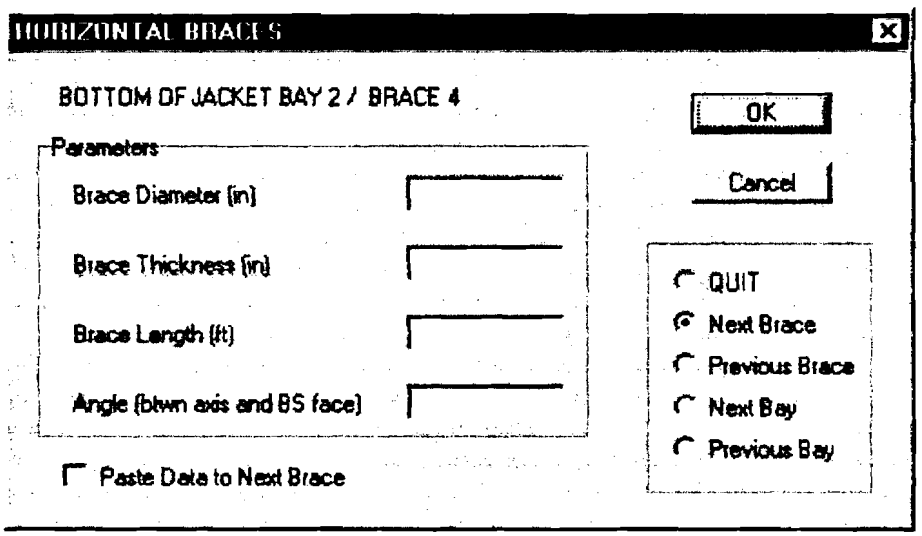

Figure 3-38: Horizontal Brace Input

As mentioned earlier, horizontal braces are not included in the capacity formulation for the platform, but must have their mass and projected areas accounted for. Horizontal braces are input in a sequential manner similar to the procedure used for joints and diagonal braces. The user must supply the diameter, thickness, length (unfortunately the program does not currently size and orient horizontal bracing members), and orientation in the horizontal plane for each horizontal brace. The actual order in which the braces are input is irrelevant. The program

organizes horizontal braces by the bottom of which bay they are in; input begins with the braces in the bottom of the deck bay and proceeds down through the jacket bays.

The angle the program uses to characterize the orientation of the brace is the angle between the axis of the brace and the end-on axis, and should be chosen to be less than or equal to 90°. This is shown in Figure 3-38.

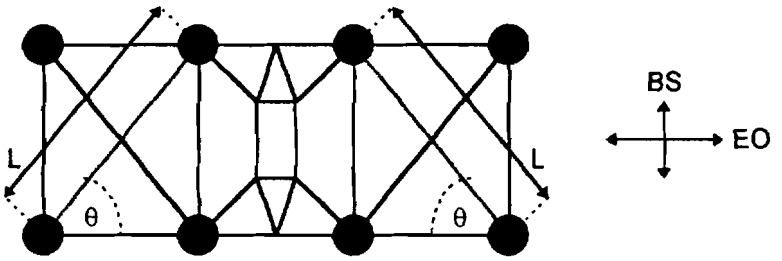

Figure 3-38: Length and Angle of Orientation for Horizontal Braces

The paste feature may be used to copy data from one brace to the next.

NOTE: the approximate sliding and bearing resistance of horizontal members in contact with the surface of the soil beneath the platform can be considered when formulating foundation capacity and strength. See Appendix G for details.

TUTORIAL: the example platform has four horizontal braces (all with diameter 18", w.t. 0.375", and length 60 ft) at the bottom of the deck bay and at the bottom of each jacket bay. Start by entering data for one brace:

- Diameter: 18
- Thickness: 0.375
- Length: 60
- Angle: 0

Now follow these steps, to quickly input the remaining braces:

1. Check paste.
2. Click OK (confirms Brace 1 at bottom of deck bay).
3. Click OK (confirms Brace 2 at bottom of deck bay).
4. Change angle to 90°.
5. Click OK (confirms Brace 3 at bottom of deck bay).
6. Click OK (confirms Brace 4 at bottom of deck bay).
7. Click OK (confirms Brace 1 at bottom of first jacket bay).
8. Click OK (confirms Brace 2 at bottom of first jacket bay).
9. Change angle to 0°.
10. Click OK (confirms Brace 1 at bottom of second jacket bay).
11. Click OK (confirms Brace 2 at bottom of second jacket bay).

12. Change angle to 90°.
13. Click OK (confirms Brace 3 at bottom of second jacket bay).
14. Click OK (confirms Brace 4 at bottom of second jacket bay).

LOCAL PARAMETERS/Main Piles

The program displays the following dialog box:

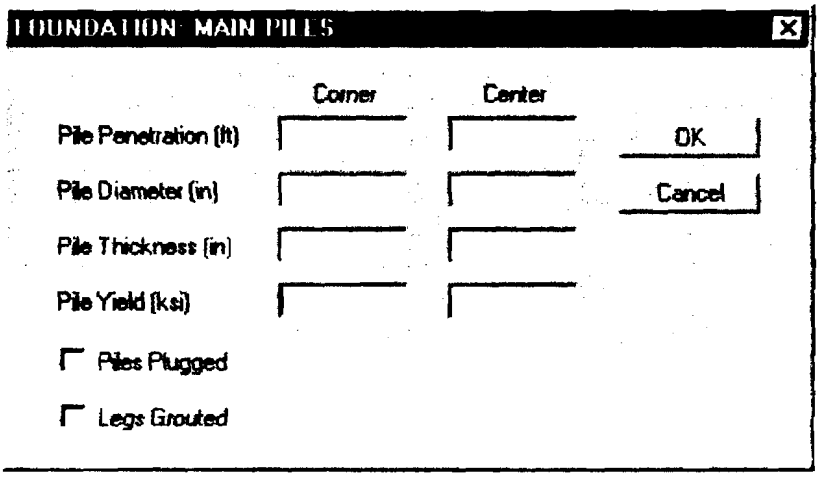

Figure 3-39: Main Pile Input Dialog Box

The user then enters diameter, wall thickness, penetration and, if desired, a specific steel yield strength different from that specified in STRUCTURE MATERIALS. In addition, the user should specify if piles are plugged, or if the jacket leg-pile annulus is grouted. As with deck and jacket legs, a user may specify corner piles as being different from center section piles for jackets with more than four legs.

NOTE: TOPCAT is intended for the analysis of platforms which are have piles of fairly uniform diameter and thickness inserted through the jacket legs. Leg (pile) performance in this case is assumed to be governed by the axial demand/capacity ratio at the pile head, as this is where axial force from overturning will be the greatest. Platforms which are supported only by skirt piles can be analyzed with TOPCAT, but the user must (1) provide data on a "dummy" main pile configuration, i.e. perhaps a pile with a penetration of one ft, and (2) check the axial capacity of the platform legs against overturning moment by hand. The weight of the "dummy" main piles must be subtracted from the structure weight.

TUTORIAL: For the example platform, the user would enter:

- Diameter: 72
- Thickness: 1
- Penetration: 150
- Plugged: yes
- Grouted: yes

LOCAL PARAMETERS/Skirt Piles

The following dialog box would appear:

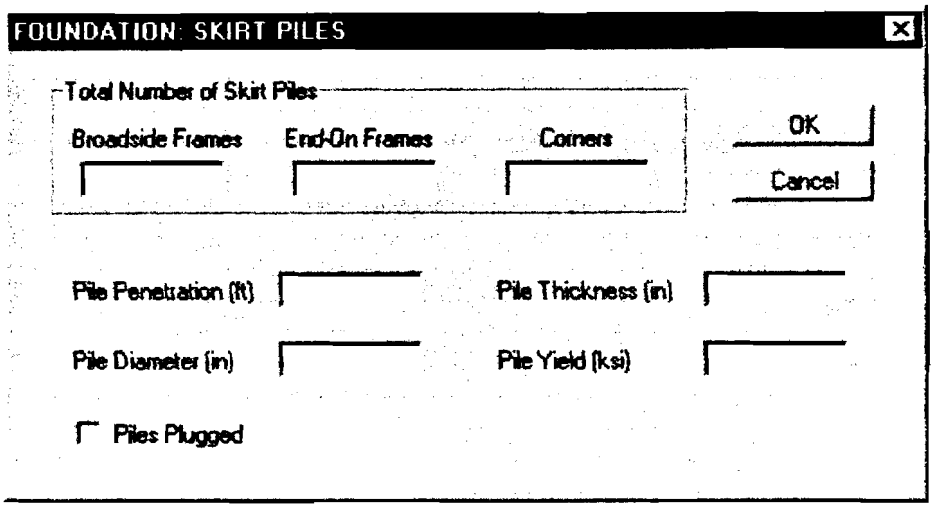

Figure 3-40: Skirt Pile Input

TOPCAT assumes that all skirt piles will be of the same type (diameter, thickness, penetration, steel yield stress, plugged/unplugged). Skirt piles are declared according to their location in the plan of the foundation.

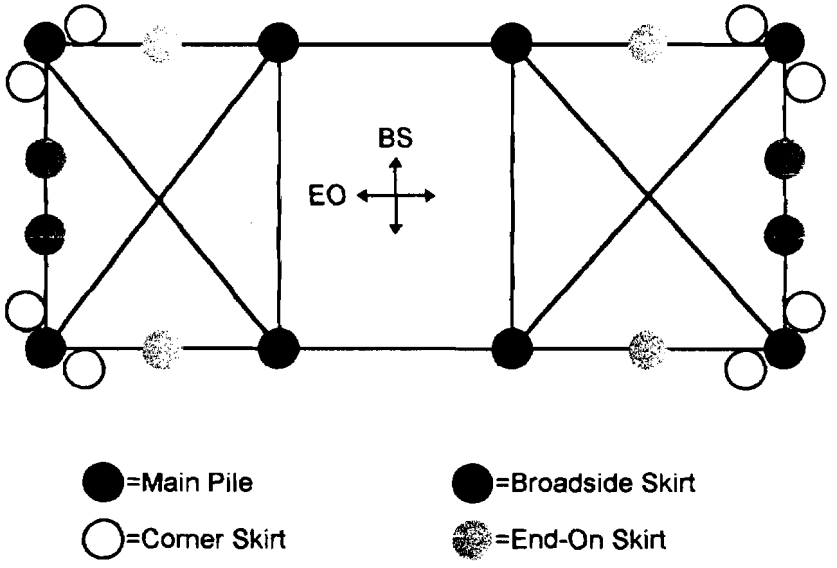

Figure 3-41: Plan View of Foundation with Skirt Pile Locations

Skirt piles which are located at the outer corners of a platform are declared as corner skirt piles; these piles are assumed to provide overturning resistance against moments on either the end-on

or broadside axis. Skirt piles which are located away from the outer corners of the platform, but within the perimeter (outside) end-on frames, should be specified as being in the end-on frames. These piles are assumed to provide resistance against overturning about the end-on axis only. Similarly, piles which are in the perimeter (outside) broadside frames, but are not at the outer corners, should be declared as being in the broadside frames. These piles are assumed to resist overturning about the broadside axis only.

LOCAL PARAMETERS/Conductors

The program displays the following dialog box:

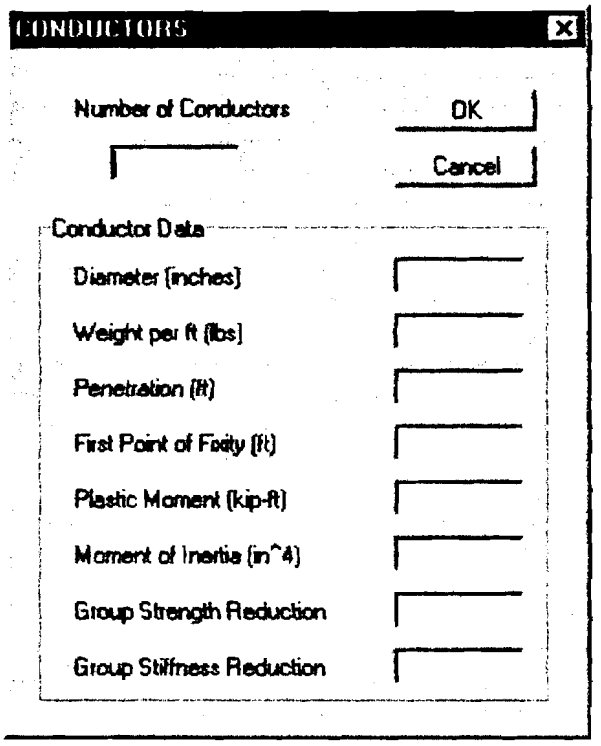

Figure 3-42: Conductor Input Dialog Box

The effect of well conductors on the lateral foundation strength and stiffness of a platform can be accounted for by TOPCAT (see Appendix G). Conductors are assumed not to possess strong vertical fixity and hence are not considered to supply vertical strength and stiffness.

NOTE: Users not wishing to include conductor contributions to foundation strength and stiffness can ignored this input. However, this input must be supplied when performing a earthquake analysis, to ensure the mass of conductors is correctly determined (simply inputting the information will not automatically include conductor contributions to foundation strength and stiffness; that calculation is activated as an analysis option, discussed later). Users simply wishing to enter data on conductors for the purpose of determining drag forces from waves and current on them must supply the more generic input described below in APPURTENANCE AREAS AND MARINE GROWTH.

The user supplies the total number of conductors, and then information on the type of conductor. As some platform operators have taken to filling unused conductors with grout, the user is asked

to supply a plastic moment capacity and cross-section moment of inertia for the conductor, in lieu of supplying a thickness and having the program calculate the plastic moment capacity and cross-section moment of inertia. In addition, the user is asked to supply biases for both the entire conductor group strength and stiffness. These biases are simple percentage modifiers, and are intended to account for possible group strength and stiffness degradation due to the close proximity of the conductors to one another. The default values are unity.

The first point of fixity refers to the height distance between the mudline and the first point of rigid attachment or framing for conductors in the platform structure. If the conductors are framed rigidly at the mudline, this distance is zero. TOPCAT does not account for gaps or flexibility of conductor framing; the program returns the approximate lateral load the conductor frames must withstand in order to fully mobilize the lateral capacity of each conductor. This must be checked separately by the user.

TUTORIAL: the example platform has no conductors, so this entry may be ignored.

LOCAL PARAMETERS/Mudline Elements:

The program displays the following dialog box:

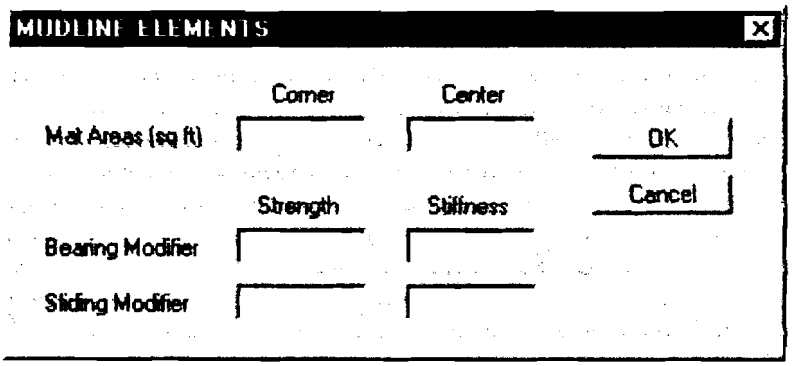

Figure 3-43: Mud Mat, Sliding and Bearing Modifiers Input

The user can supply information on mud mats for the purpose of including the strength and stiffness contributions of these components to the platform. Mud mats provide both sliding and vertical resistance and foundation level. The program can also be instructed to include the strength and stiffness contributions of mudline horizontal braces for the purpose of resisting sliding and overturning; the program makes use of the information supplied by the user for foundation level horizontal braces. These features are activated as analysis options, described later.

The bearing and sliding modifiers are simple percentage changes in unit soil sliding and bearing resistance. These resistances are discussed in Appendix G.

Mud mats are input approximately as square areas located at the base of corner and center piles. The program idealizes their area of action as shown in Figure 3-44.

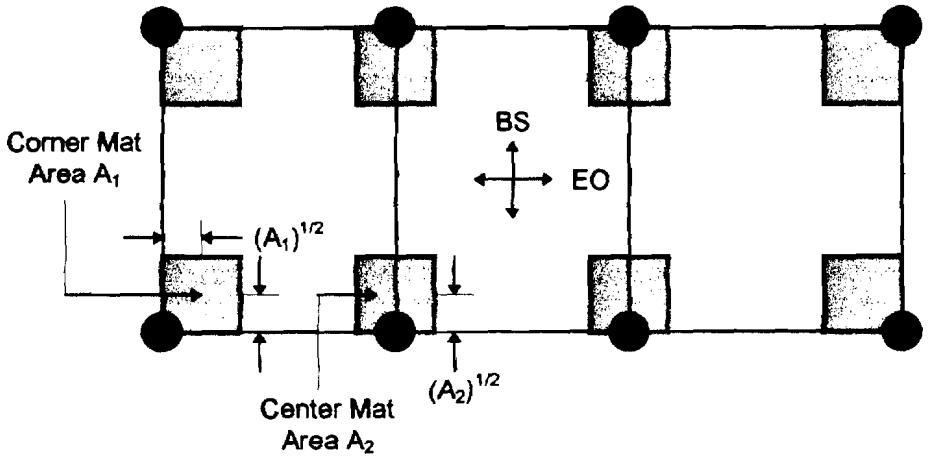

Figure 3-44: Mud Mat Locations Assumed by TOPCAT

When formulating the strength and stiffness contributions of mud mats and mudline braces, TOPCAT assumes connections between these elements and the platform are (1) rigid and stronger than the component, (2) local flexibility of the element is ignored and (3) yielding is assumed to occur in the soil beneath the element. It is left to the user to determine the applicability of these assumptions. To aid in this determination, TOPCAT returns the effective surface forces on mud mats and mudline braces when they are active as foundation elements due to sliding and vertical displacement of the platform. These surface forces may be used to check the mats and mudline braces and other platform components to which they are attached.

TUTORIAL: the example platform does not have mud mats in place, so this input may be ignored.

LOCAL PARAMETERS/Decks and Boat Landings

The user can supply projected areas and masses of decks and boat landings, so that hydrodynamic and aerodynamic loads can be calculated for these components, and so their masses can be accounted for in a modal analysis. Decks attract load to the top of the deck bay, while boat landings attract load to the top of the jacket.

When this item is selected, the program will first display the dialog box shown in Figure 3-45. Projected areas should be the approximate vertical area the deck (and structures and equipment on the deck) presents to both the broadside axis and the end-on axis, as shown in Figure 3-46. The weight of the deck should include all structural steel weight, equipment weights, and any live load the user wishes to include. Decks can be input in any order; there can be a maximum of five deck entries.

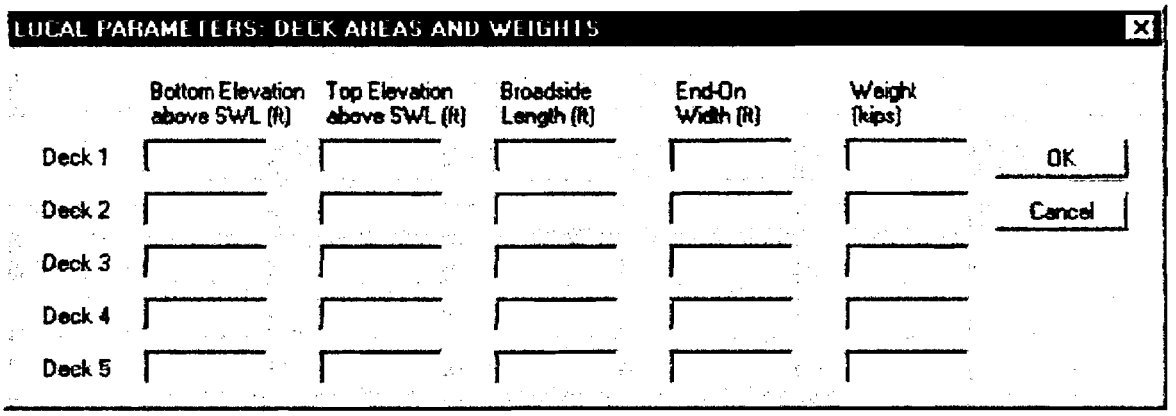

Figure 3-45: Deck Projected Areas and Weights

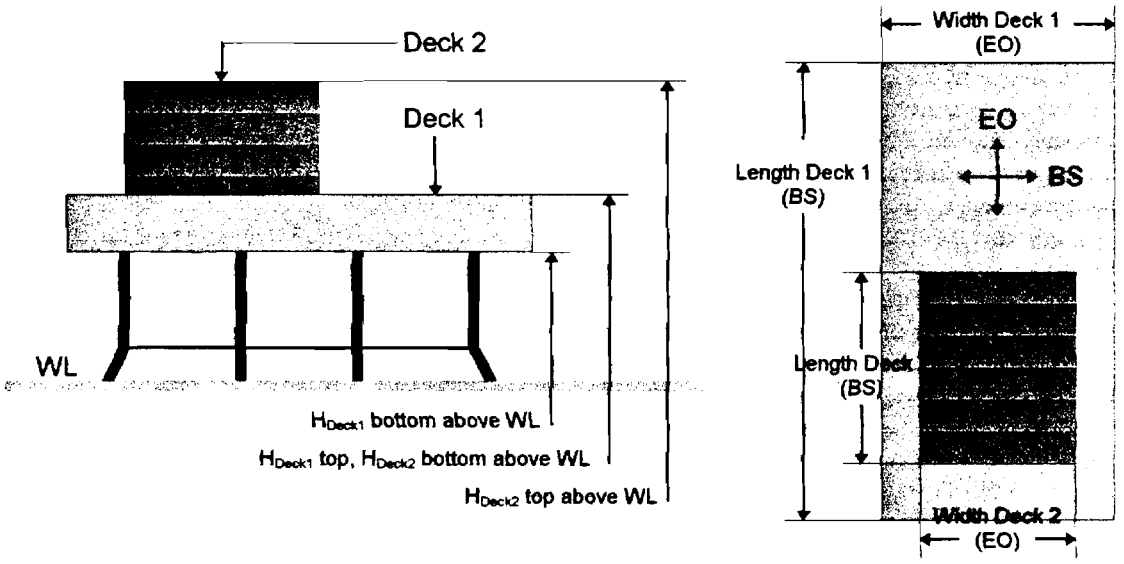

Figure 3-46: Projected Area Determination for Decks

After decks have been input, the program will display the following dialog box:

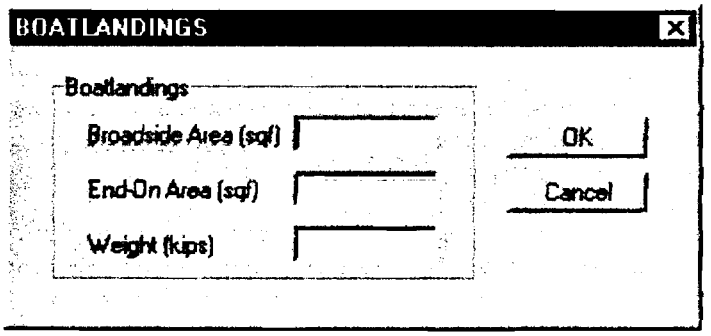

Figure 3-47: Boat Landing Projected Areas Input

The user can input the broadside and end-on projected areas of any boat landings, and the total weight (including added mass, if an earthquake analysis is being performed) of the boat landings. These areas are assumed to be lumped at the calm waterline.

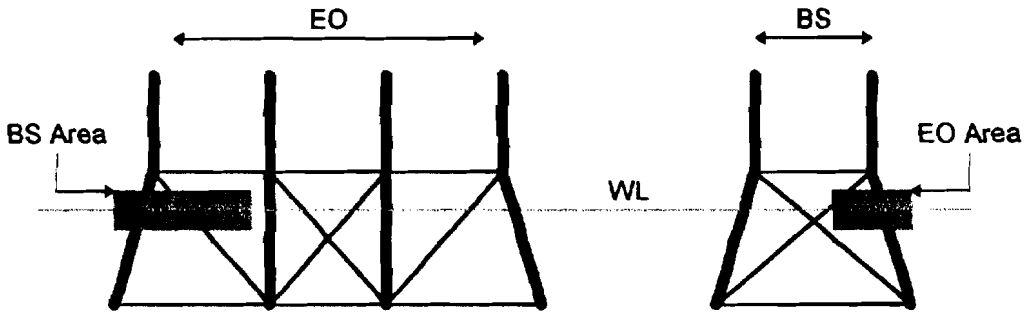

Figure 3-48: Boat Landing Areas

TUTORIAL: the example platform has one deck. The bottom of the deck is at +40 ft, and the top is at +65 ft. The BS and EO distances are both 100 ft. The weight of the deck is 5,000 kips. Make these entries for Deck 1 and click OK. The platform has no significant boat landings, so boat landing input may be ignored.

LOCAL PARAMETERS/Appurtenance Areas and Marine Growth

After selecting this item, the program will display the dialog box shown in Figure 3-49:

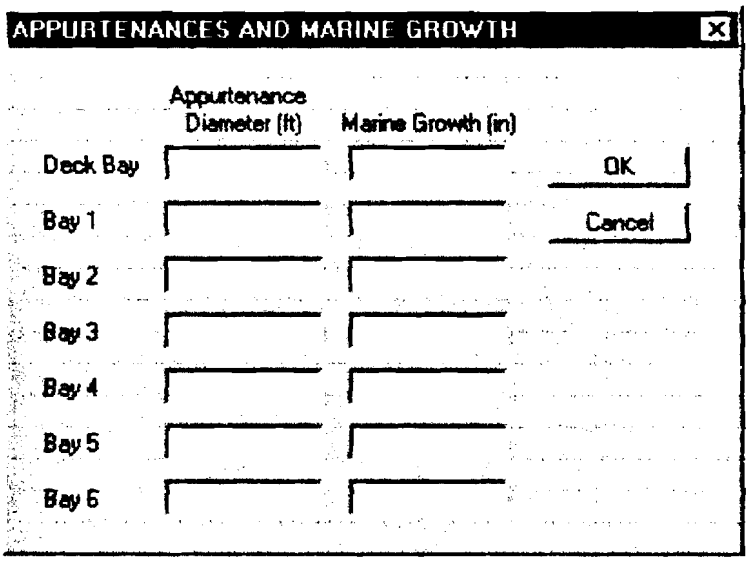

Figure 3-49: Appurtenances and Marine Growth

The user can supply information on appurtenance projected areas and marine growth. Appurtenances are any equipment attached to the platform below the deck; conductors, piping and anodes are examples of appurtenances. Marine growth represents the amount of marine

growth, expressed in inches, on platform structural members; marine growth will result in additional drag and added mass effects.

TOPCAT allows a user to enter an equivalent total width of appurtenances in each bay, including marine growth on appurtenances. The program calculates the drag forces on appurtenances in each bay based on this width, as shown in Figure 3-50.

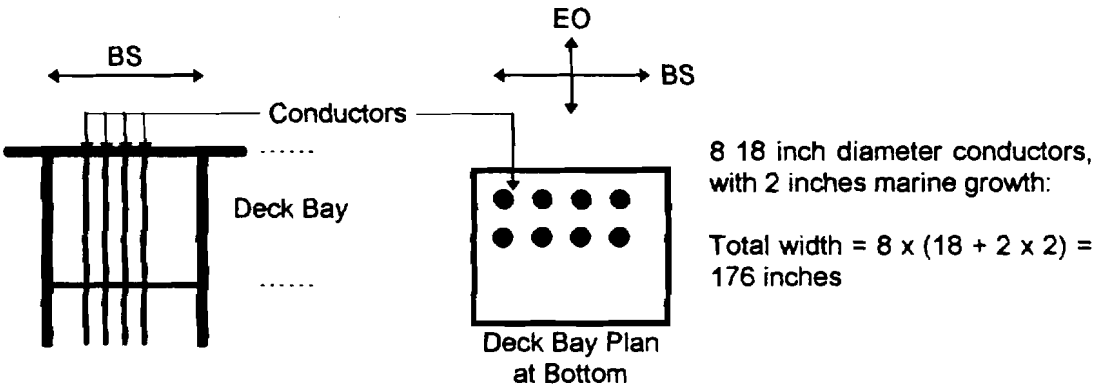

Figure 3-50: Equivalent Width of Appurtenances in a Bay

The separate marine growth entry applies only to structural members. Any specified marine growth is added (x 2) to the diameter of all structural members in the bay (including horizontal members at the bottom of the bay) for the purpose of calculating increases in drag forces and hydrodynamic added mass.

If there are more than six jacket bays, dialog boxes will appear until the user has had an opportunity to enter data in all bays.

NOTE: the appurtenance equivalent width is not used in an earthquake analysis. It is only used to estimate drag forces for storm and fatigue analyses.

TUTORIAL: the example platform has no well conductors, but it does have vertical members in the first and second jacket bay which are used to stabilize the X-braces, as shown in Figure 3-51. These members should be input as appurtenances, to ensure their drag contribution is included (the program does not model them structurally).

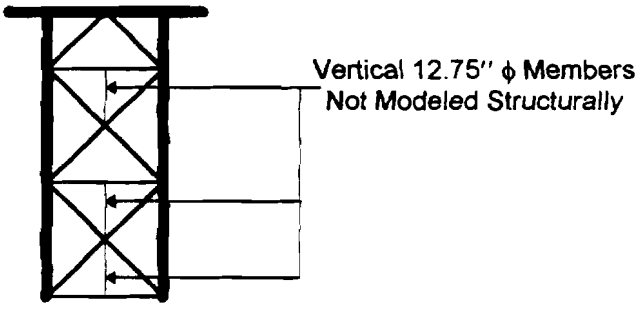

Figure 3-51: Vertical Members in Jacket of Example Platform

The members in the first jacket bay only span half of the bay elevation, so to be conservative they will be input as spanning the whole elevation. There are vertical members in each frame, so the total equivalent width will be: 4 x 12.75 / 12 = 4.25 ft for both the first and second jacket bays. The platform has no appreciable marine growth. Enter these values and click OK.

LOCAL PARAMETERS/Equipment Vibration Period

TOPCAT allows a user to determine deck-level acceleration response for mounted equipment periods of vibration when performing an earthquake analysis, as described in Appendix E. These deck-level accelerations are calculated using the response of the platform to an API (1993) response spectrum earthquake; the accelerations are determined for platform response on both principal horizontal axes and the vertical axis. Equipment response is determined as part of an earthquake analysis; it is not a separate analysis.

TOPCAT currently allows a user to only determine response for a single equipment period at a time. Future versions of the program will generate deck-level acceleration response spectra which cover a range of periods.

When this item is selected, the following dialog box appears:

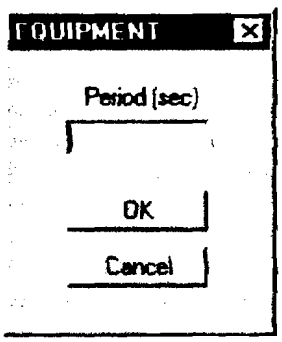

Figure 3-52: Equipment Period Input

The user inputs the equipment period, and clicks OK. Deck-level accelerations will be calculated for this period when an earthquake analysis is performed.

TUTORIAL: for the example platform, the user may leave this value unassigned.

3.7 Specifying Storm, Earthquake and Fatigue Parameters for Analysis Cases

With the structure and soil defined, the user can now proceed to defining the load sources the platform will be analyzed for; i.e. what wave, current and wind for a storm analysis, what response spectrum ZPA for an earthquake analysis, and what fatigue wave height distribution and stress parameters for a fatigue analysis.

NOTE: the user need only specify those load sources for which an analysis is desired; for example, if no earthquake analysis is being performed input for earthquakes can be ignored.

ENVIRONMENT/Wind, Wave and Current

The user can specify storm wind, wave and current (and storm surge), from which loads will be calculated based on platform projected areas. The program automatically assumes there will be two load cases: combined wind, wave and current forces from the user-specified conditions on the end-on axis, and combined wind, wave and current forces from the user-specified conditions on the broadside axis.

When this item is selected, the program displays the following dialog box:

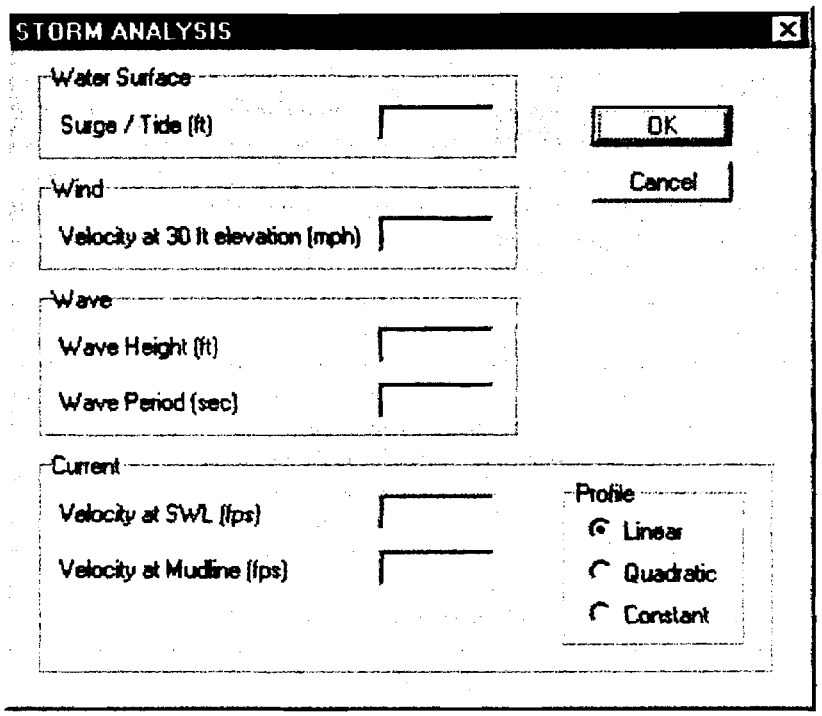

Figure 3-53: Wind, Wave and Current Input

Details on how wind, wave and current loads are calculated by TOPCAT are contained in Appendix A. The basic processes will be summarized here. The magnitude of the wind load is based on the unsubmerged projected areas of the decks, and is calculated in accordance with API Section 17 (1993) for both end-on and broadside directions. To calculate hydrodynamic loads, the program first calculates wave crest horizontal velocities for the wave height and period entered, using either Stokes Fifth-Order theory or Cnoidal theory, depending on the depth, wave height and period. These horizontal velocities, modified for directional spreading, are then summed with the current velocities (which are modified by current blockage). The total velocities are then used to calculate hydrodynamic loads. Deck loads and boat landing loads are calculated using API Section 17 (1993) procedures, while loads on members and appurtenances are calculated using the velocity-dependent component of Morison's equation. Members and appurtenances are modeled as equivalent vertical cylinders in line with the wave crest.

Wind forces are based on the gust velocity at 30 ft elevation. The user may specify current velocities as constant with depth, linear variation or quadratic variation with depth; the current specified by the user is stretched to the wave crest.

Use is automatically made of drag coefficient scaling within two fluid velocity heads of the free surface. The drag coefficient is scaled from zero at the free surface to full value at a depth of two velocity heads. Users may switch off this scaling under analysis options, described later.

TUTORIAL: enter storm conditions from API (1993). For the Santa Barbara/San Pedro Channel area, a storm tide of six ft is recommended, along with a wave height of 45 ft and a current surface velocity of 3.2 ft/sec. Based on a wave steepness of 1/20, use a period of 11 sec. Assuming the current is constant with depth. Enter these values, then click OK. These values will be used to provide storm analysis results in Section 3.9.

ENVIRONMENT/Fatigue

The user may specify parameters for a fatigue analysis of the main diagonal tubular joint connections. This analysis is conducted using the simplified fatigue analysis approach described in Appendix F. Stresses are determined for the end connections of tubular joints for storm loads on both principal axes of the platform; these stresses are assumed proportional to wave height. The stresses are then used together with a long-term wave height distribution to determining the accumulated fatigue damage to the main diagonal end connections in both the end-on and broadside frames.

When selected, the program will display the following dialog box:

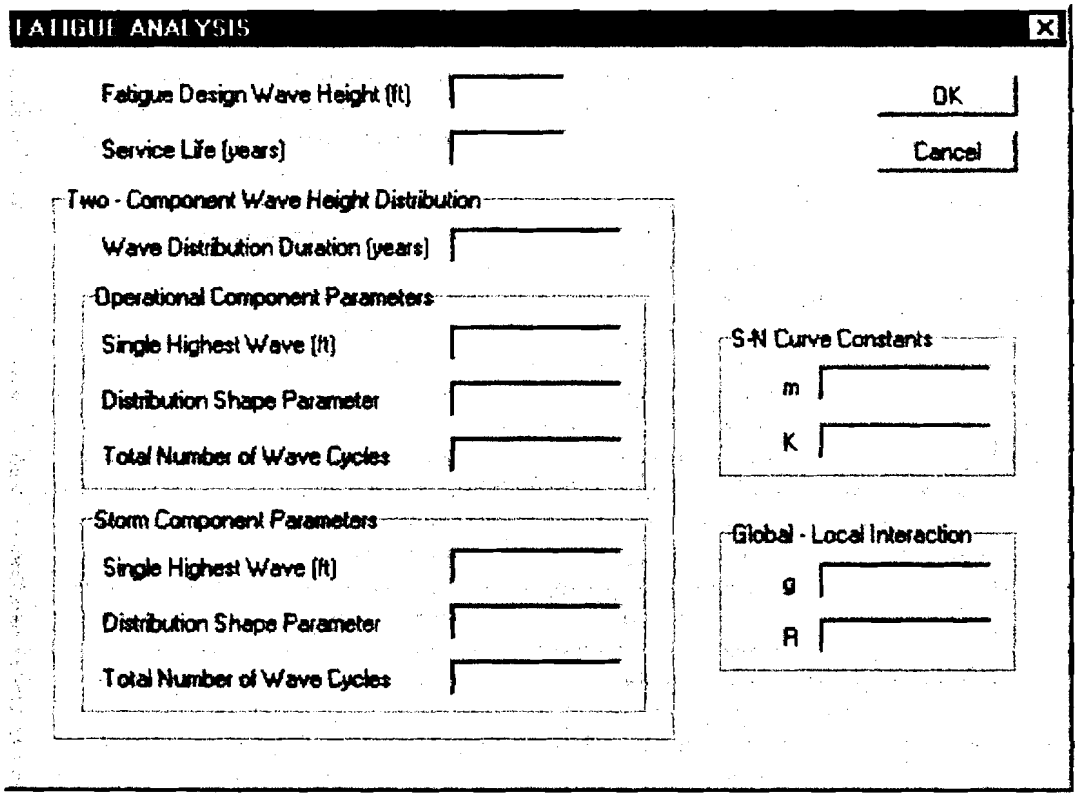

3-54: Fatigue Analysis Parameters

NOTE: users must declare tubular joints, and assign joint types to main diagonal braces, for this analysis option to function.

The fatigue design wave height defines the load pattern which will be used to determine the baseline stresses in the end connections. The wave height distribution information is specified in accordance with the wave height distribution used. A two-part distribution is assumed, like the one shown below:

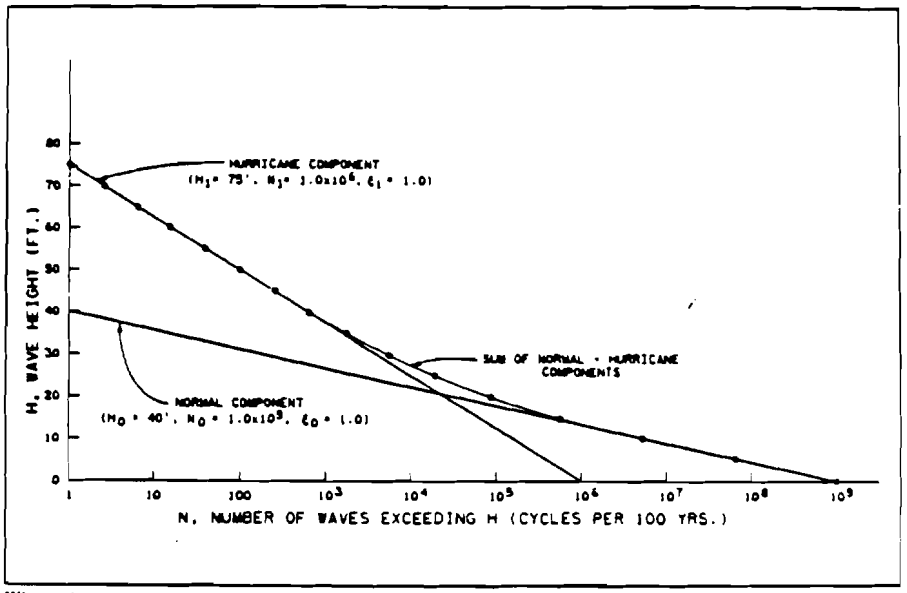

Where: H_n is the maximum normal wave height over period T.
H_1 is the maximum hurricane wave height over period T.
N_n is the number of wave cycles from normal distribution over period T.
N_1 is the number of wave cycles from hurricane distribution over period T.
T is the duration of the long-term wave height distribution.
ξ_n is the parameter defining the shape of the Weibull normal distribution. Value of 1.0 corresponding to the exponential distribution results in a straight line.
ξ_1 is the parameter defining the shape of the Weibull hurricane distribution.

Figure 3-55: Wave Height Distribution

S-N curve components m and K are taken from the S-N curve assumed to govern the connections' behavior. m is the slope of the curve, and K is the curve intercept. The curve is of the type shown in Figure 3-56. The global-local parameters are intended to modify the baseline stresses from the analysis of the platform using the fatigue design wave height. R is a parameter which related peak stress to stress range. g related the stress in a member to the wave height. Both of these parameters are described in Appendix F.

NOTE: it is important for users to recognize that this fatigue analysis is extremely approximate. It is intended to provide users with an indication as to which components in the platform are most vulnerable to fatigue damage. It is not expected to provide actual fatigue lives; the fatigue lives calculated should be taken as relative values.

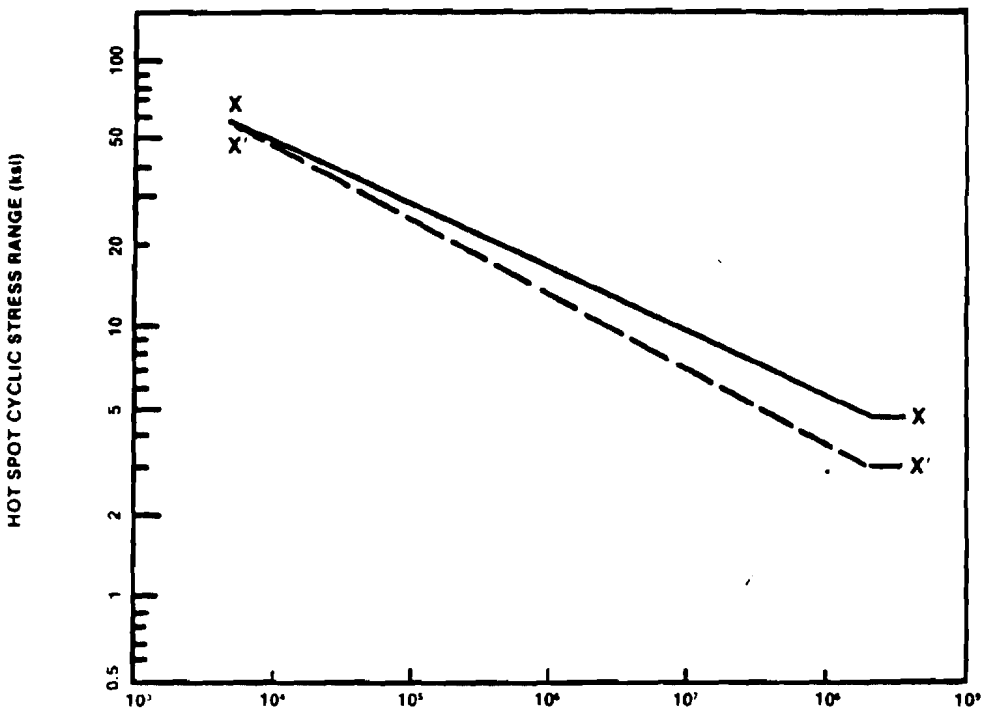

NOTE — These curves may be represented mathematically as

$$N = 2 \times 10^6 \left(\frac{\Delta\sigma}{\Delta\sigma_{ref}}\right)^{-m}$$

where N is the permissible number of cycles for applied cyclic stress range $\Delta\sigma$, with $\Delta\sigma ref$ and m as listed below.

CURVE	$\Delta\sigma ref$ STRESS RANGE AT 2 MILLION CYCLES	m INVERSE LOG-LOG SLOPE	ENDURANCE LIMIT AT 200 MILLION CYCLES
X	100 MPa (14.5 ksi)	4.38	35 MPa (5.07 ksi)
X'	79 MPa (11.4 ksi)	3.74	23 MPa (3.33 ksi)

Figure 3-56: S-N Curve

TUTORIAL: for the example problem, enter the following values:

- Fatigue Design Wave Height: 45
- Service Life: 30
- Wave Height Distribution Duration: 100
- Operational Wave Component Parameters: 20, 1, 1000000000
- Storm Wave Component Parameters: 45, 1, 1000000
- *m*: 3.74
- *K*: 179000000
- *g*: 1.3
- *R*: -0.5

These parameters will be used to generate fatigue analysis results in Section 3.9 of this tutorial.

ENVIRONMENT/Earthquake

The program displays the following dialog box:

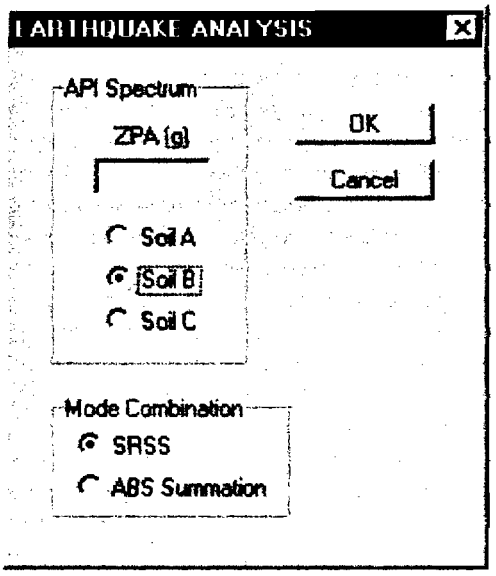

Figure 3-57: Earthquake Analysis Input

TOPCAT determines earthquake forces from modal response spectrum analysis, as described in Appendix E. The user can specify the API response spectrum ZPA and soil type (Figure 3-58), and the modal combination rule to use. Loads are determined for response on all three axes of the platform (end-on, broadside and vertical). The end-on and broadside responses are each combined with the vertical response to get the total loads on the platform foundation. Parameters selected here will also affect the mounted equipment accelerations if an equipment period has been supplied.

TUTORIAL: The user should make the following selections for the example analysis file:

- ZPA: 0.5
- Soil Type: B
- Modal Combination: SRSS

These parameters will be used to generate earthquake analysis results in Section 3.9.

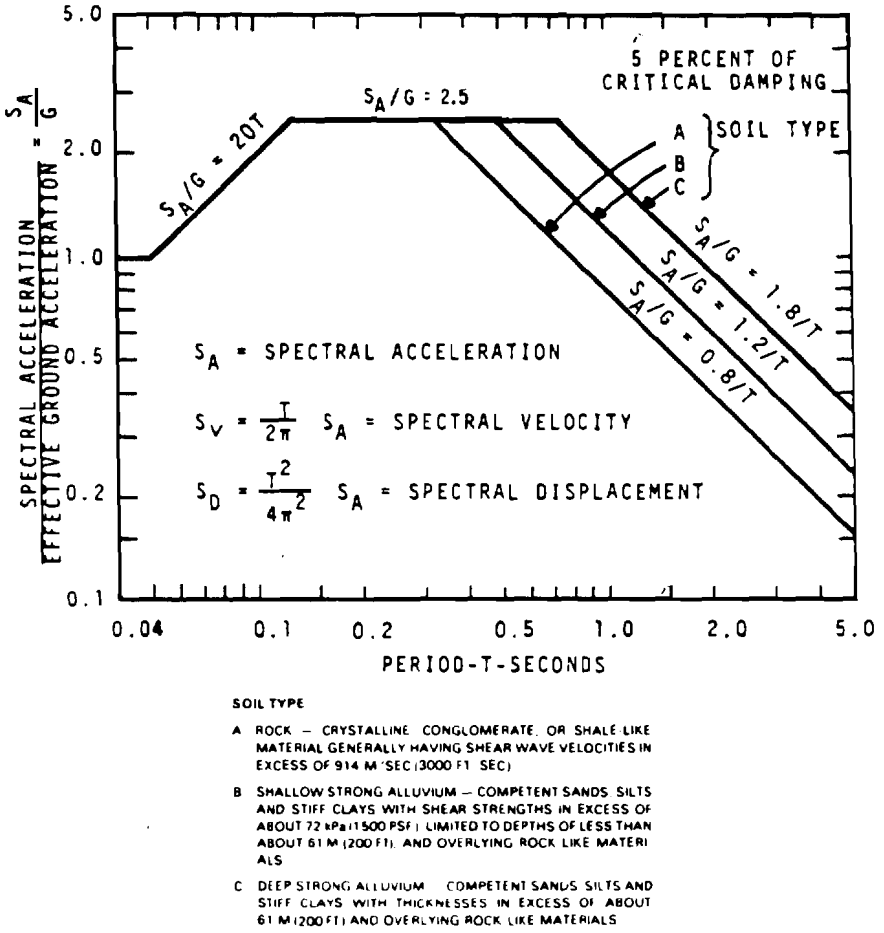

Figure 3-58: API Response Spectrum

3.8 Analysis Options

After completing construction of an input file, the user has the option of specifying some additional analysis preferences. These options are not stored in the input file, but are only active during the analysis session. These options are:

Use Design C_D/C_M:

TOPCAT defaults to a linear scaling of both the drag coefficients and the added mass coefficient within two velocity heads of the water surface. This scaling may be turned off, in which case C_D and C_M will be treated as constants.

Design Diagonal Braces:

The user need not specify the diameter and thickness of main diagonal braces. Approximate brace sizes will be determined for the platform by the program, and then used in the strength calculations. These braces are sized according to the following criteria:

$kL/r = 40$
$D/t = 33$

Note that a user must still declare the number of braces, orientations, and bracing configurations.

Turn Tubular Joints Off:

The capacities of tubular joint end connections on main diagonal braces will be ignored when calculating the effective axial capacity of the brace. This option is typically used when data on joints has been entered, and it has been found that the joints are much stronger than the attached main diagonal braces, thus distorting the demand-capacity graphs (see Section 3.9).

Always Use Stokes Fifth-Order Theory:

The program defaults to using Cnoidal wave theory for certain conditions (see Appendix A). If this option is selected, the program will always use Stokes Fifth-Order theory to calculate wave horizontal velocities.

Include Conductor Strength and Stiffness:

Conductor contributions to foundation lateral strength and stiffness will be included in an analysis. Note that this option does not have to be selected for an earthquake analysis simply to include the mass and added mass of conductors.

Include Mudline Element Effects:

The approximate contributions of mudline elements (horizontal braces and mud mats) to foundation lateral and overturning strengths and stiffnesses will be included in the analysis.

Turn Off Local Brace Loads:

Local load effects on tubular brace buckling capacity will be ignored. This option is useful in that it allows a user to calculate brace axial capacities unaffected by local loads from waves and current and from earthquake local acceleration, in order to study how axial capacity is changing in the presence of the local load.

When ANALYSIS OPTIONS is selected, the following dialog box appears:

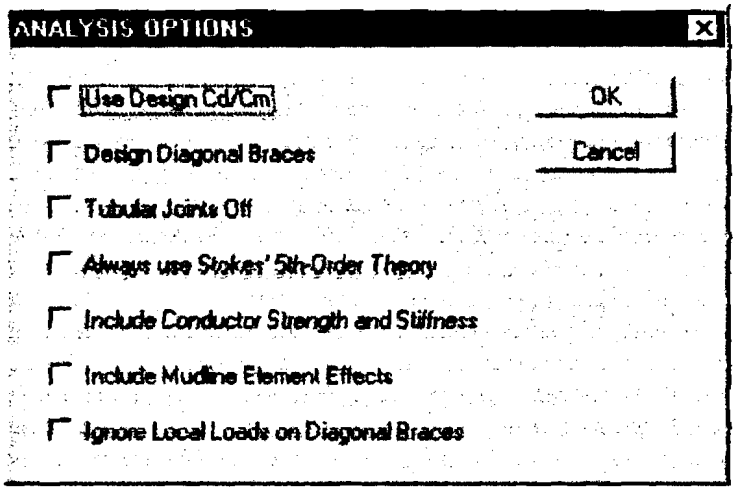

Figure 3-59: Analysis Options Input

The user may turn on or off any desired options simply by clicking the check boxes.

TUTORIAL: turn on use of design C_D/C_M, but leave all other options off.

3.9 Performing an Analysis and Obtaining Output

With the completion of all the modeling steps in Sections 3.3-3.7, and the selection of any analysis options in Section 3.8, the user is now ready to perform analyses of the input file and obtain output.

Prior to performing any calculations, it is always good practice to save newly-created input files. This ensures input data residing in the Excel environment will not be lost if the program hangs or causes other system faults.

To execute a run, simply select the desired calculation from the CALCULATION menu (Storm, Fatigue or Earthquake). TOPCAT will then read the input data, perform all necessary calculations, and then write data to tables and graphs. The user may then use the OUTPUT menu to review the graphs and tables, and use the FILE menu to print selected hardcopies of this output. In this fashion, a user can quickly perform repeated analyses of the same input file, varying loads, damage, and other analysis parameters, and quickly evaluate the results of changes.

For each type of analysis, TOPCAT will return output specifically associated with the analysis. TOPCAT has two types of output: (1) graphical output, by which important results of an analysis are highlighted in an easy-to-understand format, and (2) tabular output, by which the hard numbers for loads, capacities, and other numerical results are presented. The following sub-sections review the output available from TOPCAT.

TUTORIAL: at this point, the user may experiment by conducting storm, earthquake and fatigue analyses. Results based on the analysis of the tutorial platform are shown in the next section and Appendix T; the user may wish to compare results generated while experimenting with the

results in this tutorial. The user should review the following subsections, as well as try experimenting with the various analysis options.

OUTPUT/End-On or Broadside Demand/Capacity Graphs

The program will display a graph similar to the following:

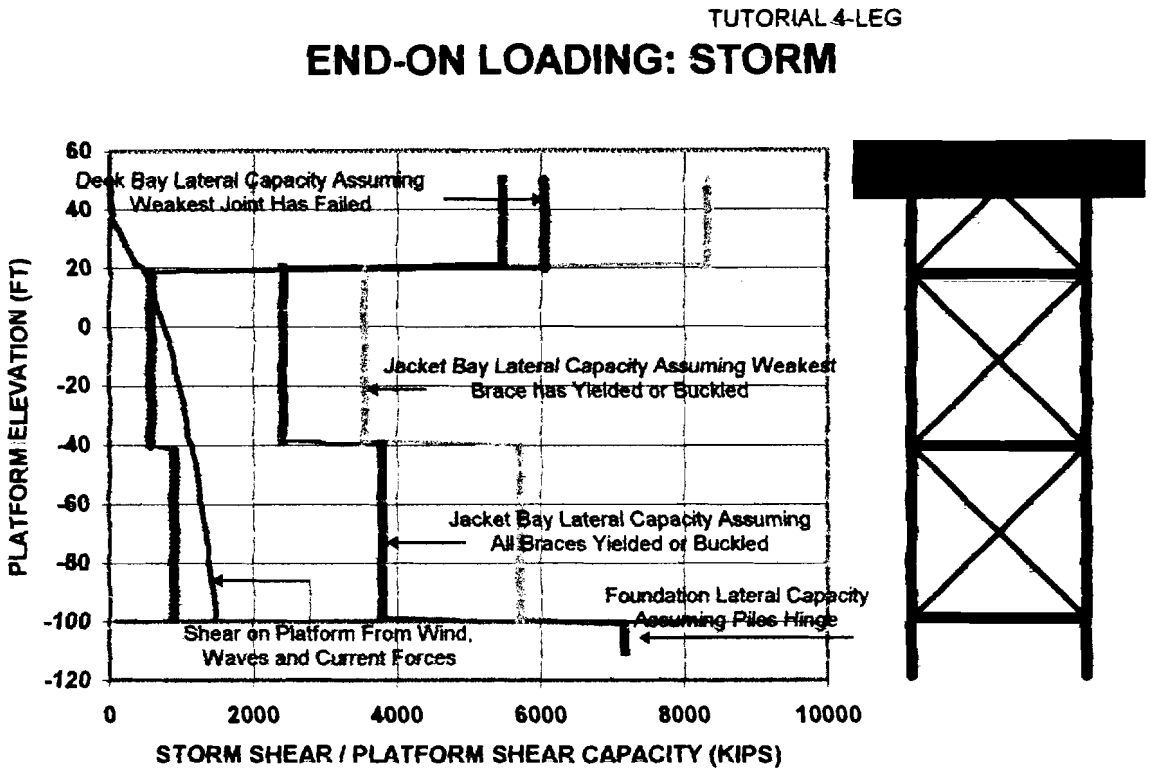

Figure 3-60: Demand/Capacity Graph (Tutorial Four-Leg Platform)

Demand/Capacity graphs are produced whenever a storm, fatigue or earthquake analysis is executed. These graphs depict the shear demand on the platform structure from lateral loads. In addition, they graphically display the capacity of the platform components (deck bay, jacket bays and foundation) to resist shear. Three "capacity" lines are produced: a lower-bound (green) line, an upper-bound (red) line, and a joint failure (black) line. For deck bays with no bracing and the foundation, the lower-bound and upper-bound capacities are the same, as only the completely plastic mechanism state is used to determine capacity. For braced bays, the lower-bound represents the capacity of the bay when the weakest brace reaches its axial capacity, while the upper-bound represents the capacity of the bay assuming all members have exceeded their yield or buckling loads. Note that if a post-buckling strength of less than 1.0 is specified for braces, the upper-bound capacity will likely be less than the lower-bound capacity. The tubular joint capacity line represents the capacity of braced bays assuming failure only occurs in the joints (i.e. no brace failure modes are considered); the line is the capacity of the bay when the weakest joint reaches its punching or pullout capacity. Unbraced deck bays and the foundation do not have a capacity line for joints, as the joint failure mechanism does not occur in these sections.

NOTE: no platform graphics are printed. The platform elevation shown in Figure 3-60 has been applied for illustrative purposes.

OUTPUT/Pile Axial RSRs

The program will display a graph as shown below:

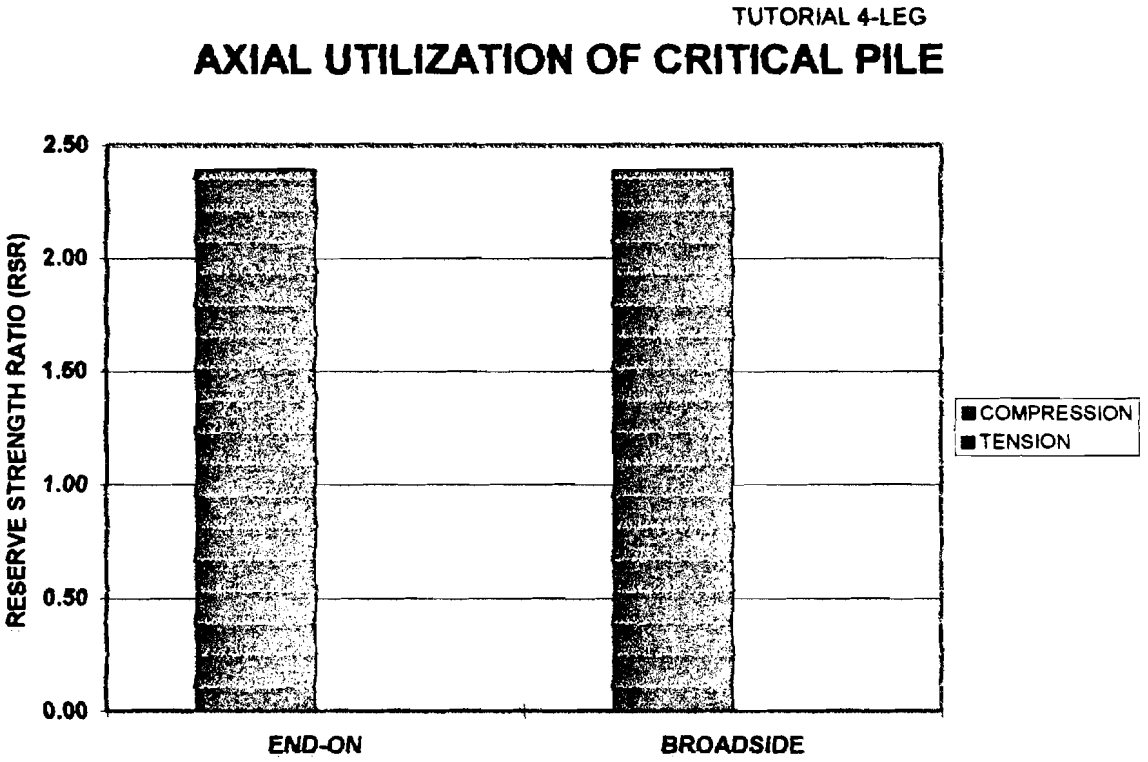

Figure 3-61: Axial Pile Reserve Strength Ratios (Tutorial Four-Leg Platform)

This simple bar chart depicts the average of pile reserve strength ratios, axial capacity / axial load, where the axial load is estimated by assuming the piles share loads from overturning or overturning and vertical force evenly. The graph is produced whenever a storm, fatigue or earthquake analysis is performed. If mats or foundation elements are active, the component of moment and vertical force carried by these elements will be deducted before the estimate is made of pile axial load.

NOTE: the graph does not shown negative RSRs. If the "pullout" force from overturning and vertical excitation is not strong enough to overcome the force from deck and structure weight, the RSR will be shown as zero.

OUTPUT/End-On or Broadside Reliability

The program will display a graph as shown below:

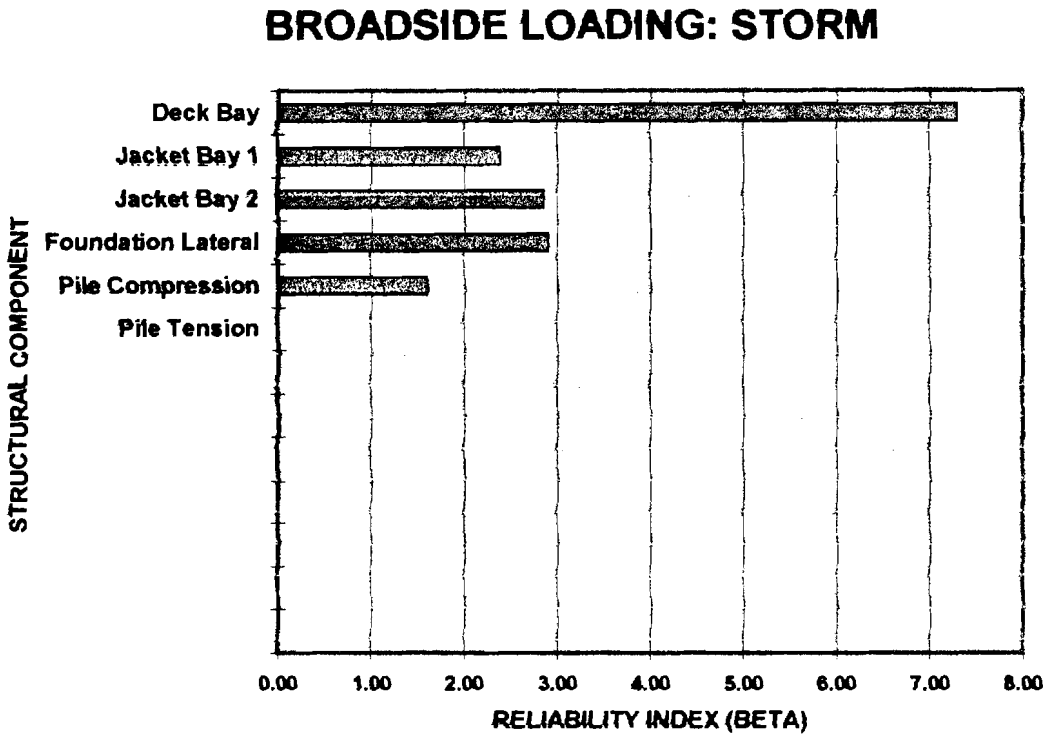

Figure 3-62: Reliability Graph (Tutorial Four-Leg Platform)

This graph depicts the reliability of platform components based on the calculated loads and capacities and including the uncertainty information supplied by the user. This graph is produced whenever a storm or earthquake analysis is performed. Deck bay and jacket bay reliability for lateral load is estimated using the mean load in the bay as the mean of the presumed component load distribution. Foundation lateral reliability is estimated using the base shear as the mean of the presumed load distribution. Pile axial compression and tension reliabilities are calculated using the average pile RSRs as the ratio of mean capacity to mean load. If the RSR is zero (i.e. no load) the reliability is returned as zero.

NOTE: TOPCAT can currently only produce reliability graphs for platforms with no more than nine jacket bays.

OUTPUT/Water Kinematics

The program will display a graph as shown in Figure 3-63. This graph shows the water particle horizontal velocities in the water column. This graph is produced when a storm or fatigue analysis is performed. The graph shows current velocity (no blockage modification), wave particle velocity (with directional spreading) and total horizontal velocity (wave plus current).

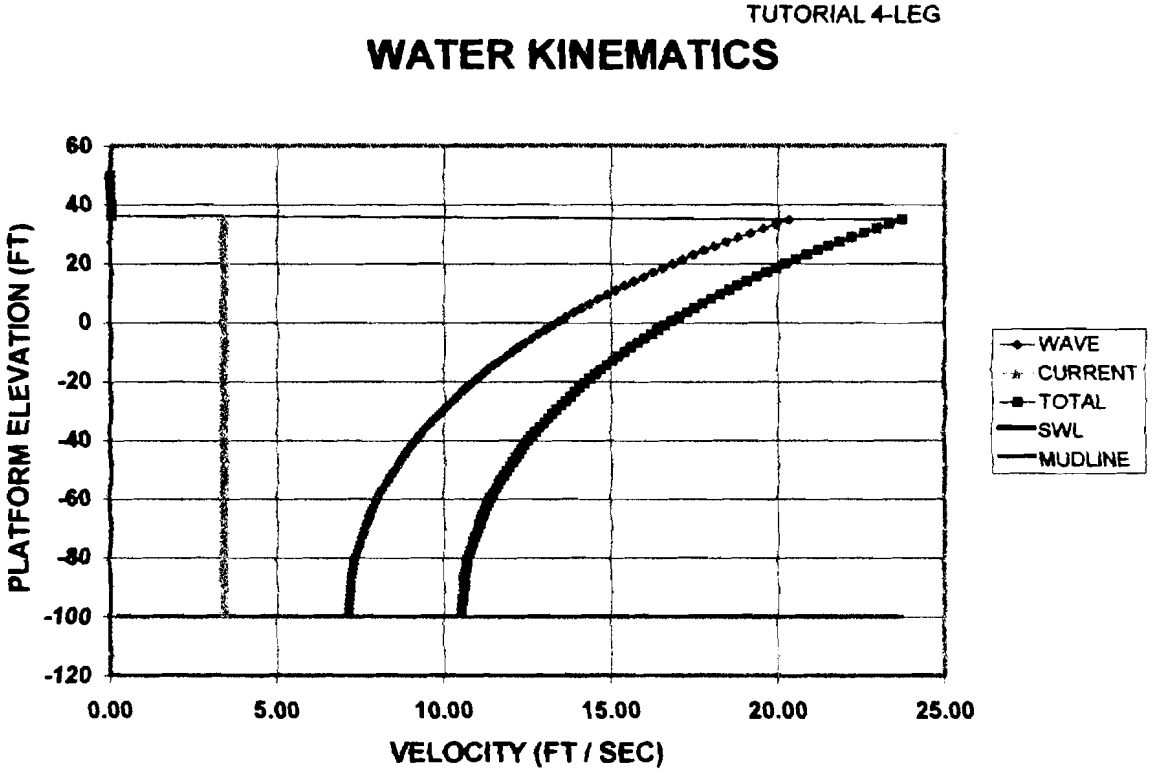

Figure 3-63: Water Kinematics Graph
(45 ft Wave, wkf = 1.0, Current 3.4 fps Constant with Depth)

OUTPUT/End-On or Broadside Mode Shapes

The program will display a graph as shown below:

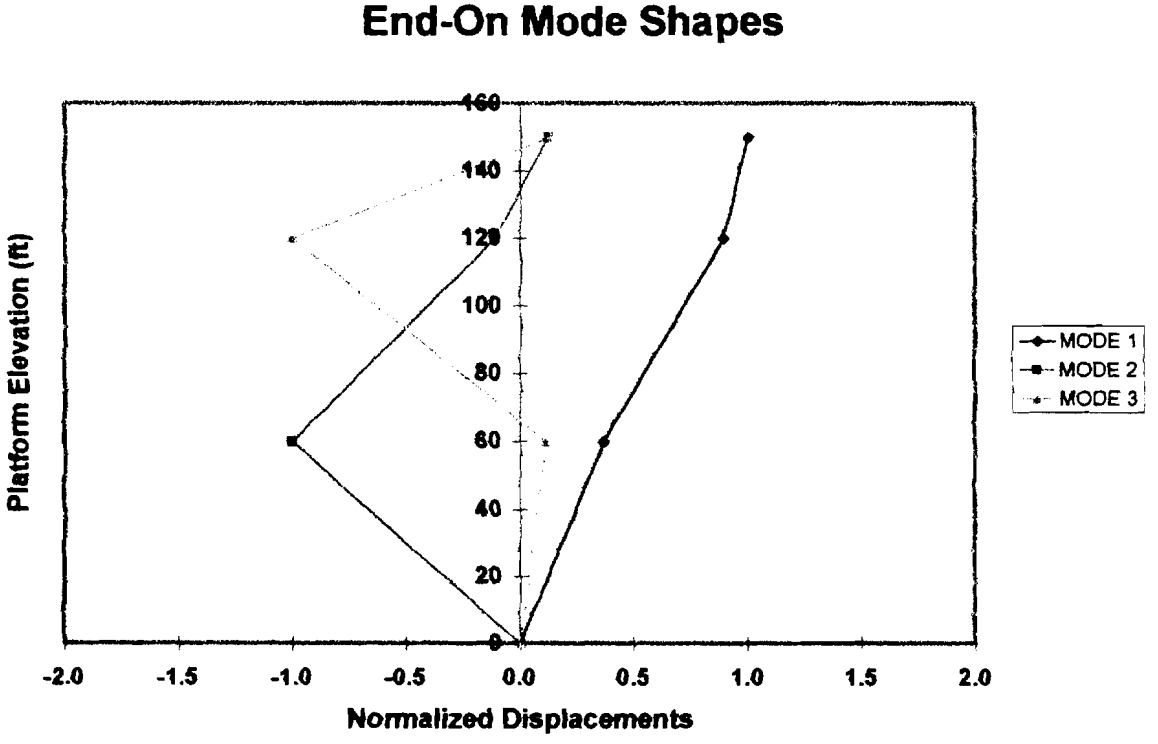

Figure 3-64: Mode Shapes (Tutorial Four-Leg Platform)

These mode shapes are determined for the platform in a fixed-base condition. The modal properties are used to calculate earthquake loads with a response spectrum. Mode shape graphs are produced when an earthquake analysis is performed.

OUTPUT/Fatigue Lives

The program will display a graph as shown:

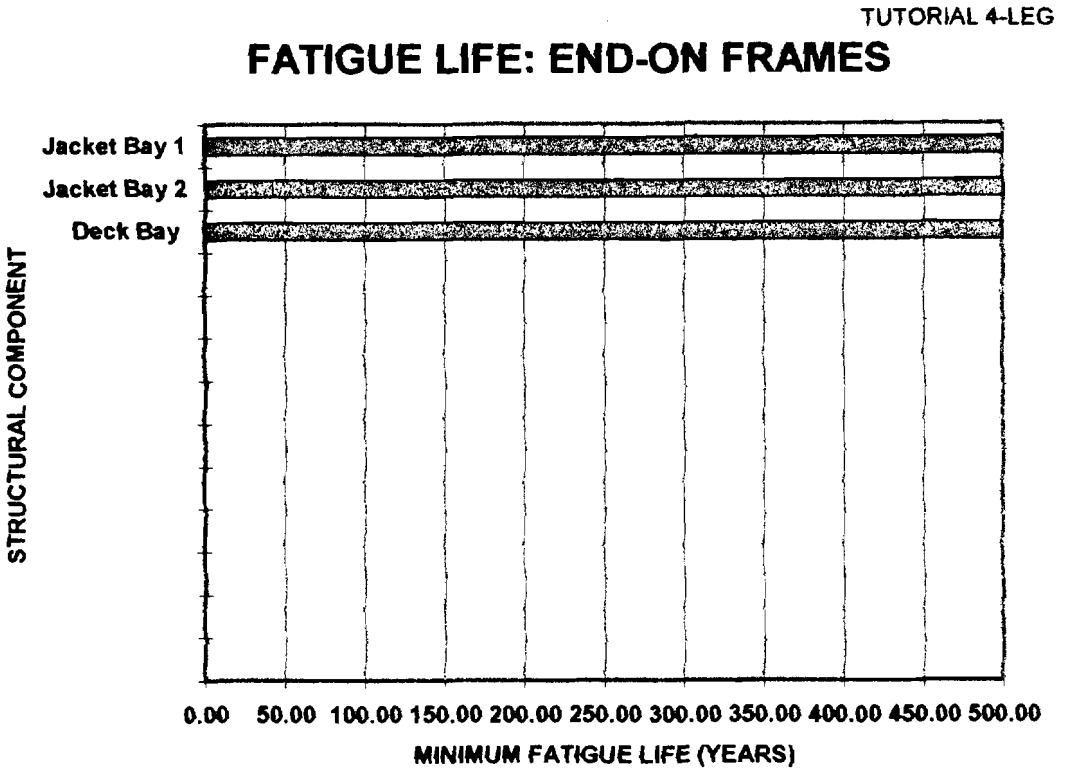

Figure 3-65: Minimum Fatigue Lives of All Joints in a Given Bay
(Tutorial Four-Leg Platform)

This graph depicts the shortest estimated joint fatigue life of all tubular joint connections in a given bay. The graph is produced each time a fatigue analysis is performed. The graph has a cap of 500 years on fatigue life for connections.

NOTE: as mentioned in previous sections, the fatigue lives calculated for joints should be taken as a relative measure. These are not absolute fatigue lives.

OUTPUT/Global Loads and Capacities

This table contains the numbers used to establish the demand/capacity and reliability graphs, and provide the user with additional information:

- Load-imposed vertical force and end-on/broadside overturning moments on the foundation.
- Platform vertical and end-on/broadside overturning capacities.

- Average pile loads, determined by assuming piles share overturning and vertical forces equally.

The table is produced each time a storm, fatigue or earthquake analysis is performed. A sample Global Loads and Capacities table is contained in Appendix T. This table comes from the analysis of the Tutorial Four-Leg Platform.

OUTPUT/Storm and Fatigue Parameters

This table contains a copy of all input information supplied by the user for storm or fatigue analysis definition. For a storm analysis, information on the wind, wave and current, water kinematic coefficients, and aero- and hydrodynamic load coefficients used in the analysis are returned to the user. In addition, it will inform the user what wave theory was used to calculate wave horizontal velocities. For a fatigue analysis, the parameters used to define the long-term wave height distribution, S-N curve, and stress range parameters are added to this table. This table is generated each time a storm or fatigue analysis is performed.

A sample Storm and Fatigue Parameters table is contained in Appendix T. This table comes from the analysis of the Tutorial Four-Leg Platform.

OUTPUT/Modal RSA and EQ Parameters

This table returns to the user all information input for earthquake analysis definition: response spectrum ZPA, spectrum soil type, and modal combination rule. In addition, it returns the numerical values of the mode shapes, periods, modal participation factors, modal masses, modal heights, lumped masses at each framing level, total vertical mass, and deck-level accelerations for a mounted equipment period. This table is generated each time an earthquake analysis is performed.

A sample Modal RSA and EQ Parameters table is contained in Appendix T. This table comes from the analysis of the Tutorial Four-Leg Platform.

OUTPUT/End-On or Broadside Fatigue Damage

These tables return the accumulated fatigue damage from a Miner's summation as well as the expected fatigue life for all main diagonal brace tubular joint connections in the platform. There is no cap on the expected life displayed for joints. The tables are generated each time a fatigue analysis is performed.

A sample Fatigue Damage table is contained in Appendix T. This table comes from the analysis of the Tutorial Four-Leg Platform.

OUTPUT/Structure Data/General Data

This table returns global and local parameter input to the user, as well as a platform steel tonnage estimate. The table is generated each time a storm or earthquake analysis is performed. The following input information is returned:

- Platform type, layout and dimensions, bay heights and numbers of diagonals
- Structure materials input
- Structure and load uncertainties
- Leg diameters and thicknesses
- Deck and boat landing areas and weights
- Appurtenance areas and marine growth on structural members
- Conductor characteristics

A sample General Data table is contained in Appendix T. This table comes from the analysis of the Tutorial Four-Leg Platform.

OUTPUT/Structure Data/Main Diagonals End-On or Broadside

These tables return user input on main diagonal braces, as well as brace axial capacities (including local load effects). This table is generated each time a storm or earthquake analysis is performed. A sample Main Diagonals table is contained in Appendix T. This table comes from the analysis of the Tutorial Four-Leg Platform.

OUTPUT/Structure Data/Tubular Joints

These tables return user input on tubular joint connection types, as well as the punching and pullout load capacities of the joints for loads on the branch axis. This table is generated each time a storm or earthquake analysis is performed. A sample Tubular Joints table is contained in Appendix T. This table comes from the analysis of the Tutorial Four-Leg Platform.

OUTPUT/Structure Data/Horizontal Frames

This table simply returns user input on horizontal bracing members. This table is generated each time a storm or earthquake analysis is performed. A sample Tubular Joints table is contained in Appendix T. This table comes from the analysis of the Tutorial Four-Leg Platform.

OUTPUT/Structure Data/Foundation

This table returns user input on the foundation. Soil layer input is returned, along with pile and mud mat areas. The axial and lateral pile head capacities and stiffnesses are also returned for each pile type, and lateral capacity and stiffness will be returned for conductors if they have been declared active for the foundation. The total projected area of mudline horizontal braces is returned. If mats and braces have been declared active, the effective surface forces these elements must resist are returned to the user. A sample Foundation table is contained in Appendix T. This table comes from the analysis of the Tutorial Four-Leg Platform.

CHAPTER FOUR: MODELING EXAMPLES

4.0 Introduction

The purpose of this chapter is to explain in further detail techniques by which less-standard platforms can be modeled using TOPCAT. The user is shown how to approximate framing configurations in bottom jacket bays where skirt piles are located. Data input for a tripod jacket is reviewed, and the special input for caissons is demonstrated for the user. This chapter assumes that a user is already familiar with the basic principals of the program, and has read and understood the tutorial in Chapter Three.

4.1 Diagonal Braces in Bays with Skirt Piles

Many older platforms with skirt piles have the skirts framed into locations in between the legs of the platform. This will lead to complications when deciding the appropriate framing configuration to use in a TOPCAT analysis, as TOPCAT automatically determines the length of diagonal braces based on the distances between jacket legs and the height of each bay.

If the configuration is similar to that shown in Figure 4-1, the bracing configuration for the diagonals around the skirt pile may be approximated as X-bracing. Similarly, the configuration in Figure 4-2 is modeled as a K-brace.

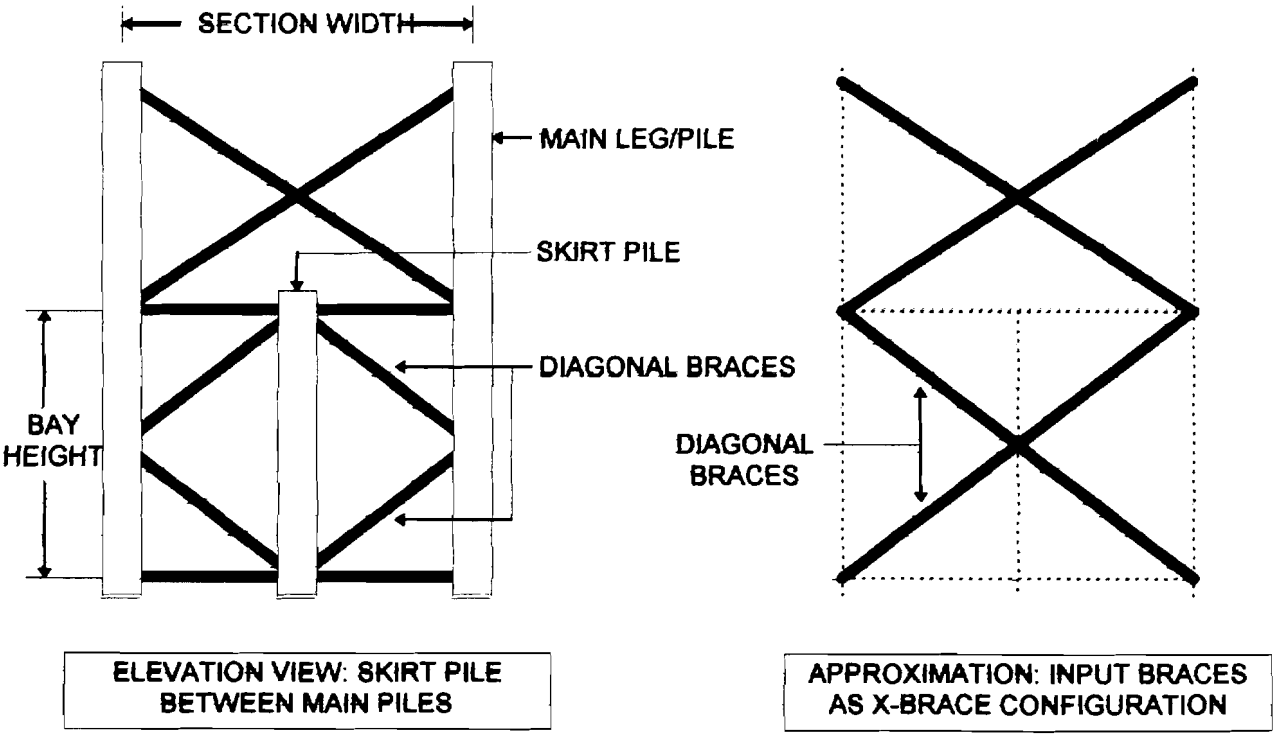

Figure 4-1: Approximate Input for Braces Around a Skirt Pile

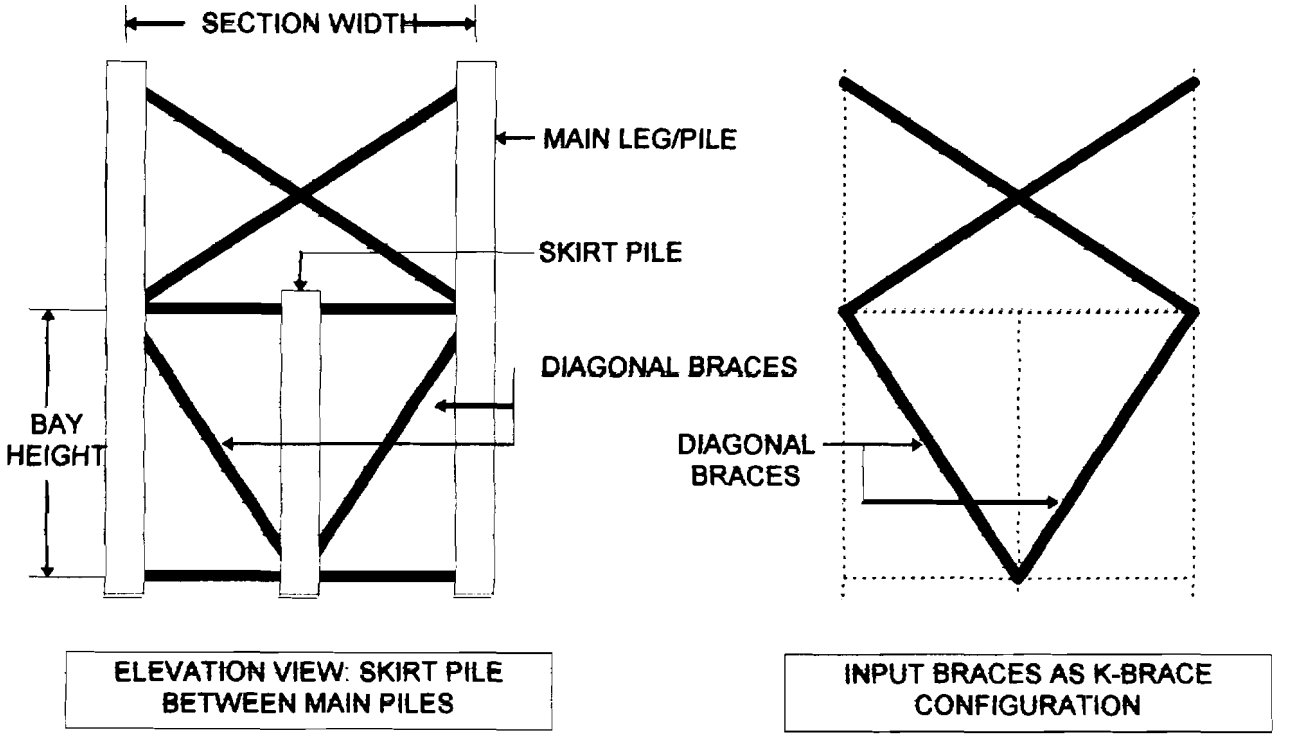

Figure 4-2: K-Brace with Skirt Pile in Center

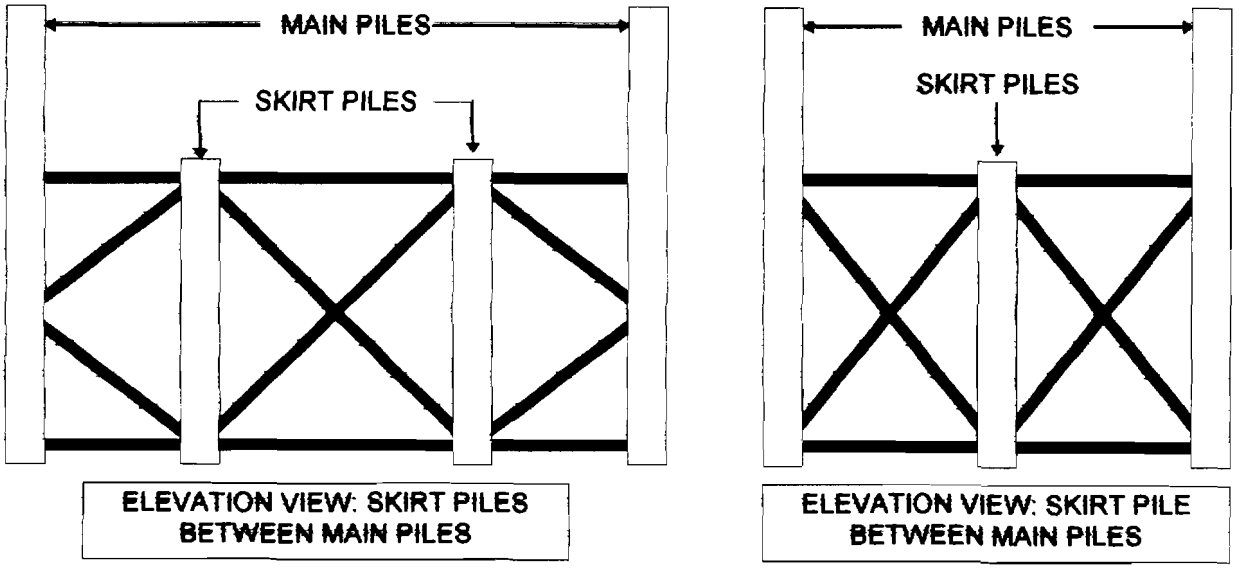

Figure 4-3: Configurations Requiring a Special Model

Configurations like the ones shown in Figure 4-3 are more problematic, as TOPCAT cannot currently size braces to multiple points in between the jacket legs. The configuration on the right of Figure 4-3 could be approximated by specifying four braces, two in a K(A) configuration

and two in a K(V) configuration; however, the braces will then have their axial strengths determined without consideration of the support point at the center of each X (as noted in Chapter Two, X-braces have their axial strengths formulated based on the length between the cross-point at the jacket legs, and not from leg to leg).

The following procedure may be used to analyze the platform for storm conditions:

1. Build an input file for the platform, with an approximation to the braces in the bottom bay. Ensure that the brace projected areas are correctly represented for load purposes.
2. Analyze the platform for the desired storm loads.
3. Record the batter forces and the total water horizontal velocity at the bottom bay.
4. Build another input file, except this time, the file will only consist of the bottom bay. Hence, specify a one-jacket bay structure, but select a platform leg layout which can be dimensioned such that the skirt piles are now in main-pile positions. For example, if the left frame of Figure 4-3 was being modeled in this way, the user could specify an eight- or twelve-leg configuration, specifying the middle section width as the width between the skirt piles. Similarly, if the right from of Figure 4-3 was being modeled in this way, the user would choose a six- or twelve-leg configuration. Enter dummy values for deck bay height, deck characteristics, pile characteristics and soil properties. Enter the diagonal braces as they should be entered, as opposed to an approximation. There is no need to input horizontals or appurtenances.
5. Analyze the second model, with a token load (i.e. wave height of one ft). However, specify a current speed such that the total water velocity at the bottom level is represented for this model (for local forces on members).
6. Take the bay capacity returned by this second analysis, and add the batter forces from the first analysis to it. This is the true capacity of the bay for the load condition considered.

This exercise points out an important ability of TOPCAT, and that is to quickly develop partial models of structures for the purpose of evaluating strength or checking attracted load. So long as the minimum input requirements are met, the program will execute correctly.

4.2 Modeling a Tripod Jacket with TOPCAT

TOPCAT provides a user the ability to analyze tripod-jacket platforms in addition to more conventional jacket types. Loads and component capacities are determined for the two axes shown in Figure 4-4. Frames 1 and 2 have equal dimensions; if the platform possesses a single vertical leg the user must specify input such that the vertical leg is B2, the vertex between Frames 1 and 2. For the broadside loading case, the direction of loading is parallel to Frame A; braces should be specified as being tension or compression based on visualizing the load as being directed from left to right. The tubular braces in Frame A are considered to govern the shear capacity of the structure bays for this direction of loading; however, the braces in Frames 1 and 2 will also provide some resistance, as described in Appendix D. Overturning for this direction of load is assumed to be resisted exclusively by piles A1 and A3. For the end-on loading case, the direction of loading is perpendicular to Frame A; braces should be specified as being tension or compression based on visualizing the load as being direction from Frame A to Pile B2.. The shear capacity of the structure bays will be determined by the strengths of the

braces in Frames 1 and 2; all three piles resist overturning for this direction but pile B2 will be twice as heavily loaded as piles A1 and A3.

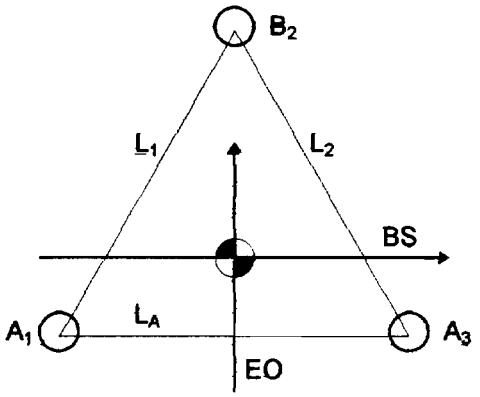

- Sides 1, 2 must have equal lengths
- Frame 1, 2 element strengths and stiffnesses are projected to EO axis to obtain components' EO strengths and stiffnesses.
- Frame 1, 2 element strengths and stiffnesses are projected to BS axis to obtain element contributions to BS strengths and stiffnesses together with Frame A elements.
- Piles A1 and A3 resist BS overturning. All piles resist EO overturning, but pile B2 carries twice the load as A1 and A3.

Figure 4-4: Tripod Principal Axes Considered by TOPCAT

TOPCAT has some important limitations when it comes to tripods. The program does not evaluate torsion arising either from mass, projected area, or stiffness eccentricities. Also, the program does not allow users to maximize loads on either Frame 1 or 2, by considering cases in-line with these frames. However, the program will return brace axial strengths for members in these frames.

Input for tripods follows the same procedures as for standard jackets. When the program requests BS and EO bracing members, the user will enter the members in Frame A for BS and the members in Frames 1 and 2 for EO. Also, horizontal braces have their orientations specified as being the angle ($\leq 90°$) between the axis of the horizontal member and an axis parallel to Frame A and the BS axis. Projected areas for decks and other non-structural members should be input such that the effective projected area is the area perpendicular to the respective axes of loading.

An example will be used to illustrate input for a tripod. Consider the simple platform in Figures 4-5 and 4-6. The platform has one jacket bay, one deck, and a single vertical pile. The user begins input by specifying the platform TYPE as "3-leg". Next, the user selects LAYOUT AND DIMENSIONS, and makes the following entries:

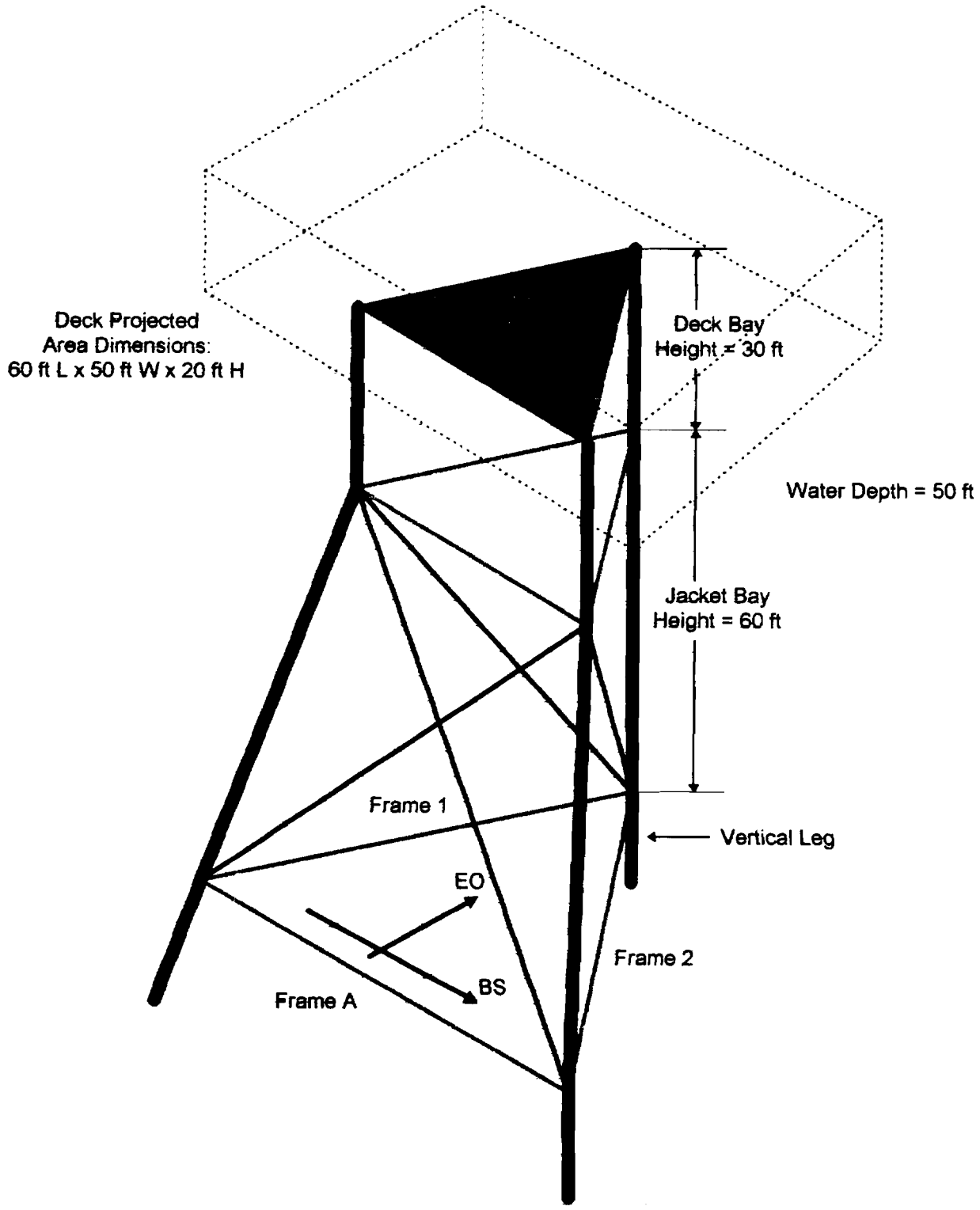

Figure 4-5: Tripod Layout

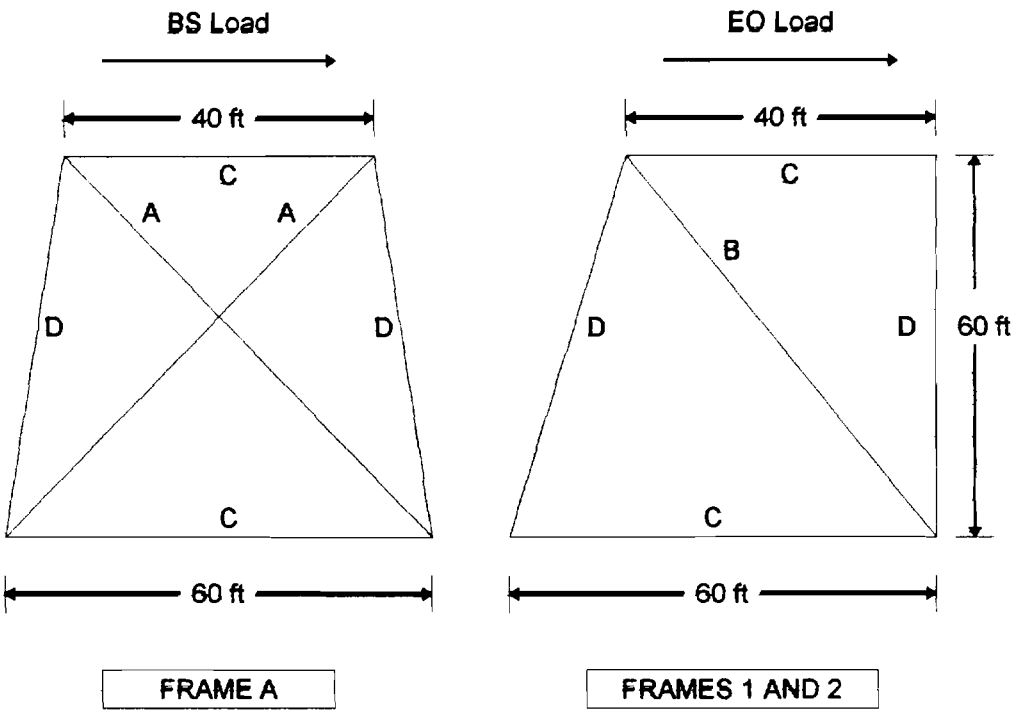

Member Dimensions

Member	Diameter (in)	Thickness (in)
Brace A	24	0.5
Brace B	30	0.625
Horizontal C	18	0.375
Jacket Leg D	70	0.875
Deck Leg	66	1
Pile	66	1

Piles are driven to 150 ft in dense sand ($\phi = 40°$, $\gamma = 0.05$ kips/ft^3)
All steel is 36 ksi
All braces have k=0.5

Figure 4-6: Tripod Frame and Member Dimensions

- Water Depth: 50 ft
- Sinkage: 0
- Decks: 1
- Jacket Bays: 1
- Vertical Leg: yes
- Skirt Piles: no
- Frame A Top Width: 40 ft
- Frame A Bottom Width: 60 ft
- Frames 1 and 2 Top Width: 40 ft

- Frames 1 and 2 Bottom Width: 60 ft

For BAY HEIGHTS AND BRACE NUMBERS, the user enters:

Deck Bay:

- Height = 30 ft
- Number of BS Braces = 0
- Number of EO Braces = 0
- Number of Horizontals = 3

Jacket Bay 1:

- Height = 60 ft
- Number of BS Braces = 2 (these are the braces in Frame A)
- Number of EO Braces = 2 (these are the total # of braces in Frames 1 and 2)
- Number of Horizontals = 3

Enter data on the soil profile and structure materials as listed above. Use the input from the Southern California Example Platform (Chapter Three) to assign force coefficients and uncertainties and biases. If desired, input for earthquake and fatigue conditions can be ignored.

Assuming no joint data is entered, the user skips ahead to entering data on main diagonal braces. The input sequence will be as follows:

Broadside Frames/ Brace 1: choose either brace in Frame A, and assign tension or compression based on the orientation. Referring back to Figure 4-6, one brace runs from upper-left to lower-right, and will be placed in compression based on the load direction. The other brace, lower-left to upper-right, will be placed in tension. Choosing the compression brace, enter:

- Orientation: compression
- Configuration: X-brace
- Position: center
- Diameter: 24 inches
- Thickness: 0.5 inches

This completes BS Brace 1. Enter the next BS Brace:

- Orientation: tension
- Configuration: X-brace
- Position: center
- Diameter: 24 inches
- Thickness: 0.5 inches

Now input must be provided for the braces in Frames 1 and 2. Again, the order of input does not matter to the program. Choosing the brace in Frame 1, and minding the direction of load, enter:

- Orientation: compression
- Configuration: single
- Position: center
- Diameter: 30 inches
- Thickness: 0.625 inches

Next, the brace in Frame 2. Note this brace's input is identical to that for Frame 1:

- Orientation: compression
- Configuration: single
- Position: center
- Diameter: 30 inches
- Thickness: 0.625 inches

This completes entry for the main diagonal braces in the platform.

Skipping now to horizontal braces, the user begins by entering data on the braces in the bottom of the deck bay. Measuring angle of orientation from the BS axis, the following entries will be made:

Brace 1: (Frame A)

- Diameter: 18 inches
- Thickness: 0.375 inch
- Length: 40 ft
- Orientation: 0°

The braces in Frames 1 and 2 would be the same except for orientation, which would be specified as 60° in both cases.

Input for the horizontal braces at the bottom of the jacket bay is similar, except that the lengths are now 60 ft for each brace.

The user should be able to input the remaining information on the platform as for any other standard jacket. Once input is complete, the user may conduct analyses of the tripod as with any other platform.

4.3 Modeling Caissons with TOPCAT

TOPCAT allows for the analysis of both braced and guyed caissons similar to MOSSII® configuration. The particulars of a caisson analysis are discussed in Appendix D. Input for a caisson analysis is relatively simple when compared to the input required for jacket-type platforms.

When a user wishes to model a braced or guyed caisson, the following steps are used:

STEP 1:
Select platform TYPE as either braced or guyed caisson.

STEP 2:
Select layout and dimensions. The program will display the following dialog box:

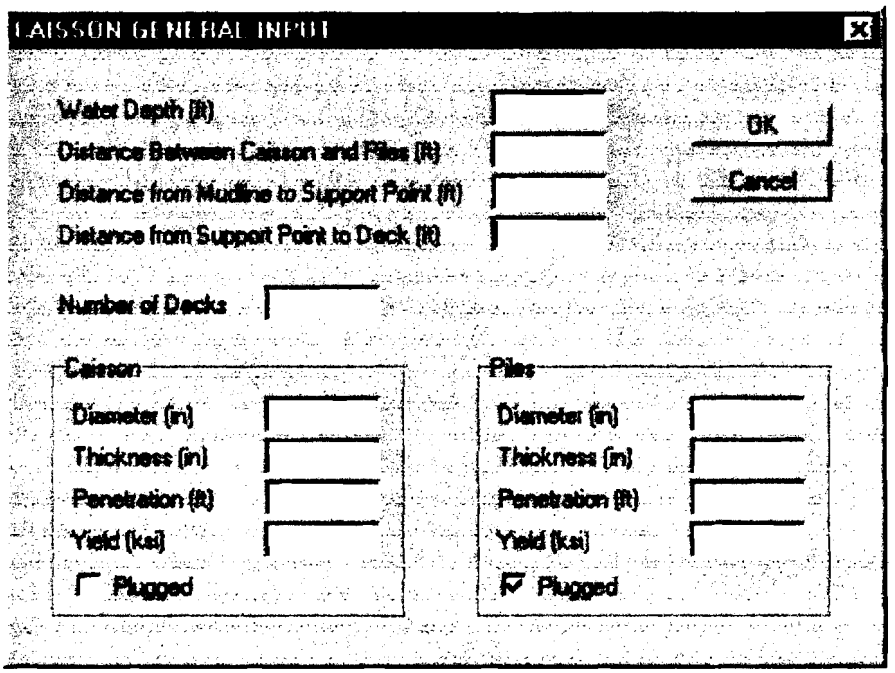

Figure 4-7: Braced or Guyed Caisson Input

The user supplies information on both the caisson and the piles which are part of the support system. The user need not assign specific yield strengths if global yield strengths will be specified in STRUCTURE MATERIALS.

STEP 3:
Upon clicking OK, the program will display a dialog box requesting information on the support. If the platform was declared as a braced caisson, the dialog box shown in Figure 4-8 will be displayed. The user inputs information on the bracing member. The connection input is intended to characterize the connection between the brace and the caisson or the brace and the pile (it is up to the user to choose which); the user simply inputs the effective connection steel area through which load is transferred. A stress concentration factor can be input if a fatigue analysis is desired; the default stress concentration factor for the connection is unity. A yield strength or brace effective length factor need not be specified if the user supplies these in STRUCTURE MATERIALS.

If instead the user declared a guyed caisson, the dialog box shown in Figure 4-9 will be displayed. The user inputs information on the cable diameter, pretension, and connection. Again, local values of yield strength will default to global values if not assigned here.

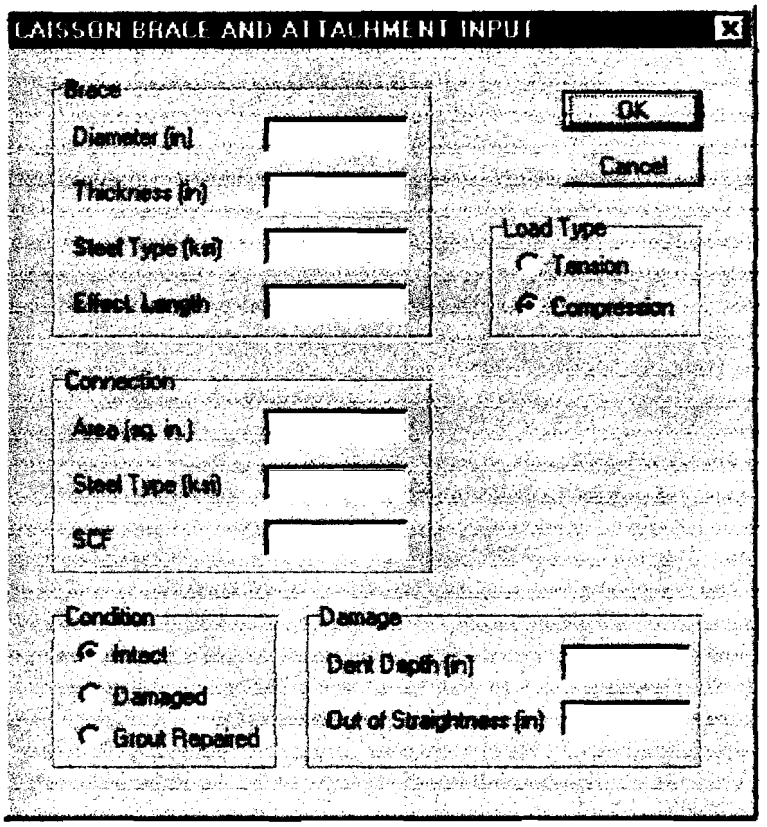

Figure 4-8: Brace Support Input

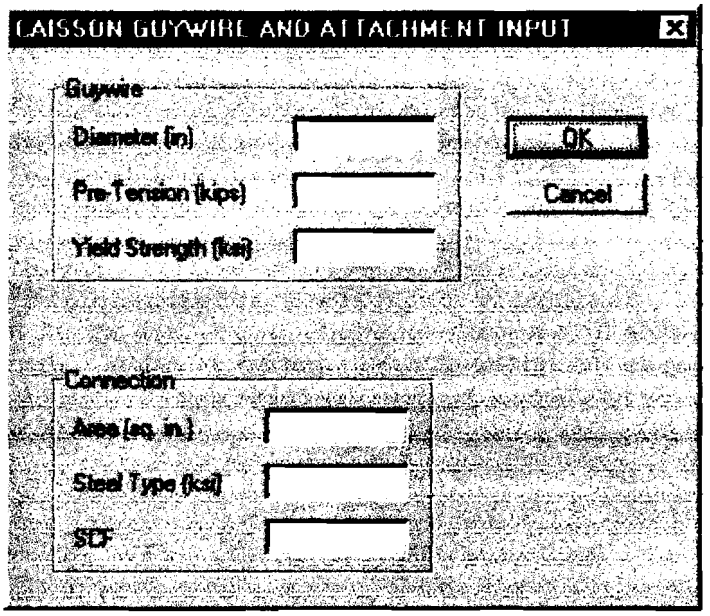

Figure 4-9: Cable Support Input

STEP 4:

The user now assigns the remaining global parameters, with the exception of BAY HEIGHTS AND NUMBERS OF DIAGONALS. The user can also specify the following local parameters: DECKS AND BOATLANDINGS, APPURTENANCES AND MARINE GROWTH, and EQUIPMENT PERIOD. All other local parameters are irrelevant to the caisson, having already been supplied in the LAYOUT AND DIMENSIONS input. Finally, the user also supplies information on the environmental conditions desired for analysis.

The program returns the same out for caissons as it does for jacket-type platforms. The shear capacity profile on the demand/capacity graphs will have four parts:

- The lateral capacity of the unsupported section of the caisson.
- The lateral capacity of the support member.
- The lateral capacity of the support connection.
- The lateral capacity of the support pile.

This is depicted in Figure 4-10.

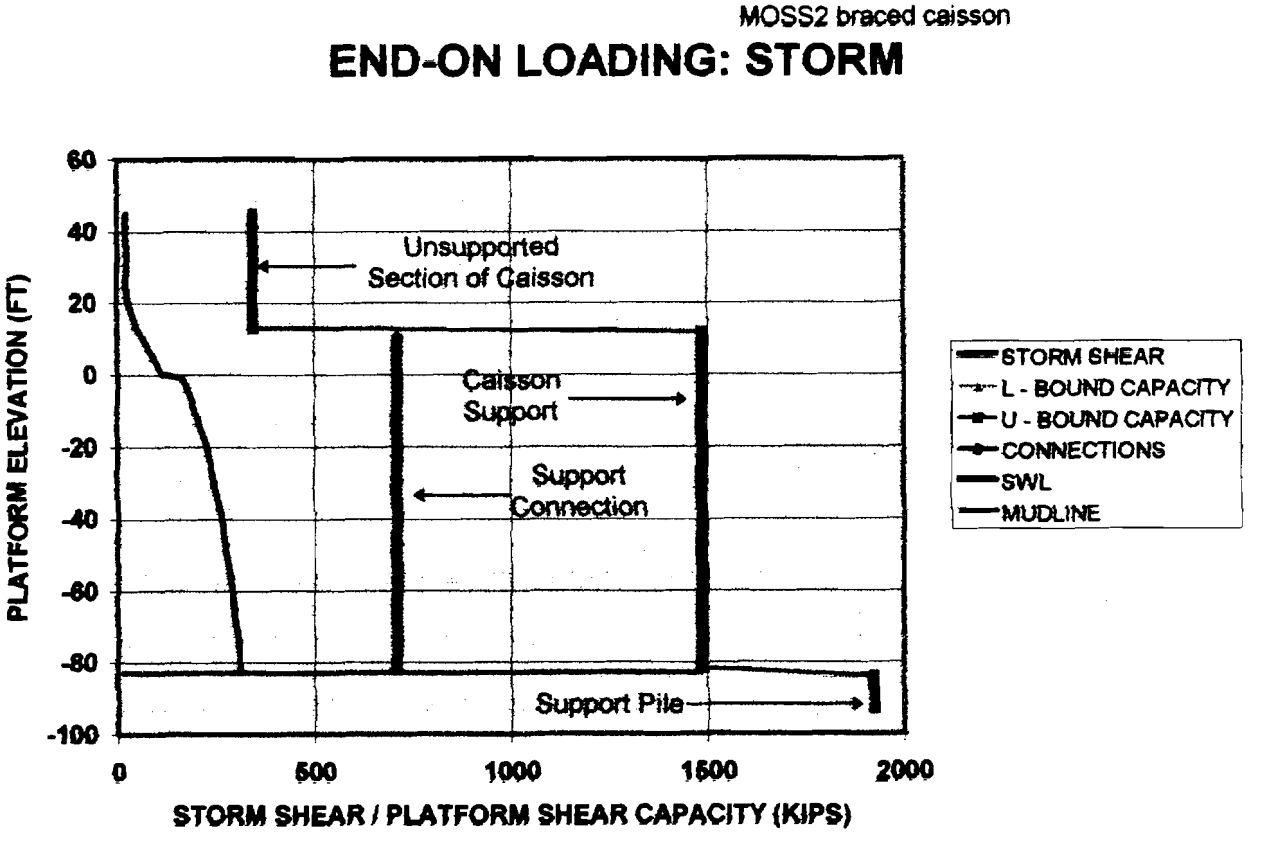

Figure 4-10: Demand/Capacity Graph for Caisson

The pile axial RSR graph shows the RSRs for both the caisson and the support pile (Figure 4-11):

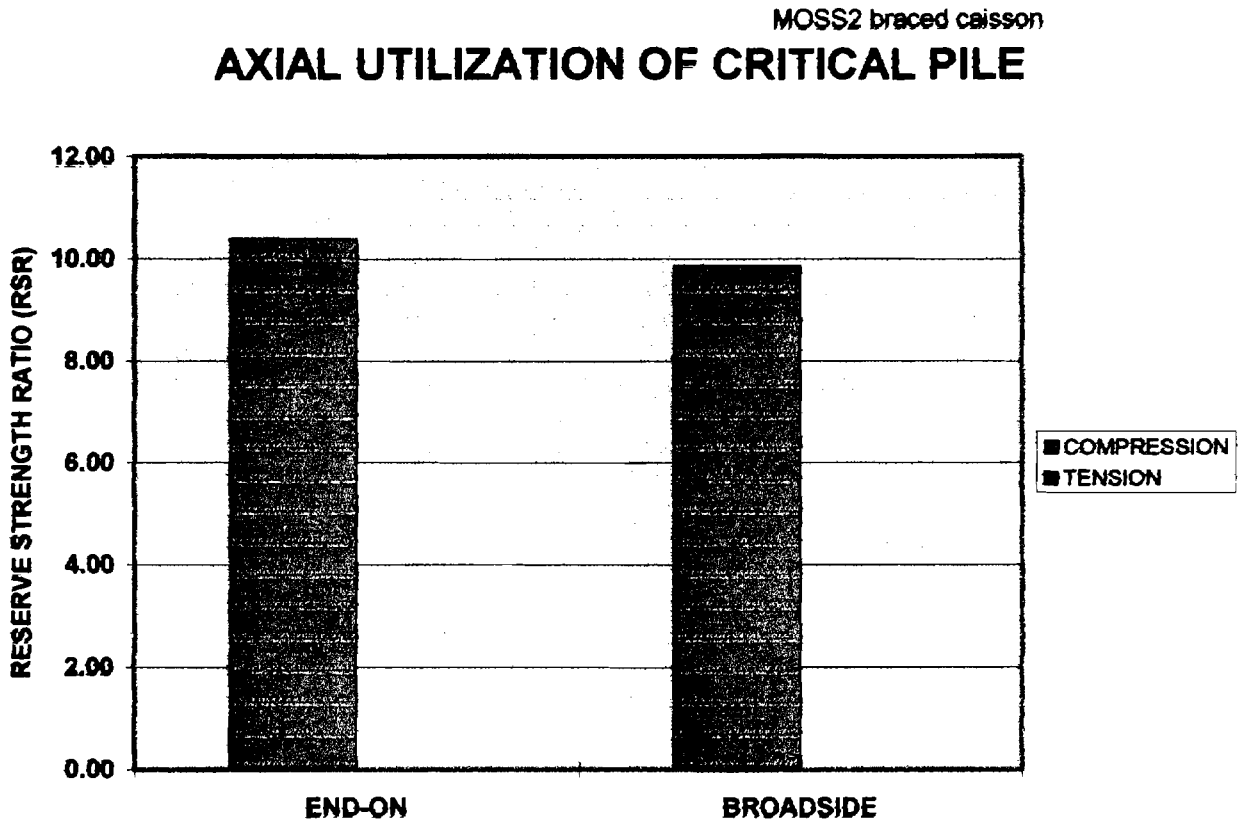

Figure 4-11: Caisson Axial RSRs

A fatigue analysis for a caisson projects the fatigue life of three parts of the platform: the support connection, the caisson wall above the support connection, and the caisson wall at the mudline. The stresses in the support are based on the axial force which must be transferred to the support, while the stresses in the caisson wall are based on the bending of the caisson. These locations are highlighted in Figure 4-12:

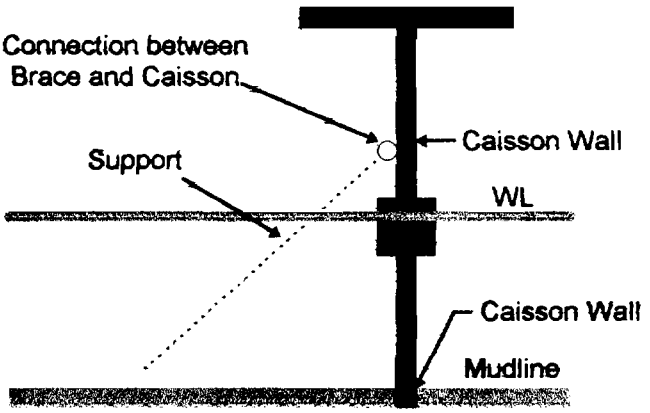

Figure 4-12: Caisson Fatigue Analysis Locations

TOPCAT returns tabular output for caissons as per a jacket-type platform, with the exception of structure data. TOPCAT generates tables only for GENERAL DATA and FOUNDATION. The strength of the support connection and support member are listed with GENERAL DATA, while the strengths and stiffnesses of the caisson and pile are listed under FOUNDATION.

APPENDIX A: SIMPLIFIED WIND, WAVE AND CURRENT LOADS ON OFFSHORE PLATFORMS

by
Mehrdad M. Mortazavi and Professor Robert G. Bea

edited by James D. Stear

Portions of this Appendix have been previously published in the following:

Mortazavi, M. M. and Bea, R. G., "A Probabilistic Screening Methodology for Steel, Template-Type Offshore Platforms," Report to Joint Industry Project Sponsors, Marine Technology and Management Group, Department of Civil and Environmental Engineering, University of California at Berkeley, CA, January 1996.

TABLE OF CONTENTS **PAGE**

A.1 INTRODUCTION

This section documents the procedures used by TOPCAT to calculate aero- and hydrodynamic loads on a platform. Wind loads are formulated and discussed first. The fluid mechanics background that is necessary to develop a simplified load calculation approach is also discussed. Finally, a simplified load model is introduced that uses an idealized structure and either Stokes Fifth-Order or Cnoidal wave theory to predict the wave loads acting on offshore platforms. This load model is verified with results from more sophisticated current and wave load generating programs commonly used in industry.

A.2 AERODYNAMIC LOADS

Wind forces acting on the exposed portions of offshore platforms are in general not as significant as the wave forces acting on these structures. However, their effect has to be included in the global and particularly in the local structural analyses of the deck structure and the topside facilities and equipment tie-downs. Wind forces are generally composed of two components: a sustained (or steady) component averaged over a longer period of time (usually over one minute) and a gust (or fluctuating) component averaged over a shorter period of time (usually less than one minute). Sustained wind velocities are used to analyze the global platform behavior and gust velocities are used to analyze the local member behavior. In case of dynamically sensitive structures such as compliant towers or tension leg platforms, more detailed dynamic wind load analyses are necessary. In such cases, wind energy representations in form of spectral densities are utilized (Ochi et al., 1986). Typical Gulf of Mexico jacket-type platforms respond to wind forces in a static way. In this research, the dynamic aspects of wind loading are neglected.

Due to surface friction, the geostrophic wind velocity is reduced in the vicinity of ocean surface. API RP 2A (API, 1993) gives the following approximation to the wind horizontal velocity profile:

$$u(1-hour,z) = u(1-hour,z_R)(z/z_R)^{0.125}$$

where z_R denotes a reference height usually taken as 10 meters. Given the wind velocity, the maximum wind force, S_a, acting on the exposed decks of the platform is given as:

$$S_a = \frac{\rho_a C_s A_d V_d^2}{2}$$

where ρ_a is the mass density of air, C_s the wind velocity pressure (or shape) coefficient, A_d the effective projected area of the exposed decks, and V_d the wind velocity at the deck elevation and for an appropriate time interval. The wind shape coefficient is a function of air turbulence, structure geometry and surface roughness.

TOPCAT allows a user to input C_s, A_d and V_d, and then calculates the wind load of a platform using the above relationship. This load is assumed to act at the top of the deck legs.

A.3 HYDRODYNAMIC LOADS: BACKGROUND

To establish the hydrodynamic loads acting on an offshore platform, three steps need to be taken: (1) establish wave, current, and storm surge information based on site specific studies including recorded or hindcasted data, (2) use an appropriate wave theory to describe the fluid motion and water particle kinematics, and (3) use a force transfer function to determine the loads acting on platform members. TOPCAT leaves the performance of (1) to the user. Background to the performance of (2) and (3) is presented in this section.

Wave Theories:

The problem of describing the wave motion has been dealt with for more than a century now. Numerous text books have been devoted to development of various wave theories and describing their results (refer to Sarpkaya and Isaacson, 1981, for a comprehensive list of references). All of these wave theories are based on the following common assumptions: the waves are two-dimensional and propagate in horizontal direction in waters with constant depth and a smooth bed. It is further assumed that the wave train profile does not change with time, no underlying current exist, and the water surface is tension-free (uncontaminated). Water itself is assumed to be incompressible, inviscid (ideal fluid), and irrotational. Figure A-1 shows the definition sketch of a wave train with H, L, d, and η, denoting wave height and length, water depth and surface elevation respectively. The governing equations of wave motion can be found in any classical text book on fluid mechanics (e.g. Sarpkaya and Isaacson 1981) and are given below for the sake of completeness.

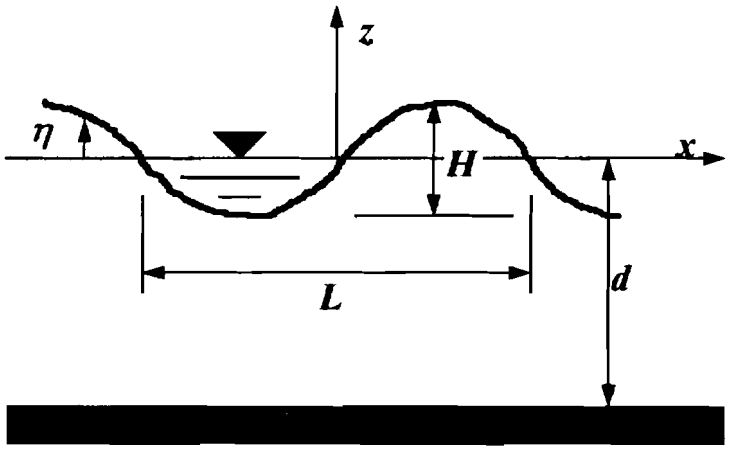

Figure A-1: Wave Train Definition Sketch

Defining a scalar function $\phi=\phi(x,z,t)$ so that the fluid velocity vector can be given by the gradient of ϕ, it can be shown that based on the assumptions stated above ϕ, the so-called velocity potential, satisfies the two-dimensional Laplace equation:

$$\nabla^2\phi = \frac{\partial^2\phi}{\partial x^2} + \frac{\partial^2\phi}{\partial z^2} = 0$$

and is subject to the following boundary conditions at water surface and seabed:

$$\frac{\partial \phi}{\partial z} = 0 \qquad \text{at } z=-d$$

$$\frac{\partial \eta}{\partial t} + \left(\frac{\partial \phi}{\partial x}\right)\left(\frac{\partial \eta}{\partial x}\right) - \frac{\partial \phi}{\partial z} = 0 \qquad \text{at } z=\eta$$

$$\frac{\partial \eta}{\partial t} + \frac{1}{2}\left[\left(\frac{\partial \phi}{\partial x}\right)^2 + \left(\frac{\partial \phi}{\partial z}\right)^2\right] + g\eta = f(t) \qquad \text{at } z=\eta$$

$$\phi(x,z,t) = \phi(x-ct,z)$$

The boundary condition at the seabed states that the velocity vector has no component in vertical direction. The kinematic boundary condition at the water surface states that the velocity component normal to the water surface is equal to the velocity of water surface in that same direction. The dynamic boundary condition at the water surface states that the pressure along the surface is constant (equal to atmospheric pressure). The last relationship is based on the assumption of periodicity of the wave train where $c=L/T$ denotes the wave celerity.

Given the wave height, period and the water depth, the question is what shape does the wave take and how to describe the water particles motion (displacements, velocities, and accelerations) throughout the flow. In solving the governing Laplace Equation subject to boundary conditions listed above, the following problems are encountered: the boundary conditions at the water surface are nonlinear and specified at a surface elevation η, which is itself unknown. The various wave theories developed in the past have tried to solve these problems with reasonable approximations. These include linear or Airy wave theory (also known as small amplitude wave theory), Stokes finite amplitude wave theories, Dean's stream function theory, and nonlinear shallow wave theories such as Cnoidal wave theory. The question of suitability of a given wave theory for a particular application is a difficult one. One selection criteria is the amount of effort needed to produce the desired results. The more advanced the theory is, the more sophisticated the tools need to be to perform the analyses. Theoretical charts have been developed that show the ranges of best fit to the free surface boundary conditions for different wave theories (e.g. Figure A-2). Experimental comparisons of different wave theories have not resulted in clear trends regarding the applicability of any particular wave theory (Sarpkaya and Isaacson, 1981).

Two approaches will be taken to determine wave kinematics for hydrodynamic load calculation. Stokes fifth-order theory will be used to calculate the kinematics in the intermediate and deep water regions, while Cnoidal theory will be used to calculate kinematics in the shallow water regime. Cnoidal theory will only be applied if the following conditions are met:

$$h/T^2 < 0.1$$

$$H/T^2 < 0.05$$

where:

h = depth from mudline to calm water surface (ft)
H = wave height (ft)
T = wave period (sec)

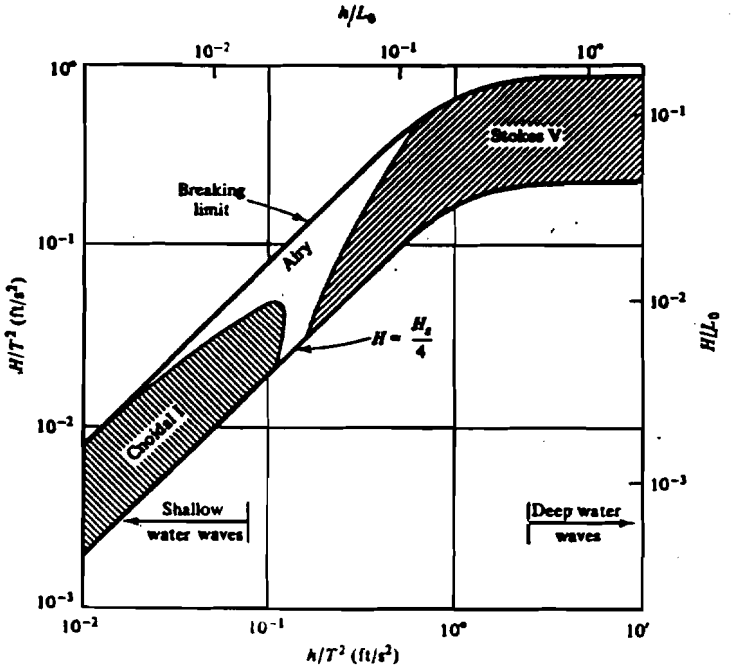

Figure A-2: Regions of Applicability of Cnoidal and Stokes Fifth-Order Wave Theory

Wave Directional Spreading:

Real storm conditions include waves from multiple directions. Directional spreading of the waves reduces the loads acting on marine structures which are computed based on a two dimensional, long crested, regular wave grid propagating in a single horizontal direction. This load reduction is mainly due to change in water particle kinematics. Wave components from different directions can partially cancel each other. The effects of wave directionality have been investigated by many authors (e.g. Dean, 1977).

The detailed treatment of the subject is not within the scope of this work. In engineering practice, wave directional spreading effects are captured by a single wave kinematics modification factor. The actual water particle velocity is estimated by multiplying the velocities based on a two-dimensional wave theory with the wave kinematics modification factor. Measurements indicate a range of 0.85 to 1.0 for highly directional seas during tropical storms to extra-tropical storm conditions (API, 1993). TOPCAT allows a user to specify a wave kinematics factor to account for directional spreading.

Currents and Current Blockage:

Currents can be a major contributor to total hydrodynamic forces acting on an offshore platform. In general, currents are generated in three ways; there are tidal, circulational, and storm generated currents. Tidal currents can be important in shallow waters of continental shelves (coastal regions and inlets). The Gulf Stream in the Atlantic Ocean and the Loop Current in the Gulf of Mexico are examples for large-scale circulational currents. Winds and pressure gradients during storms are the source of storm generated currents. These currents can be roughly estimated to have surface speeds of 1-3% of the one hour sustained wind speed during storms (API, 1993). The profile of storm generated currents is largely unknown and the subject of research.

In determining the water particle kinematics due to currents, it should be recognized that, due to existence of the structure, the current is disturbed and its speed in the vicinity of the platform differs from that in the free field. Based on experimental test data, approximate current blockage factors for typical jacket-type platforms are given in API RP 2A (API, 1993). The actual current velocity in the vicinity of the structure is obtained by multiplying the free field current speed with the current blockage factor. These factors range from 0.7 for end-on loading of eight-leg platforms to 0.9 for tripods (API, 1993). TOPCAT allows a user to specify a current blockage factor to modify the current velocity for the purpose of load calculation.

Wave and Current Loads:

Morison, Johnson, O'Brien and Schaff (1950) proposed the following formulation for the force acting on a section of a pile due to wave motion

$$F = F_i + F_d = C_m \rho V \frac{du}{dt} + \frac{1}{2} C_d \rho A u|u|$$

This formulation is widely known as the Morison equation. According to Morison et al. (1950), this force is composed of two components: an inertia component related to the acceleration of an ideal fluid around the body, F_i, and a drag component related to the steady flow of a real fluid around the body, F_d. C_m is the so-called inertia coefficient, ρ is the mass density of fluid, V is the volume of the body and du/dt is the fluid acceleration. C_d is the so-called drag coefficient, A denotes the projected area of the body normal to the flow direction, and u is the incident flow velocity relative to pile.

Vortex shedding, drag and lift forces are all phenomena observed in real (viscous) fluids due to wake formation when the fluid passes a body. These phenomena do not exist in an ideal (inviscid) fluid. They have been the subject of comprehensive research for many decades and are now well understood and described for simple, idealized cases. In such cases, numerical computations are able to simulate these phenomena with reasonable degrees of accuracy. However, these programs are not yet efficient enough to be used by engineers and designers to calculate the forces on "real" marine structures.

Although extremely simple, the Morison equation has been used for many years by researchers and engineers to calculate the wave forces on "slender" marine structures. An important assumption implicit in the Morison equation is that the incident flow remains undisturbed in the vicinity of the body. This condition is satisfied when the body is small relative to the wave

length. If the body is large relative to the wave length, the incident flow will not remain uniform and will be refracted due to presence of the body. In this case the refraction problem needs to be solved. For detailed treatment of the subject refer to Sarpkaya and Isaacson (1981). The refraction problem is not considered in this research since the platform dimensions are much smaller than the wave length in the extreme conditions underlying the ultimate strength analysis.

The drag and inertia coefficients in Morison equation have empirical nature and depend on many factors including flow characteristics, shape and roughness of the body and its proximity to sea floor or free surface. One important flow parameter reflecting its uniformity is Keulegan-Carpenter (KC) number which is defined as:

$$KC = \frac{UT}{D}$$

where U and T are the velocity amplitude and period of the oscillatory flow and D is the diameter of the cylinder. Reynolds number, Re, is another important parameter that characterizes the flow regime reflecting its turbulence and is defined as

$$Re = \frac{UD}{\nu}$$

where ν denotes the fluid viscosity. Past field tests have indicated a large scatter in the values of drag and inertia coefficients when they are plotted against either the Reynolds number or the Keulegan-Carpenter number. This scatter is largely attributable to the irregular nature of the ocean waves. Typical values for Reynolds and Keulegan-Carpenter numbers in extreme conditions are $Re > 10^6$ and $KC > 30$. For these ranges and based on experimental and field test data, mean drag and inertia coefficients are established for cylinders with smooth and rough surface (e.g. API, 1993).

A.4 SIMPLIFIED HYDRODYNAMIC LOAD MODEL

A simplified hydrodynamic load calculation model is developed and discussed in the following. Wave, current and wind forces are considered. In the case of wave loading, only the drag force component of the Morison equation is estimated. Due to 90° phase angle difference between the maximum drag and inertia force components and the relatively small dimensions of a typical jacket-type platform with respect to wave lengths and heights in an extreme condition, at the time the drag forces acting on the platform reach a maximum value the inertia forces are relatively small and hence neglected.

Wave horizontal velocities are based on Stokes fifth-order theory for intermediate and deep water depths. Using equations given by Skjelbreia and Hendrickson (1961) and Fenton (1985), computer code has been developed to calculate the kinematics. Given the wave height H, period T and water depth d, the vertical profile of maximum horizontal velocities beneath the wave crest is given as:

$$u = K_{ds} c \sum_{n=1}^{5} n \phi_n' \cosh(nks)$$

where K_{ds} is a coefficient that recognizes the effects of directional spreading and wave irregularity on the Stokes wave theory based velocities. k is the wave number and s is the vertical coordinate counting positive upward from the sea floor. c is the wave celerity and given by:

$$\frac{c^2}{gd} = \frac{\tanh(kd)}{kd}\left[1 + \lambda^2 C_1 + \lambda^4 C_2\right]$$

The crest elevation η is estimated by:

$$k\eta = \sum_{n=1}^{5} \eta_n'$$

ϕ'_n and η'_n are given functions of λ and kd. C_n are known functions of kd only and given by Skjelbreia and Hendrickson (1961). The wave number k is obtained by implicitly solving the following equation given by Fenton (1985):

$$\frac{2\pi}{T(gk)^{0.5}} - C_0 - \left(\frac{kH}{2}\right)^2 C_2 - \left(\frac{kH}{2}\right)^4 C_4 = 0$$

The parameter λ is then calculated using the equation given by Skjelbreia and Hendrickson (1961):

$$\frac{2\pi d}{gT^2} = \frac{d}{L}\tanh(kd)\left[1 + \lambda^2 C_1 + \lambda^4 C_2\right]$$

Having the parameters λ and kd, the horizontal water particle velocities and the wave crest elevation can be estimated.

Cnoidal wave theory is used to calculate the velocities for shallow water conditions. Based on a second order approximation documented by Dean and Dalrymple (1984), the horizontal velocities u at elevation z are estimated from:

$$\frac{u}{\sqrt{gd}} = \varepsilon\left(cn^2 q - h_1\right) + \varepsilon^2\left\{\left(f_1 + f_2 cn^2 q - cn^4 q\right) - \frac{3}{4\kappa^2}\left(\frac{z}{d}\right)^2\left[\kappa'^2 + 2\left(2\kappa^2 - 1\right)cn^2 q - 3\kappa^2 cn^4 q\right]\right\}$$

where:

$$\varepsilon = \frac{H}{d}$$

$$h_1 = \frac{\left(\gamma - \kappa'\right)}{\kappa^2}$$

$$f_1 = \frac{\left[-\gamma\left(6\gamma + 11\kappa^2 - 16\right) + \kappa'^2\left(9\kappa^2 - 10\right)\right]}{12\kappa^4}$$

$$f_2 = \frac{\left[2\gamma + 7\kappa^2 - 6\right]}{4\kappa^4}$$

$$q = \frac{K(\kappa)}{\pi}(kx - \omega t)\text{, 0 at wave crest location}$$

$$\kappa' = \sqrt{1-\kappa^2}$$

$$cn^2 q = \sum_{n=0}^{\infty} A_n \cos n(kx - \omega t) = \sum_{n=0}^{\infty} A_n \text{ at wave crest location}$$

$$\gamma = E(\kappa) / K(\kappa)$$

A_n are Fourier coefficients, given by:

$$A_0 = \frac{\gamma - \kappa'^2}{\kappa^2}$$

$$A_n = \frac{2\pi^2}{\kappa^2 K^2(\kappa)}\left(\frac{nr^n}{1-r^{2n}}\right)$$

where:

$$r = \exp\left(\frac{-\pi K(\kappa')}{K(\kappa)}\right)$$

$K(\kappa)$ is a complete elliptic integral of the first kind, given by:

$$K(\kappa) = \int_0^{\pi/2} \frac{1}{\sqrt{1-\kappa^2 \sin^2 x}} dx$$

while $E(\kappa)$ is a complete elliptic integral of the second kind:

$$E(\kappa) = \int_0^{\pi/2} \sqrt{1-\kappa^2 \sin^2 x} dx$$

To solve the above relationships which control u, it is necessary to solve for κ, the Jacobian elliptic function modulus. This can be done by iterating the following relationship:

$$\frac{d}{gT^2} = \frac{3\varepsilon}{16\kappa^2 K^2(\kappa)}\left(\frac{1+\varepsilon c_1 + \varepsilon c_2}{1-\varepsilon l_1}\right)^2$$

where:

$$c_1 = \frac{2-\kappa^2-3\gamma}{2\kappa^2}$$

$$c_2 = \frac{-18\kappa^4 - 88\kappa^2 - 5\gamma(15\gamma + 19\gamma^2 - 38)}{120\kappa^4}$$

$$l_1 = \frac{-10+5\kappa^2+12\gamma}{8\kappa^2}$$

For both the intermediate/deep case and the shallow case, the specified variation of current velocities with depth is stretched to the wave crest and modified to recognize the effects of structure blockage on the currents. The total horizontal water particle velocities are taken as the sum of the wave horizontal velocities and the current velocities.

The maximum drag force acting on the portions of structure below the wave crest is based on the fluid velocity pressure:

$$F_d = \frac{1}{2} C_d \rho A u|u|$$

where ρ is the mass density of water, A the effective vertical projected area of the exposed structure element, and u the horizontal velocity of water at a given point on the submerged portion of the structure element.

All of the structure elements are modeled as equivalent vertical cylinders that are located at the wave crest (Figure A-3). Appurtenances (boat landings, conductors, risers) are modeled in a similar manner. For inclined members, the effective vertical projected area is determined by multiplying the product of member length and diameter by the cube of the cosine of its angle with the horizontal.

For wave crest elevations that reach the lower decks, the horizontal hydrodynamic forces acting on the lower decks are computed based on the projected area of the portions of the structure that would be able to withstand the high pressures. The fluid velocities and pressures are calculated in the same manner as for the other submerged portions of the structure with the exception of the definition of C_d. In recognition of rectangular shapes of the structural members in the decks a higher C_d is taken. This value is assumed to be developed at a depth equal to two velocity heads (U^2/g) below the wave crest. In recognition of the near wave surface flow distortion effects, C_d is assumed to vary linearly from its value at two velocity heads below the wave crest to zero at the wave crest. (McDonald et al., 1990; Bea and DesRoches, 1993).

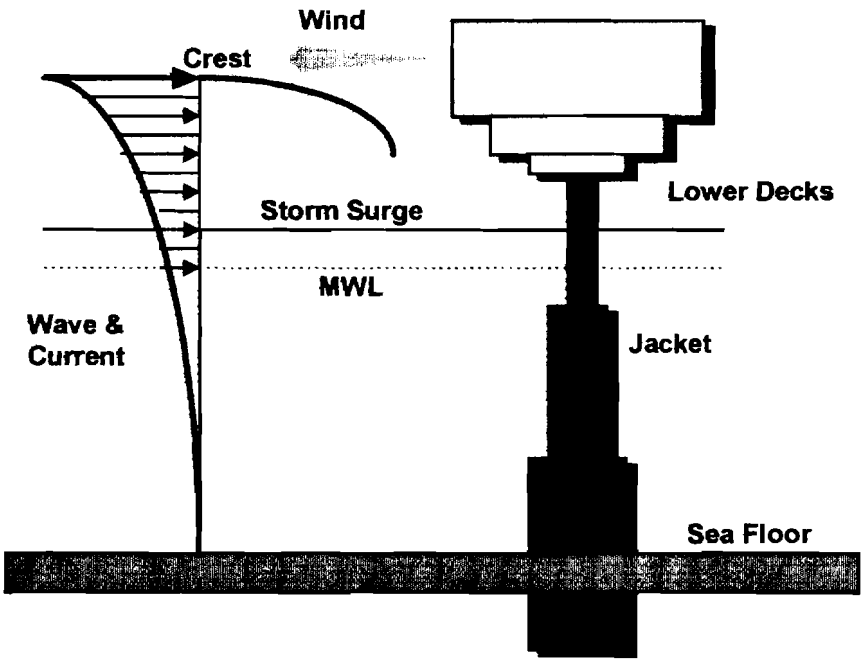

Figure A-3: Simplified Load Model

A.5 VERIFICATION OF SIMPLIFIED LOAD MODEL

The procedure used to estimate the wave forces acting on jacket structures has been verified and calibrated against results from more sophisticated computer programs. In an initial verification effort, the computer output for four design wave cases on single surface piercing cylindrical piles were used. These data were produced during an analytical wave force study conducted by Exxon and Shell Research Companies and documented by Bea (1973). In this study, the maximum wave force acting on a 3 ft diameter surface piercing cylinder was estimated where non-dimensional water depths d/gT^2 ranged from 0.022 to 0.146. Based on the simplified procedure developed in the previous sections of this chapter, the maximum wave force acting the same cylinder is also estimated using both Stokes fifth-order and depth stretched linear wave theories. A drag coefficient of C_d=0.6 is used in all cases. The results are also compared to those gained by using Dean's Charts that are developed based on ninth-order stream function theory (Dean, 1973). The results are summarized in Figures A-4 to A-7.

Figure A-4 shows the results for deep water conditions. Stokes fifth-order theory results in an estimate of base shear that is in good agreement with results reported in Exxon-Shell wave force study. Dean's Charts slightly underpredict the total force. Surprising is the result gained by using depth-stretched linear wave theory, which gives a base shear that is almost 40% less than that given by Stokes fifth-order theory. Figures A-5 and A-6 show the results for deep to intermediate water depths. Again, it can be seen that Stokes fifth-order results are in good agreement with those reported in Exxon-Shell study. Depth-stretched linear wave theory underpredicts the base shear by 40% to 50%. Dean's Charts result in total forces that are also close to those gained by using Stokes fifth-order theory. Figure A-7 shows the results for intermediate to shallow water conditions. The base shear obtained using Stokes fifth-order theory is about 10% to 15% larger

than the base shear predicted by Exxon-Shell study and that gained by using Dean's Charts. In this case, Airy wave based prediction makes up only 20% of Stokes fifth-order theory results.

Field measurements in intermediate water depths indicate that depth-stretched Airy theory provides an acceptable fit to the actual wave kinematics. With this in mind, the results plotted in Figures A-4 to A-7 indicate that wave force predictions based on finite amplitude wave theories (Stokes fifth-order or stream function) might be conservatively biased.

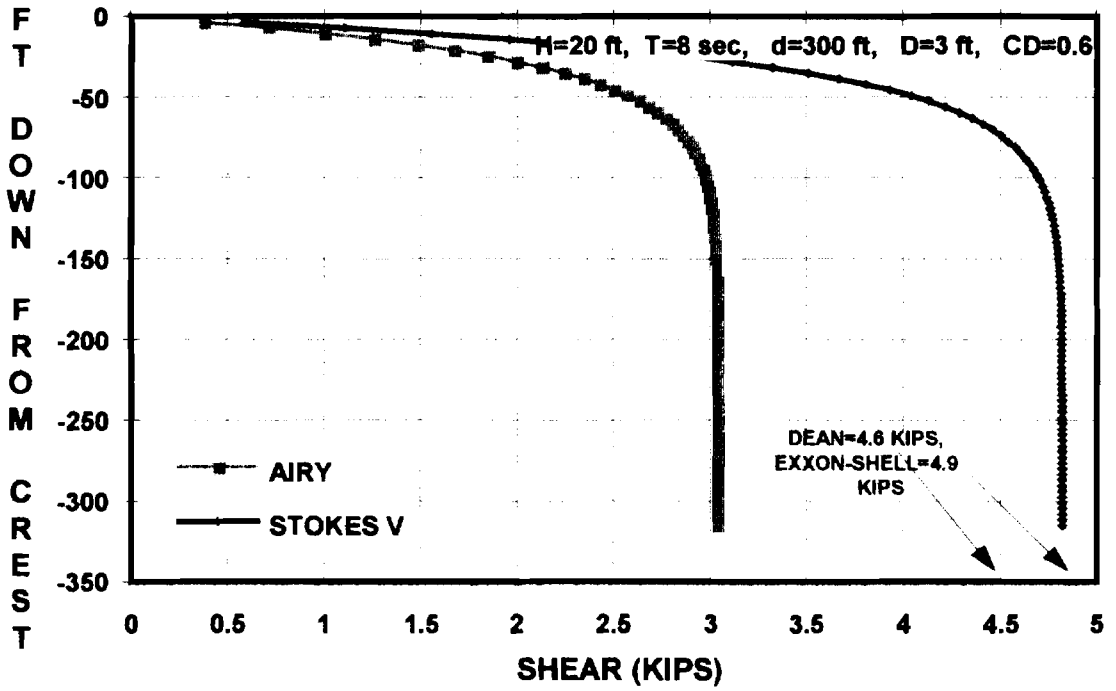

Figure A-4: Wave Force on a Vertical Surface Piercing Cylinder in Deep Water
($d / gT^2 = 0.146$)

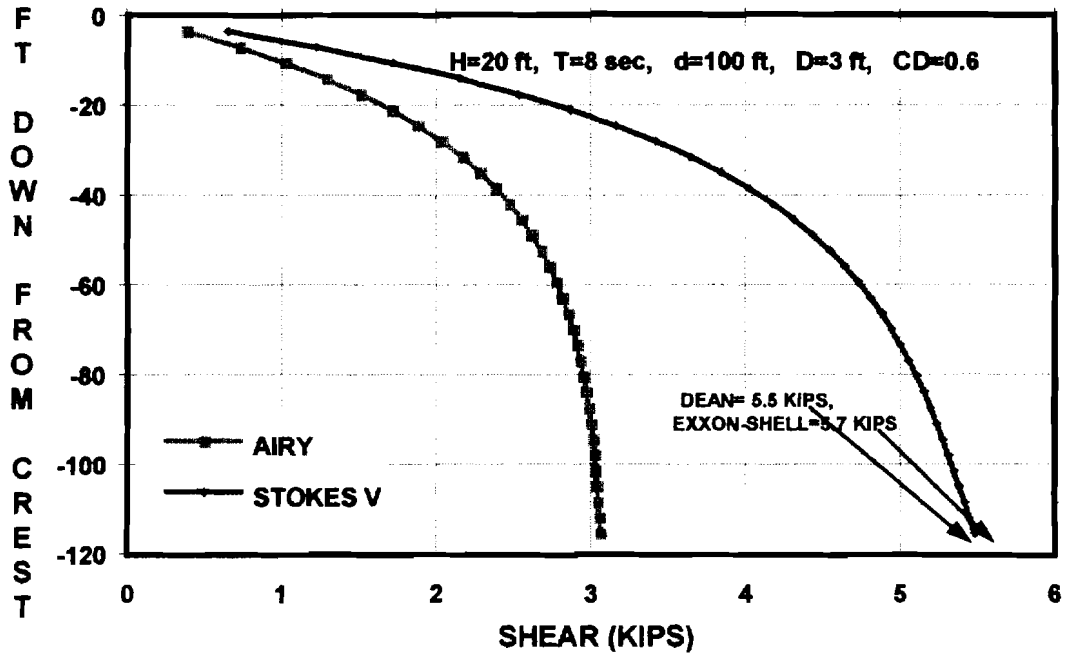

Figure A-5: Wave Force on a Vertical Surface Piercing Cylinder in Transitional Water Depth ($d / gT^2 = 0.049$)

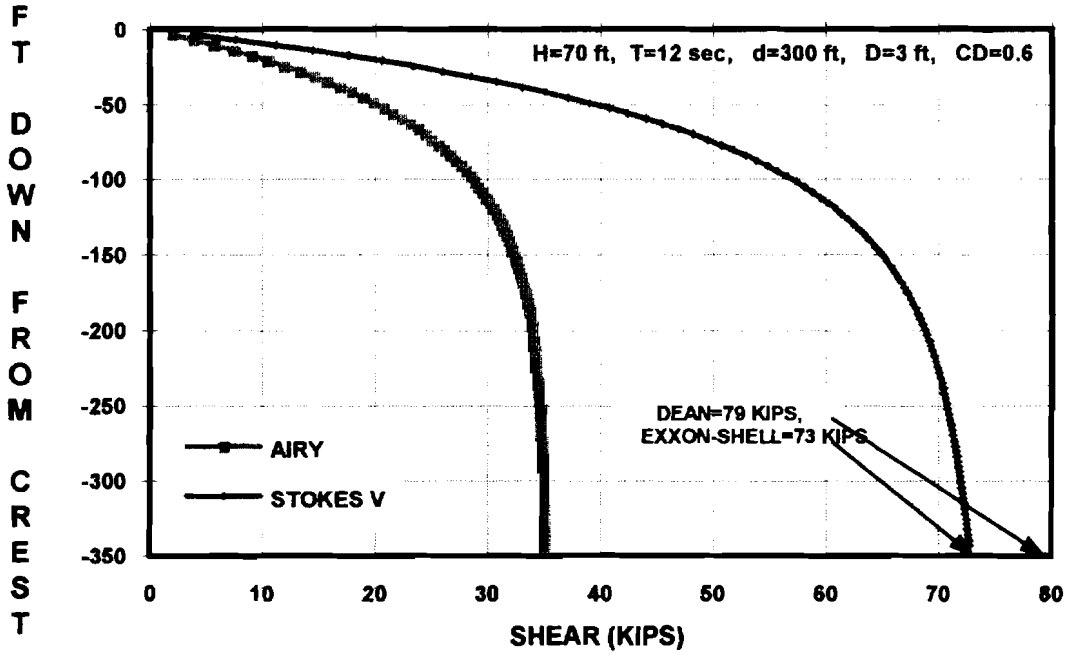

Figure A-6: Wave Force on a Vertical Surface Piercing Cylinder in Transitional Water Depth ($d / gT^2 = 0.065$)

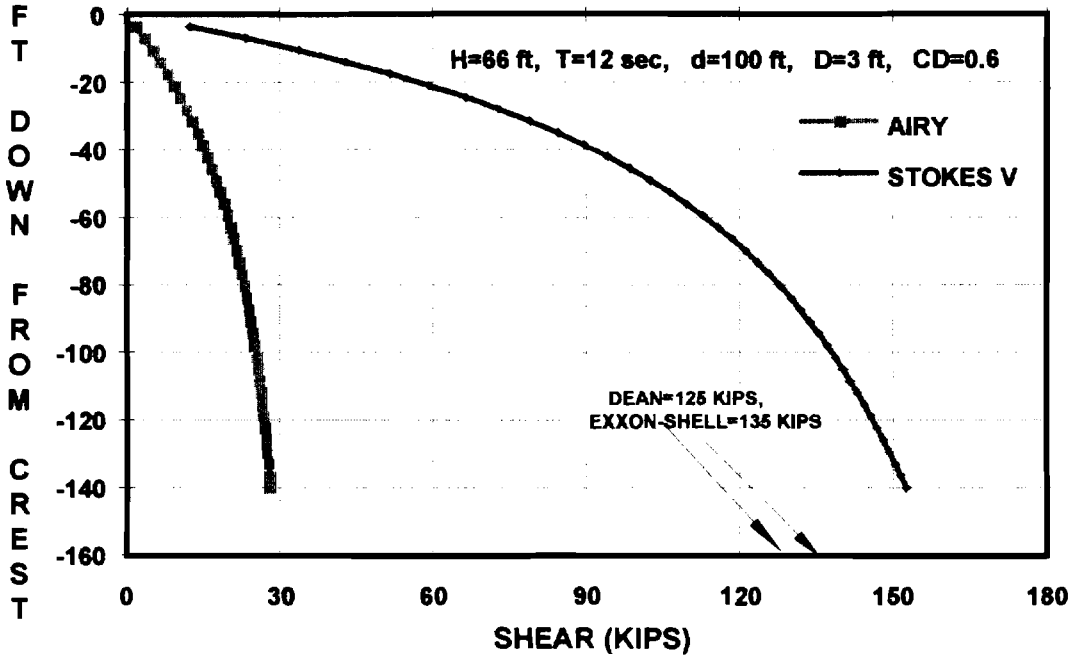

Figure A-7: Wave Force on a Vertical Surface Piercing Cylinder in Transitional Water Depth ($d / gT^2 = 0.022$)

A.6 REFERENCES

American Petroleum Institute, "Recommended Practice for Planning, Designing and Constructing Fixed Offshore Platforms - Load and Resistance Factor Design," RP 2A-LRFD, First Edition, Washington, D. C., July 1993.

Bea, R. G., "Wave Forces, Comparison of Stokes Fifth and Stream Function Theories," Engineering Note No. 40, *Environmental Mechanics,* April 1973.

Bea, R. G. and DesRoches, R., "Development and Verification of a Simplified Procedure to Estimate the Capacity of Template-Type Platforms," *Proceedings of the Fifth International Symposium on the Integrity of Offshore Structures*, D. Faulker et al., Emas Scientific Publications, 1993.

Dean, R. G., "Hybrid Method of Computing Wave Loading," OTC 3029, *Proceedings of the Offshore Technology Conference,* Houston, TX, May 1977.

Dean, R. G., and Dalrymple, R. A., *Water Wave Mechanics for Engineers and Scientists*, Prentice-Hall, New York, NY, 1984.

Fenton, J. D., "A Fifth Order Stokes Theory for Steady Waves," *ASCE Journal of Waterway, Port, Coastal and Ocean Engineering*, Vol. 111, No. 2, 1985.

MacDonald, D. T., Bando, K., Bea, R. G., and Sobey, R. J., "Near Surface Wave Forces on Horizontal Members and Decks of Offshore Platforms," Final Report, Coastal and Hydraulic Engineering, Department of Civil Engineering, University of California at Berkeley, CA, December 1990.

Morison, J. R., O'Brien, M. P., Johnson, J. W., Schaff, S. A., "The Force Exerted by Surface Waves on Piles," Petroleum Transactions AIME, Vol. 189, 1960.

Ochi, M. K., Shin, Y. S., "Wind Turbulent Spectra for Design Considerations of Offshore Structures," OTC 5736, *Proceedings of the Offshore Technology Conference*, Houston, TX, 1986.

Sarpkaya, T., and Isaacson, M., *Mechanics of Wave Forces on Offshore Structures*, Van Nostrand Reinhold Co., New York, NY, 1981.

Skjelbreia, L., and Hendrickson, J., "Fifth Order Gravity Wave Theory," *Proceedings of the 7th Conference on Coastal Engineering*, 1961.

APPENDIX B:
STRENGTH CAPACITIES OF DECK AND JACKET BAYS

by
Mehrdad M. Mortazavi and Professor Robert G. Bea

edited by James D. Stear

Portions of this Appendix have been previously published in the following:

Mortazavi, M. M. and Bea, R. G., "A Probabilistic Screening Methodology for Steel, Template-Type Offshore Platforms," Report to Joint Industry Project Sponsors, Marine Technology and Management Group, Department of Civil and Environmental Engineering, University of California at Berkeley, CA, January 1996.

TABLE OF CONTENTS **PAGE**

B.1 INTRODUCTION

The development of simplified element and component capacity estimation procedures used to predict the ultimate lateral loading capacity of a platform system are described in this appendix. Using the concept of plastic hinge theory, limit equilibrium is formulated by implementing the principle of virtual work. This is the key to the simplified ultimate limit state analysis method. Where of importance, geometric and material nonlinearities are considered. This method is being increasingly used in plastic design of simple structures or structural elements (e.g. moment frames, continuous beams). Due to the impracticality of such analyses for more complicated structures, these methods have not found broad use in design or assessment of complex structures; all possible failure modes need to be considered and evaluated to capture the "true" collapse mechanism and the associated ultimate lateral load.

Actual field experience and numerical results from three-dimensional, nonlinear analyses performed on a variety of template-type platforms indicate that in most cases certain failure modes govern the ultimate capacity of such platforms: a) plastic hinge formation in the deck legs and subsequent collapse of the deck portal, b) buckling of the main load carrying vertical diagonal braces in the jacket, c) lateral failure of the foundation piles due to plastic hinge formation in the piles and plastification of foundation soil, and d) pile pullout or pile plunging due to exceedance of axial pile and soil capacities.

Within the framework of a simplified analysis and based on experience, collapse mechanisms are assumed for the three primary components that comprise a template-type platform: the deck legs, the jacket, and the pile foundation. Based on the presumed failure modes, the principle of virtual work is utilized to estimate the ultimate lateral capacity for each component. In the following sections, this process is described in detail for the two of the primary components of a platform, the deck bay and jacket bays. Information on the capacities of foundation members is contained in Appendix G.

B.2 DECK BAY

The ultimate shear that can be resisted by an unbraced deck portal is estimated based on bending moment capacities of the tubular deck legs that support the upper decks. A collapse mechanism in the deck bay would form by plastic yielding of the leg sections at the top and bottom of all of the deck legs (Figure B-1). The interaction of bending moment and axial force is taken into account. The maximum bending moment and axial force that can be developed in a tubular deck leg is limited by local buckling of leg cross-sections. The vertical dead loads of the decks are assumed to be equally shared among the deck legs. Due to relatively large axial loads (weight of the decks and topside facilities) and large relative displacements at collapse (deck bay drift), P-Δ effect plays a role in reducing the lateral shear capacity and hence is taken into account.

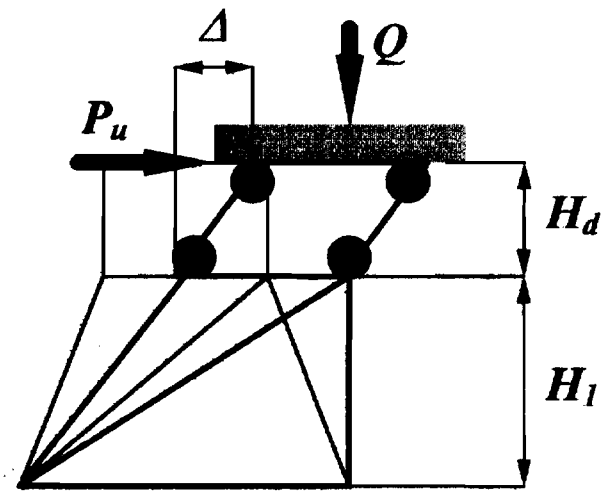

Figure B-1 : Deck Portal at Ultimate Lateral Load

Deck Bay Drift at Collapse:

To derive an estimate of P-Δ effect with out leaving the framework of a simplified analysis, simplifying assumptions are made. It is assumed that the deck structure is rigid. It is further assumed that plastic yielding of the sections at the bottom of the deck legs occur simultaneously, following the plastic yielding of the sections at the top of the legs and hence an estimate of plastic hinge rotations to calculate the deck bay drift is unnecessary. Finally, to estimate the deck bay drift at collapse, Δ, the jacket is replaced by rotational springs at the bottom of each deck leg. The spring rotational stiffness, C_r, is approximated by applying external moments, which are equal in magnitude and have the same direction, to the top of jacket legs at the uppermost jacket bay. Assuming rigid horizontal braces and fixed boundary conditions at the bottom of these jacket legs, the rotation of cross-sections at the top of the legs and hence the rotational stiffness, C_r, is determined:

$$\frac{1}{C_r} = \frac{H_1}{EI_1 \cos\beta}\left(1 - \frac{3C_s H_1^3}{4C_s H_1^3 + 12EI_1 \cos\beta}\right)$$

where C_s is an equivalent lateral stiffness coefficient

$$C_s = \frac{1}{2}\sum_i \frac{EA_i \cos^2\theta_i}{L_i}$$

summed over all diagonal braces within the uppermost jacket bay. I_1 and H_1 denote the moment of inertia of the jacket leg and the first jacket bay height respectively. E is the Young modulus, β and θ are the batter angle of the jacket legs and vertical diagonal braces respectively.

The principle of virtual force is implemented to calculate the deck bay horizontal drift at collapse:

$$\Delta = M_u H_d \left(\frac{H_d}{6EI_d} + \frac{1}{C_r} \right)$$

H_d and I_d are the height and moment of inertia of the deck legs. M_u is the ultimate moment that can be resisted by the cross-section in the presence of axial load and can be derived from the M-P interaction equation for tubular cross-sections:

$$M_u = M_{cr} \cos\left(\frac{\pi Q / n}{2P_{crl}} \right)$$

M_{cr} and P_{crl} denote the critical moment and axial load associated with local buckling of the tubular cross-section. Q denotes the total vertical deck load and n is the number of supporting deck legs.

Deck Legs Lateral Shear Strength:

Using the formulation developed above for the deck bay drift at collapse, the lateral shear capacity of the deck portal can be estimated. Equilibrium is formulated using the principle of virtual displacement. Using the actual collapse mechanism as the virtually imposed displacement, the equilibrium equation for the lateral shear capacity of the unbraced deck portal is derived including the second-order P-Δ effect:

$$P_u = \frac{1}{H_d}\left(2nM_u - Q\Delta\right)$$

B.3 JACKET BAYS

The shear capacity of each of the bays of vertical bracing that comprise the jacket is estimated including the tensile and compressive capacity of the diagonal braces and the associated joint capacities. The capacity of a given brace is taken as the minimum of the capacity of the brace or the capacity of either its joints. The batter component of axial force in the jacket legs and piles inside the jacket legs are taken into account. Where of significance, the shear forces in the legs and piles are also considered.

Ultimate Axial Strength of Tubular Braces:

The diagonal braces near the free surface are exposed to high combined bending moments and axial forces. In general, the existing bending moment result in a reduction of the ultimate axial load capacity of the brace. At the ultimate state, the large deflections result in inelastic strains. Generally an elastic-plastic load deflection (P-δ) analysis should be performed to determine the ultimate strength of the brace. The braces are treated as though there are no net hydrostatic pressures (e.g. flooded members).

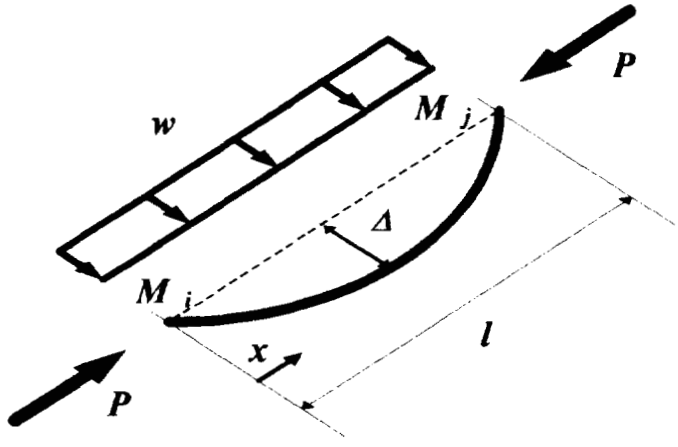

Figure B-2: Brace Element Under Compressive and Transverse Loading

The governing differential equation of the beam-column can be given as:

$$M_{xx} + \frac{P}{EI} M = -w - \frac{8P\Delta_0}{l^2}$$

where M_{xx} stands for the second derivative of bending moment with regard to the coordinate x (Figure B-2). Δ_0, P, and l are the initial out-of-straightness, axial force and unbraced length of the member respectively. The following substitutions

$$\xi = \frac{x}{l}$$

$$\varepsilon = l\sqrt{\frac{P}{EI}}$$

result in the transformed differential equation:

$$M_{\xi\xi} + \varepsilon^2 M = -wl^2 - 8P\Delta_0$$

which has the following closed-form solution:

$$M(\xi) = \frac{\sin\varepsilon(1-\xi)}{\sin\varepsilon} M(\xi=0) + \frac{\sin\varepsilon\xi}{\sin\varepsilon} M(\xi=1) + \frac{1}{\varepsilon^2}\left(\frac{\cos\varepsilon(0.5-\xi)}{\cos\frac{\varepsilon}{2}} - 1\right)(wl^2 + 8P\Delta_0)$$

Based on a three-hinge failure mode, the exact solution of the second-order differential equation for the bending moment of a beam-column is implemented to formulate the equilibrium at collapse:

$$M(\xi = 0.5) = -M(\xi = 0) = -M(\xi = 1) = M_u$$

$$M_u = \left(\frac{1}{1 + 2\dfrac{\sin 0.5\varepsilon}{\sin \varepsilon}} \right) \frac{1}{\varepsilon^2} \left(\frac{1}{\cos \dfrac{\varepsilon}{2}} - 1 \right) \left(wl^2 + 8P_u \Delta_0 \right)$$

Elastic-perfectly plastic material behavior is assumed. The ultimate compression capacity is reached when full plastification of the cross-sections at the member ends and mid-span occur (Figure B-3). It is further assumed that plastic hinges at member ends form first followed by plastic hinge formation at mid-span. *M-P* interaction condition for tubular cross-sections provides a second equation for the unknown ultimate moment M_u and axial force P_u in plastic hinges at collapse:

$$\frac{M_u}{M_p} - \cos\left(\frac{\pi P_u}{2P_p} \right) = 0$$

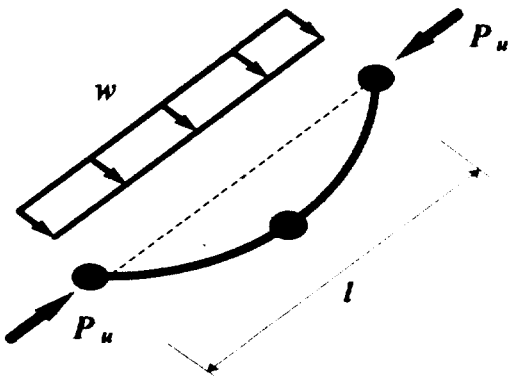

Figure B-3: Three Hinge Failure Mode for Diagonal Braces

The results have been verified with results from the nonlinear finite element program USFOS (Sintef, 1994); using the same initial out-of-straightness, Δ_0, for both simplified and complex analyses, the axial compression capacity of several critical diagonal members of different structures has been estimated. The simplified method slightly overpredicts the axial capacity of compression members (less than 10%). The initial out-of-straightness, Δ_0, is used to calibrate the axial compression capacity of braces to the column buckling curves according to API RP 2A-LRFD (API, 1993b):

$$\Delta_0 = \frac{M_p \cos\left(\frac{\pi P_{cr}}{2P_p}\right)}{8P_{cr}\left(\frac{1}{1+2\frac{\sin 05\varepsilon}{\sin\varepsilon}}\right)\frac{1}{\varepsilon^2}\left(\frac{1}{\cos\frac{\varepsilon}{2}}-1\right)}$$

where P_{cr} is the buckling load of a given brace according to API RP 2A-LRFD. Using appropriate buckling length factors, the calibrated results are in close agreement with results from USFOS (Hellan et al., 1994).

Ultimate Strength of Tubular Joints:

Because of their favorable drag characteristics, cross-sectional symmetry and the ability to provide buoyancy, tubular members are widely used in offshore structures. The stress analysis of their welded connections, often referred to as tubular joints, and the theoretical prediction of their ultimate strength has proven to be difficult. Elastic stress analysis of different joint types and geometries can be performed using a range of analytical approaches from shell theory to finite element analyses.

Experience has shown that tubular connections have a high plastic reserve strength beyond first yield, which can not be addressed by conventional linear elastic methods. Hence, empirical capacity equations based on test results have been used to predict the joint ultimate strength. Based on a data base of 137 tests of tubular joints, Yura et al. (1980) recommended one formula for both compressive and tensile ultimate capacity in the branch of a K-joint. This formula is identical to that for T and Y joints except for the additional gap factor. The test capacity was taken as the lowest of the loads at first crack, at an excessive deformation, or at first yield. For simple tubular joints with no gussets, diaphragms, or stiffeners, the capacity equations are given in Table B-1. The same capacity equations are adopted by API RP 2A-LRFD (API, 1993b).

Table B-1: Tubular Joint Capacities

Joint Type	Tension	Compression
T , Y	$\frac{f_y T^2(3.4+19\beta)}{\sin\theta}$	$\frac{f_y T^2(3.4+19\beta)}{\sin\theta}$
DT , X	$\frac{f_y T^2(3.4+19\beta)}{\sin\theta}$	$\frac{f_y T^2(3.4+13\beta)Q_\beta}{\sin\theta}$
K	$\frac{f_y T^2(3.4+19\beta)Q_g}{\sin\theta}$	$\frac{f_y T^2(3.4+19\beta)Q_g}{\sin\theta}$

Q_β is a factor accounting for geometry and Q_g is a gap modifying factor and are estimated according to the following equations:

$$Q_g = 1.8 - 0.1\frac{g}{T} \qquad \text{for} \qquad \gamma \le 20$$

$$Q_g = 1.8 - 4\frac{g}{D} \qquad \text{for} \qquad \gamma > 20$$

$$Q_\beta = \frac{0.3}{\beta(1 - 0.833\beta)} \qquad \text{for} \qquad \beta > 0.6$$

$$Q_\beta = 1.0 \qquad \text{for} \qquad \beta \le 0.6$$

g denotes the gap between branches of K-joints, $\beta = d/D$, and $\gamma = d/2T$. D, d and T are the branch and chord diameter and thickness respectively.

Effect of Shear Force in Jacket Legs and Piles:

Within the framework of a simplified analysis, the jacket has been treated as a trusswork. Plastic hinge formation in the jacket legs was not considered because this hinge development occurs at a lateral deformation that is much larger than is required to mobilize the axial capacities of the vertical diagonal braces. At the large lateral deformations required to mobilize the lateral shear capacities of the legs, the diagonal brace capacities have decreased significantly due to column buckling or tensile rupture. In general, the effect of bending moment distribution along the jacket legs on the lateral capacity has been neglected. This assumption is justified by the following example.

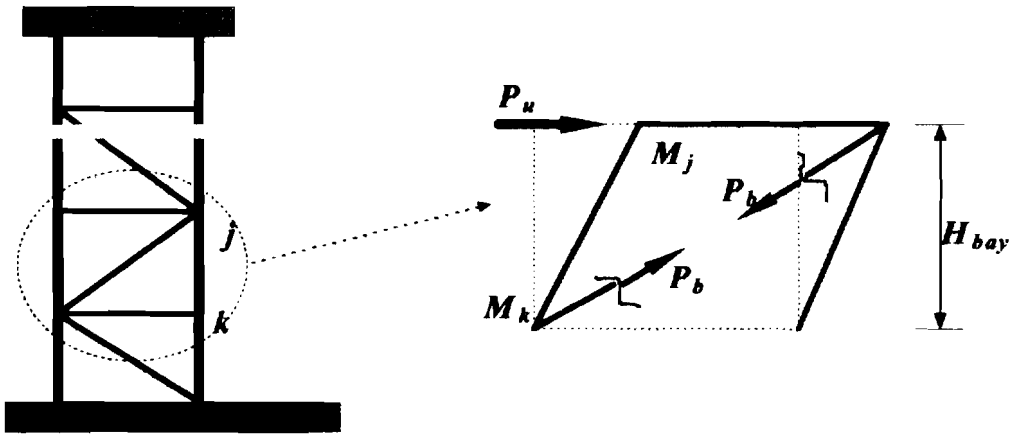

Figure B-4 : Lateral Capacity of a Jacket Bay

We impose a virtual displacement to the i^{th} jacket bay of a two-dimensional jacket frame (Figure B-4) and equate the external and internal work:

$$W^{(E)} = W^{(I)}$$

which leads to the following equilibrium equation for the given jacket bay:

$$P_u = P_{bh} + \frac{2(M_j + M_k)}{H_{bay}}$$

where P_{bh} denotes the horizontal component of brace axial force. Assuming that the magnitude of bending moment in the jacket legs is negligible:

$$M_i = M_k = 0$$

the following simplified relationship results:

$$P_u = P_{bh}$$

This assumption leads to estimates of lateral capacity of a jacket bay that are either conservative or unconservative depending on the actual bending moment distribution in the legs. However, this conservatism or unconservatism is negligible for all but the uppermost and lowest jacket bays. Due to frame action in the deck portal and rotational restraint of the legs at mud level, the jacket legs and piles inside the legs experience relatively large bending moments at these two bays. The bending moment in the legs at the lowest bay has the direction of a resisting moment and hence not considering it can only be conservative. In contrary, the shear force due to the large moment gradient at the uppermost jacket bay has the same direction as the global lateral loading. If this effect is not taken into account, the lateral capacity will be overestimated.

A simplified procedure is developed to account for the effect of shear force in the top jacket bay. Of interest is the moment distribution along the legs at this bay due to frame action in the deck portal (Figure B-5). Given the geometry of the deck portal and the load acting on deck areas, the moment distribution along the deck legs can be estimated:

$$M_0 = \frac{\frac{P_d L_d^2}{2EI} + \frac{P_d L_d}{C_r}}{\frac{L_d}{EI} + \frac{1}{C_r}} \le M_p$$

$$M_1 = M_0 - P_d L_d \le M_p$$

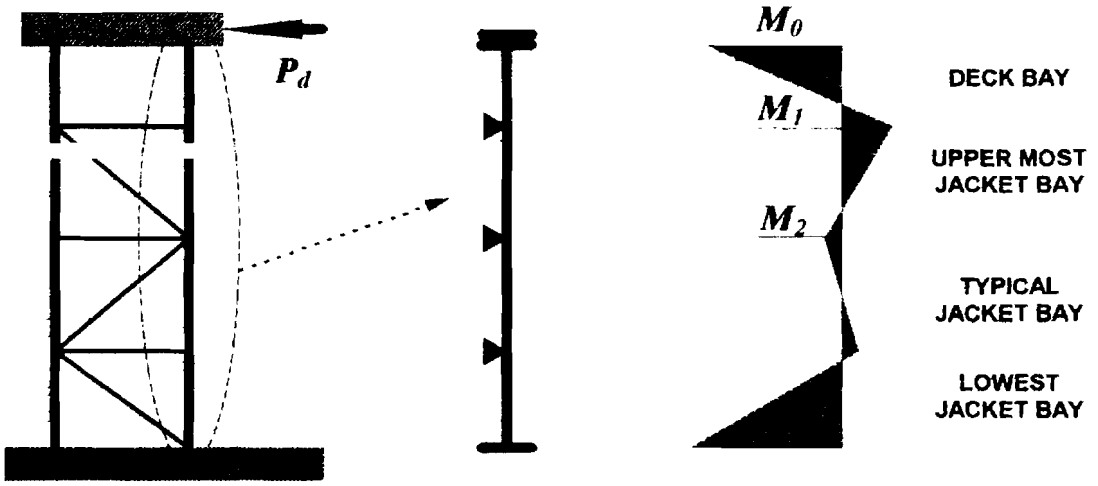

Figure B-5 : Typical Moment Distribution in Jacket Legs under Lateral Loading

Thinking of a jacket leg as a continuous beam which is supported by horizontal framings, the applied moment at the top of the leg rapidly decreases towards the bottom. Based on geometry of the structure, in particular jacket bay heights and the cross-sectional properties of the jacket leg (if nonprismatic), and in the limiting case of rigid supports, an upper bound for the desired moment distribution is estimated. For equal spans, constant moment of inertia and limiting case of rigid supports the following relationship can be derived:

$$|M_2| \leq 0.286 |M_1|$$

Jacket Bays Lateral Shear Strength:

To derive a lower-bound capacity formulation, the notion of Most Likely To Fail (MLTF) element is introduced. MLTF element is defined as the member with the lowest capacity over stiffness ratio. The lower-bound lateral capacity of a jacket bay is estimated by adding the horizontal force components of all load carrying members in the given bay at the instant of first member failure. A linear multi-spring model is used to relate the forces and displacements of diagonal braces within a bay. It is assumed that the horizontal braces are rigid. The axial force in the jacket legs due to lateral overturning moment is estimated at each bay and its batter component is added to the lateral capacity.

$$P_{u,l} = \sum_i \left(\frac{P_{u,MLTF}}{K_{MLTF}} \right) K_i + F_L$$

The summation is over all vertical diagonal braces within a given jacket bay. $P_{u,l}$ denotes the lower-bound lateral shear capacity of the jacket bay, P_u is the horizontal component of axial force in a given diagonal brace, F_L is the sum of batter components of leg forces, and K_i denotes the lateral stiffness of brace i

$$K_i = \frac{EA_i \cos\theta_i}{L_i}$$

where L, E, A, and θ denote the length, Young modulus, cross-sectional area, and the angle between the diagonal brace and the horizon respectively.

An upper-bound capacity is also formulated for each bay. After the MLTF member in compression reaches its axial capacity, it can not maintain the peak load and any further increase in lateral displacement will result in unloading of this member. Presuming that the load path remains intact (inter-connecting horizontals do not fail), a load redistribution follows and other members carry the load of the lost members until the last brace reaches its peak capacity. An empirical residual capacity modification factor, α, is introduced. Assuming elasto-perfectly plastic material behavior, α is equal to 1.0 for members in tension (neglecting strain hardening effects) and less than 1.0 for members in compression due to P-δ effects (generally in the range of 0.15 to 0.5). The upper-bound lateral shear capacity of a given jacket bay, $P_{u,u}$, is estimated by adding the horizontal component of the residual strength of all of the braces within the bay

$$P_{u,u} = \sum_i P_{ui}\alpha_i + F_L$$

B.4 DAMAGED AND REPAIRED MEMBERS

A major problem associated with assessment of an older platform is locating and evaluating the effects of defects and member damage on platform response to extreme loadings. Damage such as dents, global bending, corrosion, and fatigue cracks can significantly affect the ultimate strength of an offshore platform. Given the physical properties of damage, an estimate of the ultimate and residual strength of the damaged members is necessary to perform a strength assessment of an offshore platform system. Recently, numerous investigators have devoted their attention to this subject and several theoretical approaches have been developed addressing different types of damage (e.g. Ellinas, 1984; Ricles et al., 1992; Loh, 1993; Kim, 1992). Small and large-scale experiments have been performed to verify the analytical capacity formulations and to gain better understanding of the ultimate and post ultimate behavior of damaged and repaired tubular members.

A literature review was performed on the ultimate strength behavior of damaged and repaired tubular braces with dents, global out-of-straightness, and corrosion. Simplified methods were identified to estimate the ultimate and residual capacity of such members. In the following section, this literature review is summarized and discussed. The results of the simplified capacity estimation methods are compared with existing theoretical and experimental test results given in literature.

Dents and Global Bending Damage:

Dent-damaged tubular bracing members have been analytically studied since late 70's. The analytical methods of strength prediction developed so far can be classified into three categories (Ricles, 1993):

1. Beam-column analysis (Ellinas, 1984, Ricles et al, 1992, Loh, 1993)
2. Numerical integration methods (Kim, 1992)
3. Nonlinear finite element (FE) methods

Beam-column analysis is based on formulation of equilibrium of the damaged member in its deformed shape. The P-δ effects including the effects of out-of-straightness are considered in the equilibrium equations. The effect of dent depth is taken into account by modifying the cross-sectional properties. Numerical integration methods use empirical moment-axial load-curvature relationships to iteratively solve the differential equation of axially loaded damaged member. The empirical M-P-Φ relationship is usually based on experimental test results or finite element studies of dented tubular segments. Nonlinear FE analyses represent the most general and rigorous method of analysis. However, their accuracy and efficiency require evaluation and they are expensive and time consuming to perform.

Loh's Interaction Equations:

Developed at Exxon Production Research Company, BCDENT is a general computer program that uses M-P-Φ approach to evaluate the full behavior of dented member (Loh, 1993). The behavior of the dent section is treated phenomenologically using a set of M-P-Φ expressions. Compared with the experimental results, BCDENT gives mean strength predictions for both dented and undented members. Based on BCDENT results, Loh (1993) presented a set of new

unity check equations for evaluating the residual strength of dented tubular members. The unity check equations have been calibrated to the lower bound of all existing test data. The equations cover axial compression and tension loading, in combination with multi-directional bending with respect to dent orientation. When the dent depth approaches zero, the recommended equations are identical to API RP 2A equation for undamaged members (API, 1993b). Loh's equations for dent damaged members and those with global bending damage have been integrated in TOPCAT; the numerical relationships are listed in Section B.5.

Comparison Between Experimental and Predicted Capacities:

Based on a comparison between the experimental ultimate capacities and the corresponding predicted capacities of dented tubulars using different methods of analysis, Ricles (1993) concluded that Ellinas' formulation, which is based on first yield in the dent saddle, is overly conservative. In general, it has been found that Ellinas' approach can be either conservative or unconservative depending on the dent depth, member slenderness, and out-of-straightness. Ricles further concluded that DENTA (a computer program), Loh's interaction equations, numerical integration based on M-P-Φ relationships, and the nonlinear FEM are able to predict the capacity of the test members reasonably well.

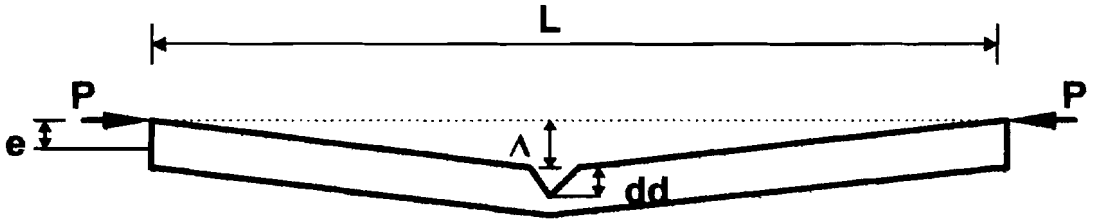

Figure B-6 : Definition Sketch for a Damaged Tubular Brace

Also, a joint industry project on testing and evaluation of damaged jacket braces was performed by PMB Engineering and Texas A&M University. Twenty salvaged braces were tested and their strength behavior compared with results gained from analyses using finite element beam column models of damaged braces. It was found that on average the analyses would overpredict the capacities by 21%. The agreement in this case is not as good as that presented by other investigators. Use of new and artificially damaged braces in other investigations may explain this inconsistency. Generally, corrosion is found to add large uncertainties to the properties of the entire member. Figure B-6 shows the definition sketch of a dent-damaged member with global out-of-straightness. Using ultimate capacity equations formulated by Ellinas (1984) and Loh (1993), the ratio of damaged compressive capacity over intact buckling capacity was estimated for ten tubular braces. The intact buckling capacity of a tubular brace was taken to be that given by API (1993b). The capacity ratios are plotted for two separate cases. Figure B-7 shows the results for no dent damage and varying global out-of-straightness, whereas Figure B-8 shows the results for no global bending damage and varying dent depth. In case of global bending damage, the two sets of results are in close agreement indicating that the second-order P-δ effects are captured coherently by both sets of formulations (Figure B-7). In case of dent-damaged tubulars, however, the results indicate significant differences in capacity predictions by the two sets of formulations. These results confirm those previously published in the literature regarding the level of conservatism of capacity equations developed by Ellinas. An attempt was made to

compare the results of different theoretical approaches to predict the compressive capacities of damaged tubulars. Nine specimen were selected from a database that represents all of the test results currently in the public domain (Loh, et al., 1992).

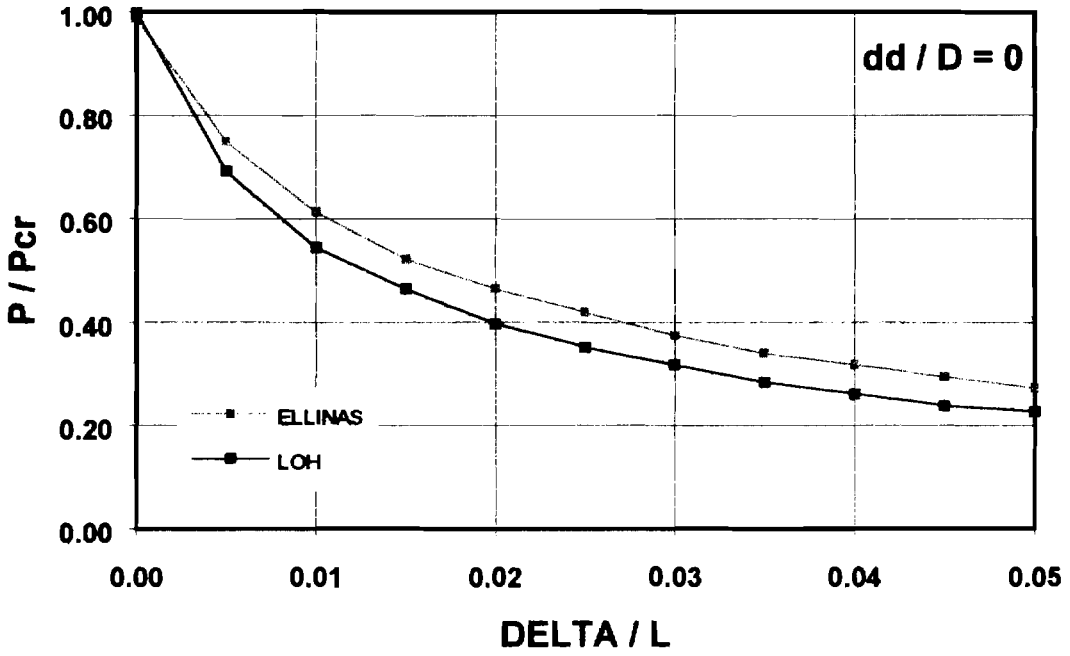

Figure B-7 : Comparison of Capacity Predictions for Tubulars with Global Bending Damage

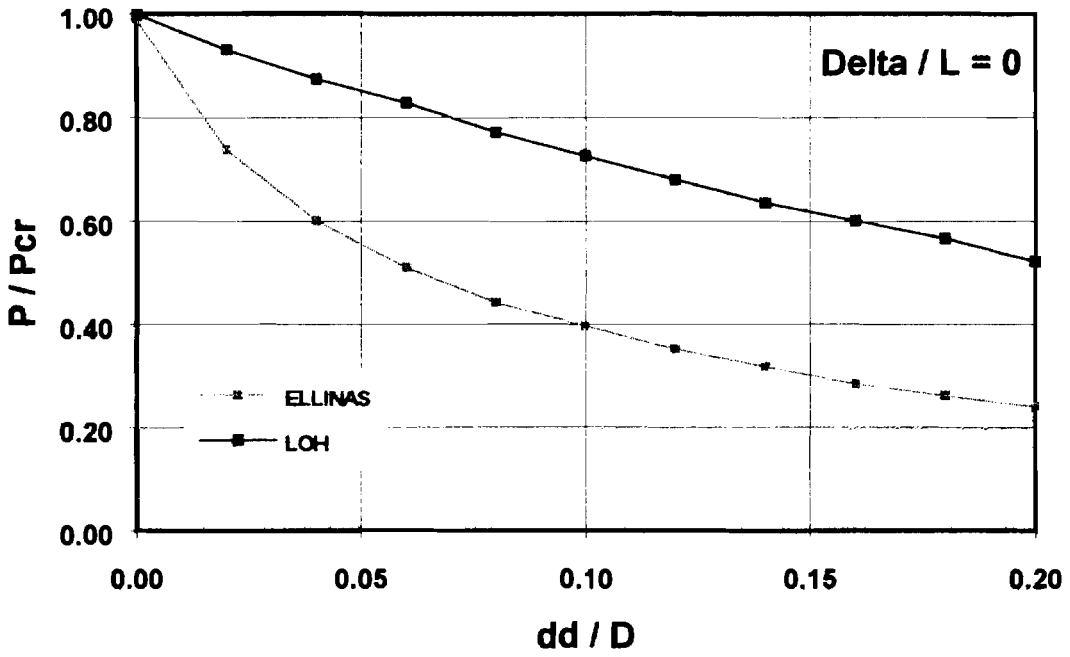

Figure B-8 : Comparison of Capacity Predictions for Tubulars with Dent Damage

Table B-2 contains the member sizes and material and damage properties. The test results are compared with those gained from the programs BCDENT (Loh, 1993), UC-DENT (Ricles et al., 1992), and capacity equations given by Ellinas (1983) and Loh (1993). The numerical results are given in Table B-3 and plotted in Figure B-9. The results indicate that for the data points presented, BCDENT capacity predictions are unbiased. Loh's formulations lead to capacity predictions that are close lower bounds of test results. Ellinas' formulation is in most cases overly conservative. UC-DENT predicts capacities that are close approximations of test results.

Based on experimental test results and parametric studies using different analytical methods, the following observations have been made and presented in the literature:

- The residual strength decreases significantly as the dent depth increases.
- For a given dent depth, the analyses show a decrease in residual strength for members with higher D/t ratio.
- The axial compression capacity decreases as the out-of-straightness increases, but the impact on ultimate moment is negligible.
- A mid-length dent location can be assumed for any dent within the middle-half section of members effective length.
- Accounting for strain hardening has only a small effect on the maximum predicted capacity.
- Lateral loadings, such as those caused by wave forces, can significantly affect dented brace capacity.
- The behavior of members with multiple forms of damage are generally dominated by one damage site.

Table B-2: Test Specimen Properties

Test	D [IN]	t [IN]	L [IN]	Sy [KSI]	E [KSI]	dd/D [%]	delta/L [%]	e/L [%]
A1	2.50	0.08	84.63	33.06	29145		0.02	
A2	2.50	0.08	84.63	33.21	30160		0.03	0.46
A3	2.50	0.08	84.63	32.77	28710	0.046	0.55	
B3	3.13	0.07	84.63	28.71	31030	0.08	0.5	
C1	4.00	0.07	84.63	30.60	29145		0.05	
C2	4.00	0.07	84.63	41.18	29870		0.05	0.46
C3	4.00	0.07	84.63	33.79	28565	0.034	0.04	
F1	16.02	0.39	305.24	44.23	28710		0.07	
F2	15.98	0.39	305.24	42.49	31030	0.124	0.18	

Table B-3: Experimental and Theoretical Capacities of Damaged Tubulars

Test	dd/D	delta/L [%]	e/L [%]	Ptest [KN]	BCDENT [KN]	LOH [KN]	ELLINAS [KN]	RICLES [KN]
A1		0.02		78.10	76.50	63.46	60.94	
A2		0.03	0.46	46.00	41.60	38.86	41.88	
A3	0.05	0.55		44.20	43.80	33.68	28.23	
B3	0.08	0.50		43.30	41.50	35.97	25.04	43.96
C1		0.05		121.00	104.80	95.37	96.48	119.66
C2		0.05	0.46	89.40	97.10	90.66	97.84	
C3	0.03	0.04		95.70	101.90	93.61	68.85	86.00
F1		0.07		3238.70	3509.90	3160.30	3192.10	3862.30
F2	0.12	0.18		2056.90	2031.70	1962.40	1068.00	2051.40

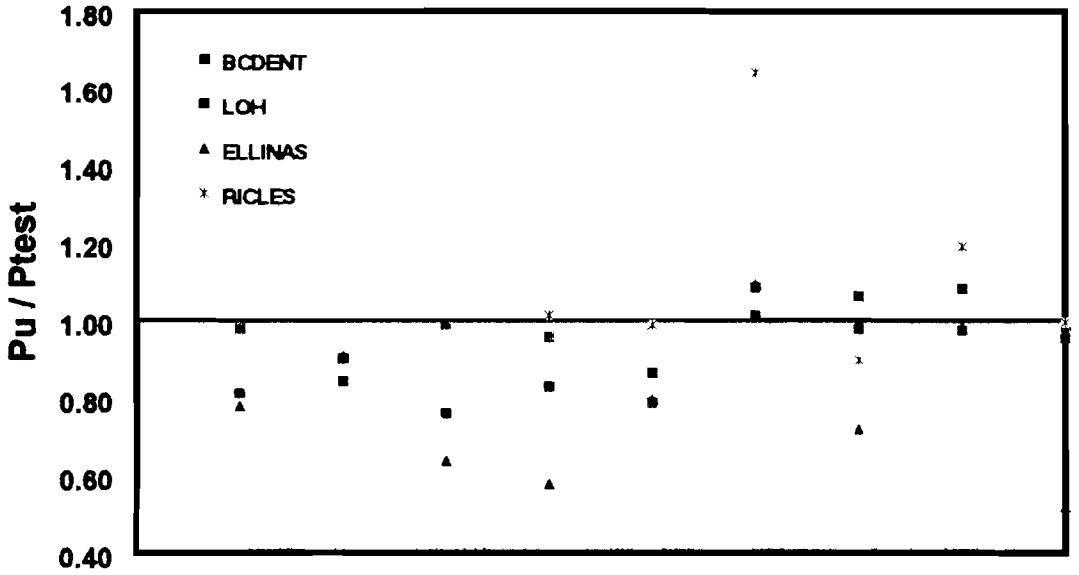

Figure B-9: Comparison of Capacity Predictions for
Tubulars with Dents and Global Bending Damage (Table B-3)

Corrosion Damage:

The marine environment is extremely corrosive. Although cathodic protection systems and protective coatings have been applied to prevent corrosion of steel members, in numerous cases corrosion damage of offshore platforms has still been observed. Corrosion results in a reduced wall thickness of the steel members which can lead to premature local buckling at the corroded areas.

Ostapenko et al. (1993) conducted experimental test on corroded tubulars from salvaged Gulf of Mexico platforms. Local buckling was reported at the most severely corroded area and an up to 50% reduction in capacity was observed. It was found that the patch with the most severe corrosion controls the local buckling of the member. Ricles and Hebor (1994) performed and presented an analytical and experimental study on patch-corroded steel tubular members. They used the results of an experimental program to verify a non-linear finite element model. The

calibrated FE model was then used to perform parametric studies and develop relationships between the residual strength of the damaged members and corrosion patch geometry. Based on a multi-variable, nonlinear regression analysis, a closed-form solution for patch-corroded tubular member strength was derived as a function of D/t ratio and corrosion patch geometry.

Grout-Repaired Tubular Members:

Given that the loss of strength of a member due to damage has a significant impact on strength and reliability of the platform system, it is desirable to apply some measure of strengthening the damaged member. Internal full-grouting or using grouted steel clamps are two economically attractive alternatives. Experimental results have shown that grouting significantly increases the capacity of damaged tubular members and therefore is a viable mean of strengthening such members. In the past practicing engineers have been applying existing analytical expressions for composite members to estimate the capacity of grout-filled damaged tubular members.

Parsanejad Method:

Responding to the need for some sort of analytical expressions, Parsanejad (1987) presented a simple analytical expression for estimating the ultimate capacity of grout-filled damaged tubular members. The analysis was based on the following simplifying assumptions: (1) full interaction exists between grout and the damaged tube and (2) grout provides sufficient support to the tube wall in the damaged region to prevent premature local buckling.

The first yield collapse criterion was adopted by Parsanejad; it was assumed that the ultimate capacity of damaged tubular member is reached when the compressive stress in the steel tube at the dent equals the yield stress. The damaged member was treated as a beam-column with uniform cross-sectional properties represented by the dented region. The total eccentricity was taken as the sum of eccentricities due to initial out-of-straightness, external load, and the distance between the original center of the tube and the centroid of the transformed cross section at the dent. Comparing the analytical results with the limited experimental results existent at the time, Parsanejad reported good agreement: the analytical results presented close lower-bound estimates of test results. The equations developed for grout repaired tubulars by Parsanejad has been integrated in TOPCAT and are listed in Section B.6.

Comparison Between Experimental and Predicted Capacities:

Ricles et al. (1993) performed experiments on thirteen large-scale damaged and repaired tubular members with two objectives: (1) assessing the residual strength of dent damaged steel tubular bracing members under combined flexural and axial load and (2) determining the effectiveness of using internal complete grouting and grouted steel clamps to repair dent damaged members.

The residual strength of damaged unrepaired and grout repaired specimens were compared to the undamaged design strength according to WSD and LRFD formats respectively. Test results were also compared to results gained from the modified Ellinas equation, computer program DENTA, and Parsanejad formulation. The following conclusions regarding grout-filled damaged tubular members are drawn by Ricles et al (1993): (1) Internal grout and grouted steel clamp repairs of a 0.1D dent damaged brace are successful in reinstating the original undamaged member's strength by arresting dent growth inwards, and (2) the predicted strength of internally grout-repaired members based on Parsanejad's method provided a close lower bound to experimental data.

B.5 LOH'S INTERACTION EQUATIONS FOR DENT-DAMAGED TUBULARS

Table B-4: Notation

A_d	effective cross-sectional area of dent section
A_0	cross-sectional area of undamaged member
A_{st}	cross-sectional area of the steel
A_s	cross-sectional area of the soil plug in pile
D	outside diameter of tubular member
dd	dent depth
ΔY	primary out-of-straightness of a dented member
ΔY_0	$=0.001\ L$
E	Young's modulus
f_y	yield stress
I_d	effective moment of inertia of dent cross-section
I_0	moment of inertia of undamaged cross-section
K_0	effective length factor of undamaged member
K	effective buckling length factor
L	unbraced member length
λ	slenderness ratio
λ_d	slenderness parameter of a dented member = $(P_{ud}/P_{Ed})^{0.5}$
M_u	ultimate moment capacity
M_{cr}	critical moment capacity (local buckling)
M_p	plastic moment capacity of undamaged member
M_{ud}	ultimate negative moment capacity of dent section
M-	negative moment for dent section
M+	positive moment for dent section
M*	neutral moment for dent section
P_{crd}	critical axial buckling capacity of a dented member ($\Delta L>0.001$)
P_{crd0}	critical axial buckling capacity of a dented member ($\Delta L=0.001$)
P_E	Euler load of undamaged member
P_u	axial compression capacity
P_{ud}	axial compression capacity of a short dented member
P_{crl}	axial local buckling capacity
P_{cr}	axial column buckling capacity
P_y	tensile capacity
r	radius of gyration
t	member wall thickness
UC	unity check

Undamaged Cross Sectional Capacities:

$$P_u = F_y A_o \qquad \text{for } \frac{D}{t} \le 60 \qquad \text{(B.1)}$$

$$P_u = F_y A_o \left[1.64 - 0.23 \left(\frac{D}{t} \right)^{0.25} \right] \qquad \text{for } \frac{D}{t} > 60 \qquad \text{(B.2)}$$

$$\frac{M_u}{M_p} = 1.0 \qquad \text{for } 0 \le \frac{F_y D}{t} \le 1500 \text{ (ksi)} \qquad \text{(B.3)}$$

$$\frac{M_u}{M_p} = 1.13 - 2.58\left(\frac{F_y D}{Et}\right) \qquad \text{for } 1500 < \frac{F_y D}{t} \le 3000 \text{ (ksi)} \qquad \text{(B.4)}$$

$$\frac{M_u}{M_p} = 0.94 - 0.76\left(\frac{F_y D}{Et}\right) \qquad \text{for } 3000 < \frac{F_y D}{t} \le 300F_y \text{ (ksi)} \qquad \text{(B.5)}$$

$$M_p = F_y t(D-t)^2 \qquad \text{(B.6)}$$

Dent-Section Properties:

$$\frac{P_{ud}}{P_u} = \frac{A_d}{A_o} = \exp\left(-0.08\frac{dd}{t}\right) \ge 0.45 \qquad \text{(B.7)}$$

$$\frac{M_{ud}}{M_u} = \frac{I_d}{I_o} = \exp\left(-0.06\frac{dd}{t}\right) \ge 0.55 \qquad \text{(B.8)}$$

Strength Check:

$$UC = \frac{P}{P_{ud}} + \sqrt{\left(\frac{M-}{M_{ud}}\right)^{\alpha} + \left(\frac{M^*}{M_u}\right)^2} \le 1.0 \qquad \text{(B.9)}$$

$$UC = \frac{P}{P_{ud}} + \sqrt{\left(\frac{M+}{M_{ud}}\right)^2 + \left(\frac{M^*}{M_u}\right)^2} \le 1.0 \qquad \text{(B.10)}$$

Stability Check:

$$UC = \frac{P}{P_{crd}} + \sqrt{\left(\frac{M-}{\left(1-\frac{P}{P_{Ed}}\right)M_{ud}}\right)^{\alpha} + \left(\frac{M^*}{\left(1-\frac{P}{P_E}\right)M_u}\right)^2} \le 1.0 \qquad \text{(B.11)}$$

$$UC = \frac{P}{P_{crd}} + \sqrt{\left(\frac{M+}{\left(1-\frac{P}{P_{Ed}}\right)M_{ud}}\right)^2 + \left(\frac{M^*}{\left(1-\frac{P}{P_E}\right)M_u}\right)^2} \le 1.0 \qquad \text{(B.12)}$$

$$\alpha = 2 - 3\frac{dd}{D} \tag{B.13}$$

Critical Buckling Capacities:

$$P_{crdo} = P_{ud}\left[1 - 0.25\lambda_d^2\right] \qquad \text{for } \lambda \le \sqrt{2} \tag{B.14}$$

$$P_{crdo} = P_{ud}\frac{1}{\lambda_d^2} = P_{Ed} \qquad \text{for } \lambda > \sqrt{2} \tag{B.15}$$

$$\frac{P_{crd}}{P_{crdo}} + \frac{P_{crd}\Delta Y}{\left(1 - \frac{P_{crd}}{P_{Ed}}\right)M_{ud}} = 1.0 \tag{B.16}$$

B.6 PARSENAJAD'S STRENGTH EQUATIONS FOR GROUT-FILLED TUBULARS

Table B-5: Notation

A_g	area of grout at the dented section
A_s	area of steel
A_{tr}, A_{tr}^*	transformed areas at the dented and undented cross section
D	mid-thickness diameter
d	depth of denth
E_g	elastic modulus of grout
E_s	elastic modulus of steel
e	external eccentricity of load
e_g	distance between centroid of grout at the dented cross section to the centroid of undented cross section
e_s	distance between centroid of steel at the dented cross section to the centroid of undented cross section
e_t	$= e + \delta + e_{tr}$
e_{tr}	distance between centroid of the dented and undented transformed cross section
I_g	moment of inertia of grout at dented cross section
I_s	moment of inertia of steel at dented cross section
I_{tr}	transformed moment of inertia of dented cross section
k	nondimensionalized parameter = $A_{tr}\, e_t / Z_{tr}$
l	effective length of member
m	nondimensionalized parameter = A_{tr} / A_{tr}^*
n	elastic modular ratio = E_s / E_g
P_u	ultimate axial capacity
P_y	full yield capacity = $A_{tr}^* \sigma_y$
r_{tr}	transformed radious of gyration of dented section
t	thickness of tubular member
Z_{tr}	transformed section modulus with respect to the dented side
α	angle shown in fig.
δ	overall bending
λ	reduced slenderness parameter
σ_a	axial stress
σ_b	bending stress
σ_e	Euler buckling stress
σ_u	ultimate axial stress
σ_y	yield stress of steel

$$\left(\frac{\sigma_u}{\sigma_y}\right)^2 - \left(\frac{1+k}{\lambda^2} + m\right)\left(\frac{\sigma_u}{\sigma_y}\right) + \frac{m}{\lambda^2} = 0 \qquad \text{(B.17)}$$

$$\kappa = \sqrt{\frac{\sigma_y}{\sigma_e}} = \frac{l}{\pi r_{tr}}\sqrt{\frac{\sigma_y}{E_s}} \qquad \text{(B.18)}$$

$$k = \frac{A_{tr} e_t}{Z_{tr}} \tag{B.19}$$

$$m = \frac{A_{tr}}{A_{tr}^*} \tag{B.20}$$

Cross-Section Properties:

$$A_{tr} = A_s + \frac{A_g}{n} \tag{B.21}$$

$$A_s = \pi D t \tag{B.22}$$

$$A_g = \frac{D^2}{4}\left(\pi - \alpha + \frac{1}{2}\sin 2\alpha\right) \tag{B.23}$$

$$n = \frac{E_s}{E_g} \tag{B.24}$$

$$\alpha = \cos^{-1}\left(1 - 2\frac{d}{D}\right) \tag{B.25}$$

$$e_{tr} = \frac{A_s e_s + \frac{A_g}{n} e_g}{A_{tr}} \tag{B.26}$$

$$e_s = \frac{D}{2\pi}(\sin\alpha - \alpha\cos\alpha) \tag{B.27}$$

$$e_g = \frac{(D\sin\alpha)^3}{12 A_g} \tag{B.28}$$

$$Z_{tr} = \frac{2I_{tr}}{D}\cos\alpha + e_{tr} \tag{B.29}$$

$$r_{tr} = \sqrt{\frac{I_{tr}}{A_{tr}}} \tag{B.30}$$

$$I_{tr} = I_s + \frac{I_g}{n} + A_s\left(e_{tr} - e_s\right)^2 + \frac{A_g}{n}\left(e_g - e_{tr}\right)^2 \approx I_s + \frac{I_g}{n} \tag{B.31}$$

$$I_s = \frac{D^3 t}{4}\left[\frac{\pi-\alpha}{2} - \frac{\sin 2\alpha}{4} + \alpha\cos^2\alpha - \frac{(\sin\alpha - \alpha\cos\alpha)^2}{\pi}\right] \quad \text{(B.32)}$$

$$I_g = \frac{D^4}{64}\left[\pi - \alpha + \frac{\sin 4\alpha}{4}\right] - \frac{D^4 \sin^6\alpha}{144 A_g} \quad \text{(B.33)}$$

$$A_{tr}^* = A_s + \frac{\pi D^2}{4n} \quad \text{(B.34)}$$

B.7 REFERENCES

American Petroleum Institute, "Recommended Practice for Planning, Designing and Constructing Fixed Offshore Platforms - Working Stress Design (RP 2A-WSD)," 20th Edition, Washington, D.C., July 1993a.

American Petroleum Institute, "Recommended Practice for Planning, Designing and Constructing Fixed Offshore Platforms - Load and Resistance Factor Design (RP 2A-LRFD)," First Edition, Washington, D.C., July 1993b.

Ellinas, C.P., "Ultimate Strength of Damaged Tubular Bracing Members," *Journal of Structural Engineering*, Vol. 110, No.2, February 1984.

Hellan, O., Moan, T., Drange, S.O., "Use of Nonlinear Pushover Analyses in Ultimate Limit State Design and Integrity Assessment of Jacket Structures," *Proceedings of the 7th International Conference on Behavior of Offshore Structures*, BOSS '94, Vol. 3, Structures, C. Chryssostomidis (Ed.), Elsevier Science Inc., New York, NY, 1994.

Kim W., Ostapenko A., "A Simplified Method to Determine The Ultimate Strength of Damaged Tubular Segment," 1992.

Loh, J.T., Kahlich, J.L., Broekers, D.L., "Dented Tubular Steel Members," Exxon Production Research Company, Offshore Division, Houston, TX, March 1992.

Loh, J.T., "Ultimate Strength of Dented Tubular Steel Members." *Proceedings of the 3rd International Offshore and Polar Engineering Conference*, Vol. 4, pp. 134-145, 1993.

Parsanejad S., "Strength of Grout-Filled Damaged Tubular Members," *Journal of Structural Engineering*, ASCE, Vol. 113, No. 3, March 1987.

Ostapenko, A., Wood, B., Chowdhury, A., Hebor, M., "Residual Strength of Damaged and Deteriorated Tubular Members in Offshore Structures," ATLSS Report No. 93-03, Lehigh University, Betlehem, PA., 1993.

Ricles, J.M., Bruin, W.M., Sooi, T.K., "Residual Strength and Repair of Dent-Damaged Tubulars and the Implication on Offshore Platform Assessment and Requalification," 1992.

Ricles, J.M., Lamport, W.P., Gillum, T.E., "Residual Strength of Damaged Offshore Tubular Bracing," OTC 6938, *Proceedings of the Offshore Technology Conference*, Houston TX, May 1992.

Ricles, J.M., Gillum, T.E., Lamport, W.P., "Grout Repair of Dent-Damaged Steel Tubular bracing," OTC 7151, *Proceedings of the Offshore Technology Conference*, Houston TX, May 1993.

Ricles, J.M., Hebor, M.F., "Residual Strength and Epoxy-based Grout Repair of Corroded Offshore Tubulars," BOSS 94, 1994.

SINTEF, "USFOS: A Computer Program for Progressive Collapse Analysis of Steel Offshore Structures," Publication N-7034, Revised Version 6.0., Trondheim, Norway, 1994.

Yura, J.A., Zettlemoyer, N., Edwards, F.E., "Ultimate Capacity Equations for Tubular Joints," OTC 3690, *Proceedings of the Offshore Technology Conference*, Houston TX, May 1980.

APPENDIX D: SIMPLIFIED STRENGTH AND STIFFNESS OF BRACED AND GUYED CAISSONS AND OF TRIPODS

by
James D. Stear and Professor Robert G. Bea

Portions of this Appendix have been previously published in the following:

Stear, J. D. and Bea, R. G., "ULSLEA Enhancements: Fatigue Analysis / Earthquake Analysis / Additional Configurations / Screening Methodologies Project Phase III," Report to Joint Industry Project Sponsors, Marine Technology and Management Group, Department of Civil and Environmental Engineering, University of California at Berkeley, CA, June 1997.

TABLE OF CONTENTS **PAGE**

D.1 INTRODUCTION

TOPCAT allows for the analysis of caissons which are supported either by braces (two identical braces at 90°) or guy-wires (three identical wires at 120°). In both cases, the lateral capacity of the caisson is assumed to be governed by a series system of the following: the brace or wire, the connection between the support and the caisson, and the anchor support.

TOPCAT also allows for the analysis of tripod platforms of either equilateral or isosceles plan, with either equal batter or a single vertical leg. Capacity is developed for two axes of loading: an axis parallel to Frame A, and an axis perpendicular to Frame A. No torsion is considered in the formulation.

D.2 BRACED CAISSONS

TOPCAT allows for the analysis of simple braced caissons of the MOSS® II type, as shown in Figure D-1. The platform consists of a single caisson of uniform diameter and thickness, two tubular braces orthogonal to one another, and two anchor piles, each of which supports one brace.

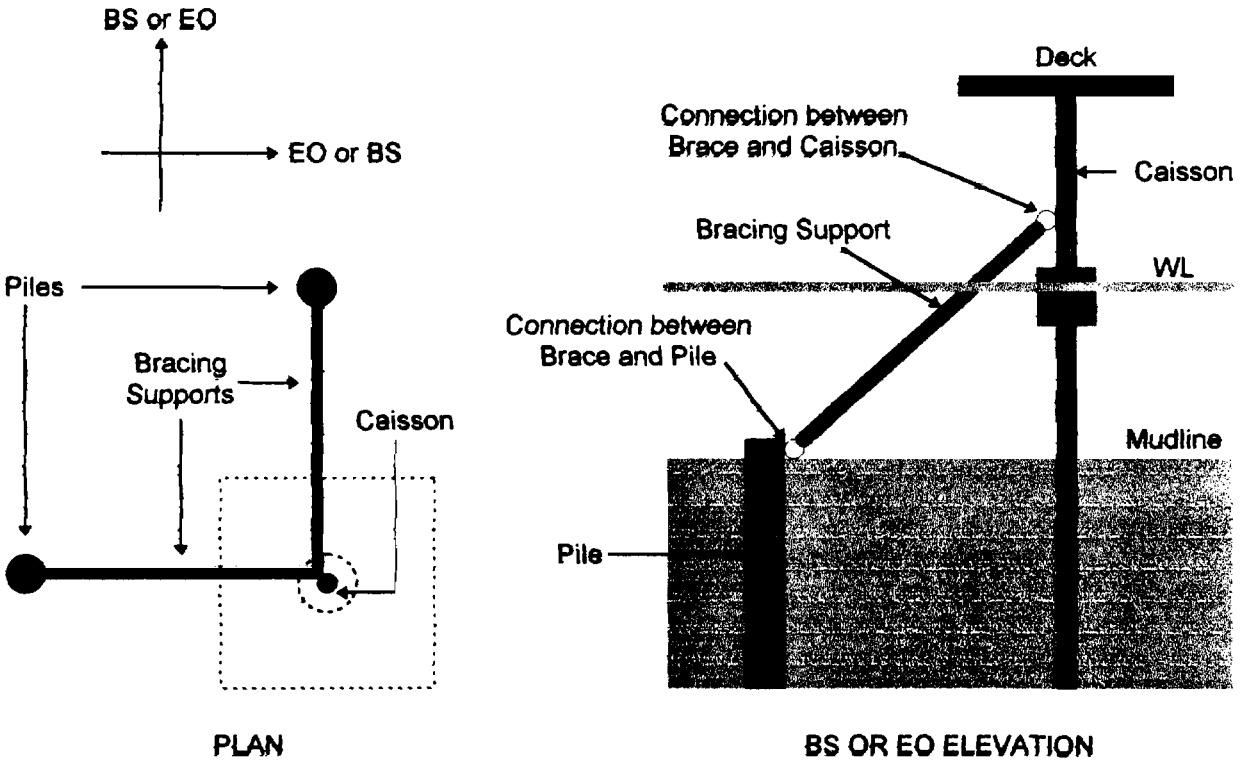

Figure D-1: Braced Caisson

The platform is assumed to have two principal axes of loading, as with jacket-type platforms. TOPCAT assumes the strength in each direction will be the same; however, a user may specify different appurtenance areas and other load attractors for the two axes. Braces are only assumed to provide support against loads parallel to their axis.

The caisson is treated as a supported cantilever beam, as shown in Figure D-2. Horizontal load is assumed to be transferred to the foundation level by the support system; the caisson itself is assumed to carry no lateral load. The caisson will, however, be subject to vertical forces, as shown in Figure D-3.

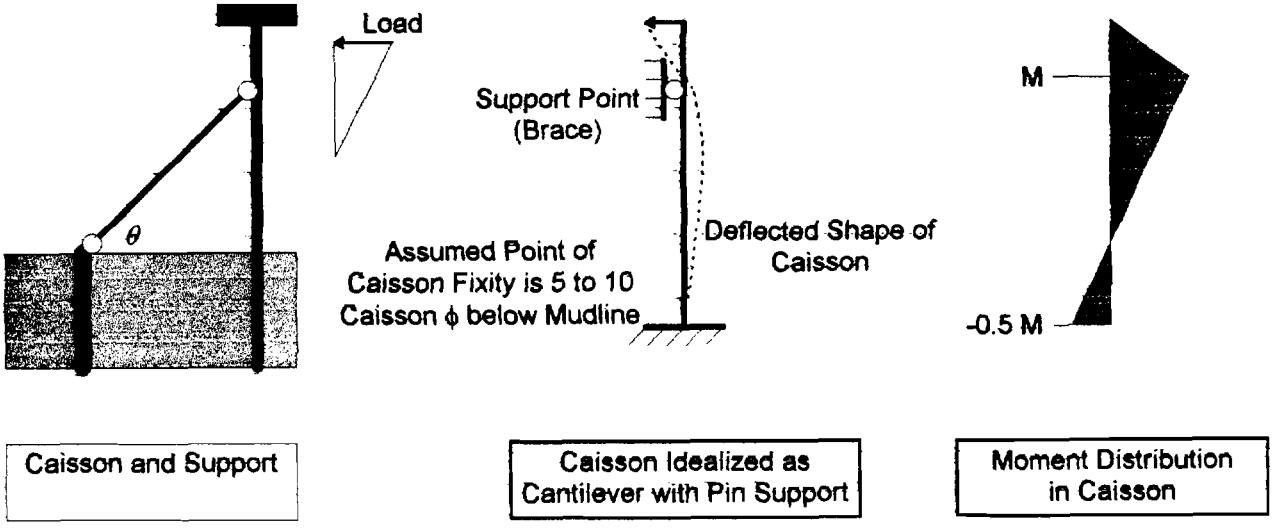

Figure D-2: Supported Caisson Idealization

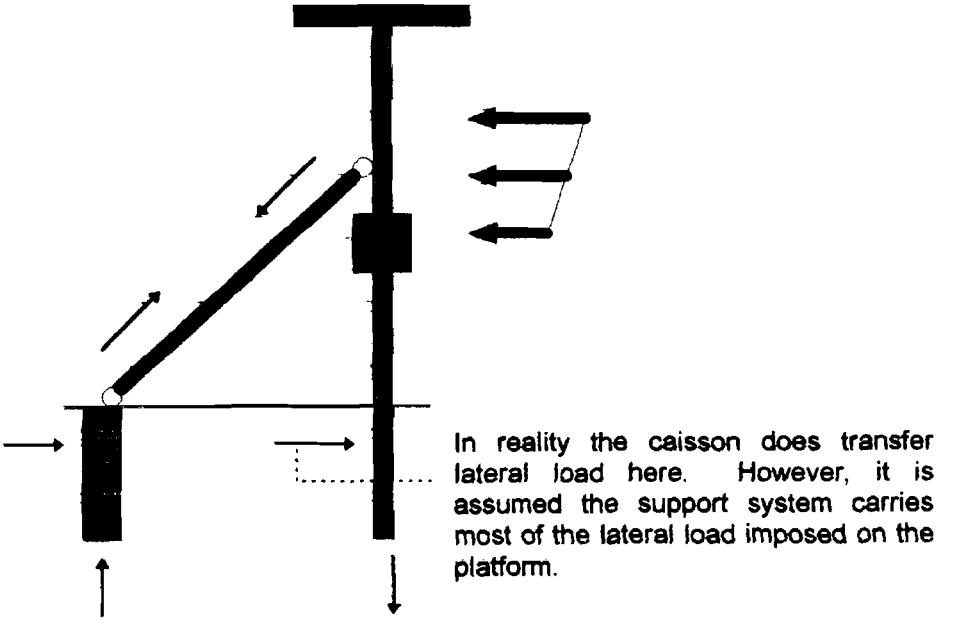

Figure D-3: Load Path in Caisson

The platform is assumed to have three modes of failure under lateral loads:

- Hinging of the caisson above the point of bracing support.
- Failure of a support, either by yielding or buckling of the bracing member, yielding of the connection between the brace and the caisson, or brace and the pile, or by pullout, plunging or lateral subsidence of the pile.
- Pull-out or plunging of the caisson.

Hinging of Caisson Above Support Point:

The ultimate capacity of the caisson above the point of bracing is assumed to be reached when a plastic hinge forms just above the bracing attachment point, as shown in Figure D-4.

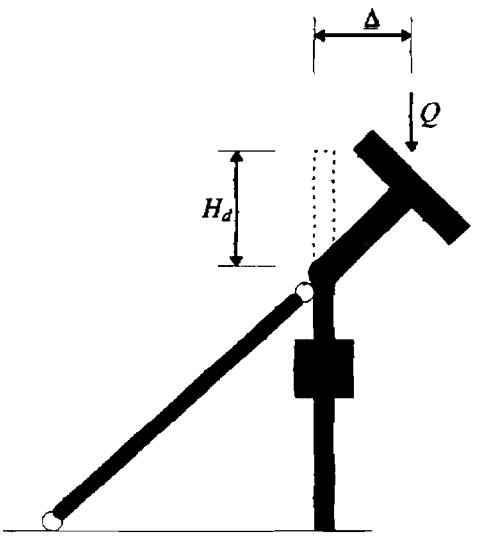

Figure D-4: Collapse Mechanism for Unsupported Section of Caisson

The equivalent horizontal load capacity is thus:

$$P_{uH} = \frac{(M_u - Q\Delta)}{H_d}$$

where:

M_u = ultimate moment capacity of caisson cross-section
Q = vertical deck load
H_d = distance from deck to bracing point
Δ = deck displacement at collapse

The ultimate moment the cross-section can support is estimated from:

$$M_u = M_{crl} \cos\left(\frac{\pi Q}{2P_{crl}}\right)$$

Where M_{crl} and P_{crl} are the critical moment and axial load associated with local buckling of the cross-section.

The deck displacement can be estimated from:

$$\Delta \cong M_u\left(\frac{H_d^2}{3EI_c} + \frac{H_d\left(H_s + 10D_c\right)}{4EI_c}\right)$$

where:

I_c = moment of inertia of caisson cross-section
D_c = diameter of caisson
H_s = height of support point above mudline

Failure in Support:
The ultimate capacity of a support will be determined by (1) the yielding or buckling capacity of the tubular brace, (2) the yield capacity of the connection between the brace and caisson or brace and pile, or (3) the pullout, plunging or lateral capacity of the pile. The capacity of the supported section will be reduced by the need to balance the bending action of the unsupported section above the support point, but will be effectively increased due to the gradual mobilization of the bending capacity of the caisson.

The effective horizontal capacity of the supported section is given by:

$$P_{u\text{-}l} = P_{u\text{-}l\text{-}support} + \frac{P_{u\text{-}l\text{-}support}}{k_{l\text{-}support}} k_{l\text{-}caisson} - \frac{3M}{2\left(H_s + 5D_c\right)}$$

where:

M = moment in caisson at point of bracing attachment, from loads above point of bracing

$k_{l\text{-}caisson}$ = horizontal cantilever stiffness of main pile, taken as $\dfrac{3EI_d}{\left(H_s + 10D_c\right)^3}$

The ultimate horizontal load capacity of the support system, $P_{u\text{-}l\text{-}support}$, should be the minimum of the following:

$A_c\sigma_y$ = yield capacity of connections, expressed as connection area A_c × steel yield stress of connections σ_y

$P_{u\text{-}brace} \cos\theta$ = horizontal component of tubular brace axial capacity in either tension or compression depending on load; θ is the angle between the brace axis and the horizontal plane

$P_{u\text{-}l\text{-}pile}$ = lateral load capacity of pile at pile head

$P_{u\text{-}z\text{-}pile} / \tan\theta$ = horizontal load at support point needed to exceed axial pile capacity

$P_{u\text{-}brace}$ is calculated following the procedure in Appendix B of the User Manual for tubular bracing members. The brace can be specified as being in tension or compression. Determination of the pile capacities $P_{u\text{-}l\text{-}pile}$ and $P_{u\text{-}z\text{-}pile}$ is performed in accordance with the procedures of Appendix G of the User Manual.

The effective horizontal stiffness of the support system for load at the support point can be approximated as a series system made up of the tubular brace and the lateral and axial pile-head stiffnesses:

$$\frac{1}{k_{l-support}} = \frac{1}{k_{l-pile}} + \frac{\tan^2\theta}{k_{z-pile}} + \frac{L}{EA\cos^2\theta}$$

where A and L are the cross-section steel area and length of the tubular brace. The connections between the brace and the pile and caisson are assumed to be rigid.

Caisson Pullout or Plunging:

The last concern is that of pull-out or plunging of the caisson. The axial capacity of the imbedded portion of the caisson is determined through application of the procedures in Appendix G of the User Manual.

Stiffnesses for Modal Analysis:

TOPCAT idealizes braced caissons as 2 DOF systems for lateral response, and an SDOF system for vertical response, as shown in Figure D-5.

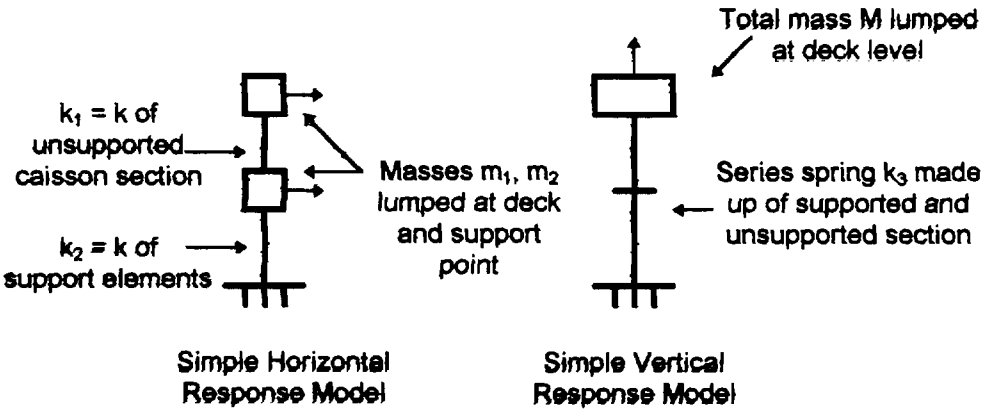

Figure D-5: Lateral and Vertical Response Models for Braced Caissons

k_1 is the lateral stiffness of the caisson above the support point, and is given by:

$$k_1 = \left(\frac{H_d^3}{3EI_c} + \frac{H_d^2\left(H_s + 10D_c\right)}{4EI_c} \right)^{-1}$$

k_2 is the lateral stiffness of the caisson and support acting together, and is given by:

$$k_2 = k_{l\text{-}support} + \frac{3EI_c}{\left(H_s + 10D_c\right)^3}$$

k_3 is found from:

$$\frac{1}{k_3} = \frac{1}{2k_{z\text{-}support} + \dfrac{H_s + 10D_c}{EA_{caisson}}} + \frac{H_d}{EA_{caisson}}$$

$k_{z\text{-}support}$ is the vertical stiffness of the support system, and is given by:

$$\frac{1}{k_{z\text{-}support}} = \frac{1}{k_{z\text{-}pile}} + \frac{\tan^2\left(90^\circ - \theta\right)}{k_{l\text{-}pile}} + \frac{L}{EA\cos^2\left(90^\circ - \theta\right)}$$

No period lengthening (User Manual Appendix E) is applied to the modal periods of the caisson; the foundation stiffnesses have been included in the stiffness formulation of the discrete model.

D.3 GUYED CAISSONS

TOPCAT also allows a user to analyze simple guyed caissons of the type shown in Figures D-6 and D-7.

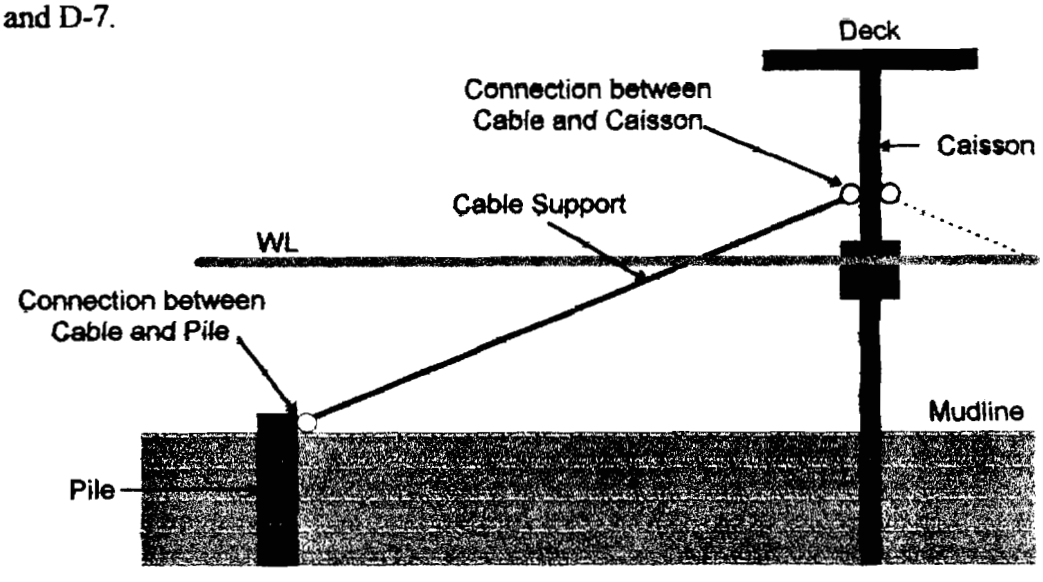

Figure D-6: Guyed Caisson Elevation View

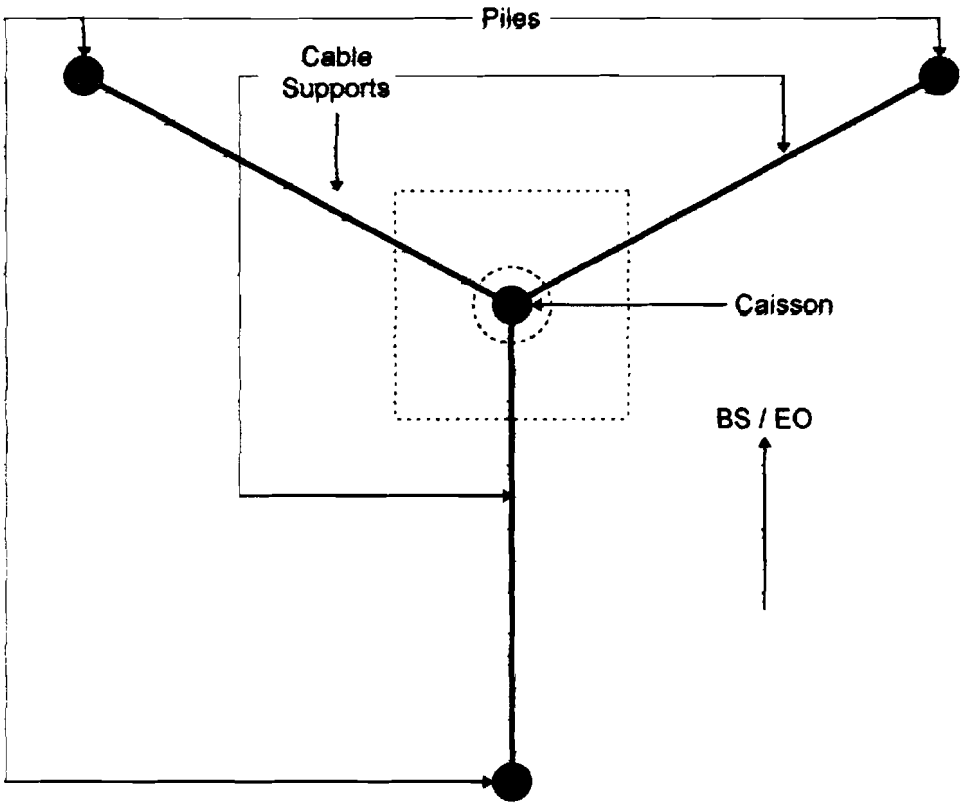

Figure D-7: Guyed Caisson Plan View

The guyed caisson is very similar to the braced caisson, except that lateral support is provided by three heavy cables, all of identical design, laid out from the axis of the caisson at 120° intervals. While two axes of loading are considered by TOPCAT, these loads are both assumed to be parallel with one of the cables. Hence, capacity is only formulated once but used for both EO and BS load cases. TOPCAT assumes the load will always place the cable in tension. Users may specify different load attractors for the two principal directions.

As with the braced caisson, lateral load on the guyed caisson is assumed to be transferred to the foundation by the support system. Hence, there are three primary failure modes:

- Hinging of the caisson above the point of cable support.
- Failure of a support, either by yielding of the cable, yielding of the connection between the cable and the caisson, or cable and the pile, or by pullout, plunging or lateral subsidence of the pile.
- Pull-out or plunging of the caisson.

The capacity of the unsupported section and the axial capacity of the caisson are determined in a manner identical to that used for braced caissons. The effective horizontal capacity of the supported section is given by:

$$P_{u\text{-}l} = P_{u\text{-}l\text{-}support} + \frac{P_{u\text{-}l\text{-}support}}{k_{l\text{-}support}} k_{l\text{-}caisson} - \frac{3M}{2\left(H_s + 5D_c\right)}$$

where:

M = moment in caisson at point of bracing attachment, from loads above point of bracing

$k_{l\text{-}caisson}$ = horizontal cantilever stiffness of main pile, taken as $\dfrac{3EI_d}{\left(H_s + 10D_c\right)^3}$

The ultimate horizontal load capacity of the support system, $P_{u\text{-}l\text{-}support}$, should be the minimum of the following:

$A_c\sigma_y$ = yield capacity of connections, expressed as connection area A_c × steel yield stress of connections σ_y

$P_{u\text{-}cable}\cos\theta$ = horizontal component of cable tension capacity; θ is the angle between the cable axis and the horizontal plane

$P_{u\text{-}l\text{-}pile}$ = lateral load capacity of pile at pile head

$P_{u\text{-}z\text{-}pile} / \tan\theta$ = horizontal load at support point needed to exceed axial pile capacity

$P_{u\text{-}cable}$ is given by:

$$P_{u\text{-}cable} = A_{cable}\sigma_y - F_{pretension}$$

where:

A_{cable} = cross-section area of cable

$F_{pretension}$ = pre-tensioning force in cable

Determination of the pile capacities $P_{u\text{-}l\text{-}pile}$ and $P_{u\text{-}z\text{-}pile}$ is performed in accordance with the procedures of Appendix G of the User Manual.

The effective horizontal stiffness of the support system for load at the support point can be approximated as a series system made up of the cable stiffness and the lateral and axial pile-head stiffnesses:

$$\frac{1}{k_{l\text{-}support}} = \frac{1}{k_{l\text{-}pile}} + \frac{\tan^2\theta}{k_{z\text{-}pile}} + \frac{L}{EA\cos^2\theta}$$

where A and L are the cross-section area and length of a cable. The connections between the cable and the pile and caisson are assumed to be rigid. If the cables in the platform have been pre-tensioned to the point at which they will not go slack for expected displacements of the support point, the value of $k_{l\text{-}support}$ calculated from the above will be doubled.

The guyed caisson is modeled like the braced caisson for the purposes of modal analysis. Stiffnesses are developed in a similar manner, and all three cables are assumed active for the purpose of vertical response.

The caisson in the guyed caisson platform is subject to an additional load $Q_{pretension}$ if the cables in the platform are pre-tensioned. This load is:

$$Q_{pretension} = 3F_{pretension} \sin\theta$$

D.4 TRIPODS

TOPCAT allows a user to analyze tripod jackets in addition to more conventional types. The tripods can have either equilateral (all frames equal sizes) or isosceles (two frames equal sizes) plan, and the platform can be specified as having a single vertical leg.

TOPCAT formulates capacities for tripod components using the same procedures as in Appendix B for standard jackets, but formulates these capacities for the two axes shown in Figure D-8.

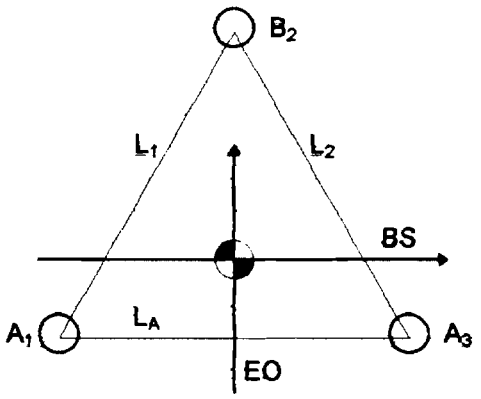

- Sides 1, 2 must have equal lengths
- Frame 1, 2 element strengths and stiffnesses are projected to EO axis to obtain components' EO strengths and stiffnesses.
- Frame 1, 2 element strengths and stiffnesses are projected to BS axis to obtain element contributions to BS strengths and stiffnesses together with Frame A elements.
- Piles A1 and A3 resist BS overturning. All piles resist EO overturning, but pile B2 carries twice the load as A1 and A3.

Figure D-8: Tripod Principal Axes

This will not affect the formulation of unbraced deck bay capacity and foundation level lateral capacity, but it will affect the formulation of jacket bay capacity and foundation overturning load sharing.

A typical tripod jacket bay is shown in Figure D-9. For loads on the BS axis, the capacity of the jacket bay is assumed to be governed by the strength of braces in Frame A, i.e. the capacities of the braces in Frames 1 and 2 are not checked for this direction of load. However, the braces in Frames 1 and 2 will provide some resistance for load on this axis. The BS capacity is thus formulated as:

$$P_{u,1\_BS} = \left(\frac{P_{u\_MLTF\_A} \cos\alpha_{MLTF\_A}}{k_{MLTF\_A}} \right) \left(\sum_i k_{i\_A} + \sum_j k_{j\_1,2} \cos^2\theta \right)$$

where:

k_{i_A} = $(EA_i\cos^2\alpha_i)/L_i$, horizontal stiffnesses of braces in Frame A

$k_{j\_1,2}$ = $(EA_j\cos^2\alpha_j)/L_j$, horizontal stiffnesses of braces in Frames 1 and 2

and $P_{u\_MLTF\_A}$, α_{MLTF_A}, and k_{MLTF_A} are the axial capacity, angle with the horizontal and horizontal stiffness of the most-likely-member-to-fail in Frame A.

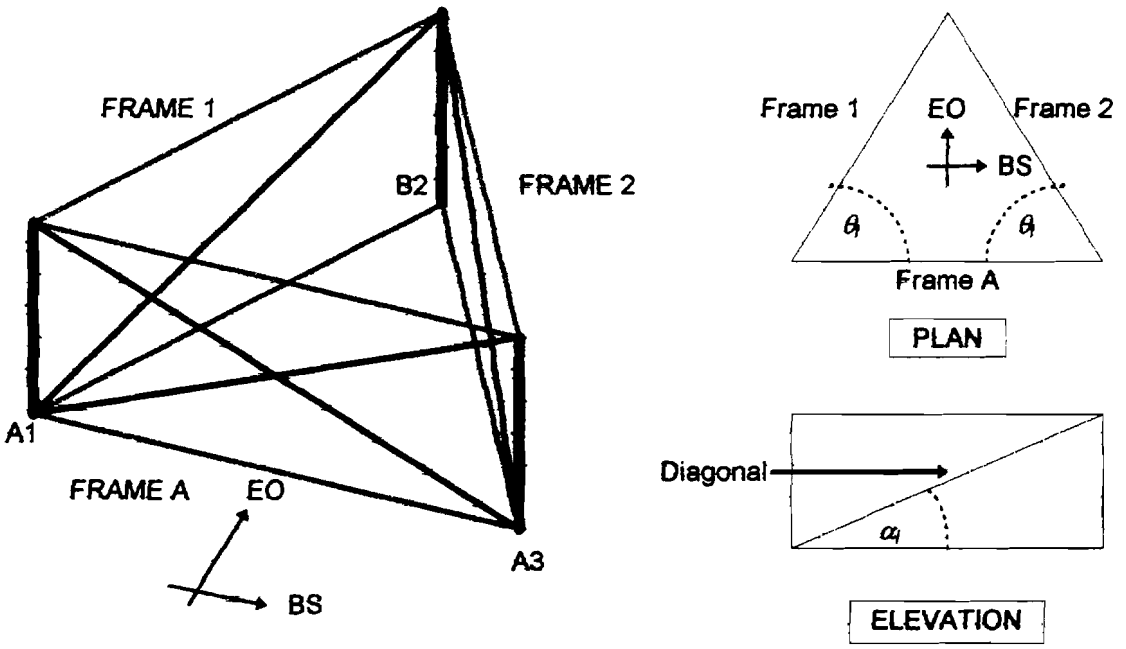

Figure D-9: Braced Bay in Tripod Jacket

For loading on the EO axis, the braces in Frames 1 and 2 are assumed to share the load, while the braces in Frame A do not contribute to the capacity. Thus the EO capacity will be given by:

$$P_{u,1\_EO} = \left(\frac{P_{u\_MLTF\_1,2} \cos\alpha_{MLTF\_1,2} \sin\theta}{k_{MLTF\_1,2} \sin^2\theta} \right) \left(\sum_j k_{j\_1,2} \sin^2\theta \right)$$

where:

$k_{j\_1,2}$ = $(EA_j\cos^2\alpha_j)/L_j$, horizontal stiffnesses of braces in Frames 1 and 2

and $P_{u\_MLTF\_1,2}$, $\alpha_{MLTF\_1,2}$, and $k_{MLTF\_1,2}$ are the axial capacity, angle with the horizontal and horizontal stiffness of the most-likely-member-to-fail from both Frames 1 and 2.

For the purpose of determining the axial loads on piles for the axial RSR calculations, it is assumed that piles A1 and A3 share the loads from overturning caused by BS loads equally, and that pile B2 provides no resistance. Hence, overturning resistance is:

$$M_{u\_BS} = \left(\frac{L_A}{2} \right) \left(P_{z\_A1} + P_{z\_A3} \right)$$

For overturning caused by loads on the EO axis, it is assumed that pile B2 is subject to twice as much load as piles A1 and A3. This is due to the assumption that the foundation rotates as a rigid plate, and hence, for rotation about the centroid of the foundation, pile B2 will be subject to twice as much axial displacement as piles A1 and A3. Overturning capacity is:

$$M_{u\_EO} = \left(\frac{L_{1,2} \sin\theta}{3} \right) \left(P_{z\_A1} + P_{z\_A3} \right) + \left(\frac{2L_{1,2} \sin\theta}{3} \right) \left(P_{z\_B2} \right)$$

APPENDIX E:
SIMPLIFIED STRENGTH-LEVEL EARTHQUAKE ANALYSIS OF FIXED STEEL OFFSHORE PLATFORMS

by
James D. Stear and Professor Robert G. Bea

Portions of this Appendix have been previously published in the following:

Stear, J. D. and Bea, R. G., "Earthquake Analysis of Offshore Platforms / Screening Methodologies Project Phase III," Report to Joint Industry Project Sponsors, Marine Technology and Management Group, Department of Civil and Environmental Engineering, University of California at Berkeley, CA, June 1997.

TABLE OF CONTENTS **PAGE**

E.1 INTRODUCTION

Approximately 100 template-type offshore platforms have been installed in seismically-active regions of the world's oceans. As new regions with the potential for significant seismic activity are now beginning to be developed, methods are needed to assist in the preliminary design of the structures which will be placed in those regions. In addition, geological studies have identified the potential for significant or increased seismic activity in regions once believed to be far removed from seismic hazard; structures within these regions are in need of assessment for earthquake loads or re-assessment for increased earthquake loads.

Given the increasing importance of seismic considerations for offshore structures, the Marine Technology and Management Group at U.C. Berkeley initiated a study as part of its Screening Methodologies for Offshore Platforms project to find means of defining and determining the demands an earthquake may impose on an offshore structure. Strength-Level earthquake demand calculation procedures developed during this study have been implemented with the TOPCAT platform assessment program.

The demand calculation procedure utilizes modal response spectrum analysis (RSA) for the purposes of calculating load demands on offshore structure components. It is assumed the components (deck legs, diagonal braces, foundation piles) respond in the elastic or near-elastic regions of load-displacement behavior. Platform horizontal modes and periods are determined from modal analysis of a simple lumped-mass shear-frame fixed-base model of the structure. The first horizontal mode periods are lengthened to account for foundation and tower-bending flexibility. A simple SDOF model is used to estimate the first vertical period, and it is assumed all vertical mass participates in this mode. These modal properties are then used with response spectrum analysis to find loads. Loads estimated using this procedure are directly compared with the load capacities of components currently calculated by the TOPCAT program.

The simplified modal response spectrum procedure has been verified against the results of detailed 3-D response spectrum analyses of an 8-leg structure and a 12-leg structure, as well as against both 3-D response spectrum and 3-D time-history analyses of a 4-leg structure.

A procedure for the calculation of peak accelerations for deck-mounted equipment has also been implemented into the TOPCAT program. These accelerations may be used to determine forces for the design equipment mountings.

E.2 RSA FOR MDOF SYSTEMS

Response spectrum analysis (RSA) is an excellent means of determining strength-level earthquake demands for large platforms in a simple yet accurate manner. As a background to applying this approach to the analysis of offshore platforms, the RSA approach for application to multi-degree-of-freedom (MDOF) systems must first be reviewed. What follows is a summary of the modal RSA approach; readers desiring additional information should consult Chopra (1995).

In applying RSA to the evaluation of a large, complicated structure, an analyst must follow several important steps. First, the vibration properties of the structure (mode shapes, periods and

damping ratios) must be determined. This may be done either experimentally (taking actual vibration measurements of the structure in the field), semi-empirically (through application of a code-type estimating procedure such as that contained within the Uniform Building Code), or by developing a numerical model and solving for the properties of free vibration. As the first approach is relatively difficult to perform, and the second approach may involve too many generalities (for example, not accounting for stiffness discontinuities along the height of the structure), numerical modeling offers the most practical means at getting estimates of the vibration properties. A typical numerical model of a platform structure may be seen in Figure E-1:

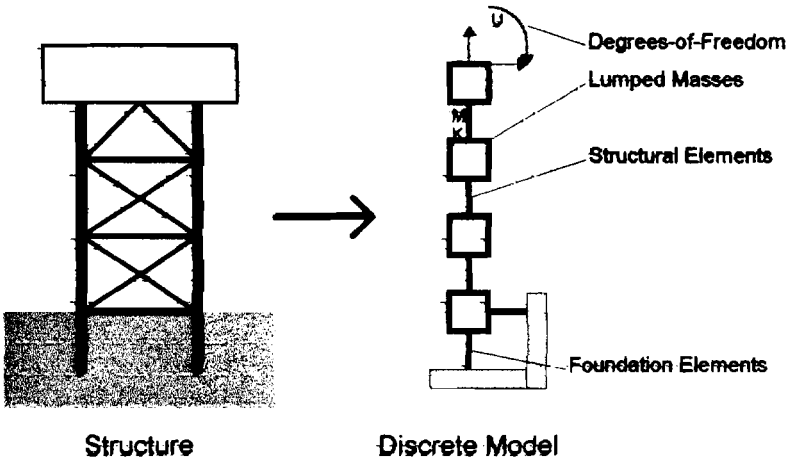

Figure E-1: Discrete Numerical Model of Structure

Free vibration, neglecting damping, of a MDOF system is governed by:

$$\mathbf{m}\ddot{\mathbf{u}} + \mathbf{k}\mathbf{u} = \mathbf{0}$$

where:

$\mathbf{m}$	=	square matrix of lumped masses
$\mathbf{k}$	=	square matrix of stiffness properties
$\ddot{\mathbf{u}}, \mathbf{u}$	=	vectors of acceleration and displacement of each lumped mass

This equation of dynamic equilibrium represents a series of uncoupled differential equations governing the free response of the system. The free vibration properties of the system will be found by the solution of the resulting matrix eigenvalue problem:

$$\mathbf{k}\phi_n = \omega_n^2 \, \mathbf{m}\phi_n$$

where:

ϕ_n	=	natural shape of vibration for mode n
ω_n	=	natural frequency of vibration for mode n

This problem is the subject of classical modal analysis, and has been studied extensively over the years for a variety of physical problems.

Once the mode shapes and frequencies of the system have been determined, and estimates have been made of the damping ratios ξ_n associated with each mode, the response spectrum appropriate to the location of the structure may be consulted to find the peak responses associated with each mode. A response spectrum is a record of the peak responses (either displacement, velocity, or acceleration) of a group of single-degree-of-freedom (SDOF) systems with various natural periods and values of damping subjected to a time-history of excitation. When developing a seismic response spectrum, this excitation will be a time-history of earthquake excitation. A response spectrum may be developed from the use of a single excitation record, or it may be developed from an ensemble of such records. In the later case, the resulting spectrum is "smoothed" along the overall peak responses irrespective of the exact record; this is referred to as a "design spectrum," and it represents an enveloping of the peak responses which might be expected at the site in question. A typical response spectrum is shown in Figure E-2.

It should be noted that applying the RSA approach to MDOF systems requires the use of a linear response spectrum, i.e. one that has been developed from the peak responses of SDOF systems possessing linear force-displacement relationships. This is a requirement as the mode shapes and frequencies developed for the MDOF system from free vibration analysis assume linear relationships govern the displacement of each DOF.

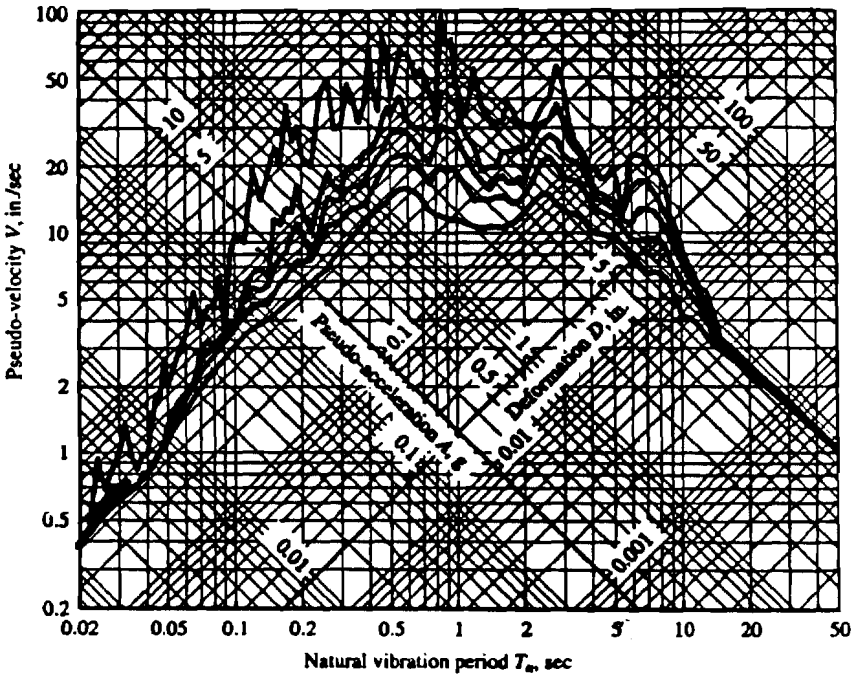

Figure E-2: Response Spectrum for El Centro, Damping is 0, 2, 5, 10, 20%

From the response spectrum in Figure E-2, values of peak displacement D_n specific to each natural frequency ω_n and damping level ζ_n can be read. The equivalent static forces associated with each mode for the excitation may then be found from:

$$\mathbf{f}_n = \mathbf{s}_n A_n$$

where:

$\mathbf{s}_n = \Gamma_n \mathbf{m} \boldsymbol{\phi}_n$ = distribution of modal inertia forces

with:

$\Gamma_n = L_n^h / M_n$ = modal participation factor

$L_n^h = \sum_{j=1}^{N} m_j \phi_{jn}$

$M_n = \sum_{j=1}^{N} m_j \phi_{jn}^2$ = generalized mass

$A_n = \omega_n^2 D_n$ = pseudo-acceleration; mA is equal to the peak value of the elastic resisting force for a SDOF system

and: n = mode index
j = DOF index

The static forces $\mathbf{f}_n$ may then be used to find member forces and nodal displacements due to each mode using structural analysis. Typical mode-specific responses for the structure modeled as shown in Figure E-1 would be given by:

$V_{in} = \sum_{j=1}^{N} \mathbf{f}_{jn}$ = shear for i^{th} level

$M_{in} = \sum_{j=1}^{N} (h_j - h_i)\mathbf{f}_{jn}$ = bending moment at i^{th} level

$u_{in} = \Gamma_n D_n \phi_{in}$ = displacement of node i

To estimate the peak or maximum value of a response quantity, the mode-specific values of the response quantity are first found and then combined. The method of combination is important, as it represents the approximate "phasing" or point in time each peak response occurs relative to every other peak. Various recommendations have been made at to how to combine these responses; most common are the square-root sum of the squares (SRSS), absolute sum (ABS), and complete quadratic combination (CQC). ABS is usually far too conservative and is seldom used. SRSS provides excellent estimates of peak response estimates when the natural frequencies of the individual modes are well-separated. CQC is intended to account for correlation between modes and hence capture effects when modal frequencies are close together. Another proposed combination rule is NRL (Naval Research Laboratory) SRSS; this rule combines the absolute value of the first mode's response with a SRSS of the remaining modes.

NRL-SRSS is intended to provide better enveloping of the results of response history analysis, as it has been shown that SRSS tends to give response predictions on the low side of response history analysis. To bound the expected strength demands, TOPCAT will allow a user to select either the ABS or SRSS modal response combination rules.

Another issue which must be addressed is the number of modes which must be included to capture a given response quantity to the desired degree of accuracy. Some quantities, such as roof displacement, will be dominated by the first one or two modes or a large (5+ DOF) structure, whereas base shear may require substantially more. However, review of the modal properties of several typical platforms indicate excellent load estimates can be obtained using perhaps three horizontal modes in either direction and a single vertical mode. Therefore, TOPCAT will focus on determining at most three horizontal modes for each principal platform direction, and will estimate one vertical mode.

E.3 SIMPLE MODAL RESPONSE MODELS FOR PLATFORMS

Following previous work performed by Mortazavi (1996), it is assumed the load capacity of a typical offshore platform is governed by the performance of two critical components (see Figure E-3): bays in the structure (both deck leg and jacket sections) and the foundation.

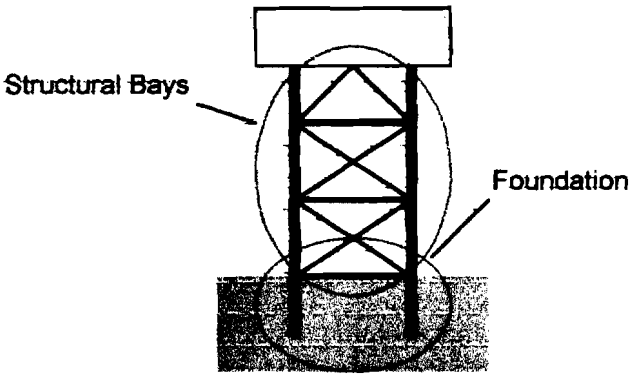

Figure E-3: Critical Components in a Jacket-Type Platform

A bay in the structure consists of a series of parallel elements (either diagonal braces or unbraced leg sections) which act primarily to resist horizontal loads. The load capacity of a bay is determined by calculating the horizontal load needed to bring the weakest element in the bay to a failure state (either buckling of a brace in a braced section, or hinging of a leg in an unbraced section).

The foundation also consists of a series of parallel elements: the piles (both main and skirt) which support the structure. Foundation capacity is determined by calculating both the axial and lateral load capacity of the individual piles.

The strength demands calculated should therefore be in terms of loads on these critical components. Hence, it will be necessary to estimate horizontal loads (story and base shear demands) on both the structural bays and foundation elements, and vertical loads (axial from both overturning and vertical excitation) on the foundation elements.

To estimate loads in the horizontal and vertical directions, it is necessary to develop a response model or models which capture the performance of the structure in these directions. The bays in the structure will be subject to the greatest load demands when the load direction is parallel with one of the two principal horizontal axes; hence, response models should be developed for each of these directions. Loads on the foundation elements may be found from the loads calculated on the principal axes together with (in the case of axial demand) loads calculated in the vertical direction; therefore, a vertical response model is also needed. If it is further assumed that responses in these three directions are independent of one another (i.e. displacement in one direction does not induce displacement in the other two), then it is possible to develop relatively simple separate response models as shown below in Figure E-4:

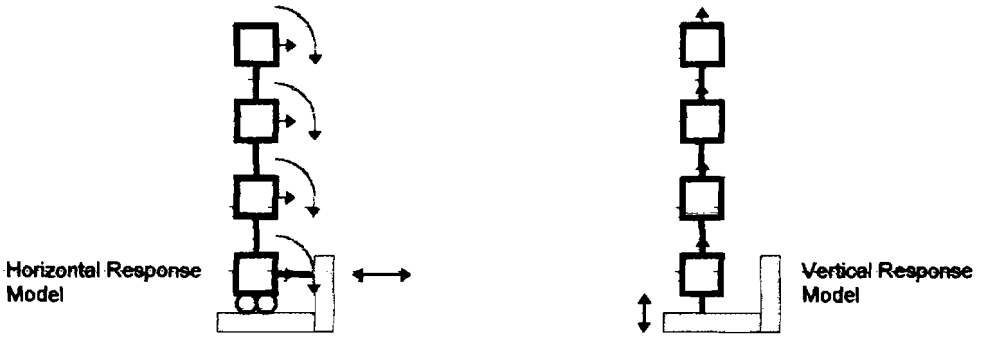

Figure E-4: Response Models for Horizontal and Vertical Excitation

The scope of this demand modeling will be limited to structures which possess mass and stiffness symmetry on their two principal horizontal axes; hence, lateral-torsional action will not be considered. While symmetric structures may undergo "accidental" torsion due to spatial variations in the applied ground motion, these variations are very difficult to predict, and in most cases accidental torsion results in increases in member forces of less than 4% (Chopra, 1995). Analysts should be aware of this possibility, however, and allow suitable margin for it.

With the demand calculations now reduced to the analysis of three uncoupled response models, it is now desirable to reduce the detail of each model further, in order to simplify the procedures necessary for the modal analysis of each model. However, in the course of simplifying the models, care must be taken to ensure that essential characteristics of response are not lost or distorted.

The models for horizontal response will be examined first. As shown in Figure E-4, these are simple lumped mass models (masses lumped as each level or horizontal framing in the structure), with the elements between the DOF representing the combined stiffnesses of the structural members between each horizontal level (i.e. bay or story stiffnesses). The lowest element in the model represents the foundation stiffness.

It would be highly desirable to eliminate the rotational DOF from the structural portion of the model, and to isolate the foundation portion of the model from the structural portion. This would reduce the computational effort to one of solving a matrix eigenvalue problem with diagonal mass and tri-diagonal stiffness matrices (a common formulation for a shear-type building); this type of matrix eigenvalue problem may be readily solved through application of iterative techniques such as the Rayleigh-Stoddola method (Clough, Penzien, 1975). However, these DOF represent significant aspects of structural response, which cannot be neglected. Instead, several simplifying procedures by which the overall effects these DOF can be accounted for will be applied.

Veletsos and Boaz (1979) have proposed a two-stage procedure by which the period-lengthening effects of foundation flexibility (horizontal as well as rotational) may be accounted for without explicit inclusion in the mass and stiffness formulations used for the modal analysis. Recognizing that foundation effects are concentrated in the first mode responses of a MDOF system, it is possible to first determine the periods and mode shapes of the structure as though it were supported on a fixed base, and then modify the first mode period to account for foundation flexibility effects. In addition, guidelines for adjusting the modal damping ratio to account for foundation sources of damping are also given. It must be noted that the forces acting on the foundation itself must necessarily be approximated, as the foundation mass is not considered in the fixed-base analysis of the structure. This procedure assumes that non-linearity in the soil stiffness and damping will be small, and that cyclic degradation of strength and stiffness may be accounted for by using cyclic test strength and stiffnesses in the model.

The effective fundamental period of a MDOF structure undergoing horizontal excitation can be expressed by:

$$\tilde{T}_1 = T_1 \sqrt{1 + \frac{k_1^*}{K_x}\left[\frac{1}{1-(T_o/\tilde{T}_1)^2} + \frac{K_x h_1^{*2}}{K_\theta}\right]}$$

where:

T_1 = fundamental period of the fixed-base structure

T_o = natural period of foundation mass

$k_1^* = \dfrac{4\pi^2 M_1^*}{T_1^2}$ = effective horizontal stiffness of the fundamental mode of the fixed-base structure

K_x = horizontal stiffness of foundation

K_θ = rotational stiffness of foundation

$h_1^* = \dfrac{L_1^\theta}{L_1^h}$ = effective modal height of fundamental mode of fixed-base structure

$M_1^* = \Gamma_1 L_1^h$ = effective modal mass of fundamental mode of fixed-base structure

$$L_1^{\theta} = \sum_{j=1}^{N} h_j m_j \phi_{j1}$$

The fundamental period of the fixed-base structure is found from modal analysis, whereas the natural period of the foundation mass may be estimated from:

$$T_o = 2\pi\sqrt{\frac{W_o}{gK_x}}$$

where:

W_o = weight of foundation mass included in model
g = acceleration due to gravity

The weight of the foundation mass included in the model consists of the weight of any horizontal framing and mud mats on the bottom of the jacket structure, the weight of pile steel in the foundation and the weight of soil contained within the piles. For TOPCAT, pile steel and soil mass associated with a depth of ten pile diameters will be included in the foundation mass.

K_x and K_θ represent pile group stiffnesses, and can be estimated using procedures outlined in Appendix G of the User Manual. The effective damping ratio for the fundamental mode of the structure may be expressed as:

$$\tilde{\xi} = \xi_o + \frac{\xi}{(\tilde{T}_1 / T_1)^3}$$

where:

ξ = damping factor of the fundamental mode for the fixed-base structure (usually 2%-5%, from local hysteresis in the steel)
ξ_o = equivalent foundation damping, which is a viscous equivalent damping of the work done in local plastification of soil beneath the platform (in the range of 1% to 15%, depending on the magnitude of excitation)

TOPCAT does not make modifications of the damping associated with different modes. All modes are assumed to have the 5% damping associated with the API response spectrum.

To obtain an estimate of the shear imposed on the foundation, the maximum base shear of the fixed-base structure (considering all modes) is combined with an approximate value of the inertia force of the foundation mass:

$$V_o = \frac{W_o A_o}{g} + \sum_{i=1}^{N} V_i \qquad \text{(for ABS combination, can also use SRSS)}$$

where:

A_o = pseudo-acceleration of the foundation mass calculated from the response spectrum
V_i = base shear contribution of each individual mode

A volume of soil equal to the volume contained within the pile is considered to ride with the pile as it moves. The volume of soil is that associated with ten pile diameters depth below the mudline.

The rotational DOF in the structural portion of the model represent the overall bending or cantilever action of the platform. The effect of this action is to lengthen the periods of the first few horizontal vibration modes, and to increase the displacements of the top DOF relative to the lower ones (Figure E-5).

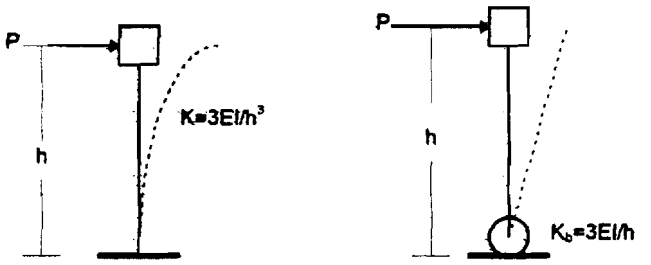

Figure E-5: Approximating Bending Effects of Structure

It will be assumed that the changes in mode shape are small, and hence will be neglected. The period-lengthening effects of cantilever action can be bounded by modifying the fixed-base response of the structure in a manner similar to that proposed by Veletsos and Boaz (1979). The bending of the structure is assumed to be similar to the rotation of a rigid structure on a flexible base. To give similar tip displacements for the same tip load, the stiffness of the rotational element may be estimated from:

$$K_b = 3EI/h$$

where:

I = moment of inertia of the structure cross-section, based on pile areas (or pile and leg areas, if grouted)
h = height of the structure
E = modulus of elasticity

This rotational spring is then considered to act in series with the spring K_θ which represents foundation rotational flexibility.

Two additional effects which have not been explicitly included in the model need to be addressed: batter effects and P-Δ effects. For a battered structure, the legs of the structure will

contribute to the shear resistance in each story of the structure (increasing in effect towards the bottom of the structure); this will increase the stiffness of the structure and hence lower the period. The magnitude of this effect is unknown (and perhaps impossible to generalize across many configurations); however for the purposes of this study it will be assumed to be small.

P-Δ effects can play an important role in increasing the effective load on a structural bay or story; they also contribute to lengthening the period of the first natural mode of response. Previous research (Gates, et al., 1977) has indicated these changes are small for structures in shallow to medium depths, and hence they will be neglected here as well.

With these simplifications made, the platform may be modeled as a shear frame, with lumped masses at the levels of horizontal framing. The stiffness of each bay will be approximated by considering only the stiffness contributions of the diagonal braces in each bay (each bay a parallel system of braces) or the stiffness contributions of the jacket legs and piles if there are no braces (again, a parallel system of elements).

$$k_{bay-braced} = \sum_{i=1}^{n_{braces}} \frac{EA_i}{L_i} \cos^2 \theta_i$$

$$k_{bay-unbraced} = \sum_{i=1}^{n_{legs}} \frac{6EI_i}{L_i^3}$$

Hydrodynamic effects of the response of vibrating structures have been studied extensively by both numerical and experimental means (Goyal, Chopra, 1989). While it is generally accepted that for submerged slender members (length to diameter ratios less than ten) hydrodynamic damping (both viscous and radiation) can be neglected, the effects of the mass of fluid both displaced and entrained by the movement of the members can substantially change the vibration characteristics of the structure. The common approach to account for this effect is to assume a certain amount of "added" hydrodynamic mass rides with the members of the structure; this amount is assumed to be constant for the purposes of determining the mass properties of the structure. The amount of mass to include depends upon the size, orientation and depth of the members as well as the manner of excitation (Goyal, Chopra, 1989). For circular members undergoing periodic motion it is generally taken to be equal to the mass of the volume of fluid displaced by the member. It should be noted that recent experience (Bannon, Penzien, 1992) suggests that this approach may over-estimate the actual amount of added mass.

The approximate added mass per unit length for cylindrical members undergoing translation is (Newmark, Rosenblueth, 1971):

$$m_{added} = \rho_w \pi r^2 \sin \theta$$

where:

ρ_w = density of the surrounding fluid
r = radius of the member
θ = the angle between the cylindrical length axis and the direction of translation

Added mass is also dependent upon the proximity of the member to the free surface. Goyal and Chopra (1989) have documented the variation of added mass along the height of circular cylinders of various diameters; it is demonstrated that the added mass begins to drop off rapidly when within 0.1 H_o of the water's surface. Hence, the following approximations are used to scale the amount of added mass included in the weight of the structure:

$$m_{added}(z) = m_{added} \text{ when } z > 0.1\ H_o$$

$$m_{added}(z) = m_{added}(z / 0.1\ H_o) \text{ when } z \leq 0.1\ H_o$$

where:

z = depth below the surface
H_o = water depth

This added mass is included in the lumped masses of the structure model when considering both lateral and vertical excitation. It should be noted that the estimation of added mass effects on tower structures subject to earthquake excitation is still an area of active research. Recent experience with two offshore structures have indicated the use of current techniques leads to possible overestimation of added mass effects (Bannon, Penzien, 1992). This can have serious consequences on demand estimates, as it leads to inaccuracies in period estimates. Experimental results obtained by Clough (1960) indicate that the added mass associated with a member is strongly dependent on the member's flexibility; Clough (1960) suggests the use of added mass coefficients ranging from 0.6 for flexible members to 1.0 for stiff members in order to account for this dependence. TOPCAT will allow a user to specify the added mass coefficient for tubular braces; for all other members it is assumed to be unity.

With the horizontal model defined, a vertical model must be developed. As the main quantity of interest which comes from the analysis of vertical response is the axial load demand on the foundation piles, the model will be reduced in scope so that this quantity can be estimated without much detail. Hence, a model consisting of one DOF is proposed (see Figure E-6). The mass of the structure, including hydrodynamic mass, is lumped at the DOF; the stiffness element consists of the axial stiffnesses of the piles above the mudline (together with the jacket legs, if the legs are grouted) acting in series with the axial stiffnesses of the piles below the mudline.

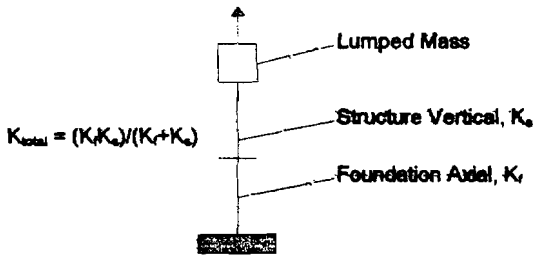

Figure E-6: Simplified Vertical Response Model (SDOF)

The use of these simple models to estimate modal properties together with response spectrum analysis to estimate earthquake forces will be referred to as Simplified Response Spectrum Analysis, or SRSA. Calculation routines have been incorporated into TOPCAT to allow it to perform SRSA of jacket- and caisson-type platforms.

The approach utilized within the TOPCAT program to find mode shapes and periods for horizontal response is based upon the conversion of the problem $\mathbf{k}\phi_n = \omega_n^2 \mathbf{m}\phi_n$ to standard form, $\mathbf{A}\phi_n = \lambda_n \phi_n$, and then solving for the eigenvectors and eigenvalues through iteration. This process has attracted much attention in engineering; readers desiring additional information are referred to Timoshenko, Young and Weaver (1974) and to Parlett (1980). The essential steps of the iteration process are listed below:

1. Start with an arbitrary trial vector, ϕ_n, and solve $\mathbf{A}\phi_n = \mathbf{y}$.
2. Obtain an estimate of the associated eigenvalue, λ_n, by taking the ratio between components of ϕ_n and y having the same index; hence $\lambda_n \approx y_i / \phi_{ni}$.
3. Normalize y by y_i to get $\bar{\mathbf{y}}$. Check to see if all $\bar{y}_i = \phi_{ni}$; if this condition is met, ϕ_n is a valid eigenvector and λ_n the correct associated eigenvalue. If not, set $\phi_n = \bar{\mathbf{y}}$ and return to step 1.

This iteration process has the useful characteristic of always converging to the largest eigenvalue and associated eigenvector. The vibration problem $\mathbf{k}\phi_n = \omega_n^2 \mathbf{m}\phi_n$ can be transformed to the standard form by multiplying both sides by $\mathbf{k}^{-1}$ and dividing both sides by ω_n^2. Hence the rearranged problem is now of the form $\mathbf{A}\phi_n = \lambda_n \phi_n$, where $\mathbf{A} = \mathbf{k}^{-1}\mathbf{m}$ and $\lambda_n = 1/\omega_n^2$. The solution will converge to the largest value of λ_n, which conveniently coincides with the inverse of the square of the lowest natural frequency; this is of course the frequency associated with the first mode of vibration.

In order to obtain eigenvectors and eigenvalues associated with higher modes, it is necessary to ensure that successive eigenvectors are orthogonal to one another (the orthogonality condition, $\phi_i \mathbf{m} \phi_j = 0$, ensures that the work done by i^{th} mode inertia forces going through j^{th} mode displacements is zero). This may be accomplished by enforcing the orthogonality condition when determining successive eigenvectors. This process is shown in the following section.

With the eigenvector ϕ_1 determined, and with a trial vector ϕ_2 estimated, applying the orthogonality condition $\phi_1 \mathbf{m} \phi_2 = 0$ gives (assuming a diagonal mass matrix):

$$m_{11}\phi_{11}\phi_{21} + m_{22}\phi_{12}\phi_{22} + m_{33}\phi_{13}\phi_{23} + \ldots + m_{jj}\phi_{1j}\phi_{2j} = 0$$

Solving for ϕ_{21} (this is an arbitrary choice) gives:

$$\phi_{21} = -\frac{m_{22}\phi_{12}\phi_{22}}{m_{11}\phi_{11}} - \frac{m_{33}\phi_{13}\phi_{23}}{m_{11}\phi_{11}} - \ldots - \frac{m_{jj}\phi_{1j}\phi_{2j}}{m_{11}\phi_{11}}$$

Calculating ϕ_{21} using the above expression prior to using ϕ_2 as a trial vector ensures orthogonality between ϕ_2 and ϕ_1. This may be accomplished using the following matrix multiplication:

$$\phi_{2\,\text{trial}} = \mathbf{T}_{S1}\phi_2$$

where: $$\mathbf{T}_{S1} = \begin{bmatrix} 0 & -\frac{m_{22}\phi_{12}}{m_{11}\phi_{11}} & -\frac{m_{33}\phi_{13}}{m_{11}\phi_{11}} & \dots & -\frac{m_{jj}\phi_{1j}}{m_{11}\phi_{11}} \\ 0 & 1 & 0 & \dots & 0 \\ 0 & 0 & 1 & \dots & 0 \\ \dots & \dots & \dots & \dots & \dots \\ 0 & 0 & 0 & \dots & 1 \end{bmatrix}$$

$\mathbf{T}_{S1}$ is referred to as a "sweeping" matrix, as it acts to sweep out or suppress the first mode characteristics and allow the second mode to be come dominant. As $\mathbf{T}_{S1}$ is used with each iteration of ϕ_2, it may be used to reformulate $\mathbf{A}$ according to $\mathbf{A}_{S1} = \mathbf{A}\mathbf{T}_{S1}$, and then operate directly on the reformulated matrix.

Higher modes may be determined by successive application of sweeping matrices. For example, a sweeping matrix $\mathbf{T}_{S2}$ for removing the dominance of ϕ_2 may be constructed, and then used together with $\mathbf{T}_{S1}$ to allow the third mode ϕ_3 to become dominant. This matrix $\mathbf{T}_{S2}$ would be constructed by using the fact that $\phi_1 \mathbf{m} \phi_3 = 0$ and $\phi_2 \mathbf{m} \phi_3 = 0$. This gives the following:

$$m_{11}\phi_{11}\phi_{31} + m_{22}\phi_{12}\phi_{32} + m_{33}\phi_{13}\phi_{33} + \ldots + m_{jj}\phi_{1j}\phi_{3j} = 0$$
$$m_{11}\phi_{21}\phi_{31} + m_{22}\phi_{22}\phi_{32} + m_{33}\phi_{23}\phi_{33} + \ldots + m_{jj}\phi_{2j}\phi_{3j} = 0$$

Using the first equation to find a relationship for ϕ_{31}, the following relationship can be developed for ϕ_{32}:

$$\phi_{32} = -\frac{m_{33}\left(\phi_{11}\phi_{23} - \phi_{21}\phi_{13}\right)}{m_{22}\left(\phi_{11}\phi_{22} - \phi_{21}\phi_{12}\right)} - \frac{m_{44}\left(\phi_{11}\phi_{24} - \phi_{21}\phi_{14}\right)}{m_{22}\left(\phi_{11}\phi_{22} - \phi_{21}\phi_{12}\right)} - \ldots - \frac{m_{jj}\left(\phi_{11}\phi_{2j} - \phi_{21}\phi_{1j}\right)}{m_{22}\left(\phi_{11}\phi_{22} - \phi_{21}\phi_{12}\right)}$$

The sweeping matrix is thus:

$$\mathbf{T}_{S2} = \begin{bmatrix} 1 & 0 & 0 & \dots & 0 \\ 0 & 0 & -\frac{m_{33}\left(\phi_{11}\phi_{23} - \phi_{21}\phi_{13}\right)}{m_{22}\left(\phi_{11}\phi_{22} - \phi_{21}\phi_{12}\right)} & \dots & -\frac{m_{jj}\left(\phi_{11}\phi_{2j} - \phi_{21}\phi_{1j}\right)}{m_{22}\left(\phi_{11}\phi_{22} - \phi_{21}\phi_{12}\right)} \\ 0 & 0 & 1 & \dots & 0 \\ \dots & \dots & \dots & \dots & \dots \\ 0 & 0 & 0 & \dots & 1 \end{bmatrix}$$

This is then used together with $\mathbf{T}_{S1}$ to reformulate **A** according to $\mathbf{A}_{S2} = \mathbf{A}\mathbf{T}_{S1}\mathbf{T}_{S2}$.

E.4 VERIFICATION OF SIMPLIFIED METHOD

It is necessary to verify the accuracy of these simple models. The Southern California Example Platform was selected for analysis by both the SRSA approach and by traditional 3-D response spectrum analysis. This platform is a hypothetical symmetric four-leg production platform (see Figure E-7). The structure is designed for 100 ft water depth. The deck is at +50 ft MWL and supports a load of 5,000 kips. The main diagonals in the first jacket bay are 24 inch-diameter (w.t. 1 inch in top portions and 0.5 inch in bottom portions), while those in the second bay are 30 inch-diameter (w.t. 0.625 inch); the diagonals in the deck bay are 36 inch-diameter (w.t. 0.75 inch). The legs are 78 inch-diameter (w.t. 0.875 to 1.125 inches); they are grouted, and possess heavy joint cans. The piles are 72 inch-diameter (w.t. 1 to 1.5 inches), and are designed for 150 ft penetration in medium to stiff clay. The main structure is A36 steel.

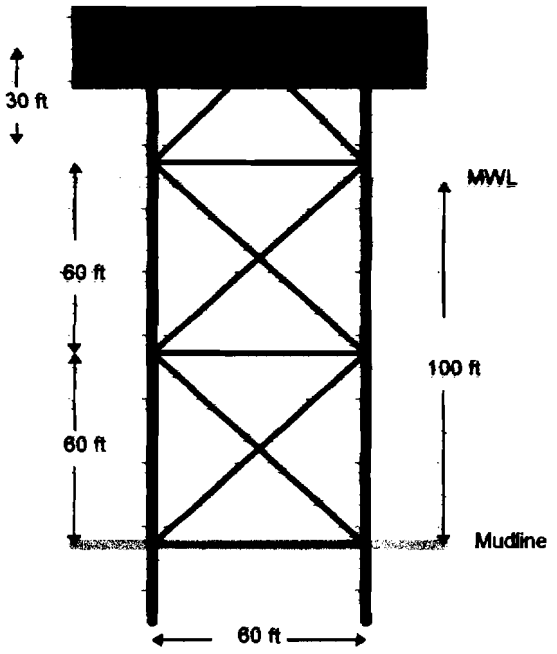

Figure E-7: Southern California Example Platform

Both a 3-D response spectrum analysis and a simplified response spectrum analysis were performed for this platform to estimate horizontal load demands. For both analyses, the masses and pile head vertical and horizontal stiffnesses listed by Gates, et al. (1977) were used. SRSS was used to combine modal responses.

A comparison of predicted modal properties can be seen in Figures E-8 and E-9. The first horizontal period estimated as part of the SRSA evaluation is 3% below the period estimated by 3-D modal analysis. The simplified modal analysis predicts subsequent horizontal periods much lower than those from 3-D modal analysis; the difference is attributed to the concentration of

foundation flexibility in the first horizontal mode. The mode shapes are obviously quite different, as the simplified modal analysis treats the structure as having a fixed base.

Loads predicted by the SRSA evaluation are at most 11% below those predicted by the 3-D analysis. The difference is attributed to the higher values of modal participation that were evident for the 3-D analysis. Overall, though, the comparison is quite good.

The simplified approach provides good estimates of the fundamental vibration properties of the platform. However, this platform is fairly short, and does not have a flexible jacket (the legs are grouted). Platforms in very deep water will respond in a manner which will most likely require the inclusion of the tower bending mode in a more accurate manner. Also, previous experience (Stear, Bea, 1998) has indicated that platforms with ungrouted jackets possess much more flexibility that those with grout due to the additional "warping" the jacket will exhibit.

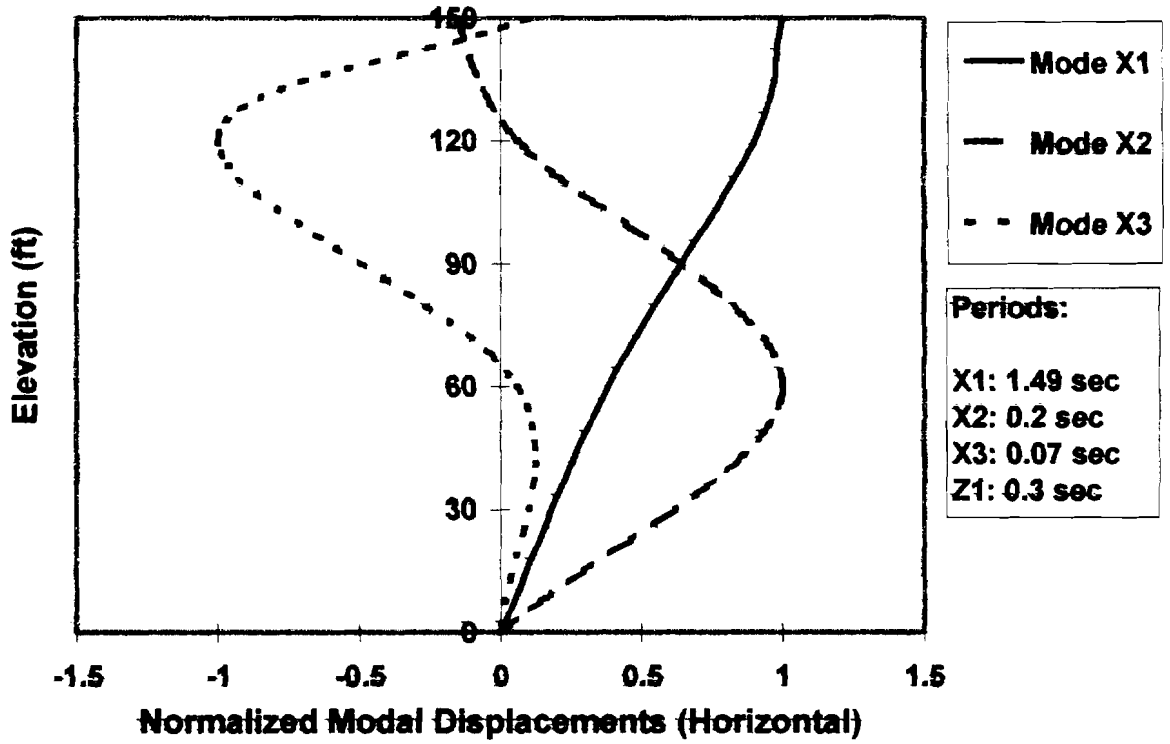

Figure E-8: Mode Shapes and Periods Estimated from Simple Analysis

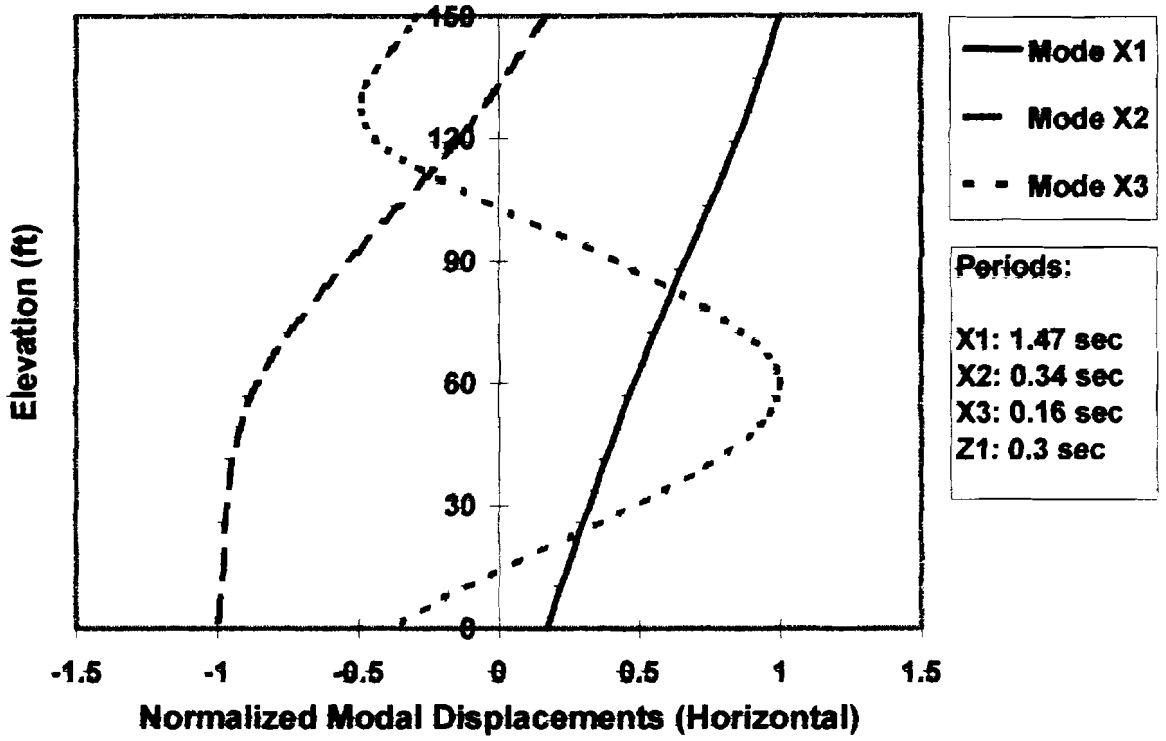

Figure E-9: Mode Shapes and Periods Estimated from 3-D Analysis

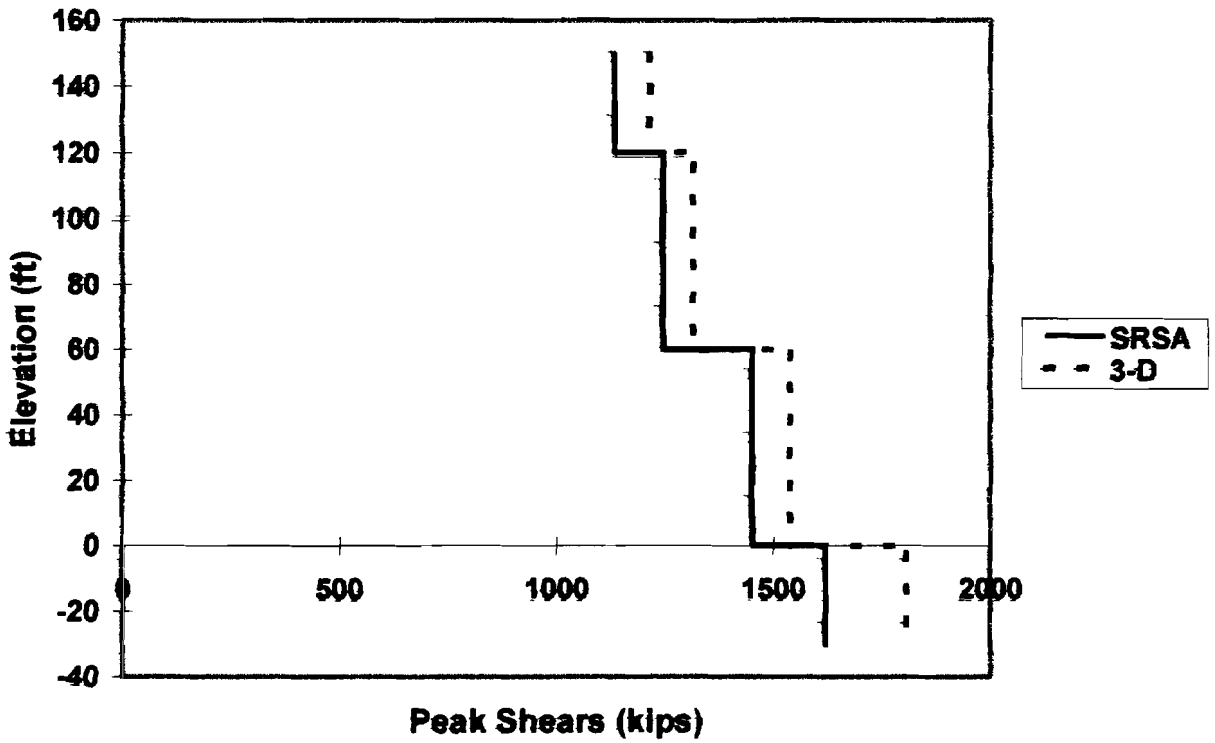

Figure E-10: Peak Shears Estimated by SRSA and 3-D RSA

E.5 DECK-LEVEL ACCELERATIONS

A simplified engineering approach proposed by Biggs and Roesset (1970) to define earthquake floor accelerations for equipment, piping, and other facilities mounted on the decks of drilling and production platforms is discussed in this section; this approach has been integrated into the TOPCAT program. The approach is based on relatively simple calculations that require as input the platform ground motion elastic response spectra, the platform primary response periods and mode shapes, and the estimated weights and periods of the equipment of concern. The formulation of this approach is founded on the results from comparable developments of floor spectra guidelines for nuclear power plants, buildings, and refinery vessels and piping.

The Biggs and Roesset (1970) approach has the following advantages. The method is relatively simple, and fast. Only the response spectrum and the dynamic characteristics (mode shapes, periods, and damping ratios) of the structure and the equipment are required. No time history analysis is needed. The procedure can be applied to multiple-degrees-of-freedom (MDOF) pieces of equipment or piping. The method allows for different damping ratios for the equipment and the structure. Advanced dynamic analysis knowledge is not required. Even though interaction of topsides and platform masses is not considered, as the ratio of mass of the equipment to the mass of the structure approaches zero, the effects become negligible. This is generally the case for offshore platforms. Neglecting the interaction effects tends to make the design more conservative.

The approach does, however, have the following disadvantages. The method does not account for interaction of the platform and topsides masses. The mass of the equipment is assumed to be light enough compared to the mass of the structure to ignore interaction effects. Thus, the dynamic characteristics of the structure remain the same after mounting equipment. This interaction may or may not be significant. However, as stated above, ignoring interaction makes a more conservative design. The method assumes lumped mass systems. Theoretical results are calibrated to more closely match empirical results.

Bowen and Bea (1995) have developed an equipment acceleration magnification ratio diagram for use in determining accelerations on mounted equipment (Figure E-11). This diagram has been based on synthesis of the analytical approaches developed by Biggs and Roessett (1970) and calibrated with additional results from analyses of offshore platforms subjected to earthquake time histories (Bowen, Bea, 1995). The acceleration magnification ratio diagram represents a mean result. Based on the time history results available to this study, at a given period ratio (ratio of equipment period, T_e, to structure period, T_s) the coefficient of variation of the acceleration magnification ratio is estimated to range from 10% to 15%.

The magnification ratio diagram proposed is based on a structure damping ratio of 5% and an equipment damping ratio of 2%. As appropriate, other damping ratios can be used to develop other magnification ratio diagrams. The developments are based on linear elastic response of the platform and topsides and are applicable to API Strength Level Earthquake (SLE) conditions.

There are two limiting cases of equipment response that are important to understand. The first is the case of rigid equipment in which the equipment is very stiff compared with the supporting structure. An example might be a horizontal separator skid that is mounted on the platform deck. The equipment simply must move in the same manner as its support. The motion and the maximum acceleration of the equipment mass, A_e, must be the same as that of the supporting point on the structure, A_s. Thus $A_e = A_s$.

The second limiting case is that of very flexible equipment. An example might be a flare boom or flare stack mounted on the platform deck. The period of the equipment, T_e, is much greater than that of the supporting structure, T_s. The internal distortion of the structure is relatively unimportant and the equipment behaves as though it was supported directly on the ground. In this case, the maximum acceleration of the equipment is equal to the maximum acceleration of the ground.

Between these two limiting cases, there is interaction between the equipment and the structure. The structure behaves as a frequency filter, developing harmonic components with frequencies equal to the modal frequencies of the structure. If the equipment has a natural frequency close to one of these harmonic components, the motion can be amplified. Near the point of resonance ($T_e \approx T_s$), the maximum acceleration of the equipment can be several times that of the supporting structure. The amplification (A_e / A_s) will be proportional to the number of cycles of motion, N (for low damping $A_e / A_s \approx N\pi$). Given a sufficient number of cycles (e.g. $N \geq 3$), the amplification is limited by damping ($A_e / A_s \approx 0.5\xi$). Based on the results of time history analyses of structures with mounted equipment (Bowen, Bea, 1993), the relationship between accelerations for structure and equipment may be expressed as shown in Figure E-11.

The procedure to find the appropriate acceleration for use in determining equipment tie-down forces is organized into five steps:

1. Obtain the acceleration at the DOF x corresponding to the point of equipment support for each structure vibration mode i:

$$\ddot{u}_{xi} = \Gamma_i \phi_{xi} SA_i$$

2. Obtain the spectral accelerations for the equipment modes j:

$$\ddot{u}_j = SA_j$$

3. If the ratio of T_{ej} / T_{si} is less than 1.25, modify the structure's acceleration $\ddot{u}_{xi}$ at the DOF of attachment by the ratio of A_{ej} / A_{si} taken from Figure E-11 and assign to $\ddot{u}_{ij}'$:

$$\ddot{u}_{ij}' = \left(\frac{A_{ej}}{A_{si}}\right)\ddot{u}_{xi}$$

4. Otherwise, modify the equipment mode's spectral acceleration by A_{ej} / A_{si} , and assign to $\ddot{u}_{ij}''$:

$$\ddot{u}_{ij}'' = \left(\frac{A_{ej}}{A_{si}}\right) SA_j$$

5. Perform the above tasks for each mode of the structure. When done, combine the resulting accelerations according to the following to get the equipment modal acceleration:

$$\ddot{u}_j = \sqrt{\sum_{i \text{ over all } ii} \left(\ddot{u}_{ij}'\right)^2 + \frac{\sum_{i \text{ over all } ii} \left(\Gamma_i \phi_{xi} \ddot{u}_{ij}''\right)^2}{\sum_{i \text{ overall all structure modes}} \left(\Gamma_i \phi_{xi}\right)^2}}$$

Repeat the above tasks for each equipment mode. This will provide spectral accelerations for all equipment modes, after which forces can be determined using modal analysis procedures.

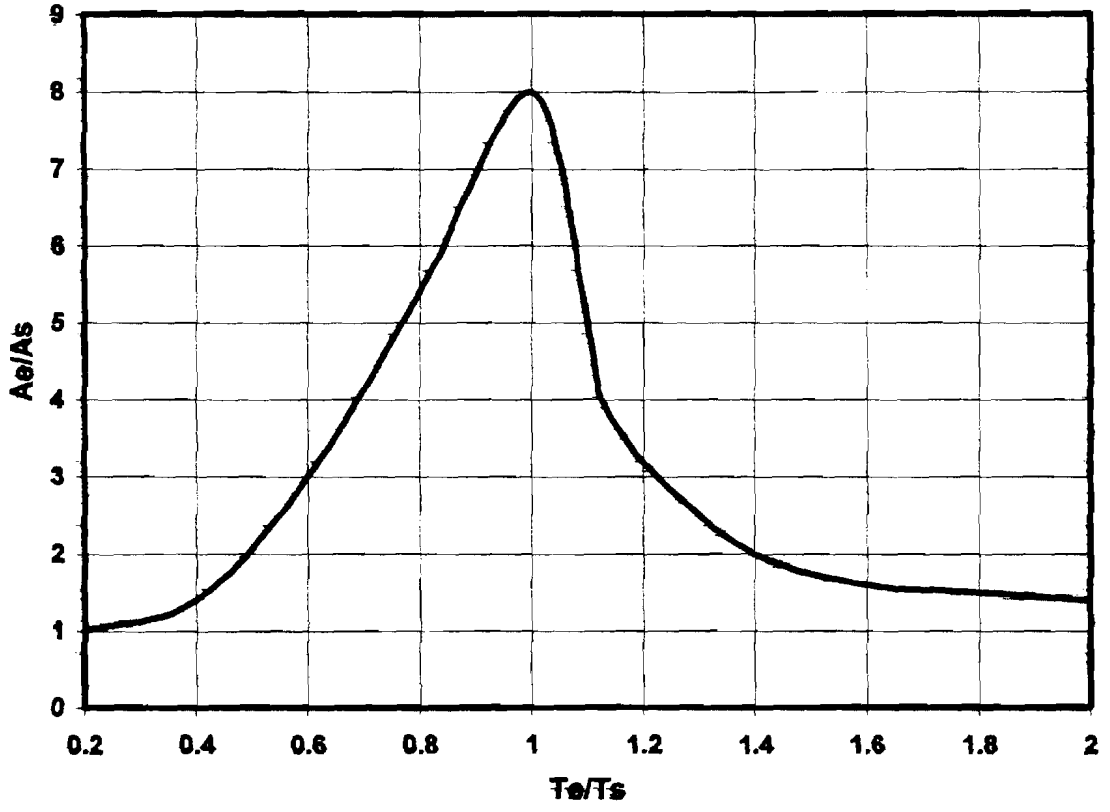

Figure E-11: Equipment/Structure Amplification Ratios (Bowen, Bea, 1993)

E.6 REFERENCES

American Petroleum Institute, "Recommended Practice for Planning, Designing and Constructing Fixed Offshore Platforms - Load and Resistance Factor Design," API Recommended Practice 2A-LRFD (RP 2A-LRFD), 1st Edition, Washington, D. C., July 1993.

Bannon, H., and Penzien, J., "Working Group Report on Structural Performance," *Proceedings of the International Workshop on Seismic Design and Reassessment of Offshore Structures*, editor: W. D. Iwan, California Institute of Technology, Pasadena, CA, December 7-9 1992.

Biggs, J. M., *Introduction to Structural Dynamics*, McGraw - Hill, New York, NY, 1964.

Biggs, J. M., and Roesset, J. M., "Seismic Analysis of Equipment Mounted on a Massive Structure," Seismic Design of Nuclear Power Plants, editor: R. J. Hansen, M.I.T. Press, 1970.

Bowen, C. M., and Bea, R. G., "Simplified Earthquake Floor Response Spectra for Equipment on Offshore Platforms," *Proceedings of the International Workshop on Wind and Earthquake Engineering for Coastal and Offshore Facilities*, Department of Civil Engineering, University of California at Berkeley, CA, January 17-19 1995.

Chopra, A. K., *Dynamics of Structures - Theory and Applications to Earthquake Engineering*, Prentice-Hall, Englewood Cliffs, NJ, 1995.

Clough, R. W., "Effects of Earthquakes on Underwater Structures," *Proceedings of the 2nd World Conference on Earthquake Engineering*, Tokyo, 1960.

Clough, R. W., and Penzien, J., *Dynamics of Structures*, McGraw - Hill, New York, NY, 1975.

Gates, W. E., Marshall, P. W., and Mahin, S. A., "Analytical Methods for Determining the Ultimate Earthquake Resistance of Fixed Offshore Structures," *Proceedings of the Offshore Technology Conference*, OTC 2751, Houston, TX, May 1977.

Goyal, A., and Chopra, A. K., "Earthquake Analysis and Response of Intake-Outlet Towers," Report No. UCB/EERC-89/04, Earthquake Engineering Research Center, University of California at Berkeley, CA, July 1989.

Mortazavi, M., "A Probabilistic Screening Methodology for Use in Assessment and Requalification of Steel, Template-Type Offshore Platforms," Report to Joint Industry Project Sponsors, Department of Civil Engineering, University of California at Berkeley, CA, 1996.

Newmark, N. M., and Rosenblueth, E., *Fundamentals of Earthquake Engineering*, Prentice-Hall, Englewood Cliffs, NJ, 1971.

Parlett, B., *The Symmetric Eigenvalue Problem*, Prentice-Hall, Englewood Cliffs, NJ, 1980.

Timoshenko, S., Young, D. H., and Weaver, W., jr., *Vibration Problems in Engineering*, 4th Edition, John Wiley and Sons, New York, NY, 1974.

Uniform Building Code, 1994.

Veletsos, A. S., and Boaz, I. B., "Effects of Soil-Structure Interaction of Seismic Response of a Steel Gravity Platform," *Proceedings of the Offshore Technology Conference*, OTC 3404, Houston, TX, May 1979.

APPENDIX F:
SIMPLIFIED FATIGUE ANALYSIS FOR TUBULAR CONNECTIONS IN JACKET-TYPE PLATFORMS

by
James D. Stear and Professor Robert G. Bea

Portions of this Appendix have been previously published in the following:

Stear, J. D. and Bea, R. G., "ULSLEA Enhancements: Fatigue Analysis / Earthquake Analysis / Additional Configurations / Screening Methodologies Project Phase III," Report to Joint Industry Project Sponsors, Marine Technology and Management Group, Department of Civil and Environmental Engineering, University of California at Berkeley, CA, June 1997.

TABLE OF CONTENTS **PAGE**

F.1 INTRODUCTION

A decision as to the serviceability of a structure should be based not only upon strength, but also upon durability (resistance to fatigue damage). Hence, it is desirable to devise some means of evaluating the fatigue damage potential of critical platform structural elements within the framework of a simplified analysis process.

Platform components particularly vulnerable to fatigue damage are the tubular joints between members. If improperly detailed, they can give rise to very high stress concentrations, which in turn will lead to a rapid accumulation of fatigue damage.

A simplified approach to estimate fatigue damage for tubular joint connections of main diagonal braces has been implemented in the TOPCAT program. This approach is based upon the one outlined in API RP 2A-LRFD (1993), by which the fatigue damage in a structural element is related to the distribution of wave heights affecting the structure over a fixed period of time. The stress at a joint due to a user-specified wave load pattern is calculated; this stress is then combined with information on the long-term distribution of waves in the area (a combined spectrum of both typical and extreme waves) together with S-N parameters in order to give a generic estimate of accumulated damage. This estimate is then used to rank the joints so that a qualitative assessment of potential problem areas can be made.

This approach assumes fatigue damage will most likely occur in those joints to which main diagonal braces are attached; hence, its application is limited to that class of joint (Figure F-1). Only loading parallel to the principal axes of the platform is considered when estimating the base stress at a connection from which the cyclic stress is calculated.

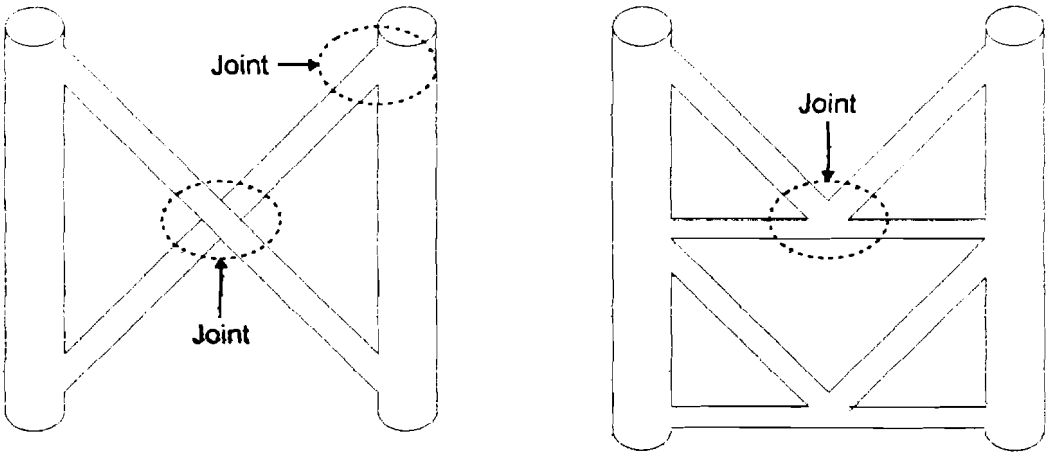

Figure F-1: Tubular Joint Connections of Main Diagonals

F.2 ANALYTICAL APPROACH

The approach taken to calculate fatigue damage for tubular joints is based on four assumptions:

1. The maximum stress range at the critical area in the joint is dependent only on the wave heights, and is related to them as follows:

$$S = CH^{g_{stress}}$$

where:

S = maximum stress range
C = calibrated constant
H = wave height
g_{stress} = calibrated exponent

2. The S-N curve characterizing the fatigue behavior is given by:

$$NS^m = K$$

where:

N = number of cycles to failure at a given S
m = empirical constant
K = empirical constant

3. Miner's rule applies. This is given by:

$$D = \sum_i \frac{n_i}{N_i}$$

where:

D = total fatigue damage
n_i = number of cycles of stress range S_i
N_i = number of cycles to failure given stress range S_i

4. The long-term wave-height distribution can be represented as a sum of two Weibull distributions, one of which represents typical waves while the other represents storm waves. These distributions are given by their cumulative distribution functions:

$$F_{H_0}(h) = 1 - \exp\left[-\left(\frac{h}{H_0}\right)^{\xi_0} \ln N_0\right]$$

and:

$$F_{H_1}(h) = 1 - \exp\left[-\left(\frac{h}{H_1}\right)^{\xi_1} \ln N_1\right]$$

where:

H_i = maximum wave height for time considered
N_i = number of waves for time considered
ξ_i = Weibull distribution parameter

Based on these assumptions, a closed-form solution for the fatigue damage may be obtained (Nolte, Hansford, 1976):

$$D_d = \frac{T_d C^m}{K}\left(Y_0 + Y_1\right)$$

where:

$$Y_0 = \frac{N_0}{T_{spectrum}} H_0^{g_{stress}m}\left(\ln N_0\right)^{\frac{g_{stress}m}{\xi_0}} \Gamma\left(1 + \frac{g_{stress}m}{\xi_0}\right)$$

and:

$$Y_1 = \frac{N_1}{T_{spectrum}} H_1^{g_{stress}m}\left(\ln N_1\right)^{\frac{g_{stress}m}{\xi_1}} \Gamma\left(1 + \frac{g_{stress}m}{\xi_1}\right)$$

D_d is the fatigue damage accumulated over the specified duration of service T_d.

C should be determined from "fatigue design wave" conditions; this may be done as follows:

$$C = \frac{S_f}{H_f^{g_{stress}}}$$

where:

H_f = fatigue design wave height
S_f = maximum stress range corresponding to H_f

S_f may be evaluated from:

$$S_f = S_p(1 - R)$$

where:

S_p = peak stress in component due to static application of forces from H_f
R = stress cycle ratio

With some rearranging, the accumulated fatigue damage may then be expressed by:

$$D_d = \frac{T_d}{K}\left(\frac{S_p(1\text{-}R)}{H_f^{g_{stress}}}\right)^m \left(Y_0 + Y_1\right)$$

This accumulated damage value may then be used to make qualitative comparisons of joint performance. A high damage value for a joint may indicate it is a potential problem, and hence may need careful inspection.

F.3 FATIGUE DAMAGE PARAMETERS

To evaluate the accumulated fatigue damage for a given joint, the parameters K, m, g_{stress}, R, H_0, H_1, ξ_0, ξ_1, N_0, N_1, H_f, and $T_{spectrum}$ must be determined. The calculation of S_p is discussed in Section A.4.

K and m will be specified by the S-N curve chosen for the joint being analyzed. The X S-N curve (for welds with profile control) and the X′ S-N curve (for welds without profile control) provided by API RP 2A-LRFD (1993) may be used for a conservative assessment, as shown below:

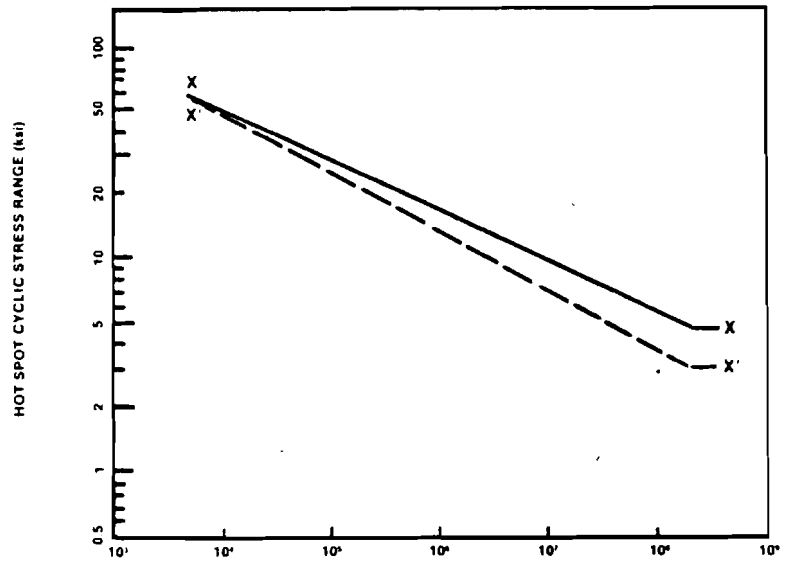

NOTE — These curves may be represented mathematically as

$$N = 2 \times 10^6 \left(\frac{\Delta\sigma}{\Delta\sigma_{ref}}\right)^{-m}$$

where N is the permissible number of cycles for applied cyclic stress range $\Delta\sigma$, with $\Delta\sigma_{ref}$ and m as listed below

CURVE	$\Delta\sigma_{ref}$ STRESS RANGE AT 2 MILLION CYCLES	m INVERSE LOG-LOG SLOPE	ENDURANCE LIMIT AT 200 MILLION CYCLES
X	100 MPa (14.5 ksi)	4.38	35 MPa (5.07 ksi)
X′	79 MPa (11.4 ksi)	3.74	23 MPa (3.33 ksi)

Figure F-2: S-N Curves from API (1993)

g_{stress} is a constant relating the wave height to the stress range at a particular location. Luyties and Geyer (1987) indicate that for structures having natural periods of three seconds or less, g_{stress} may be taken as 1.2 for components at the waterline, and as 1.3 for all other members. R is typically taken to be the total base shear cycle ratio (i.e. maximum base shear divided by minimum base shear for a single wave cycle), as described by API RP 2A-LRFD (1993) and Luyties and Geyer (1987). Typical values of R range from -0.15 to -0.5 and are dependent upon water depth.

H_0, H_1, ξ_0, ξ_1, N_0, N_1 and $T_{spectrum}$ must be specified according to the joint distribution of typical and storm waves to be found in the region where the structure is sited. This distribution must reflect wave encounters for the specified duration T_d. Similarly, H_f should be selected as the maximum wave height expected for the duration T_d. It is worth noting that for most cases this specified wave will not inundate the decks of the platform; should situations arise in which the specified wave does inundate the decks, the calculated stress S_p due to this wave will be conservatively high due to the inclusion of deck inundation forces in the component load calculation. A sample two-part distribution is shown below:

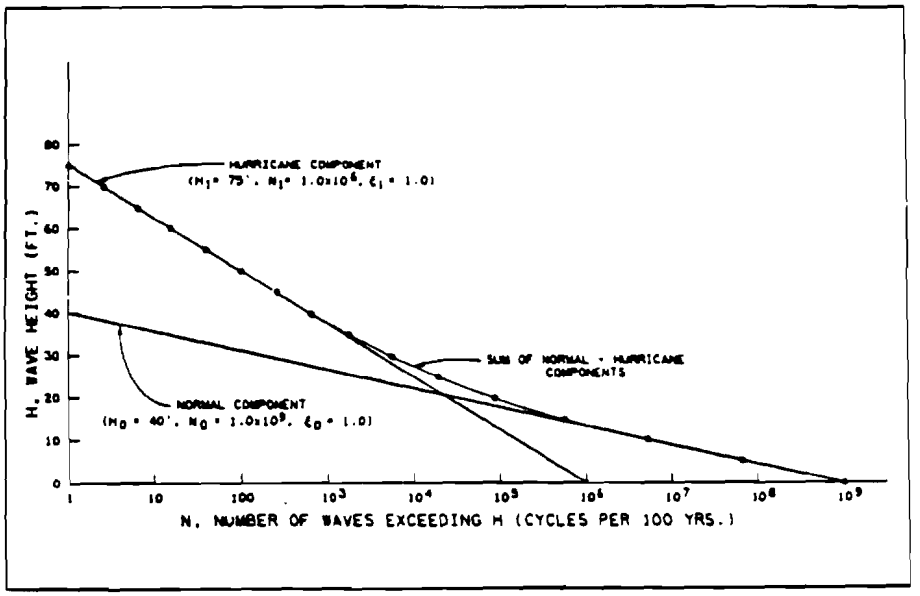

Where: H_n is the maximum normal wave height over period T.
H_1 is the maximum hurricane wave height over period T.
N_n is the number of wave cycles from normal distribution over period T.
N_1 is the number of wave cycles from hurricane distribution over period T.
T is the duration of the long-term wave height distribution.
ξ_n is the parameter defining the shape of the Weibull normal distribution. Value of 1.0 corresponding to the exponential distribution results in a straight line.
ξ_1 is the parameter defining the shape of the Weibull hurricane distribution.

Figure F-3: Two-Part Wave Height Distribution (API, 1993)

F.4 CALCULATING THE PEAK STRESS

Calculation of the stresses in a tubular joint can be a very time consuming and complicated process. Much effort may be expended in trying to refine estimates of the forces affecting the joint, and considerable detail may be applied in constructed a model which relates the stresses in the joint to the applied forces. A simplified approach to capturing the relationship between the forces acting on the structure and the stress at the joint is therefore proposed, in order to reduce the complexity of input information and calculation effort required.

The stresses existing in a joint are assumed to be dominated by two components:

1. Stresses induced by the axial force carried by the attached diagonal bracing member
2. Stresses due to bending induced in the attached diagonal bracing member by local hydrodynamic forces

Therefore, the following steps must be taken:

1. The global load or story shear due to the application of H_f must be calculated
2. The component of the story shear carried axially by the brace attached to the joint must be found
3. The bending moment due to local hydrodynamic forces from H_f at the brace end connected to the joint must be calculated

With the axial force and the moment known, the stress at the brace-joint interface may be estimated using simple mechanics:

$$\sigma = \frac{F_{axial}}{A_{brace}} + \frac{M_{end} r_{brace}}{I_{brace}}$$

The stresses due to axial force and bending may be further modified by stress concentration factors in order to relate the simply-calculated stresses to the peak stress which exists in the welded region:

$$S_p = (SCF)\sigma_{axial} + (SCF)\sigma_{bending}$$

Axial Force in Brace:

To find the axial force in the brace attached to the joint under evaluation, it is first necessary to find the load carried by the jacket bay in which the brace is located. The amount of load actually carried by the brace itself is estimated by considering the brace to be part of a parallel system of elements which all share the same lateral displacement imposed by the load on the bay.

The lateral forces imposed by H_f on the structure may be calculated as described in Appendix A. The story shear existing at the midpoint of the jacket bay in which the brace is located is taken as the force carried by that bay.

The bay in which the attached brace is located is considered to resist the applied load as a system of parallel elements, those elements being the braces in the bay (Figure F-4).

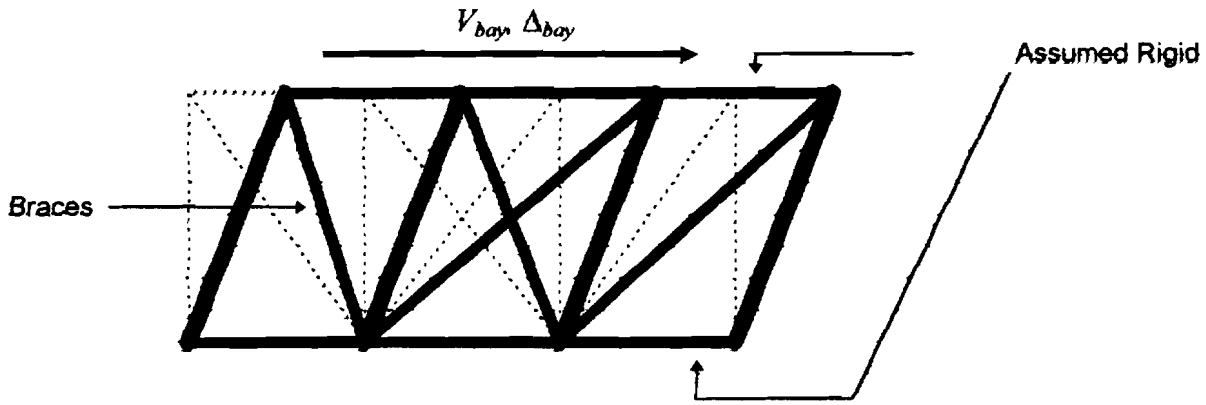

Figure F-4: Idealized Jacket Bay Behavior

Assuming that rigid framing exists above and below the bay, all braces in the bay will therefore share the same imposed lateral displacement due to the load. The lateral stiffness for the bay may be formulated as:

$$k_{bay} = \sum k_i \cos^2 \theta_i$$

where:

k_i = axial stiffness of each individual brace, i.e. $\frac{EA}{L}$

θ_i = angle between each brace and the horizontal

The lateral displacement of the bay may then be estimated as:

$$\Delta_{bay} = \frac{V_{bay} - F_L}{k_{bay}}$$

where:

V_{bay} = lateral load carried by bay

F_L = lateral load carried by battered legs

The axial force in an individual brace is then calculated according to:

$$F_{axial\,i} = k_i \Delta_{bay} \cos\theta_i$$

Moment at Brace End:

To find the moment at the brace end, i.e. where it connects to the joint being evaluated, it is necessary to find the local distributed load along the length of the brace. Then, together with assumptions as to the end fixity of the brace at the joint, this may be used to calculate the moment at the end of the brace by simple beam theory.

The distributed load w on individual braces due to H_f may be calculated as described in Appendix A. By conservatively assuming the ends of the brace to be completely fixed (and hence may develop large bending moments), the moment at the brace end may be found from:

$$M_{end} = \frac{wL^2}{12}$$

Together with the estimate of axial force in the brace, the moment may be used to calculate the stress at the brace-joint interface.

Stress Concentration Factors:

TOPCAT uses the stress concentration factors from API (1993) as a default. Users may override these factors by supplying their own.

Table F-1: Tubular Joint *SCFs*

Connection	Axial *SCF*	In-Plane Bending *SCF*
Chord K	$1.8\sqrt{\gamma}\tau\sin\theta$	$1.2\sqrt{\gamma}\tau\sin\theta$
Chord T/Y	$3.06\sqrt{\gamma}\tau\sin\theta$	$2.04\sqrt{\gamma}\tau\sin\theta$
Chord X, $\beta < 0.98$	$4.32\sqrt{\gamma}\tau\sin\theta$	$2.88\sqrt{\gamma}\tau\sin\theta$
Chord X, $\beta \geq 0.98$	$3.06\sqrt{\gamma}\tau\sin\theta$	$2.04\sqrt{\gamma}\tau\sin\theta$
All Braces	$1.0+0.375\left(1+\sqrt{\tau/\beta}SCF_{chord}\right) \geq 1.8$	

$$\beta = d/D \qquad \tau = t/T \qquad \gamma = D/(2T)$$

where:
- d = brace diameter
- D = chord diameter
- t = brace thickness
- T = chord thickness
- θ = angle between chord and brace axes

F.5 REFERENCES

American Petroleum Institute, "Recommended Practice for Planning, Designing, and Constructing Fixed Offshore Platforms - Load and Resistance Factor Design," API Recommended Practice 2A-LRFD (RP 2A-LRFD), 1st Edition, Washington, D. C., July 1993.

Luyties, W. H., and Geyer, J. F., "The Development of Allowable Fatigue Stresses in API RP2A,", Proceedings of the Offshore Technology Conference, OTC 5555, Houston, TX, 1987.

Nolte, K. G., and Hansford, J. E., "Closed-Form Expressions for Determining the Fatigue Damage of Structures Due to Ocean Waves," Proceedings of the Offshore Technology Conference, OTC 2606, Houston, TX, 1976.

APPENDIX G:
FOUNDATION STRENGTH AND STIFFNESS

by
James D. Stear and Professor Robert G. Bea

Portions of this Appendix have been previously published in the following:

Stear, J. D. and Bea, R. G., "Earthquake Analysis of Offshore Platforms / Screening Methodologies Project Phase III," Report to Joint Industry Project Sponsors, Marine Technology and Management Group, Department of Civil and Environmental Engineering, University of California at Berkeley, CA, June 1997.

TABLE OF CONTENTS **PAGE**

G.1 INTRODUCTION

This appendix documents the procedures used by the TOPCAT program to determine foundation strength and stiffness. It is organized into three sections: (1) strength of piles, (2) stiffness of piles and effect on platform vibration properties, and (3) strength and stiffness of mud mats and other mudline elements.

G.2 STRENGTH CAPACITY OF PILES AS MEASURED AT THE PILE HEAD

Horizontal Foundation Capacity:

The horizontal strength capacity of the foundation is estimated based on the assumptions that (1) the supporting piles will yield by forming plastic hinges at the base of the jacket and at some depth below the mudline, and that (2) all piles yield simultaneously (Figure G-1). The lateral load applied at the pile head which results in the formation of the two-hinge mechanism is determined by successively checking for the location of the second plastic hinge which will form when the pile fails (the first is assumed to be at the base of the jacket). A hinge depth d_{hinge} is initially selected, and then the lateral capacity is approximated using two physical relationships.

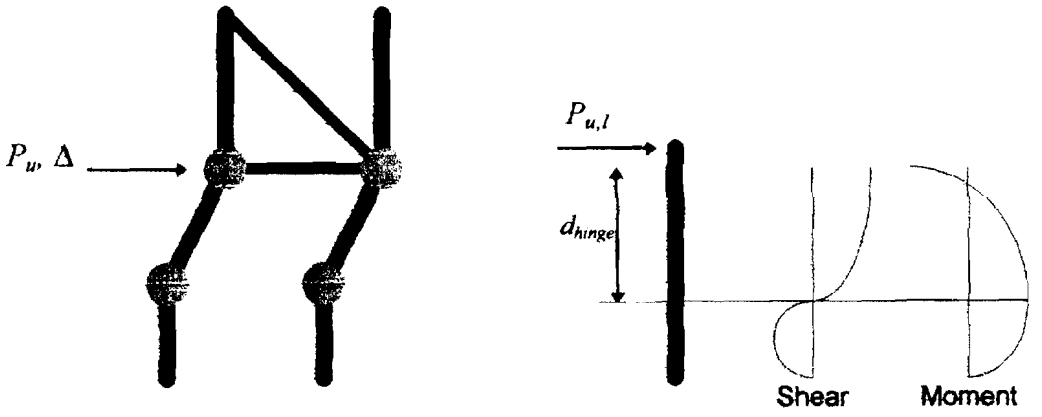

Figure G-1: Foundation Lateral Collapse Mechanism

The first relationship is formulated assuming the selected point is the point of zero shear, and hence the pile lateral capacity $P_{u,l}$ can be obtained by summing up the incremental lateral capacity of the soil to this depth:

$$P_{u,l} = \int_0^{d_{hinge}} p_s(z)dz$$

where:

$p_s(z)$ = unit soil strength at depth z

The second relationship is formulated using virtual work; the virtual displacement is the rotation of the second hinge:

$$P_{u,l} = \left[2M_u + \int_0^{d_{hinge}} z \cdot p_s(z)dz\right] \cdot \left(\frac{1}{d_{hinge}}\right)$$

where:

M_u = plastic moment capacity of pile section computed using P-M interaction

When the values of lateral capacity calculated using the two methods are in agreement, the true location of the hinge has been found, and hence the two values represent the correct lateral capacity.

NOTE: caissons and their supporting piles are assumed to fail in a one-hinge mechanism. The relationships used to solve lateral capacities for these members use M_u and not $2M_u$.

Unit pile soil resistance for cohesive soils with undrained shear strength S_u is taken to be:

$$p_s = 9S_uD$$

where D is the pile diameter. This formulation is supported by studies documented by Matlock (1970) and Randolph, et al. (1984) based on results for smooth piles. Unit soil resistance for cohesionless soils is estimated using a relationship from Broms (1964):

$$p_s = 3\gamma \cdot z \cdot D \cdot K_p$$

where:

$$K_p = \tan^2\left(45 + \frac{\phi}{2}\right)$$

and:

γ = submerged unit weight of the soil
ϕ = effective angle of internal friction of the soil

The total lateral strength capacity of the foundation is thus taken to be:

$$P_u = \sum_{i=1}^{N_{pile}} P_{u,l_i} + F_L$$

where F_L is the horizontal component of the batter force existing in the piles from overturning.

Pile head force-displacement relationships will be affected by both the loading rate and the number of extreme load cycles. If the loading rate is high, the effective strength and stiffness as measured at the pile head will increase, as documented by Bea (1980). Figure G-2 depicts the load-rate dependence phenomenon as observed in testing.

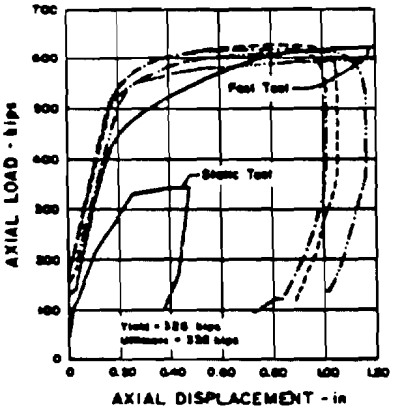

Figure G-2: Load-Rate Dependence for Piles

Cyclic inelastic loading on a pile will result in reductions in observed strength and capacity as measured at the pile head (Bea, 1980). Figure G-3 depicts these changes based on the results of pile testing.

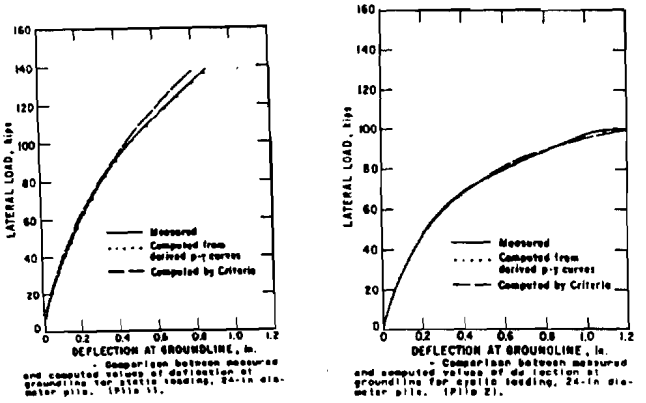

Figure G-3: Changes in Lateral Strength and Stiffness for Piles Subject to Cyclic Loading, from Holmquist, Matlock (1976)

Neither of these effects is explicitly considered by TOPCAT. Instead, users are given the opportunity to apply biases according to individual judgment.

The piles of a jacket-type platform are not the only foundation load-carrying members. Mud mats, mudline braces and conductors can provide additional capacity. approximations for additional capacity from these elements have been documented in Section G.4.

Foundation Overturning Capacity:

Foundation overturning capacity is determined from the axial strength and ductility of the piles. The procedure by which the axial capacities Q of piles are determined is straightforward: the individual soil layer friction contributions and, for the case of compression loading, the bottom

layer end-bearing capacities, are determined and then summed; Q is taken as the minimum of either this sum or the pile yield strength F_yA:

$$Q = qA_p - wL_p - P_z + \int_0^{L_p} f(z)A_s dz$$

where:

q = normal end yield force per unit of pile-end area
f = shear yield force per unit of embedded shaft surface area
A_p = area of pile tip
A_s = embedded shaft surface area per unit length of pile
A = steel cross-section area of pile
L_p = pile length
w = weight of pile and soil plug per unit length
P_z = vertical force from first platform vertical mode

The end-bearing capacity can only be mobilized when the friction capacity of the internal soil plug exceeds the end-bearing capacity.

The bearing strength q of cohesive soil with undrained shear strength S_u is:

$$q = 9S_u$$

The ultimate shaft friction is estimated from the following relationship:

$$f = \kappa S_u$$

where κ is the side resistance factor. Focht and Kraft (1986) provide values for K as a function of S_u:

Table G-1: Side Resistance Factor for Cohesive Soils, from Focht and Kraft (1986)

S_u, ksf	κ
< 0.5	1.0
0.5 to 1.5	1.0 to 0.5
> 1.5	0.5

For cohesionless soils, the ultimate bearing capacity is estimated from:

$$q = N_q \sigma_v$$

N_q is a bearing capacity factor dependent on the friction angle ϕ of the soil. σ_v is the effective pressure at the pile tip. The unit shaft resistance per unit length of pile is taken to be:

$$f = k\sigma_{vl} \tan\theta$$

where:

k = lateral earth pressure coefficient, assumed to be 0.8 (API, 1993)
σ_{vi} = effective overburden pressure at depth
θ = friction angle between soil and pile, taken as ϕ - 5°

The unit shaft resistance and unit end-bearing capacity cannot increase indefinitely with pile penetration; the following limiting values for N_q, q and f are used from Focht and Kraft (1986):

Table G-2: Limiting Values of N_q, q and f, from Focht and Kraft (1986)

ϕ, degrees	N_q	q, ksf	f, ksf
20	8	40	1.0
25	12	60	1.4
30	20	100	1.7
35	40	200	2.0

With the pile capacities determined, the rotation capacity of the foundation will be given by:

$$M_{f-rot} = \sum_{i=1}^{npile} Q_i L_{xi}$$

where L_x is the distance from the pile to the axis of rotation.

Axial load tests performed on piles indicate inelastic behavior of the type shown in Figure G-4. As will lateral loading of piles, the axial pile head load-displacement behavior will exhibit reductions in strength when subjected to inelastic cycling. Also, the axial strength and stiffness measured at the pile head will increase for high loading rates. These affects are not explicitly considered by TOPCAT; however, a user may supply biases to implicitly account for them.

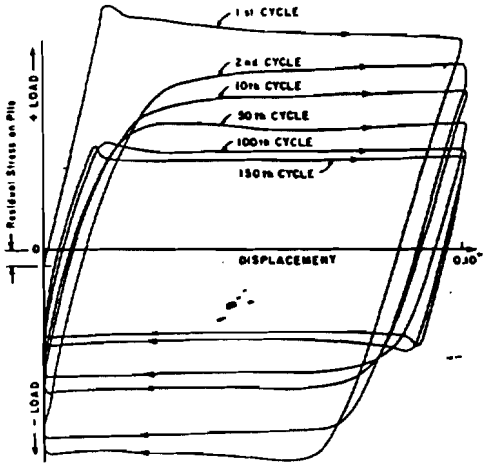

Figure G-4: Cyclic Axial Loading of Pile in Soft Clay (Reese, Cox, 1975)

Mud mats and mudline braces can provide additional capacity against overturning. While these elements are not included in the capacity formulations described in this section, approximations for additional capacity from these elements have been documented in Section G.4.

G.3 PILE HEAD LATERAL AND VERTICAL STIFFNESS APPROXIMATIONS

As the foundation is a significant source of platform flexibility, it is important that the associated stiffness properties of the foundation be well represented. Typically, the stiffness contributions of mud mats and mudline braces are ignored, while stiffnesses for piles and conductors are developed by modeling the pile as a segmented beam supported by springs, and then developing pile-head load-deflection behavior from these models. Developing pile-head behavior using this approach can be quite time-consuming.

In lieu of using the above procedure, a number of approximate approaches are available to estimate pile-head stiffnesses. Perhaps the most common approach to estimating lateral pile-head stiffnesses is to consider the pile to be a beam fixed at the mudline and fixed at some depth L (between five and ten pile diameters) below the mudline:

$$k_x = \frac{12EI}{L^3}$$

A similar approach is commonly used to estimate pile-head vertical stiffnesses. The vertical stiffness is derived by considering the basic stiffness EA/L of the pile column and then modifying this stiffness for the mechanism by which vertical loads are transferred to the surrounding soil. Various transfer mechanisms are shown below in Figure G-5.

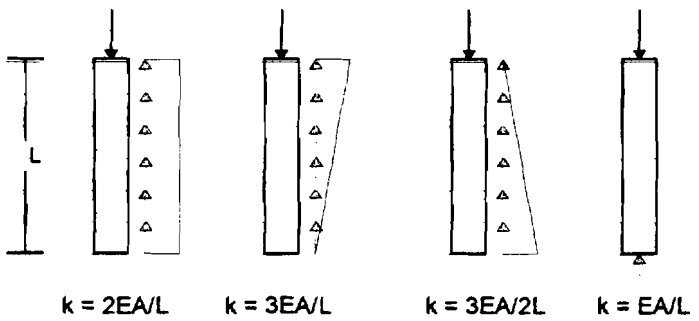

Figure G-5: Vertical Load Transfer Mechanisms for Imbedded Piles

An alternative for pile-head horizontal stiffness is that used by Penzien (1975) in a series of studies of offshore platforms subjected to earthquakes:

$$k_x = 18.2Gr\frac{(1-\upsilon^2)}{(2-\upsilon)^2}$$

where:

G = shear modulus of the foundation soil

υ = Poisson's ratio for the foundation soil
r = pile radius

This horizontal stiffness k_x is derived using elastic half-space theory and assuming the pile is deeply imbedded. Unless the foundation is extremely soft, the horizontal loads will be transferred quite rapidly to the surrounding soil with depth. Hence, the horizontal stiffness of each pile may be derived by considering the pile-head to be a rigid circular footing supported on an elastic medium. It is assumed to connection between the pile and jacket is rigid and allows for no pile-head rotation.

Another approach to estimating pile head stiffnesses is that suggested by Dobrey (1980). These approximations are based on previous work by Novak (1974) and Blaney, et al. (1976). Assuming foundation strength to rely upon soil elastic modulus and assuming as a basis a beam on an uniform elastic foundation, pile-head stiffnesses take the form:

$$k_z = 0.8\frac{E_p A}{r}\left(\frac{E_s}{E_p}\right)^{0.5}$$

$$k_x = 2\frac{E_p I}{r^3}\left(\frac{E_s}{E_p}\right)^{0.75}$$

$$k_\theta = 1.6\frac{E_p I}{r}\left(\frac{E_s}{E_p}\right)^{0.25}$$

$$k_{\theta x} = -1.2\frac{E_p I}{r^2}\left(\frac{E_s}{E_p}\right)^{0.5}$$

where:

E_p = Elastic modulus of pile material
E_s = Elastic modulus of soil material
I = Moment of inertia of pile steel cross-section

Assuming there is no applied moment at the pile head, the effective horizontal stiffness may be represented by:

$$k_{x\,\text{effective}} = k_x - \frac{k_{\theta x}^2}{k_\theta + k_{\theta\,\text{structure}}}$$

This effective stiffness will vary depending on the amount of rotational stiffness supplied by the structure attached to the pile head, $k_{\theta\ structure}$. These formulas are intended for intermediate values of E_s/E_p, and r/L ratios in the range of 10 to 50.

A comparison has been made between the various approximate pile-head stiffness and those derived during the course of two example platform analyses. One platform was a four-leg structure in 100 ft of water, with 72 " diameter piles driven to 150 ft through stiff clay. The other was an eight-leg structure in 265 ft of water, with two sets of piles. The corner piles were 66" diameter, and were driven to 260 ft. The center piles were 48" diameter, and were driven to 230 ft. Pile-head stiffnesses from the different approximations along with those used in the examples are shown below in Tables G-3 and G-4:

Table G-3: Horizontal Pile-Head Stiffnesses (kips/in)

Diameter	$12EI/L^3$ L=5D	$12EI/L^3$ L=10D	Penzien kx	Dobry kx	3-D kx
72"	1093	136	870	515	469
66"	1640	205	598	623	260
48"	1640	205	435	623	135

Table G-4: Vertical Pile-Head Stiffnesses (kips/in)

Diameter	3EA/L	EA/L	Dobry kz	3-D kz
72"	10933	3644	2915	3150
66"	8541	2847	3787	4496
48"	7069	2356	3787	2825

There is much variation between the approximate methods and the springs derived for the 3-D analyses. However, it must be remembered that these estimates may be obtained with much less effort than constructing and analyzing a segmented pile model. Furthermore, given the fact that soil properties may possess significant biases due to sampling and testing methods, there will be an element of variation to the springs derived from detailed analyses; this must be recognized by the analyst. The best of action when making use of these approximations is to select sets which will provide upper and lower bounds on the stiffnesses.

To study the effect of foundation flexibility on the horizontal response of a platform, the axial and horizontal pile-head stiffnesses used with two platforms were varied with respect to the values calculated from the detailed analysis (see Tables G-3 and G-4). The variation in fundamental horizontal period for both Platforms are shown below in Figures G-6 and G-7:

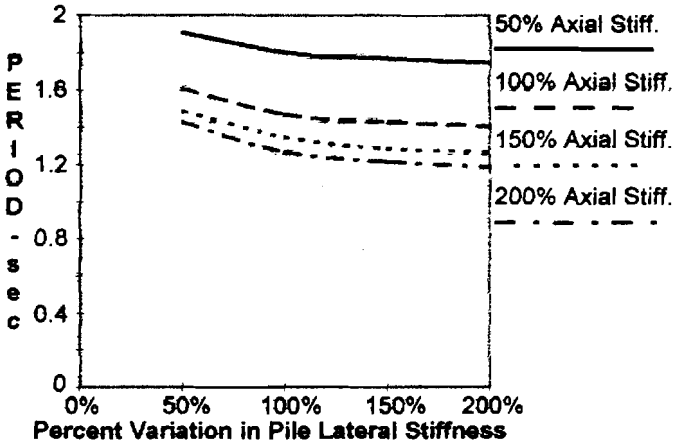

Figure G-6: Four-Leg Platform, Variation in Fundamental Period

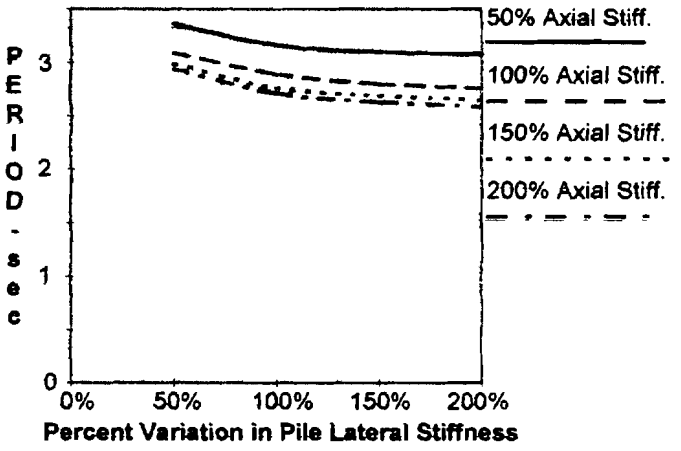

Figure G-7: Eight-Leg Platform, Variation in End-On Fundamental Period

Varying the stiffnesses for the four-leg platform may change the period by as much as 33%. This could have a significant effect on calculated loads, depending upon the response spectrum being used. For the eight-leg platform, the maximum variation is 14%. This is less significant, and is due to the larger flexibility of the ungrouted 8-leg jacket. Nevertheless, it is important to recognize that there may be significant variation in the pile stiffnesses due to factors beyond the control of the analyst.

TOPCAT adopts the basic pile stiffness approximations of EA/L and $12EI/(10D)^3$. The user may apply biases to these values in order to cover a wider range of possibilities.

G.4 INCREASES IN FOUNDATION STRENGTH AND STIFFNESS FROM CONDUCTORS, MUD MATS AND MUDLINE BRACES

It is now possible to evaluate the effects of conductors, mud mats and mudline braces on foundation strength and stiffness with TOPCAT. After entering data on these components, and selecting one or both of the analysis options "Include Conductor Strength and Stiffness Effects" and "Include Mudline Element Strength and Stiffness Effects," the strength and stiffness contributions of these elements will be added to the overall foundation capacity.

Conductors:

Conductors are treated as piles which offer lateral support only. Their lateral strength and stiffness are determined the same as for piles (G.2 and G.3). Group effect modifiers for both strength and stiffness may be entered by the user to bias these characteristics. The user must supply the number of conductors, as well as conductor diameter, plastic moment capacity, moment of inertia, weight per unit length, distance from mudline to first point of fixity (if no framing exists at mudline), and penetration. The user should check to ensure that sufficient framing strength exists at the first point of fixity to ensure the full lateral capacity of the conductors can be mobilized.

Mudline Elements:

Mud mat and mudline brace foundation capacity contributions are determined using approaches suggested by Section 6.13 of API RP 2A-WSD (1993) for mat foundations. It is assumed that these elements are very strong and stiff compared to the underlying soil; hence strengths and stiffnesses will be dictated by the soil properties. Bearing and sliding capacities for these elements are determined using the following:

For elements founded on cohesive soils (clays):

$Q = 5.14cA$ maximum bearing strength

$H = cA$ maximum sliding strength

where:

c = undrained shear strength of soil

A = foundation contact area

For elements founded on cohesionless soils (sands):

$Q = 0.3\gamma' BN_\gamma A$ maximum bearing strength

$H = c'A + Q\tan\phi'$ maximum sliding strength

where:

γ' = effective unit weight of soil

B = minimum lateral foundation dimension, assumed to be unity

$N_\gamma = 2(N_q + 1)\tan\phi'$

$N_q = \left(\exp\left[\pi\tan\phi'\right]\right)\left(\tan^2\left(45° + \phi'/2\right)\right)$

ϕ' = effective friction angle of Mohr envelope

c' = effective cohesion intercept of Mohr envelope, assumed 0 for sand

A = foundation area

Bearing and sliding stiffnesses are assumed to be controlled by the supporting soil. The following values of soil stiffness per unit area are used:

Table G-5: Bearing Stiffness as Related to Bearing Strength (Barkan, 1962)

Soil Group	Bearing Stress (kips/ft^2)	Vertical Stiffness (kips/ft^3)
Weak	3 or less	190
Medium	3 to 7	190 to 310
Strong	7 to 10	310 to 620
Rock	10 or more	620

The vertical stiffness is selected based on the bearing capacity of the soil as determined from the API RP 2A-LRFD (1993) Section 6.13 relationships listed above. The sliding stiffness is taken to be 50 % of the vertical stiffness, as suggested by Barkan, (1962).

The lateral capacity and stiffness provided by mudline elements are taken as the product of the contact areas of all mats and mudline braces (the contact areas for braces are assumed to be DL) with the soil sliding strength and stiffness. These values may be modified by the user using bias factors. The mudline element lateral strength and stiffness are added to the lateral strength and stiffness provided by piles and conductors. The user should be aware that the combined mat-pile-conductor foundation capacity assumes fully plastic behavior by all foundation strength mechanisms, and that all of these mechanisms are assumed to become active (i.e. achieve full strength) prior to any occurrence of instability caused by excessive platform deflection at the mudline.

For the purpose of determining mudline element contributions to platform overturning capacity, it is assumed that the base of the platform rotates as a rigid plate, and that all piles and mudline elements act as springs connected to this plate. The overturning moment capacity of the platform is based upon the base rotation which will result in the first incidence of pile yielding (in either tension or compression). The TOPCAT program first determines the amount of base rotation which is needed to fulfill this condition for both end-on and broadside loading. Once the base rotation is determined, the moment resulting from action of the foundation mudline elements through this rotation is calculated. This moment is approximated using the following relationship:

$$M = F\frac{L}{4}\left[\frac{\left(A_{braces} + A_{mats}\right)}{2}\right]$$

where:

$$F = Min\left[\frac{L}{2}k_{bearing}\theta, \sigma_{bearing}\right]$$

and:

L = length of base on side perpendicular to axis of rotation
A_{braces} = contact area of all mudline braces
A_{mats} = contact area of all mud mats
$k_{bearing}$ = unit bearing stiffness as determined from Table G-5
$\sigma_{bearing}$ = unit bearing resistance as determined from API Section 6.13

It is assumed that mats and mudline braces actively contribute to strength and stiffness only when placed in compression; i.e. they do not provide support against uplift. Hence, only 50 % of the total mat and brace contact areas are used to determine the effective resisting moment from these elements. Furthermore, to simplify further it is assumed that the centroid of the area of mudline element action is halfway between the axis of rotation and the outer edge of the base ($L/4$). The soil resistance at the prescribed rotation is taken to be the minimum of either the resultant unit force found using the soil bearing stiffness at the outer edge of the base or the maximum bearing capacity of the soil. This moment is then added to the moment determined based on axial action of the piles to obtain the total overturning moment capacity. The moment

capacity from mudline elements is also used to supplement the effective axial capacity of the piles used in determining pile reserve strength ratios; an "equivalent" axial resistance is estimated from:

$$P = \frac{M}{Ln_{pile}}$$

where n_{pile} is the total number of piles providing axial resistance. This value is then added to the axial strength of the piles and the reserve strength ratios are then evaluated.

The user must carry out independent checks of mudline braces, mud mats and mud mat connections, and other elements which may be in the load path in order to ensure these elements can carry the load required to develop full capacity in the soil for both bearing and sliding conditions. To aid in this assessment, TOPCAT returns the surface forces which will be induced on mudline elements as the sliding and bearing capacities of the underlying soil is mobilized. The user should also be aware that mats and braces on soil, piles in soil and conductors in soil may have very different stiffnesses; hence very stiff elements may reach capacity at levels of displacement much smaller than those required to mobilize the capacity of flexible elements. This can have serious consequences if the stiff elements will fail in a manner which results in strength loss, i.e. the breaking of connections or member rupture; as a result it may not be possible to achieve the fully-plastic bearing and sliding mechanisms currently assumed by the program.

G.5 REFERENCES

American Petroleum Institute, "Recommended Practice for Planning, Designing and Constructing Fixed Offshore Platforms - Working Stress Design," Recommended Practice 2A-WSD (RP 2A-WSD), 20th Edition, Washington, D. C., July 1993.

Barkan, D. D., *Dynamics of Bases and Foundations*, McGraw-Hill, New York, NY, 1962.

Bea, R. G., "Dynamic Response of Piles in Offshore Platforms," Dynamic Response of Pile Foundations: Analytical Aspects, editors: M. W. O'Neill and R. Dobry, ASCE, New York, NY, 1980.

Blaney, G. W., Kausel, E., and Roesset, J. M., "Dynamic Stiffness of Piles," Proceedings of the 2nd International Conference on Numerical Methods in Geomechanics, ASCE, Blacksburg, VA, 1976.

Broms, B. B., "Lateral Resistance of Piles in Cohesionless Soils," Proceedings, ASCE, Vol. 90, No. SM3, May 1964.

Dobry, R., Vicente, E., and O'Rourke, M., "Equivalent Spring and Damping Coefficients for Individual Piles Subjected to Horizontal Dynamic Loads," paper submitted for publication in the Journal of the Geotechnical Division, ASCE, 1980.

Focht, J. A., and Kraft, L. M., "Axial Performance and Capacity of Piles," Planning and Design of Fixed Offshore Platforms, editors: McClelland, B., and Reifel, M. D., 1986.

Holmquist, D. V., and Matlock, H., "Resistance-Displacement Relationships for Axially-Loaded Piles in Soft Clay," OTC-2774, Proceedings of the Offshore Technology Conference, Houston, TX, May 1976.

Matlock, H., "Correlations for Design of Laterally Loaded Piles in Soft Clay," Proceedings of the Offshore Technology Conference, Houston, TX, May 1970.

Novak, M., "Dynamic Stiffness and Damping of Piles," Canadian Geotechnical Journal, Vol. 11, No. 4, 1974.

Penzien, J., "Seismic Analysis of Platform Structure-Foundation Systems," Proceedings of the Offshore Technology Conference, OTC 2352, Houston, TX, May 1975.

Randolph, M. F., Houlsby, G. T., "The Limiting Pressure on a Circular Pile Loaded Laterally in Cohesive Soil," Geotechnique, London, England, 1984.

Reese, L. C., and Cox, W. R., "Field Testing and Analysis of Laterally Loaded Piles in Stiff Clay," OTC-2312, Proceedings of the Offshore Technology Conference, Houston, TX, May 1975.

APPENDIX H: SIMPLIFIED RELIABILITY ANALYSIS OF PLATFORM COMPONENTS

by
Mehrdad M. Mortazavi and Professor Robert G. Bea

edited by James D. Stear

Portions of this Appendix have been previously published in the *following:*

Mortazavi, M. M. and Bea, R. G., "A Probabilistic Screening Methodology for Steel, Template-Type Offshore Platforms," Report to Joint Industry Project Sponsors, Marine Technology and Management Group, Department of Civil and Environmental Engineering, University of California at Berkeley, CA, January 1996.

TABLE OF CONTENTS **PAGE**

H.1 INTRODUCTION

Large uncertainties associated with loadings and capacities add another dimension to the complexity of the problem of structural integrity assessment of offshore platforms. Due to these large uncertainties and relatively high consequences of failure of offshore platforms, in particular in North Sea region, these structures have been the subject of comprehensive reliability analyses in the past (e.g. Thoft-Christensen et al., 1982, Nordal et al., 1988). In general, there are two types of uncertainty; natural or aleatory (Type I) and unnatural or epistemic (Type II). The source of the aleatory uncertainties is the inherent randomness of stochastic processes (e.g. the uncertainty associated with the prediction of the annual maximum wave height for a given site). Basically, this type of uncertainty is information insensitive and can not be reduced. The epistemic uncertainties are partially due to our lack of thorough understanding of the physics of the problem (physical modeling uncertainties) and partially due to lack of data (statistical modeling uncertainties)(e.g. uncertainties associated with the wave kinematics given the wave height and period). This type of uncertainty is in general information sensitive and can be reduced. More research can lead to our better understanding of the physical processes and help enhance the physical modelings and hence reduce the uncertainties associated with them. More experiments and field measurements can lead to improvements of statistical modelings and help reduce the uncertainties associated with the modeling parameters. It is often difficult to clearly distinguish between the two types of uncertainty.

One effective mean of representing Type II uncertainties is through characterizing "biases". Bias is defined as the ratio of the true to the predicted value of a random variable. By establishing and evaluating the statistical properties of the bias (mean and standard deviation), conservatism or unconservatism implicit in the simplified modeling assumptions can be captured and taken into account.

A simplified deterministic structural integrity assessment approach has been developed for offshore platforms, and integrated into the TOPCAT program. This approach is described in the following section. Taking into account the Type I and Type II uncertainties associated with loadings and capacities and using the concepts of structural reliability theory and the deterministic safety assessment formulations developed in this and previous appendices, a simplified probabilistic safety assessment approach has been also developed and is described in this appendix.

H.2 DETERMINISTIC FAILURE ANALYSIS

The process is summarized in Figure H-1. The geometry of the platform is defined by specifying a minimum amount of data. These include the effective deck areas and weights, the proportion and topology of jacket legs, braces, and joints and of the foundation piles and conductors. The projected area and mass characteristics of appurtenances such as boat landings, risers, and well conductors are specified. If marine fouling is present, the variation of the fouling thickness with depth is also defined. Specialized elements are designated including grouted or ungrouted joints, braces, and legs. In addition, damaged or defective elements are included. Dent depth and initial out-of-straightness are specified for braces with dents and global bending defects. Element capacity reduction factors are introduced to account for other types of damage to joints, braces,

and foundation (corrosion, fatigue cracks, etc.). Steel elastic modulus, yield strength, and effective buckling length factor for vertical diagonal braces are specified. Soil characteristics are specified as the depth variation of effective undrained shear strength for cohesive soils or the effective internal angle of friction for cohessionless soils. Scour depth around the piles is also specified.

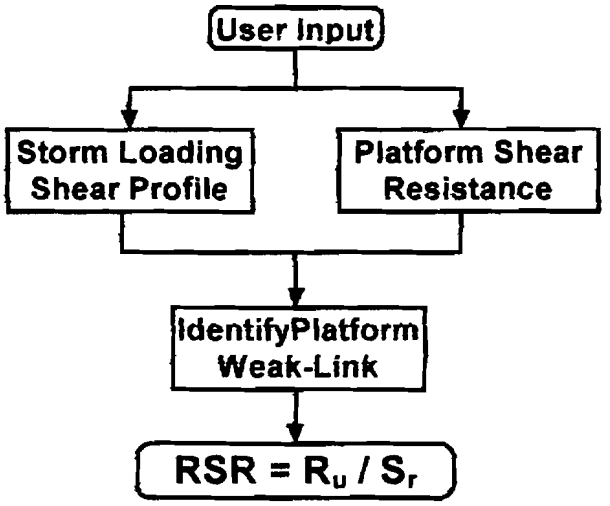

Figure H-1: Deterministic Failure Analysis

Collapse mechanisms are assumed for the three primary components that comprise a template-type platform: the deck legs, the jacket, and the pile foundation. Based on the presumed failure modes, the principle of virtual work is utilized to estimate the ultimate lateral capacity for each component and a profile of horizontal shear capacity of the platform is developed (Appendices B, D and G).

For storm conditions, wind speed at the deck elevation, wave height and period, current velocity profile, and storm water depth need to be defined. These values are assumed to be collinear and to be the values that occur at the same time. Generally the load combination is chosen to be wind speed component and current component that occur at the same time and in the same principal direction as the expected maximum wave height. The wave period is generally taken to be expected period associated with the expected maximum wave height. To calculate wind loadings acting on the exposed decks the effective drag coefficient needs to be defined. Similarly, the hydrodynamic drag coefficients for smooth and marine fouled members have to be defined. Modification factors are introduced to recognize the effects of wave directional spreading and current blockage.

For earthquakes, a response spectrum must be specified in order to obtain modal accelerations. The added mass associated with submerged members must be determined, and estimates of modal damping ratios must be made. An appropriate modal combination rule must be selected to obtain total demands on components.

Comparison of the shear demands and forces from overturning with the platform component capacities identifies the weak link in the platform system. The base shear or total lateral loading at which the capacity of this weak link is exceeded defines the static ultimate lateral capacity of

the platform R_{us}. The static lateral loading capacity is corrected with a loading effects modifier, F_v, to recognize the interactive effects of transient loadings and nonlinear hysteretic platform response (Bea and Young, 1993).

$$R_u = R_{us} F_v$$

With these results, the Reserve Strength Ratio (*RSR*) can be determined as:

$$RSR = \frac{R_u}{S_r}$$

where S_r denotes the reference total maximum lateral loading.

H.3 PROBABILISTIC FAILURE ANALYSIS

The development of a simplified method to assess the structural reliability of conventional template-type offshore platforms is described in this section. The primary objectives are to identify the potential failure modes and weak-links of the structure and to estimate bounds on the probability of system failure by taking into account the biases and uncertainties associated with loadings and capacities (Figure H-2).

With this in mind, the maximum static force acting on a platform is treated as a function of random variables. Its statistical properties are derived considering the uncertainties associated with environmental conditions, structure conditions, and force calculation procedures. The expected capacity of the platform and the uncertainty associated with it are also characterized. The simplified ultimate limit state analysis procedures described in other appendices are utilized to estimate an expected or best estimate capacity of the platform. The uncertainties associated with this capacity are estimated using a combination of series components and parallel elements. The series components are the superstructure (deck), the substructure (jacket), and the foundation. The capacity of the platform is assumed to be reached when the capacity of anyone of these components is reached. Within each component there are parallel elements; deck legs, braces, joints, and piles. In order for a component to reach its upper-bound capacity, all of the parallel elements have to fail.

The proposed reliability analysis in this appendix is based on a first order second moment (FOSM) approach. A study is made of the implications of the simplified FOSM method. In the case of an eight-leg drilling and production platform located in Gulf of Mexico, the results from FOSM reliability analysis are compared with those from first and second order reliability methods (FORM and SORM).

H.4 STRUCTURAL COMPONENT AND SYSTEM RELIABILITY

Component Reliability:

The reliability analysis formulated in this chapter is based on the assumption of two-state structural components; a component can be in a safe- or fail-state. Furthermore it is assumed that the uncertainties associated with the state of the component can be described by random

variables. For the basic structural component with the resistance R and load S, the probability of failure is equal to the probability that the load exceeds the resistance:

$$p_f = P[R < S]$$

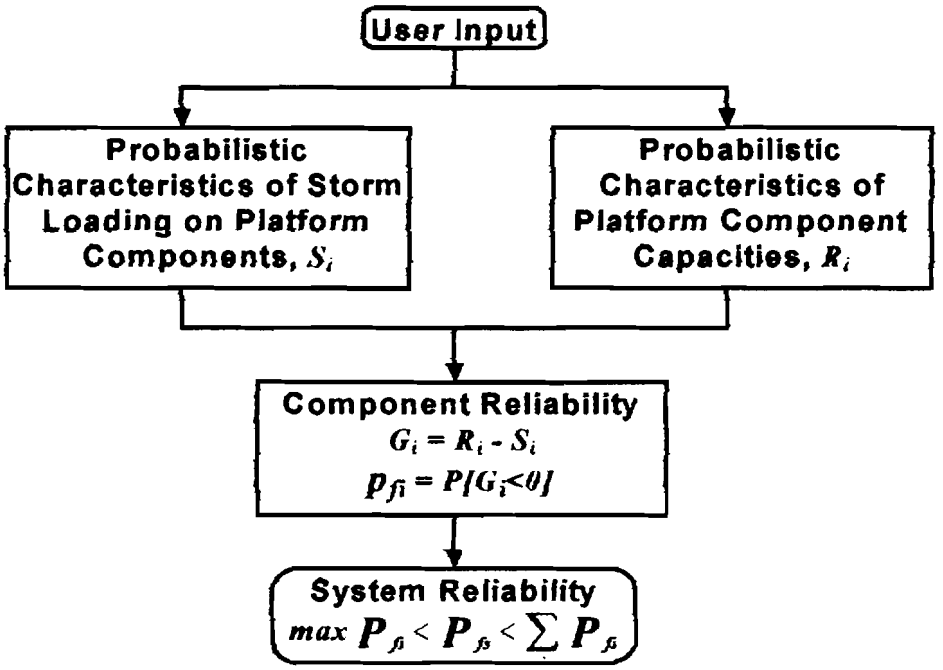

Figure H-2: Probabilistic Failure Analysis

Assuming that R and S are random variables with the joint probability density function $f_{RS}(r,s)$, the probability of failure can be written as:

$$p_f = \iint_{r \le s} f_{RS}(r,s)\,dr\,ds$$

In general, the resistance R and the load S are themselves functions of random variables. Assuming $X(x_1, x_2, ..., x_n)$ to be a set of random variables that completely describe the load and resistance characteristics with a joint probability density function $f_X(x)$, and further assuming that the state of the component is described by a function $g(x)$ so that $g(x) -<0$ indicates failure, the probability of failure can be given by the n-fold integral:

$$p_f = \int_{g(x) \le 0} f_X(x)\,dx$$

$g(x)$ is often referred to as limit state function. Problems associated with evaluating the above integral include: a) $f_X(x)$ may not be completely known due to lack of statistical data, b) the limit state function, $g(x)$, may not completely describe the true state of the component, and c) even in absence of problems stated above, integrating the above integral can be a formidable task (Der Kiureghian, 1994).

To circumvent these problems, reliability measures under incomplete statistical information have been developed. Indeed much of the early work on reliability analysis was based on such measures. The complete handling of the subject is not within the scope of this dissertation, however, the background used to develop simplified reliability analysis formulations for jacket offshore structures is summarized in the following.

Based on a mean value first order second moment (MVFOSM) approximation and using the load and capacity equations formulated earlier in this and other appendices, the mean and standard deviation of loads acting on and capacities of platform components can be estimated. Given that the resistance R of a component is a function of random variables $(x_1, x_2, ..., x_n)$, its first two statistical moments can be given by:

$$\mu_F \approx F(M_x)$$

and:

$$\sigma_F^2 \approx \nabla F|_{M_x} \Sigma \nabla F^T|_{M_x}$$

where:

$$M_x = \begin{bmatrix} \mu_{x_1} & \mu_{x_2} & \cdots & \mu_{x_n} \end{bmatrix}$$

is the mean vector of the resistance function and:

$$\Sigma = \begin{bmatrix} \sigma_{x_1}^2 & \rho_{x_1x_2}\sigma_{x_1}\sigma_{x_2} & \cdots & \rho_{x_1x_n}\sigma_{x_1}\sigma_{x_n} \\ \rho_{x_2x_1}\sigma_{x_2}\sigma_{x_1} & \sigma_{x_2}^2 & \cdots & \rho_{x_2x_n}\sigma_{x_2}\sigma_{x_n} \\ \cdots & \cdots & \cdots & \cdots \\ \rho_{x_nx_1}\sigma_{x_n}\sigma_{x_1} & \rho_{x_nx_2}\sigma_{x_n}\sigma_{x_2} & \cdots & \sigma_{x_n}^2 \end{bmatrix}$$

defines the covariance matrix, whereas:

$$\nabla F = \begin{bmatrix} \frac{\partial F}{\partial x_1} & \frac{\partial F}{\partial x_2} & \cdots & \frac{\partial F}{\partial x_n} \end{bmatrix}$$

is the gradient vector of the resistance function which is evaluated at the mean vector. The same formulations can be written for the load function S. Defining a safety margin as:

$$M = \ln(R) - \ln(S)$$

The probability of failure may then be estimated from:

$$P_f = CDF\left(\frac{M - \mu_M}{\sigma_M}\right)$$

where:

μ_M – mean value of the safety margin
σ_M – standard deviation of the safety margin

Assuming the demand on and capacity of the component may both be described by log-normal distributions, the exact reliability index may be solved explicitly. It is given by:

$$\beta = \frac{\mu_M}{\sigma_M}$$

where:

$$\mu_M = \ln\left(\frac{\mu_R}{\mu_S}\sqrt{\frac{1+V_S^2}{1+V_R^2}}\right)$$

$$\sigma_M^2 = \ln\left(1+V_R^2\right) + \ln\left(1+V_S^2\right) - 2\ln\left(1+\rho_{RS}V_R V_S\right)$$

μ_R, σ_R – mean and coefficient of variation of resistance function
μ_S, σ_S – mean and coefficient of variation of demand function
ρ_{RS} – correlation between demand and resistance

The probability of failure is thus:

$$P_f = \Phi(-\beta)$$

where $\Phi(.)$ is the standard normal variate function. Note that these equations and those derived for jointly normally distributed loads and capacities are the only known exact and closed form solutions of the probability of failure for non-trivial distributions of loads and capacities.

System Reliability:
Unimodal bounds on probability of failure of a series system, p_{fs}, can be estimated by:

$$\max\left(P_{fi} < P_{fs} < \sum_i P_{fi}\right)$$

where p_{fi} denotes the probability of failure of the i^{th} component. The lower bound is based upon the assumption of perfect correlation among all component failure modes. The upper bound is based upon the assumption of no correlation among the component failure modes. In general, unimodal bounds are useful when there exists a dominating failure mode. However, in case of offshore platforms, the failure of different structural components has been shown to be strongly correlated mainly due to common dominating uncertainties in loading variables (Thoft-Christensen and Baker, 1982, Nordal et al., 1988).

H.5 PROBABILISTIC LOADING AND CAPACITY FORMULATIONS

The uncertainties and biases associated with storm loads will be discussed first. Given the wave height and its associated period, there are uncertainties associated with predicting the wave kinematics (water particle velocities and accelerations). The primary source of these uncertainties is the incomplete physical modeling of the complex processes. Wave theories that try to predict the wave kinematics have been developed based on many idealizing assumptions, including wave regularity, directionality, and propagation (Appendix A). Given the water particle kinematics, there also are uncertainties associated with predicted local and global forces acting on an offshore platform. The primary source of these uncertainties is the force calculation model and the associated empirical drag and inertia coefficients (Bea; 1990; Haver, 1995).

Offshore engineering research has traditionally used field measurements and laboratory experiments to calibrate existing wave kinematics and load models and establish the uncertainties associated with the predictions of these models. The Conoco Test Structure (Bea et al. 1986) and Ocean Test Structure (Haring et al. 1979) are two examples of highly instrumented platforms to measure wave kinematics and forces on offshore structures. The measured data indicates that the primary difference between predicted and measured wave kinematics and forces is due to irregularity and directional spreading of real waves generated during intense storms.

Given the wave height, the API wave and current force calculation procedure is expected to result in unbiased estimates of the forces acting on offshore platforms provided appropriate coefficients are used (Heideman and Weaver, 1992). The kinematics modification factors and the force coefficients recommended in API RP 2A (API, 1993a) guidelines are based on large numbers of experimental test data and field measurements. For a given Keulegan-Carpenter number (e.g. KC>30), the uncertainties associated with the force coefficients are found to be rather small (COV=0.05) (Haver, 1995).

Wave height is the governing parameter in the API load calculation procedure. However, various investigators have found that wave forces can be more closely correlated to wave crest elevations (Haver, 1995). This is particularly true, if the crest elevation exceeds the elevation of lower platform decks. The probabilistic characteristics of wave-in-deck loadings are of extreme importance for structural risk assessment studies of offshore platforms. Tromans et al. (1992) found that the only significant source of modeling uncertainty relates to wave-in-deck forces which is due to modeling uncertainties in local water particle kinematics close to the free surface. For predicted wave-in-deck forces, a total coefficient of variation of 70% has been suggested by Petrauskas et al. (1994). For a given wave height, a conditional COV for predicted wave-in-deck force of 0.35 has been recommended by API (1994).

Hydrodynamic wave forces on platform decks are not only important due to their magnitude, but also because of their effect on the global load pattern. A load pattern that includes relatively large deck forces can result in failure modes different from those predicted based on a load pattern that does not include wave-in-deck forces (Loch and Bea, 1995).

Earthquake loads also contain many uncertainties. There exists great variation in the magnitude, duration and rate of energy release of all earthquakes; this uncertainty translates directly into the random nature of ground-level displacements a structure subjected to an earthquake. Determining the demands is further complicated by the uncertainties existing in the structure's response characteristics, i.e. the masses, stiffnesses and damping of platform components. Finally, the modal response spectrum load calculation procedure will introduce additional uncertainty by virtue of its lack of addressing the phasing of the individual modal responses.

To perform structural risk analyses of a platform, it is necessary to characterize the limit states of the structure and the uncertainties associated with them. In this research, the ultimate limit state of the structure at collapse is considered (as opposed to serviceability limit state). With the exception of foundation capacities, the uncertainties associated with the ultimate static capacity of structural components are small compared to loading related uncertainties. In some case studies, the platform capacity is assumed to be a deterministic value (Bea and Smith, 1987; Haver, 1995). This capacity is estimated by performing nonlinear structural analyses (e.g. pushover analyses) using mean values or best estimates for capacity parameters. The probability of failure is estimated as the likelihood that the random load exceeds the deterministic capacity. In a general case, however, the uncertainties associated with platform component capacities need to be considered. This is particularly true, when a foundation failure mode is a potential collapse mechanism. The large uncertainties associated with foundation axial and lateral capacities are primarily due to the inherent variability of ocean floor soils, soil sampling and testing procedures, the complexity of marine sub-sea construction, and modeling of pile-soil and loading interaction (Bea, 1990).

Considering a platform as a series of structural components, its structural reliability can be evaluated by using the formulations given earlier. The series components are the superstructure (deck), each bay of the substructure (jacket), and the foundation. The capacity of the platform is reached when the capacity of any one of these components is reached. Within each component there are parallel elements; deck legs, braces, joints, and piles. In order for a component to reach its upper-bound capacity, all of the parallel elements have to fail.

Using a first-order Taylor-series approximation around the mean point, the required means and standard deviations of loads and capacities can be computed. By specifying the means of input variables, the mean lateral load acting on components and the mean component capacities are estimated. Simplified loading and capacity equations have been developed in the previous appendices. Some of these equations are used in this section and are repeated for the sake of completeness.

Storm Loading Formulation:
A combination of storm wind load and hydrodynamic wave and current loads is considered:

$$S = S_w + S_h$$

The wind load is given by:

$$S = K_w V_{wd}^2$$

where K_w is a structure dependent loading parameter, and V_{wd} is the wind speed that occurs at the same time as the maximum wave height.

The total integrated hydrodynamic drag force acting on a surface piercing vertical cylinder can be expressed as:

$$S_h = K_d K_u H^2$$

K_u is an integration function that integrates the velocities along the cylinder and is a function of wave steepness and the wave theory used to estimate the velocities. K_d is a force coefficient and a function of mass density of water ρ, diameter of the cylinder D, and drag coefficient C_d. The mean forces acting on the elements are integrated and the shear force at each component level is calculated. These integrated shear forces define the means of the load variables S_D for deck, S_{Ji} for each jacket bay, and the base shear S_F for the foundation bay. The coefficient of variation of the wave load is given as:

$$V_S = \sqrt{V_{Kd}^2 + V_{Ku}^2 + \left(2V_H\right)^2}$$

The dominating storm loading parameters are the maximum wave height and its associated period. An evaluation of the uncertainties in the wind forces does not play a major role and is not included.

Earthquake Load Formulation:

The mode-specific load demand calculated on a MDOF structure from a response spectrum is:

$$\mathbf{f}_n = \mathbf{s}_n A_n$$

where:

$\mathbf{s}_n = \Gamma_n \mathbf{m} \phi_n$ = distribution of modal inertia forces

with:

$\Gamma_n = L_n^h / M_n$ = modal participation factor

$L_n^h = \sum_{j=1}^{N} m_j \phi_{jn}$

$M_n = \sum_{j=1}^{N} m_j \phi_{jn}^2$ = generalized mass

$A_n = \omega_n^2 D_n$ = pseudo-acceleration; mA is equal to the peak value of the elastic resisting force for a SDOF system

and:

n = mode index
j = DOF index

Ordinates from a response spectrum, $D_n(T)$, typically have uncertainties in the range of 40% to 80% (Bazzurro, Cornell, 1994). Furthermore, many spectra are selected with a bias of +1 or +2 standard deviations from the mean. The selection of the ordinate is driven by the modal period T and modal damping ratio ξ. T is dependent upon the mass and stiffness properties of the platform. While the mass and stiffness of the steel structure and equipment are likely to have low uncertainties, there is possibly great uncertainty associated with the added mass appropriate to the analysis, and great uncertainty associated with the stiffness properties of the foundation. Added mass is related to the frequency of vibration of the structure through the water. The stiffness at the foundation level may exhibit softening with increasing load amplitude, while at the same time an increase in the modal damping ratio ξ may become evident as local plastification of the soil beneath the platform and around the pile tops occurs. For platforms with ungrouted jackets, additional damping will result with increasing levels of excitation at the jacket legs and piles begin to slide against one another, dissipating energy through friction. Variability in the stiffnesses and masses will also have an impact on the mode shapes of the platform, which in turn will change the loads determined for components. Finally, the uncertainty in the true phase between modal responses will further complicate the force determination procedure.

In lieu of a more rigorous evaluation, it will be assumed that the uncertainties affecting the earthquake loads calculated from responses spectrum analysis are controlled by the uncertainty in the spectral ordinate associated with the first mode in each principal direction. Therefore, the uncertainty in the total demands from the response spectrum analysis will be taken as:

$$V_{Total\_Response} = V_{D\_1st\_Mode}$$

Capacity Formulations:

Deck Bay Shear Capacity:
A mechanism in the deck leg bay would form when plastic hinges are developed at the top and bottom of all of the deck legs. Using this failure mode as a virtual displacement, virtual work principle can be utilized to estimate the deck leg shear resistance R_d (Appendix B):

$$R_d = \frac{1}{H_d}\left(2nM_u - Q\Delta\right)$$

where:

$$\Delta = M_u H_d\left(\frac{H_d}{6EI_d} + \frac{1}{C_r}\right)$$

$$M_u = M_{cr}\cos\left(\frac{\pi Q/n}{2P_{crl}}\right)$$

The moment capacity of the legs M_{cr} and the local buckling capacity P_{crl} are treated as random variables. Assuming perfect correlation between M_{cr} and P_{crl}, the variance of deck legs capacity can be given as:

$$\sigma_{Rd}^2 = \sigma_{Mcr}^2\left(\frac{\partial R_d}{\partial M_{cr}}\right)^2 + \sigma_{Pcrl}^2\left(\frac{\partial R_d}{\partial M_{crl}}\right)^2 + 2\sigma_{Mcr}\sigma_{Pcrl}\left(\frac{\partial R_d}{\partial M_{cr}}\right)\left(\frac{\partial R_d}{\partial M_{crl}}\right)$$

where:

$$\frac{\partial R_d}{\partial M_{cr}}, \frac{\partial R_d}{\partial P_{crl}}$$

are the partial derivatives of the deck legs shear capacity R_d with respect to critical moment and buckling capacities M_{cr} and P_{crl}, evaluated at the mean values μ_{Mcr} and μ_{Pcrl}.

Jacket Bay Shear Capacity:

Shear capacity in a given jacket bay is assumed to be reached when the vertical diagonal braces or their joints are no longer capable of resisting the lateral load acting on the jacket bay. Tensile and compressive capacity of the diagonal braces, the associated joint capacities, and the batter component of axial forces in the legs due to overturning moment are included to estimate the jacket bay shear capacity. The capacity of a given brace is taken as the minimum of the capacity of the brace or the capacity of either its joints.

It should be noted that the diagonal brace capacities are negatively correlated with the lateral loading. To implicitly account for this correlation, the strength equation is rewritten in the following format:

$$P_u = \frac{M_u}{8\Delta_0\left(\frac{1}{1+2\frac{\sin 0.5\varepsilon}{\sin\varepsilon}}\right)\frac{l}{\varepsilon^2}\left(\frac{1}{\cos\frac{\varepsilon}{2}}-1\right)} - \left(\frac{wl^2}{8\Delta_0}\right)$$

Thus the variance of the compression capacity of a brace can be given by:

$$\sigma_{Pu}^2 = \sigma_{Pcr}^2 + \left(\frac{l^2}{8\Delta_0}\right)^2\sigma_w^2$$

where it is assumed that Δ_0 is a deterministic parameter and that the first term in the strength equation equals the buckling load of the brace in the absence of lateral distributed load w:

$$P_{cr} = \frac{M_u}{8\Delta_0 \left(\frac{1}{1+2\frac{\sin 0.5\varepsilon}{\sin \varepsilon}} \right) \frac{1}{\varepsilon^2} \left(\frac{1}{\cos \frac{\varepsilon}{2}} - 1 \right)}$$

Joints are not considered in the reliability formulation.

To estimate the lateral capacity of a given jacket bay, it is assumed that interconnecting horizontal brace elements are rigid. Thus, the lower-bound capacity of the n^{th} jacket bay R_{Jn}, which is associated with the first member failure in that bay, can be given as (Appendix B):

$$R_{Jn} = \sum_i \alpha_n K_i + F_L$$

where F_L is the sum of batter components of axial pile and leg forces in the given bay and:

$$\alpha_n = \frac{P_{u,MLTF} \cos \theta_{MLTF}}{K_{MLTF}}$$

is the lateral drift of the n^{th} jacket bay at the onset of first member failure. K_i are deterministic factors accounting for geometry and relative member stiffness ($\alpha_i K_i$ = horizontal shear force of brace element i at the onset of first brace or joint failure within the given bay). Assuming that there is no correlation between the capacity of the MLTF member and lateral shear in the jacket legs, the variance of the lower-bound capacity of the n^{th} jacket bay can be given as:

$$\sigma_{RJn}^2 = \left(\sum_i K_i \right)^2 \sigma_\alpha^2 + B_{FL}^2 \sigma_{FL}^2$$

where:

$$\sigma_\alpha = \frac{\sigma_{Pu,MLTF}}{K_{MLTF}}$$

B_{FL} denotes the bias associated with the batter component of axial leg forces F_L.

The upper-bound capacity of the n^{th} jacket bay R_{Jn}, which is associated with failure of all main load carrying members in that bay, can be given as (Appendix B):

$$R_{Jn} = \sum_i \alpha_i R_i + F_L$$

where R_i is the horizontal component of resisting force of the joint-brace element i. α_i account for the post-yielding behavior of semi-brittle brace or joint elements ($\alpha_i R_i$ = residual strength of element i) and are assumed to have deterministic values. Assuming perfect correlation among the member capacities R_i and R_j within the given bay, the variance of the upper-bound capacity of the n^{th} jacket bay can be given as:

$$\sigma_{RJn}^2 = \sum_{i,j} \alpha_i \alpha_j \sigma_{Ri} \sigma_{Rj} + \left(B_{FL} \sigma_{FL}\right)^2$$

Foundation Capacity:

Two basic types of failure mode in the foundation are considered: lateral and axial. The lateral failure mode of the piles is similar to that of the deck legs. In addition to moment resistance of the piles, the lateral support provided by foundation soils and the batter shear component of the piles are considered. The lateral and axial capacity equations for piles in sand and clay are given in Appendix G. These formulations are used to calculate the best estimate capacities. Considering the uncertainties in soil and pile material properties, the uncertainties associated with foundation capacities can also be estimated. However, due to lack of data regarding modeling uncertainties, the total uncertainties associated with axial and lateral pile capacities are used in this research, which implicitly include the uncertainties associated with soil and pile parameters and capacity modeling. The uncertainty associated with the batter component of the pile force is added to the total capacity uncertainty for vertically driven piles.

Load tests and recent post-hurricane Andrew studies on marine foundations (PMB, 1995) have indicated that the traditional foundation capacity prediction procedures are conservatively biased (Appendix G). Major sources of bias are found to be the dynamic nature of loadings and soil sampling and testing.

Bea (1987) found the following to be two of the important influences of dynamic loadings on offshore pile foundations: (1) decrease in the capacity and stiffness due to cyclic loading and (2) increase in the capacity and stiffness due to high rates of loading. Another source of bias in the foundation capacities is the quality of soil samples. Soil sample disturbance is unavoidable. Some of the sources of sample disturbance are drilling, sampling, significant pressure relief, packaging, transport and preparation for testing (Bea, 1987). Laboratory testing is also a source of bias in soil strength parameters.

H.6 EXAMPLE APPLICATION

Using the formulations developed in the previous sections, the structural reliability of an offshore platform is determined. Located in the main pass area of the Gulf of Mexico, the 8-leg template-type platform is installed in a water depth of approximately 271 feet (Figure H-3). Designed and installed in 1968-70, the platform is exposed to high environmental loading developed by hurricanes passing through the Gulf. Because of its dominance, only wave force is considered. According to oceanographic studies performed for the site, the 100 year return period wave height, H_{100}, is 70 feet. The uncertainties associated with the expected annual maximum wave height predictions are assumed and given in Table H-1. Considering these uncertainties result in a total bias of B_H = 1.1 and a coefficient of variation of V_H = 0.34. Assuming Lognormal and Type I Extreme Value distributions, the probabilistic characteristics of

the expected annual maximum wave height are given in Table H-2. The wave height distribution parameters were determined by fitting the tails of the distributions to the predicted extreme wave heights. The variabilities of the force coefficients given by Bea (1990) were used to estimate the uncertainties associated with the wave forces (Table H-3). These estimates are consistent with the simplified analytical models employed to calculate the loadings.

It should be noted that once the wave crest elevation exceeds the platform lower deck elevation, the load pattern changes significantly and the total forces acting on the platform increase much faster than before. In the presented example, this fact has not been accounted for. In general, the problem can be circumvented by considering conditional probabilities ($p_f|H$). In this case, the total probability of failure can be estimated by:

$$p_f = \int_h p_f\Big|_H f_H(h)dh$$

Based on the background developed in the previous sections of this chapter, structural reliability of the example platform is studied for the two principal orthogonal directions. For each load direction, eight different failure modes are identified and analyzed; one in the superstructure, five in the substructure, and two foundation failure modes.

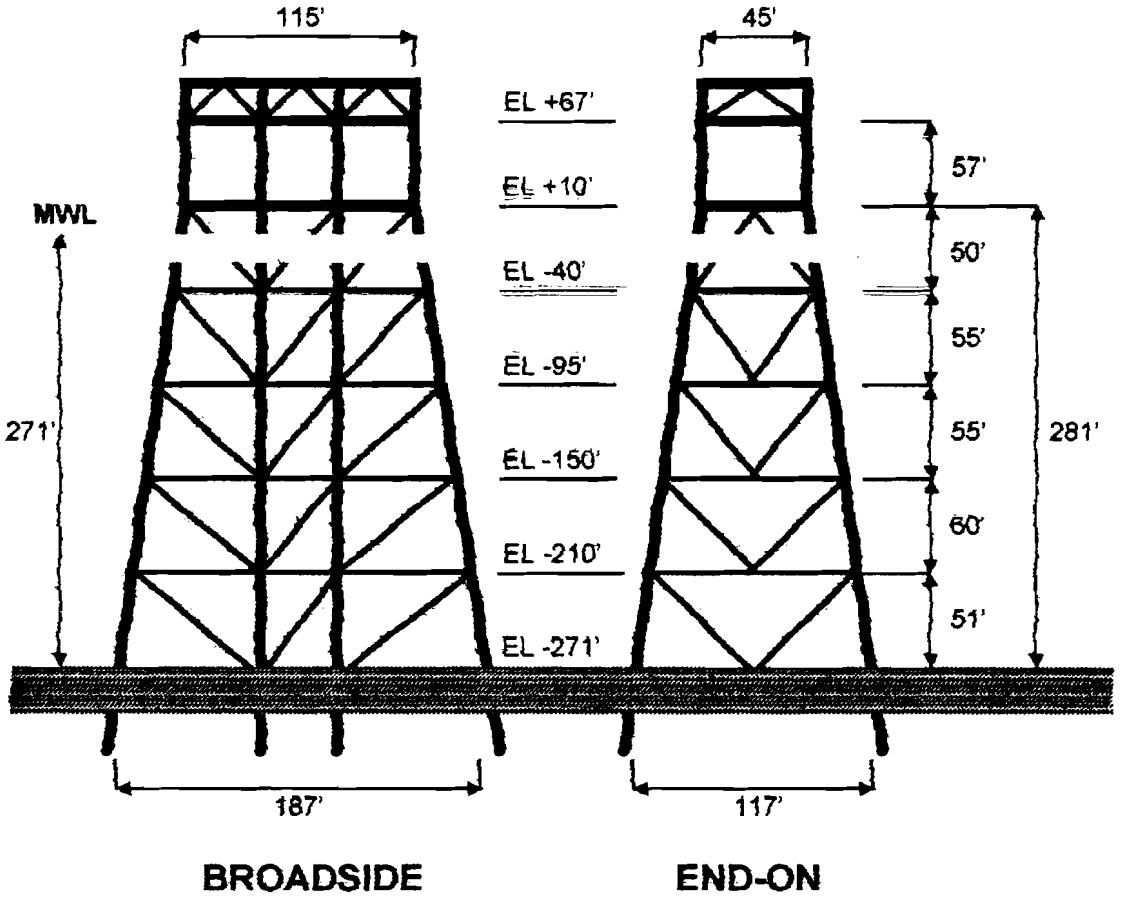

Figure H-3: Example Platform Elevations

Table H-1: Wave Height Uncertainties (Example Platform)

	σ_{lnH}	Bias (B_H)	σ_{lnBH}
H_{max}	0.3	1.1	0.13

Table H-2: Probabilistic Characteristics of the Maximum Wave Height (Example Platform)

$f_H(h)$	μ_H (ft)	σ_H (ft)
Lognormal	34.5	11.7
Type I largest	34.0	11.4

Table H-3: Force Coefficient Uncertainties (Bea, 1990)

	σ_{lnK}	Bias (B_K)	σ_{lnBk}
K_u	0.1	0.41	0.47
K_d	0.1	1.67	0.23

For critical bending moment M_{cr}, local buckling capacity P_{crl}, and global buckling capacity of diagonal braces P_{cr}, the mean-value curves given by Cox (1987) are utilized. These are:

$$M_{cr} = M_p\left[1.113\exp\left(\frac{-1.638 f_y D}{Et}\right)\right]$$

$$P_{crl} = P_y\left[1.79 - 0.25\left(\frac{D}{t}\right)^{0.25}\right]$$

$$P_{cr} = P_y\left(1.03 - 0.24\lambda^2\right) \text{ for } 0 < \lambda < 1.7$$

where:

$$M_p = Zf_y$$

$$P_y = Af_y$$

$$\lambda = \left(\frac{KL}{\pi r}\right)\sqrt{\frac{f_y}{E}}$$

where Z, λ, and K are the plastic section modulus of the cross-section, slenderness ratio of the member, and buckling length factor respectively. For bending resistance, a combined coefficient of variation (COV) of 0.106 is given by Cox (1987). The COV for local buckling is 0.117, which includes the test uncertainties, uncertainties in steel yield strength, and uncertainties associated with fabrication. This value is reported to be constant over the entire range of practical values of Et/fyD and D/t respectively. The uncertainties of column resistance over a practical range of λ are given in Table H-4 (Cox, 1987). In addition to uncertainties associated with test and

fabrication, the uncertainties associated with yield stress f_y, elastic modulus E, and effective column length factor K are included in the column resistance uncertainty.

Table H-4: Column Resistance Uncertainties (Cox, 1987)

λ	0.4	0.6	0.8	1.0	1.2	1.4
COV	0.099	0.100	0.106	0.119	0.150	0.212

A tubular joint failure mode is not included in the presented reliability analysis since the leg-pile annulus and the joints are grouted and the joints are significantly stronger than the braces. In a general case, the joints' capacity and the uncertainties associated with it can be considered.

In the presented example, the upper-bound capacity formulation is used for the jacket bays. Deterministic values are assigned to brace residual strength factors α, which are calibrated to give results consistent with those gained from a detailed nonlinear pushover analysis of the studied platform (Bea , et al. 1995a,b,c). In a general case however, the α factor is unknown and can be considered as a random variable itself. The uncertainty associated with this variable reflects the modeling uncertainty introduced by using simplifying assumptions regarding residual strength of compression braces and stiffness properties of inter-connecting horizontal braces.

Table H-5: Lateral Pile Capacity Uncertainties (Tang, 1990)

Lateral Capacity in:	Bias	COV
Clay	0.92	0.20
Sand	0.81	0.21

Table H-6: Axial Pile Capacity Uncertainties (Tang, 1988)

Axial Pile Capacity in:	Bias	COV
Sand	0.9	0.47 - 0.56
Clay	1.3 - 3.7	0.32 - 0.53

Due to lack of data regarding the pile capacity modeling uncertainty, the total uncertainties recommended by Tang and Gilbert (1990) are used, which are based on test results and implicitly include the model uncertainties (Table H-5). The uncertainty associated with the batter component of the pile force is added to the total capacity uncertainty given for vertical piles. Available test data on axially loaded piles indicate a very wide range in capacity bias. The uncertainties associated with axial capacities of driven piles are given by Tang (1988) (Table H-6). Current studies of the performance characteristics of platforms subjected to storm loadings indicates that the mean biases in lateral and axial pile capacities indicated in Tables H-5 and H-6 represent a lower bound (mean biases in the range of 2 to 3) (Bea et al. 1995b; 1995c).

To study the effect on FOSM results of different probability distributions of maximum wave height and nonlinear limit state functions, the computer program CALREL (Liu et. al., 1989) was used to perform FORM and SORM analyses in addition to FOSM analysis. In the case of lognormally distributed loads and capacities, the results from the simplified FOSM analysis and those from more sophisticated FORM and SORM are given in Tables H-7 and H-8 and Figures H-3 and H-4. FORM and SORM analyses have also been performed assuming Type I Extreme Value distribution for annual maximum wave height. No significant changes in the reliability

indices are observed. The FOSM safety indices are close approximations to those determined from the FORM and SORM analyses.

The results indicate that the most probable failure mode in both loading cases involves the failure of the diagonals in the second jacket bay. The large uncertainties in storm loadings are due to uncertainties in force calculations and those associated with predicted wave heights. The large uncertainties in jacket bay capacities are mainly due to uncertainties associated with the lateral loading and the load-capacity correlation which is implicitly accounted for in this analysis.

The uncertainties in lateral capacity of jacket bays are larger for the broadside loading direction than the end-on loading direction. This can be explained by the fact that for the broadside loading case, compressive buckling of diagonal K-braces govern the failure of the jacket, whereas in the case of end-on loading, tensile yielding of diagonal braces govern the ultimate lateral loading capacity of the jacket. The compressive buckling of the braces is associated with much larger uncertainties than the tensile yielding. The foundation piles have safety indices that are comparable with those in the superstructure.

Table H-7: Component Reliabilities Based on FOSM, FORM and SORM Analyses, Broadside Loading (Example Platform)

BROADSIDE LOADING	LOAD (KIPS)	BIAS	C.O.V.	CAP (KIPS)	BIAS	C.O.V.	FOSM β	FOSM Pf	FORM β	SORM β
DECK LEGS	197	0.83	1.03	2606	1.00	0.11	3.84	1.34E-04	3.51	3.51
JACKET										
BAY1	544	0.83	1.03	2632	1.00	0.06	2.61	4.52E-03	2.46	2.46
BAY2	521	0.83	1.03	2621	1.00	0.24	2.22	1.32E-02	2.08	2.12
BAY3	638	0.83	1.03	4130	1.00	0.45	2.41	8.07E-03	2.41	2.47
BAY4	641	0.83	1.03	5702	1.00	0.49	2.67	3.85E-03	2.75	2.80
BAY5	643	0.83	1.03	6157	1.00	0.48	2.75	2.94E-03	2.84	2.90
FOUNDATION										
LATERAL	643	0.83	1.03	7700	0.81	0.56	2.69	3.58E-03	2.67	2.67
AXIAL	1035	0.83	1.03	4063	1.5	0.31	2.52	5.79E-03	2.49	2.49

Table H-8: Component Reliabilities Based on FOSM, FORM and SORM Analyses, End-on Loading (Example Platform)

END-ON LOADING	LOAD (KIPS)	BIAS	C.O.V.	CAP (KIPS)	BIAS	C.O.V.	FOSM β	FOSM Pf	FORM β	SORM β
DECK LEGS	120	0.83	1.03	2606	1.00	0.11	4.22	1.20E-05	4.10	4.10
JACKET										
BAY1	424	0.83	1.03	1954	1.00	0.07	2.43	7.51E-03	2.29	2.29
BAY2	498	0.83	1.03	2046	1.00	0.10	2.26	1.13E-02	2.12	2.14
BAY3	515	0.83	1.03	2380	1.00	0.15	2.39	8.54E-03	2.25	2.28
BAY4	518	0.83	1.03	2538	1.00	0.20	2.43	7.62E-03	2.28	2.32
BAY5	520	0.83	1.03	2892	1.00	0.26	2.51	6.02E-03	2.38	2.43
FOUNDATION										
LATERAL	520	0.83	1.03	7200	0.81	0.53	2.88	1.96E-03	2.85	2.85
AXIAL	856	0.83	1.03	4063	1.5	0.31	2.74	3.12E-03	2.70	2.70

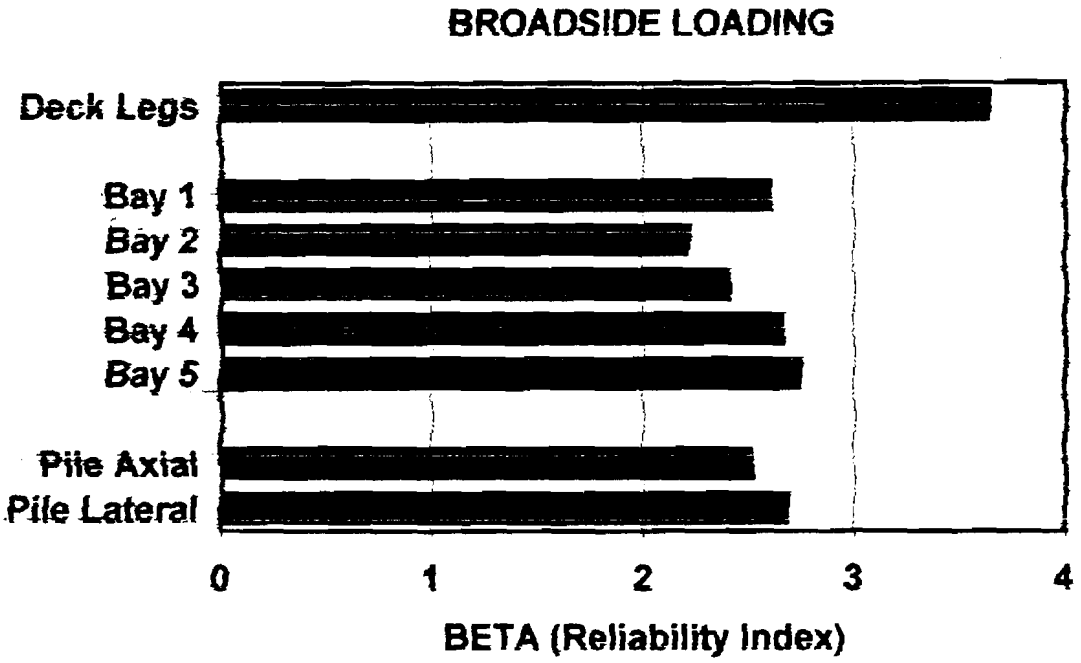

Figure H-4: Annual Component Safety Indices for Broadside Loading (Example Platform)

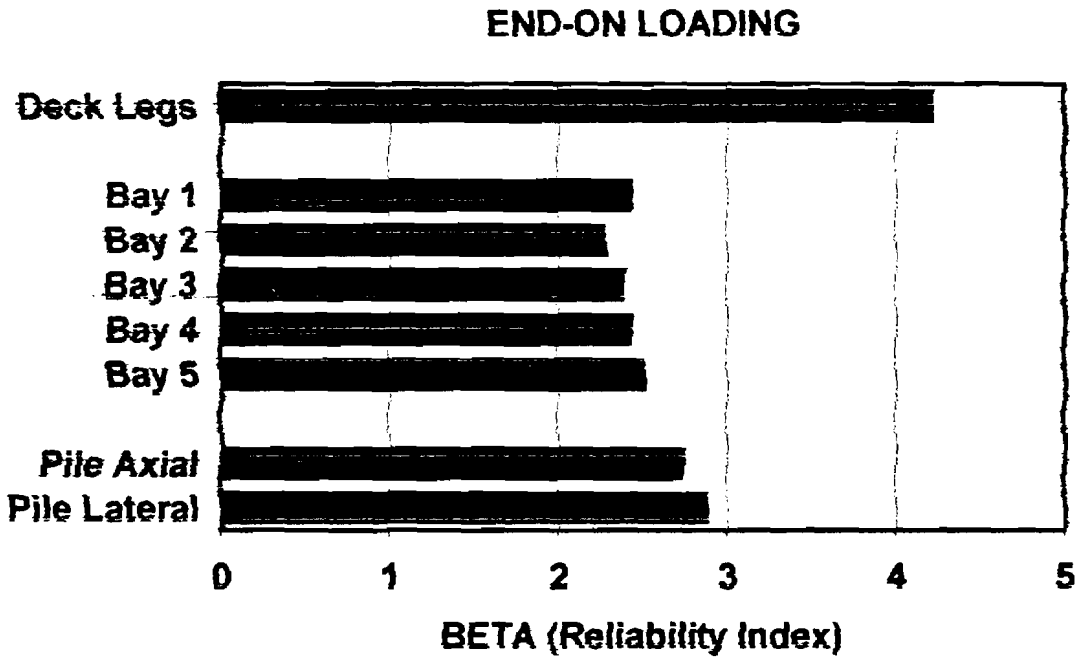

Figure H-5: Annual Component Safety Indices for End-on Loading (Example Platform)

Based on the FOSM results, unimodal bounds on annual probabilities of failure are estimated for both loading directions and given in Table H-9. The failure probabilities range from about 1% per year to 4% per year depending on the assumptions regarding correlation of the failure modes. Given the large loading uncertainties relative to those of the component capacities, one would expect the correlation of the failure modes to be nearly unity (Nordal et al. 1988). Thus, the most realistic failure probability would be represented by the lower-bound results.

Table H-9: Unimodal Bounds on annual p_f (Example Platform)

Loading	Lower-Bound p_{f_L}	Upper-Bound p_{f_U}
End-on	0.011	0.046
Broadside	*0.013*	*0.042*

H.7 REFERENCES

American Petroleum Institute (API), "Recommended Practice for Planning, Designing and Constructing Fixed Offshore Platforms - Working Stress Design (RP 2A-WSD)," 20th Edition, Washington, D.C., July 1993a.

American Petroleum Institute (API), "Recommended Practice for Planning, Designing and Constructing Fixed Offshore Platforms - Load and Resistance Factor Design (RP 2A-LRFD)," First Edition, Washington, D.C., July 1993b.

American Petroleum Institute (API), "API RP 2A-WSD 20th Edition, Draft Section 17.0, Assessment of Existing Platforms," Houston, TX, November 1994.

Bazzurro, P., and Cornell, C. A., "Seismic Hazard Analysis of Nonlinear Structures I: Methodology," *Journal of Structural Engineering*, ASCE, Vol. 120, No. 11, November 1994.

Bea, R.G., Pawsey, S.F., Litton, R.W., "Measured and Predicted Wave Forces on Offshore Platforms," OTC No. 5787, *Proceedings of the Offshore Technology Conference*, Houston, TX, 1986.

Bea, R.G., Smith, C.S., "AIM (Assessment, Inspection, Maintenance) and Reliability of Offshore Platforms," Marine Structural Reliability Symposium, Virginia. pp57-75, 1987.

Bea R.G., "Dynamic Response of Marine Foundations." *Proceedings of the Ocean Structural Dynamics Symposium '84*, Oregon State University, Corvallis, OR, September 1987.

Bea R.G., "Reliability Based Design Criteria for Coastal and Ocean Structures." The Institution of Engineers, Australia, 11 National Circuit, Barton, ACT, Australia, 1990.

Bea, R.G., Young, C., "Loading and Capacity Effects on Platform Performance in Extreme Condition Storm Waves & Earthquakes," OTC No. 7140, *Proceedings of the Offshore Technology Conference*, Houston, TX, 1993.

Bea, R.G., Loch, K., Young, P., "Evaluation of Capacities of Template-Type Gulf of Mexico Platforms," *Proceedings of the 5th International Offshore and Polar Engineering Conference*, ISOPE-95, The Hague, The Netherlands, June 11-16, 1995b.

Bea, R.G., Mortazavi, M., Loch, K., Young, P., "Verification of A Simplified Method to Evaluate the Capacities of Template-Type Platforms," OTC 7780, *Proceedings of the Offshore Technology Conference*, Houston TX, May 1995c.

Bea, R.G., Mortazavi, M., Loch, K., Young, P., "Verification of A Second Generation Simplified Method to Evaluate the Storm Loadings on and Capacities of Steel Template-Type Platforms," Proceedings, Energy and Environmental Expo 95, American Society of Mechanical Engineers, Houston, Texas, January 1995d.

Cox, J.W., "Tubular Member Strength Equations for LRFD," Final Report API PRAC Project 86-55., 1987.

Der Kiureghian, A., "Structural Reliability." Lecture Notes, Department of Civil Engineering, University of California, Berkeley, 1994.

Haring, R.E., Spencer, L.P., "The Ocean Test Structure Data Base." Proceedings, Civil Engineering in the Oceans IV, Vol. II, ASCE, New York, pp 669-683, September 1979.

Haver, S., "Uncertainties in Force and Response Estimates," E&P Forum, The Oil Industry International Exploration & Production Forum, Offshore Structures/Metocean Workshop, E&P Forum Report No. 3.15/229, 1995.

Heideman, J.C., Weaver, T.O., "Static Wave Force Procedure for Platform Design," *Proceedings of Civil Engineering in the Oceans V*, College Station, Texas, American Society of Civil Engineers, New York, NY, 1992.

Liu, P.L., Lin, H.Z., Der Kiureghian, A., "CALREL User Manual." Report No.UCB/SEMM-89/18, Dept. of Civil Engineering, University of California at Berkeley, 1989.

Loch, K.J., Bea, R.G., "Determination of the Ultimate Limit States of Fixed Steel-Frame Offshore Platforms Using static Pushover Analyses." Report to U.S. Minerals Management Service and Joint Industry Project Sponsors, Marine Technology Development Group, University of California at Berkeley, May 1995.

Nordal, H., Cornell, C.A., Karamchandani, A., "A System Reliability Case Study of an Eight-leg Jacket Platform," Report No. RMS-3, Department of Civil Engineering, Stanford University, 1988.

Petrauskas, C., Botelho, D.L.R., Krieger, W.F., and Griffin, J.J., "A Reliability Model for Offshore Platforms and its Application to ST 151 H and K Platforms During Hurricane Andrew (1992)," *Proceedings of the Behavior of Offshore Structure Systems*, BOSS '94, Massachusetts Institute of Technology, 1994.

PMB Engineering Inc., "Further Evaluation of Offshore Structures Performance in Hurricane Andrew - Development of Bias Factors for Pile Foundation Capacity," Report to American Petroleum Institute and Minerals Management Service, San Francisco, CA., December 1995.

Tang, W.H. and Gilbert R.B., "Offshore Lateral Pile Design Reliability." Research Report for Project PRAC 87-29 sponsored by the American Petroleum Institute, 1990.

Tang, W.H., "Offshore Axial Pile Design Reliability", Research Report for Phase 1 of the Project PRAC 86-29B sponsored by the American Petroleum Institute, 1988.

Thoft-Christensen, P., Baker, J., "Structural Reliability Theory and Its Applications," Springer-Verlag, 1982.

Tromans, P. S., and van de Graaf, J. W., "A substantiated Risk Assessment of a Jacket Structure," OTC 7075, *Proceedings of the Offshore Technology Conference*, May 1992.

APPENDIX T:
SAMPLE OUTPUT FROM TOPCAT FOR THE SOUTHERN CALIFORNIA EXAMPLE PLATFORM

by
James D. Stear and Professor Robert G. Bea

TABLE OF CONTENTS

GLOBAL PARAMETERS OF PLATFORM

Southern California Example Platform

Session Name Southern California Example Platform

Platform Type	4-leg Jacket
Number of Decks	1
Number of Jacket Bays	2
Water Depth (ft)	100

SPECIAL CHARACTERISTICS

Bracing in Deck Bay

PLATFORM GEOMETRY

Broadside Frames Top Width (ft)	60
Broadside Frames Base Width (ft)	60
End-On Frames Top Width (ft)	60
End-On Frames Base Width (ft)	60

STRUCTURAL LAYOUT

	Height (ft)	Diagonals BS Frames	Diagonals EO Frames	Horizontals Bay Floor	Corner Legs D (in)	Corner Legs t (in)	Appurt. Sum D (ft)	Marine Growth (in)
Deck Bay	30	4	4	4	72	1		
Jacket Bay 1	60	4	4	4	79	1.125	4.25	
Jacket Bay 2	60	4	4	4	78	0.875	4.25	

PLATFORM DECKS

	Bottom Elev. (ft)	Top Elev. (ft)	Broadside Width (ft)	End-On Width (ft)	Weight (kips)
Deck 1	40	65	100	100	5000

BOAT-LANDINGS

General Structure Data:

Projected Area, End-On (ft^2)
Projected Area, Broadside (ft^2)
Total Weight (Kips)

CONDUCTORS

Total Number
D (in)
Penetration (ft)
Fixity Above Mudline (ft)
Weight (kips / ft) 0
Plastic Moment (kip-ft)
Moment of Inertia (ft^4)
Group Strength Reduction (%)
Group Stiffness Reduction (%)

PLATFORM TONNAGE ESTIMATE

Deck Section	5000 kips
Jacket	854 kips
Piles	820 kips
TOTAL	6674 kips

GLOBAL MATERIAL PARAMETERS

Steel Yield Stress (ksi)	36
Elastic Modulus (ksi)	29000
Brace Effective Length Factor, k	0.5
Brace Post-Buckling Strength Factor	0.3

BIASES AND UNCERTAINTIES

Structural:

	Bias	COV

Main Diagonal Strength	1	0.3
Tubular Joint Strength	1	0.3
Pile Axial Capacity	1	0.4
Pile Lateral Capacity	1	0.4
Pile Axial Stiffness	3	0.4
Pile Lateral Stiffness	1	0.4

Load:

	Bias	COV
Wave-in-Deck Force	1	0.4
Wave Force on Jacket	1	0.4
Earthquake Spectral Acceleration	1	0.8

LOCAL PARAMETERS
End-On Main Diagonals

Southern California Example Platform

Jacket Bay 1 Brace #	D (in)	t (in)	Bay Position	Load Type	Bracing Pattern	Joint i Type #	Joint j Type #	Condition	Dent Depth (in)	Out-of-Straight (in)	Pu (kips)
1	24	0.5	center	comp.	X	3	2	intact	0	0	1289
2	24	0.5	center	comp.	X	3	2	intact	0	0	1289
3	24	0.5	center	tens.	X	3	2	intact	0	0	1328
4	24	0.5	center	tens.	X	3	2	intact	0	0	1328

Jacket Bay 2 Brace #	D (in)	t (in)	Bay Position	Load Type	Bracing Pattern	Joint i Type #	Joint j Type #	Condition	Dent Depth (in)	Out-of-Straight (in)	Pu (kips)
1	30	0.625	center	comp.	X	4	5	intact	0	0	2036
2	30	0.625	center	comp.	X	4	5	intact	0	0	2036
3	30	0.625	center	tens.	X	4	5	intact	0	0	2075
4	30	0.625	center	tens.	X	4	5	intact	0	0	2075

Deck Bay Brace #	D (in)	t (in)	Bay Position	Load Type	Bracing Pattern	Joint i Type #	Joint j Type #	Condition	Dent Depth (in)	Out-of-Straight (in)	Pu (kips)
1	36	0.75	center	comp.	K (A)	1		intact	0	0	2949
2	36	0.75	center	comp.	K (A)	1		intact	0	0	2949
3	36	0.75	center	tens.	K (A)	1		intact	0	0	2988
4	36	0.75	center	tens.	K (A)	1		intact	0	0	2988

LOCAL PARAMETERS
Broadside Main Diagonals

Southern California Example Platform

Jacket Bay 1 Brace #	D (in)	t (in)	Bay Position	Load Type	Bracing Pattern	Joint i Type #	Joint j Type #	Condition	Dent Depth (in)	Out-of-Straight (in)	Pu (kips)
1	24	0.5	center	comp.	X	3	2	intact	0	0	1289
2	24	0.5	center	comp.	X	3	2	intact	0	0	1289
3	24	0.5	center	tens.	X	3	2	intact	0	0	1328
4	24	0.5	center	tens.	X	3	2	intact	0	0	1328

Jacket Bay 2 Brace #	D (in)	t (in)	Bay Position	Load Type	Bracing Pattern	Joint i Type #	Joint j Type #	Condition	Dent Depth (in)	Out-of-Straight (in)	Pu (kips)
1	30	0.625	center	comp.	X	4	5	intact	0	0	2036
2	30	0.625	center	comp.	X	4	5	intact	0	0	2036
3	30	0.625	center	tens.	X	4	5	intact	0	0	2075
4	30	0.625	center	tens.	X	4	5	intact	0	0	2075

Deck Bay Brace #	D (in)	t (in)	Bay Position	Load Type	Bracing Pattern	Joint i Type #	Joint j Type #	Condition	Dent Depth (in)	Out-of-Straight (in)	Pu (kips)
1	36	0.75	center	comp.	K (A)	1		intact	0	0	2949
2	36	0.75	center	comp.	K (A)	1		intact	0	0	2949
3	36	0.75	center	tens.	K (A)	1		intact	0	0	2988
4	36	0.75	center	tens.	K (A)	1		intact	0	0	2988

LOCAL PARAMETERS
Tubular Joints

Southern California Example Platform

Joint #	Type	Grouted?	Chord D (in)	Chord t (in)	Branch D (in)	Gap in K (in)	Angle (degrees)	+Pu (kips)	-Pu (kips)
1	K	no	80	1.875	36	18	45	2140	2140
2	K	no	80	1.875	24	18	45	2263	2263
3	X	no	24	0.5	24	0	90	202	266
4	K	no	80	1.875	30	18	45	2617	2617
5	X	no	30	0.625	30	0	90	315	415
6	Y	no	80	1.875	30	0	45	2617	2617

LOCAL PARAMETERS
Horizontal Braces

Southern California Example Platform

Horizontal Frame 1

Brace #	D (in)	t (in)	L (ft)	Angle w/BS
1	18	0.375	60	90
2	18	0.375	60	90
3	18	0.375	60	0
4	18	0.375	60	0

Horizontal Frame 2

Brace #	D (in)	t (in)	L (ft)	Angle w/BS
1	18	0.375	60	90
2	18	0.375	60	90
3	18	0.375	60	0
4	18	0.375	60	0

Horizontal Frame 3

Brace #	D (in)	t (in)	L (ft)	Angle w/BS
1	18	0.375	60	90
2	18	0.375	60	90
3	18	0.375	60	0
4	18	0.375	60	0

FOUNDATION

Southern California Example Platfon

SOIL PROPERTIES

Number of Soil Layers: 1

Layer 1: Clay

Undrained Shear Strength, Mudline (kip / ft^2)	2.5
Undrained Shear Strength, Pile Tips (kip / ft^2)	4.5
Submerged Unit Weight of Soil (lbs / ft^3)	50

Scour Depth (ft) 0

PILES

Main Piles: Corner

D (in)	72	Lateral Capacity (kips)	1793
t (in)	1	Axial Capacity, Tension (kips)	5262
L (ft)	150	Axial Capacity, Compression (kips)	5652
Plugged?	yes	Lateral Pilehead Stiffness (kips / in)	137
		Axial Pilehead Stiffness (kips / in)	10781

NOTE: Pile Self-Weight Has Been Deducted From Axial Capacities

Mud Mats and Mudline Braces

Contact Areas (ft^2)

Mudline Braces (total area)	361
Corner Mud Mats (each mat)	

	Bearing	Sliding
Strength Factor		

Stiffness Factor

Contact Surface Loads (kip / ft^2)

Max Bearing	0
Max Sliding	0

Storm and Fatigue Analysis Parameters

SURGE, WIND, WAVE AND CURRENT		Southern California Example Platfon
Surge / Tide Level (ft)	6	
Wind Velocity, 30 ft Elevation (mph)	58	
Wave Height (ft)	45	Wave Kinematic Theory Used: Stokes
Wave Period (sec)	11	
Current Velocity, SWL (fps)	3.4	
Current Velocity, Mudline (fps)		
Current Velocity Profile	Constant	
LOAD FACTORS AND FORCE COEFFICIENTS		
Global Load Factor	1	
Water Kinematics:		
Current Blockage, Cb	0.8	
Directional Spreading, wkf	1	
Hydrodynamic Drag Coefficients, Cd:		
All Members and Appurtenances	1.05	
Deck 1	2.5	
Wind Speed Coefficients, Cs:		
Deck 1	1	

T10

Southern California Example Platform

WATER KINEMATICS

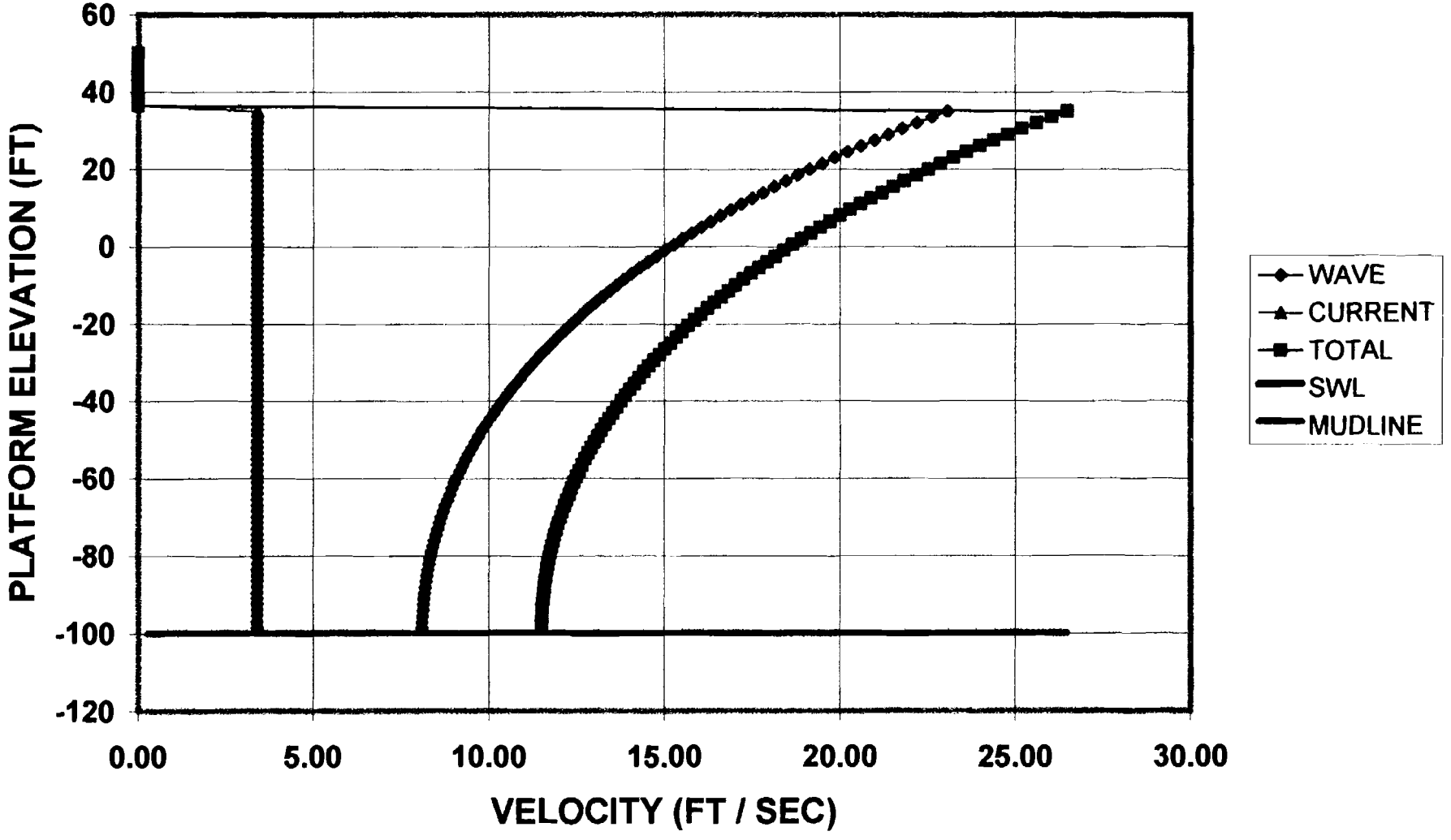

ANALYSIS TYPE: storm

Southern California Example Platfon

SHEARS AND SHEAR CAPACITIES

	End-On Demand / Capacity					Broadside Demand / Capacity				
	Shear Demand (kips)	LO-Bound Capacity (kips)	HI-Bound Capacity (kips)	TJ-Bound Capacity (kips)	Batter Forces (kips)	Shear Demand (kips)	LO-Bound Capacity (kips)	HI-Bound Capacity (kips)	TJ-Bound Capacity (kips)	Batter Forces (kips)
Deck Bay	572	8320	5474	6052	0	572	8320	5474	6052	0
Jacket Bay 1	1422	3514	2406	570	0	1422	3514	2406	570	0
Jacket Bay 2	1819	5703	3790	891	0	1819	5703	3790	891	0
Foundation	1819	7170	7170		0	1819	7170	7170		0

BASE-LEVEL FORCES

End-On

Base Shear (kips)	1819
Overturning Moment (kip-ft)	165023

Broadside

Base Shear (kips)	1819
Overturning Moment (kip-ft)	165023
Vertical Force (kips)	0

GLOBAL FOUNDATION CAPACITIES

Horizontal (EO) (kips)	7170
Horizontal (BS) (kips)	7170
Vertical (+) (kips)	21049
Vertical (-) (kips)	22606

Moment (EO) (kip-ft)	654833
Moment (BS) (kip-ft)	654833

APPROXIMATE PEAK PILE LOADS

End-On

Lateral (kips)	455
Vertical, Tension (kips)	125
Vertical, Compression (kips)	2625

Broadside

Lateral (kips)	455
Vertical, Tension (kips)	125
Vertical, Compression (kips)	2625

SAFETY INDICES

	End-On	Broadside
Deck Bay	6.77	6.77
Jacket Bay 1	1.93	1.93
Jacket Bay 2	2.42	2.42
Foundation Lateral	2.52	2.52
Pile Compression	1.41	1.41
Pile Tension	6.86	6.86

Southern California Example Platform

END-ON LOADING: STORM

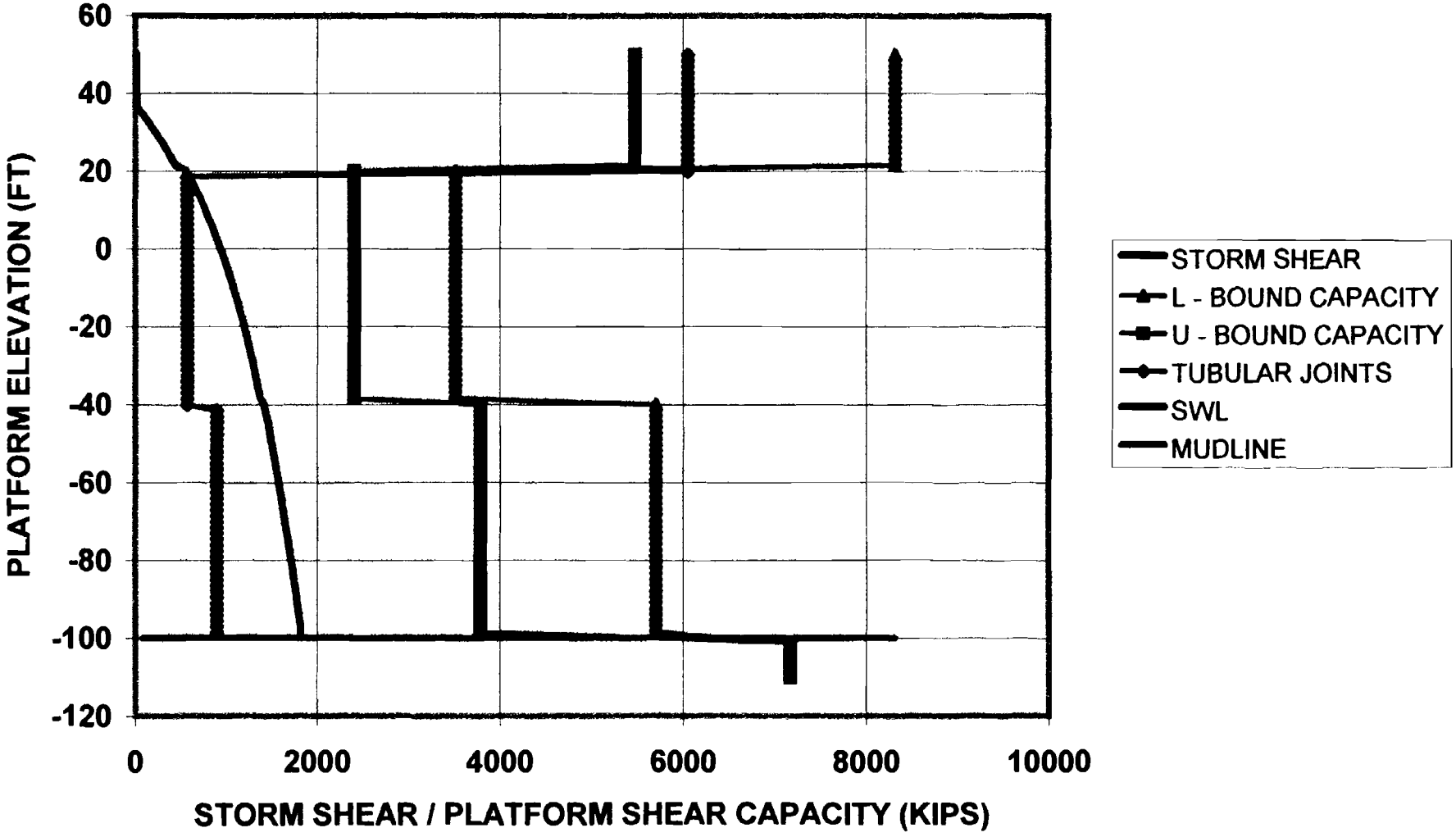

T14

Southern California Example Platform

BROADSIDE LOADING: STORM

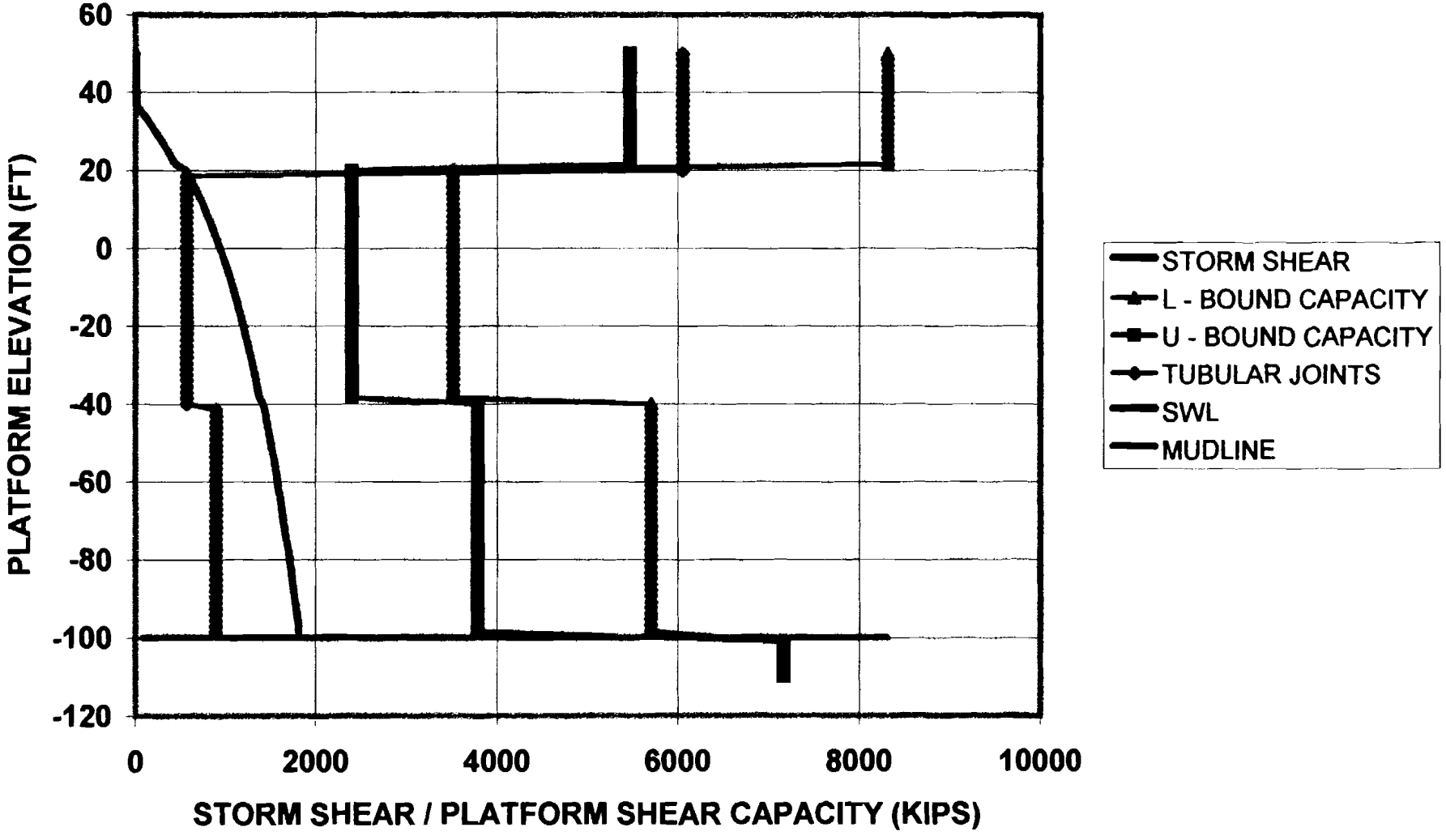

Southern California Example Platform

AXIAL UTILIZATION OF CRITICAL PILE

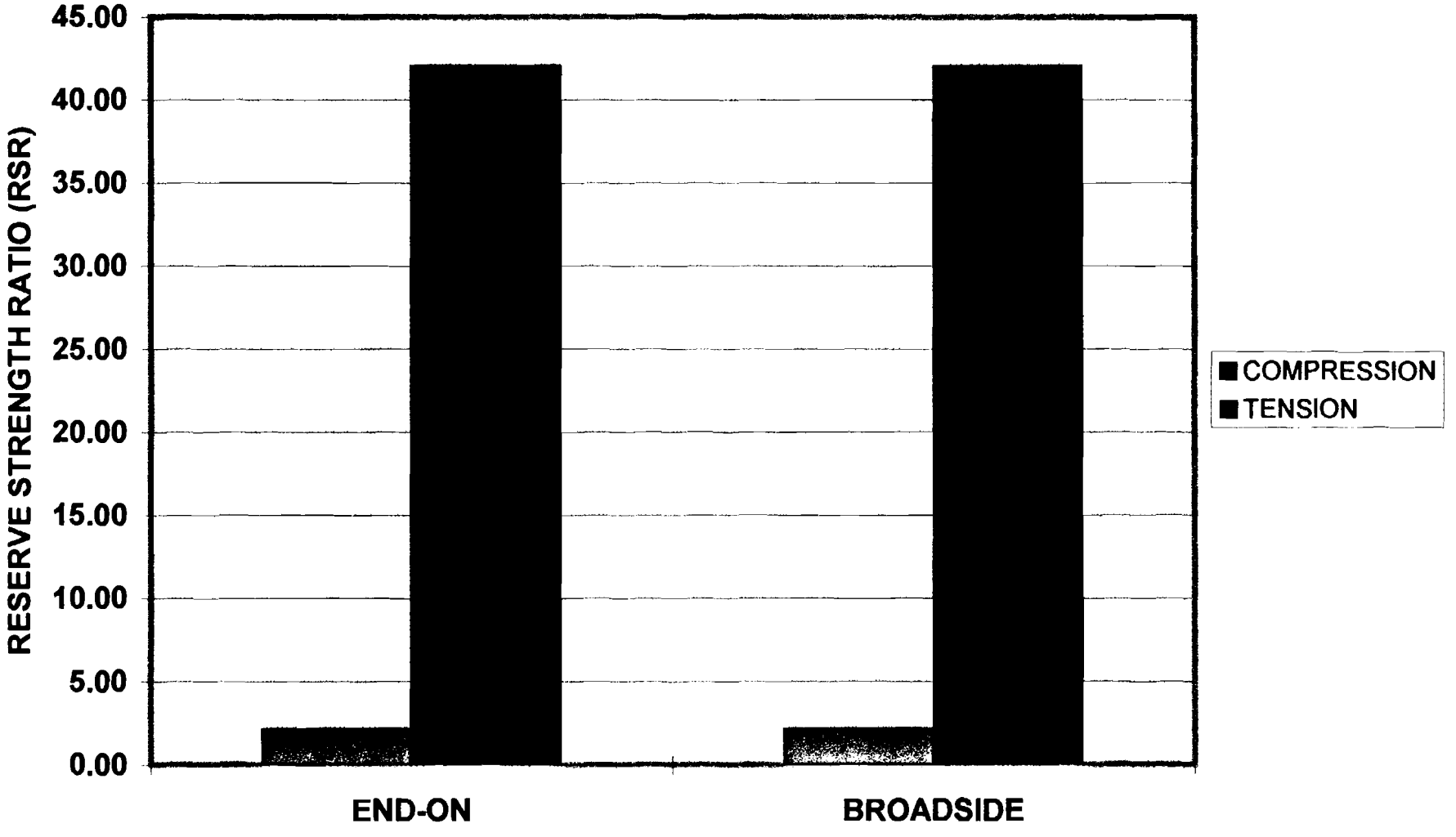

END-ON LOADING: STORM

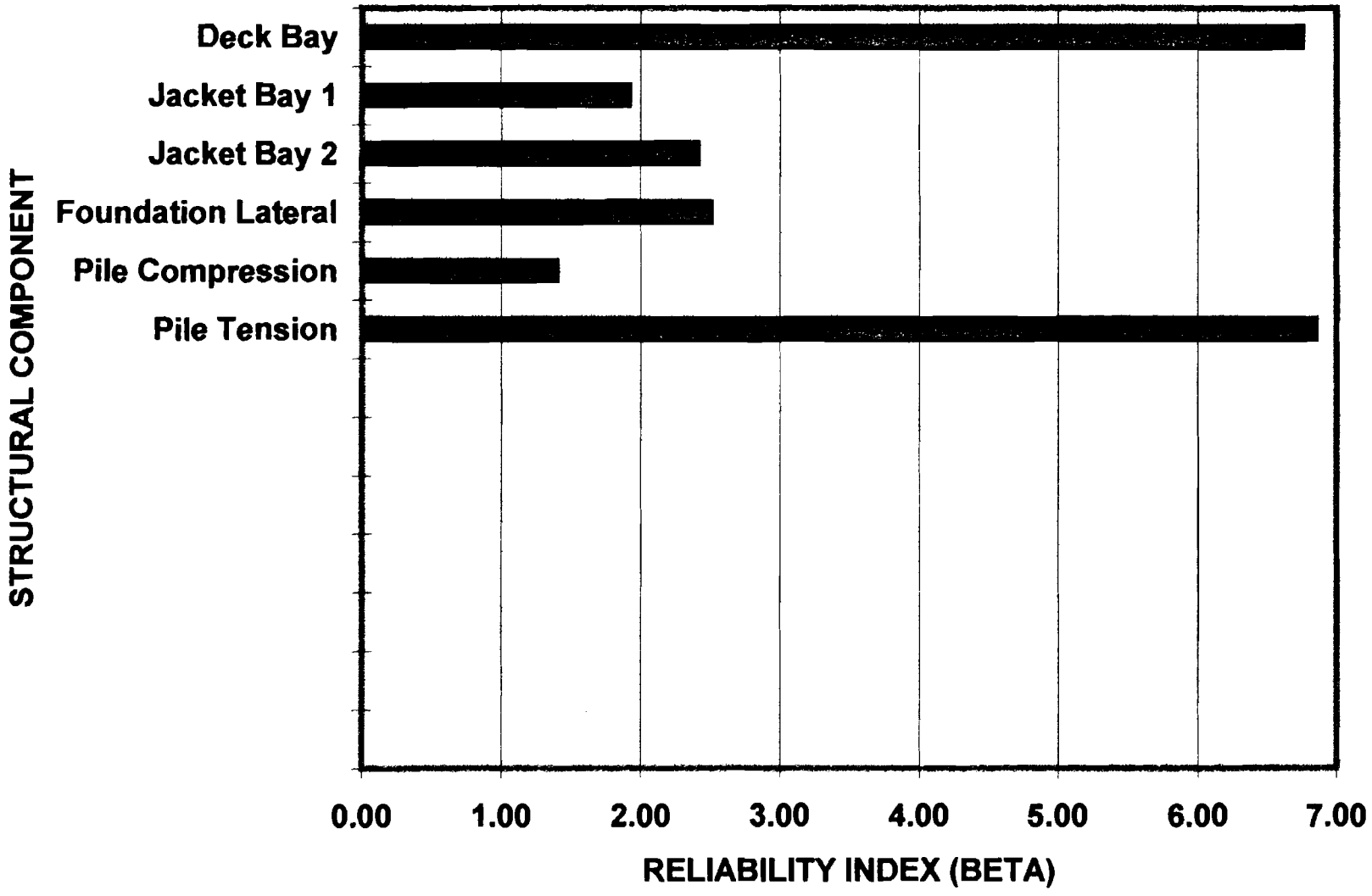

BROADSIDE LOADING: STORM

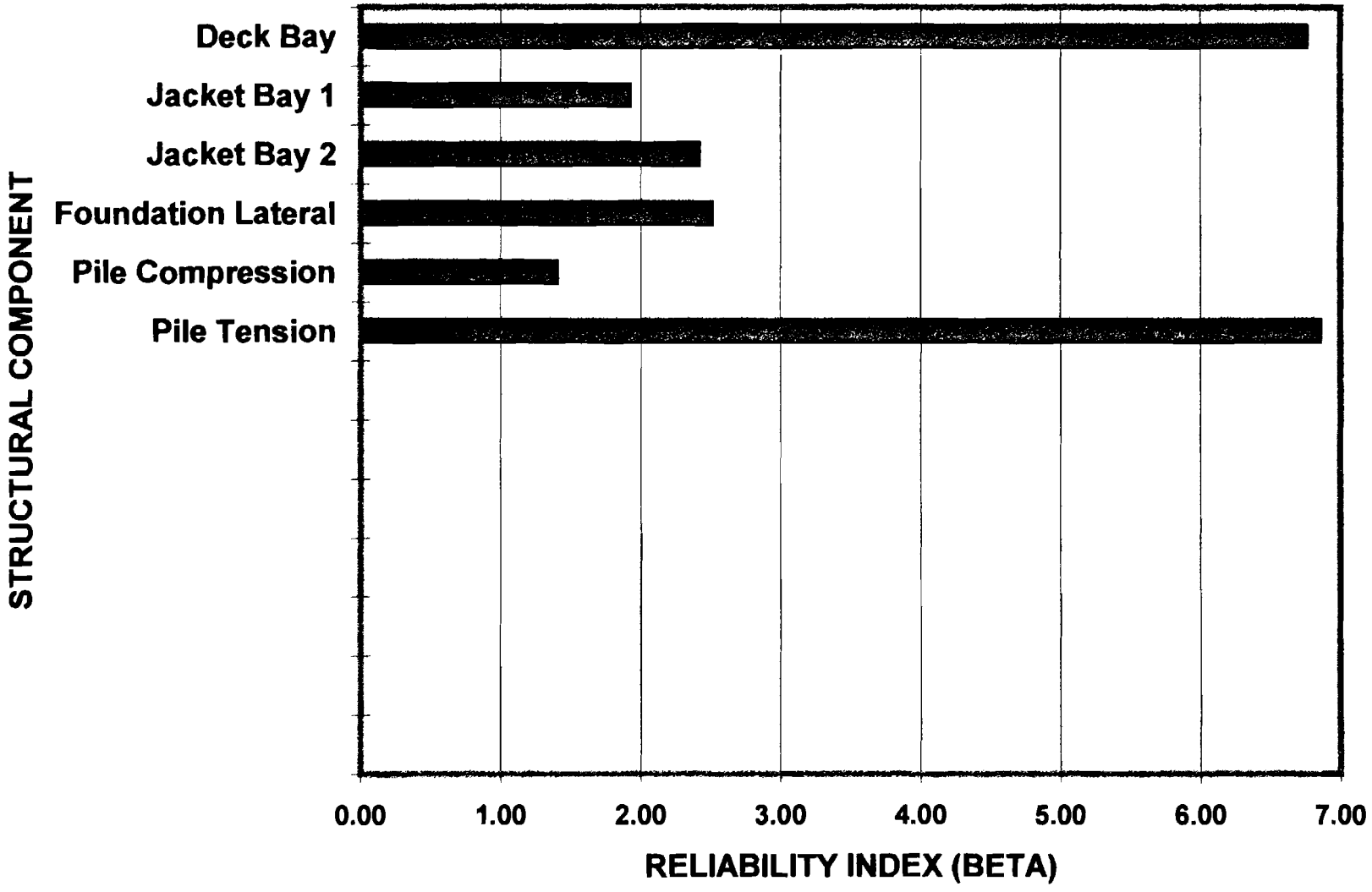

SURGE, WIND, WAVE AND CURRENT

Surge / Tide Level (ft)	6
Wind Velocity, 30 ft Elevation (mph)	58
Wave Height (ft)	45
Wave Period (sec)	11
Current Velocity, SWL (fps)	3.4
Current Velocity, Mudline (fps)	
Current Velocity Profile	Constant

Wave Kinematic Theory Used: Stokes

LOAD FACTORS AND FORCE COEFFICIENTS

Global Load Factor	1
Water Kinematics:	
Current Blockage, Cb	0.8
Directional Spreading, wkf	1
Hydrodynamic Drag Coefficients, Cd:	
All Members and Appurtenances	1.05
Deck 1	2.5
Wind Speed Coefficients, Cs:	
Deck 1	1

FATIGUE ASSESSMENT PARAMETERS

S-N K	1.79E+09
S-N m	3.74
Global-Local g	1.3
Global-Local R	-0.5
Exposure Period (years)	30

T19

Storm and Fatigue Analysis Parameters

Operational Component of Spectrum:	
H0 (ft)	20
Eta0	1
N0 (cycles)	1E+09
Storm Component of Spectrum:	
H1 (ft)	45
Eta1	1
N1 (cycles)	1000000
Spectrum Period (years)	100

T20

FATIGUE DAMAGE RATING AND EXPECTED LIFE
Broadside Tubular Joints

Jacket Bay 1

Brace #	Joint i Type	Joint i Damage	Joint j Type	Joint j Damage	Life (years)
1	3	32.2439	2	0.0011	1
2	3	32.2439	2	0.0011	1
3	3	32.2439	2	0.0011	1
4	3	32.2439	2	0.0011	1

Jacket Bay 2

Brace #	Joint i Type	Joint i Damage	Joint j Type	Joint j Damage	Life (years)
1	4	0.0123	5	0.0005	2441
2	4	0.0123	5	0.0005	2441
3	4	0.0123	5	0.0005	2441
4	4	0.0123	5	0.0005	2441

Deck Bay

Brace #	Joint i Type	Joint i Damage	Joint j Type	Joint j Damage	Life (years)
1	1	0.0001		0	361450
2	1	0.0001		0	361450
3	1	0.0001		0	361450
4	1	0.0001		0	361450

FATIGUE DAMAGE RATING AND EXPECTED LIFE
End-On Tubular Joints

Jacket Bay 1

Brace #	Joint i Type	Joint i Damage	Joint j Type	Joint j Damage	Life (years)
1	3	32.2439	2	0.0011	1
2	3	32.2439	2	0.0011	1
3	3	32.2439	2	0.0011	1
4	3	32.2439	2	0.0011	1

Jacket Bay 2

Brace #	Joint i Type	Joint i Damage	Joint j Type	Joint j Damage	Life (years)
1	4	0.0123	5	0.0005	2441
2	4	0.0123	5	0.0005	2441
3	4	0.0123	5	0.0005	2441
4	4	0.0123	5	0.0005	2441

Deck Bay

Brace #	Joint i Type	Joint i Damage	Joint j Type	Joint j Damage	Life (years)
1	1	0.0001		0	361450
2	1	0.0001		0	361450
3	1	0.0001		0	361450
4	1	0.0001		0	361450

FATIGUE LIFE: END-ON FRAMES

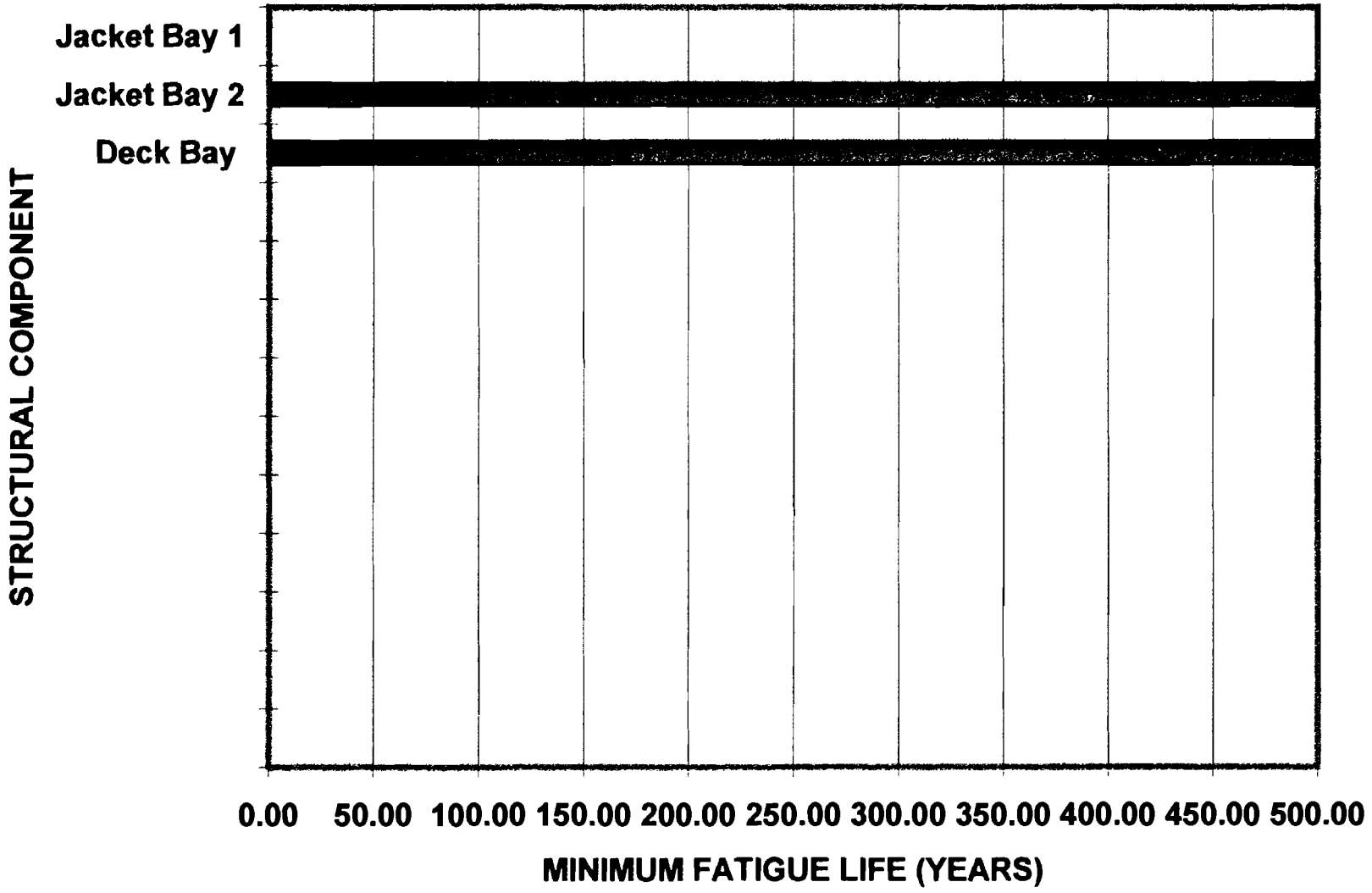

FATIGUE LIFE: BROADSIDE FRAMES

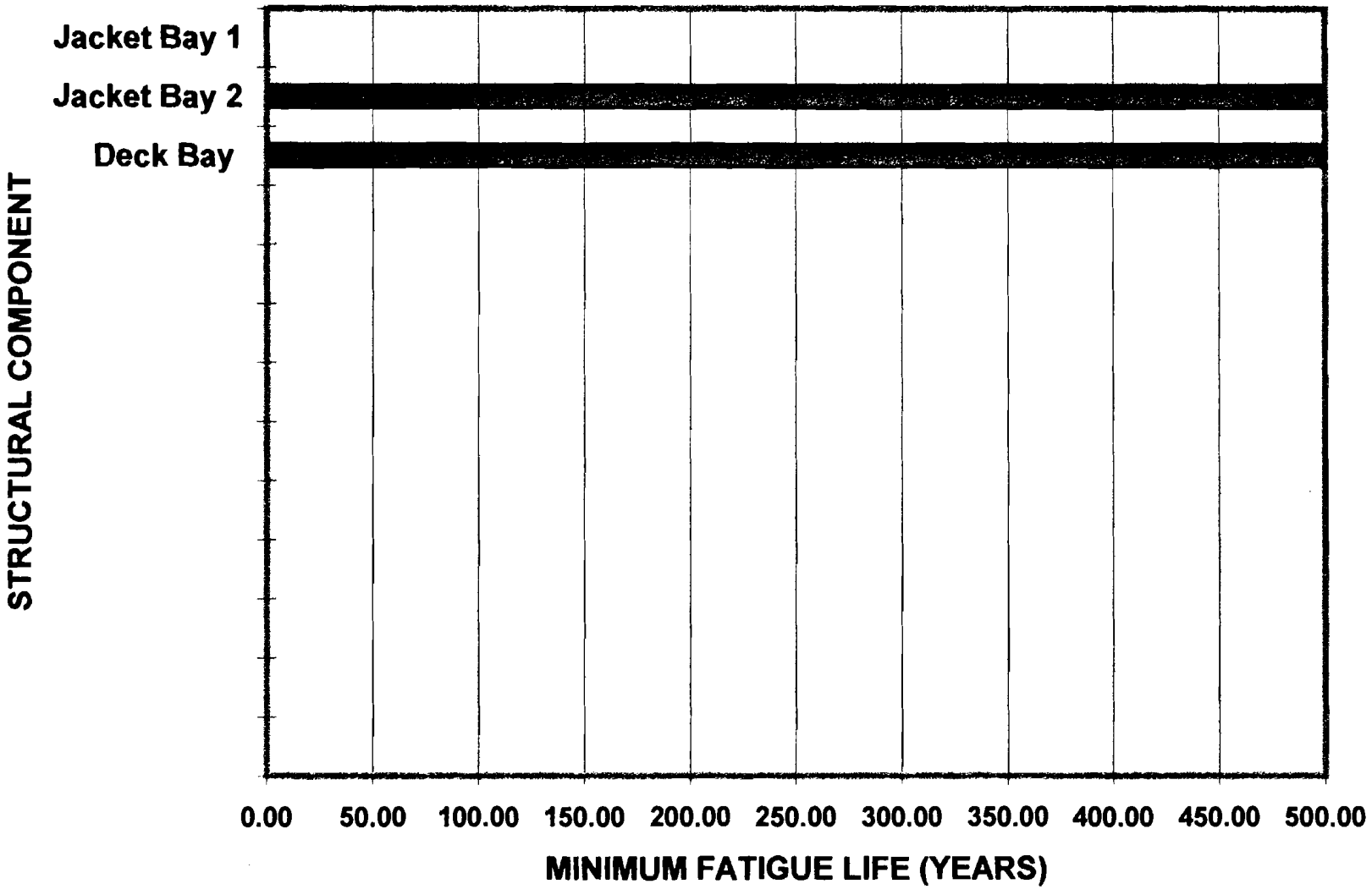

PERIODS AND MODE SHAPES

Southern California Example Platf

	Broadside Response			End-On Response		
Mode:	1	2	3	1	2	3
Modal Period (sec):	1.53	0.17	0.08	1.53	0.17	0.08
Modal Participation Factor:	1.07	-0.6	0.03	1.07	-0.6	0.03
Modal Height (ft):	139	6	476	139	6	476
Modal Mass x g (kips):	6982	556	1	6982	556	1
Deck Level	1	0.121	0.142	1	0.121	0.142
Horizontal Frame 1	0.898	-0.115	-1	0.898	-0.115	-1
Horizontal Frame 2	0.369	-1	0.133	0.369	-1	0.133
Horizontal Frame 3	0	0	0	0	0	0

Vertical Response

1
0.14

Horizontal Masses x g (kips)

BS	EO
5191	5191
900	900
1448	1448
1169	1169

Vertical Mass x g (kips):
7879

DECK-LEVEL SPECTRAL ACCELERATIONS FOR EQUIPMENT

Fundamental Period of Equipment (sec): 0

BS Acceleration (g): 0.4
EO Acceleration (g): 0.4
Z Acceleration (g): 0.63

RESPONSE SPECTRUM ANALYSIS PARAMETERS

Spectrum ZPA (g) 0.5
Soil Type B
Modal Combination Rule SRSS

Hydrodynamic Added Mass Coefficient, Cm 1

T25

Southern California Example Platform

End-On Mode Shapes

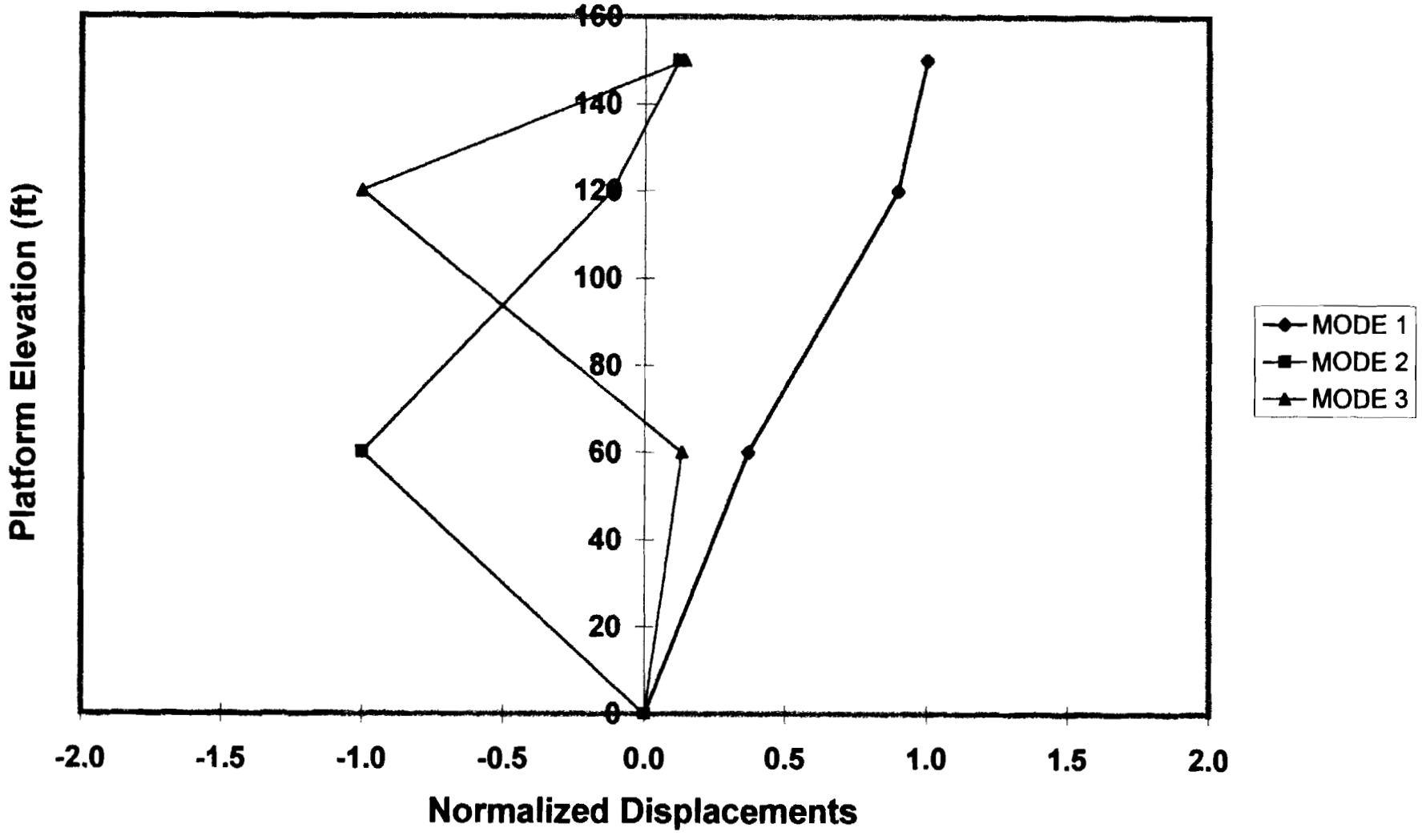

T26

Southern California Example Platform

Broadside Mode Shapes

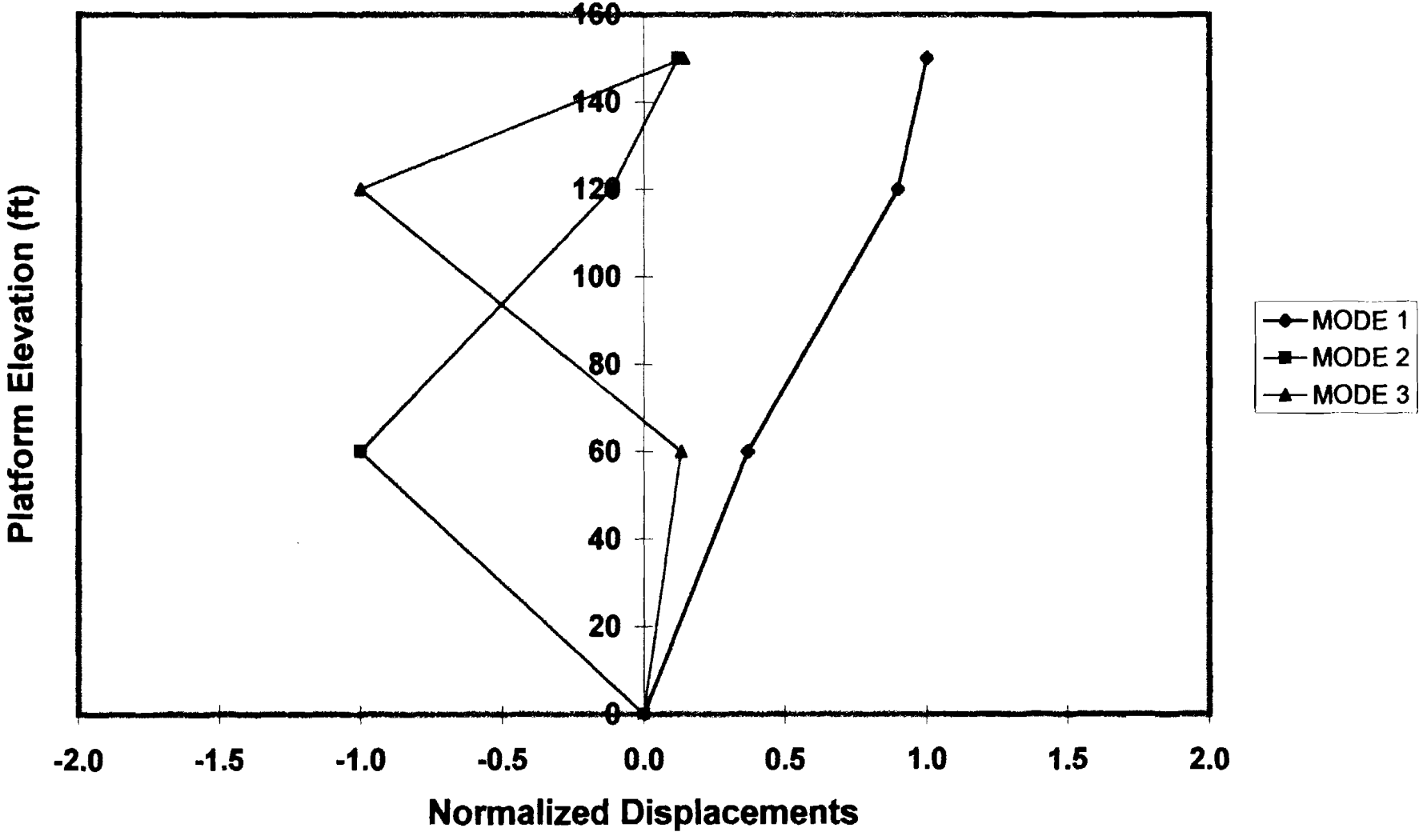

727

ANALYSIS TYPE: quake

Southern California Example Platfor

SHEARS AND SHEAR CAPACITIES

	End-On Demand / Capacity					Broadside Demand / Capacity				
	Shear Demand (kips)	LO-Bound Capacity (kips)	HI-Bound Capacity (kips)	TJ-Bound Capacity (kips)	Batter Forces (kips)	Shear Demand (kips)	LO-Bound Capacity (kips)	HI-Bound Capacity (kips)	TJ-Bound Capacity (kips)	Batter Forces (kips)
Deck Bay	2224	8122	5445	6052	0	2224	8122	5445	6052	0
Jacket Bay 1	2542	3484	2401	570	0	2542	3484	2401	570	0
Jacket Bay 2	2822	5569	3770	891	0	2822	5569	3770	891	0
Foundation	3178	7170	7170		0	3178	7170	7170		0

BASE-LEVEL FORCES

End-On

Base Shear (kips)	3178
Overturning Moment (kip-ft)	379963

Broadside

Base Shear (kips)	3178
Overturning Moment (kip-ft)	379963
Vertical Force (kips)	4924

GLOBAL FOUNDATION CAPACITIES

Horizontal (EO) (kips)	7170
Horizontal (BS) (kips)	7170
Vertical (+) (kips)	21049
Vertical (-) (kips)	22606

Moment (EO) (kip-ft)	654833
Moment (BS) (kip-ft)	654833

APPROXIMATE PEAK PILE LOADS

End-On

Lateral (kips)	794
Vertical, Tension (kips)	3147
Vertical, Compression (kips)	5647

Broadside

Lateral (kips)	794
Vertical, Tension (kips)	3147
Vertical, Compression (kips)	5647

SAFETY INDICES

	End-On	Broadside
Deck Bay	2.15	2.15
Jacket Bay 1	0.68	0.68
Jacket Bay 2	1.16	1.16
Foundation Lateral	1.23	1.23
Pile Compression	0.22	0.22
Pile Tension	0.86	0.86

Southern California Example Platform

END-ON LOADING: EARTHQUAKE

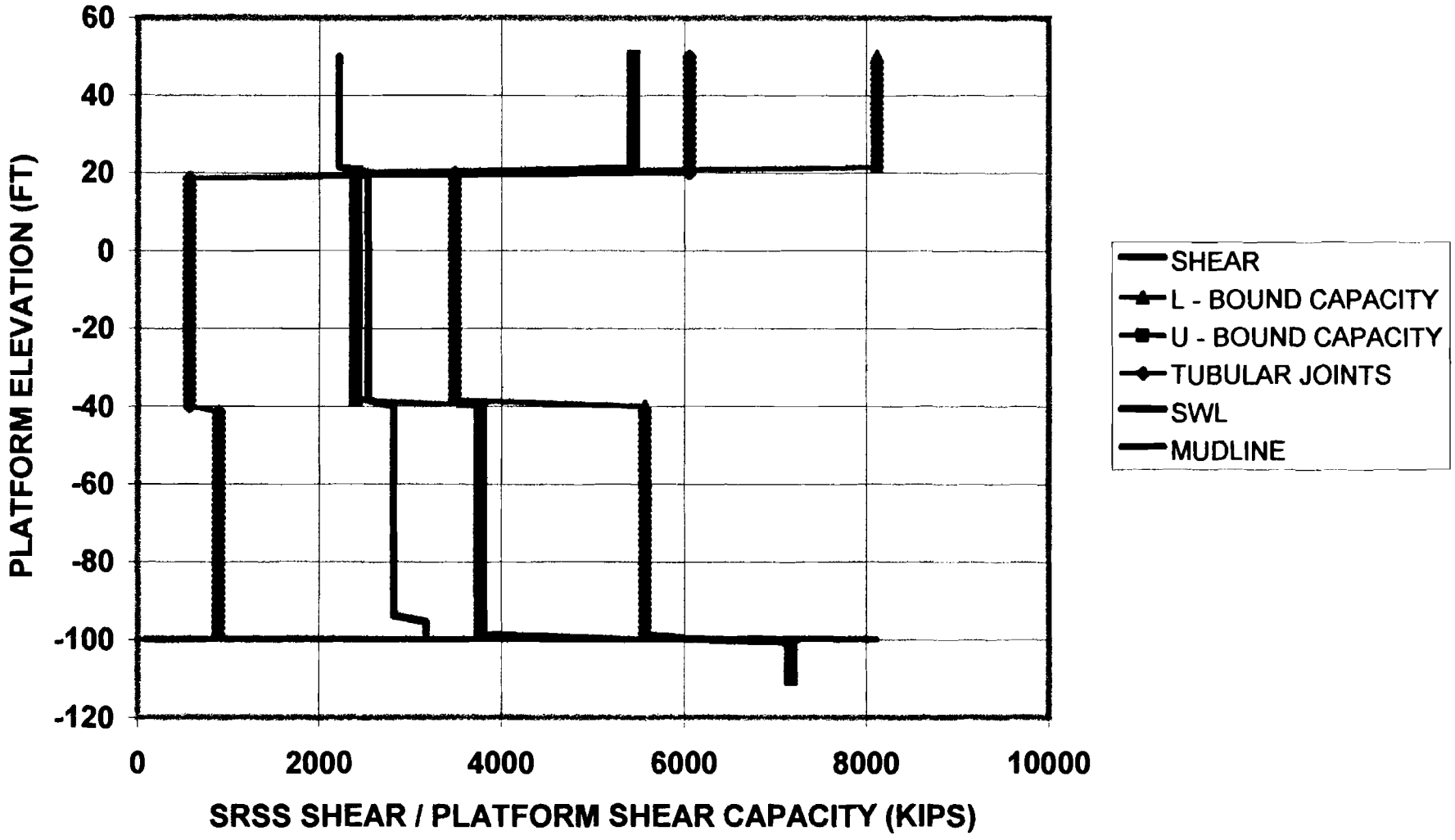

Southern California Example Platform

BROADSIDE LOADING: EARTHQUAKE

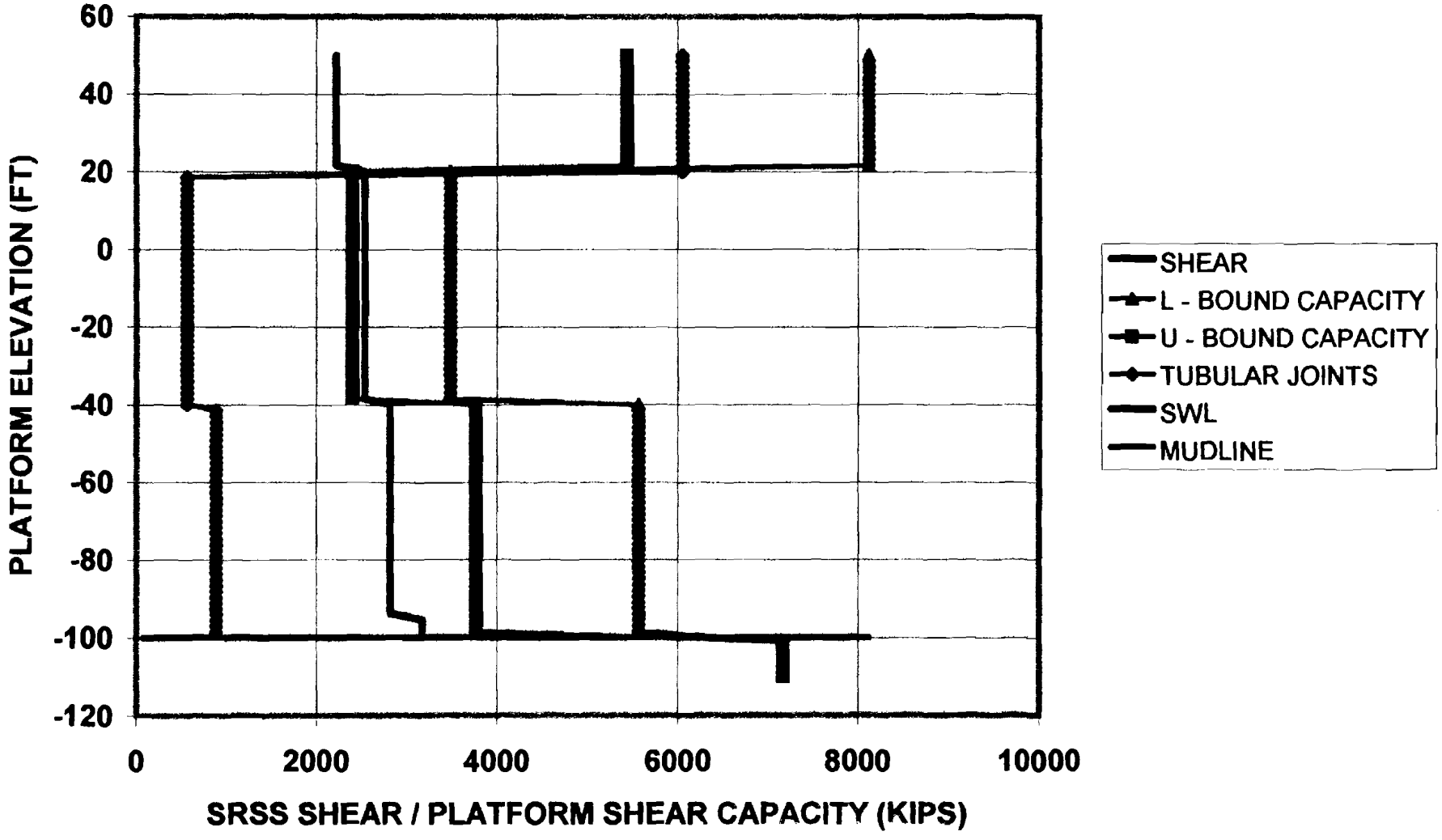

Southern California Example Platform

AXIAL UTILIZATION OF CRITICAL PILE